Structural Basis of Guest-Host Interaction in the Gastrointestinal Delivery of Lipophilic Bioactive Compounds using Protein-based Vehicles

Ogadimma Desmond Okagu

A thesis submitted in partial fulfillment of the requirements for the Doctorate in Philosophy degree in Chemistry

Department of Chemistry and Biomolecular Sciences

Faculty of Science

University of Ottawa

GENERAL DECLARATION

This thesis generated two book chapters, three original research articles published in international peer reviewed journals and two original research manuscripts submitted for consideration for publication. The motivation for this project was the quest to understand the "structural basis of guest-host interaction in the gastrointestinal delivery of lipophilic bioactive compounds using protein-based vehicles".

The research candidate bore the responsibility of conceptualization of idea, formal analysis, investigation, methodology, validation, visualization, writing, review, and editing. This research was conducted at the University of Ottawa under the supervision of Professor Chibuike C. Udenigwe. The inclusion of co-authors in the manuscripts of various chapters indicates that there were a few minor internal collaborations, and their contribution fits within the main subject framework of this study.

I hereby declare that the data and materials contained in this thesis have not previously been published by another author or approved for the award of a diploma or degree by any institution, except where appropriate acknowledgement has been made. Since no animal or human was used in this study, no research ethics approval was required for it or its inclusion.

Signed by: …….

Date: April 3, 2023

Ogadimma Desmond Okagu
(PhD Candidate)

The peer-reviewed scientific articles published or submitted by the candidate, which were used in formulating this thesis, are listed in the table below.

Thesis Chapter	Title of Publication	Type of Publication	Status of Publication	Candidate Contribution
1	Protein-based nanodelivery systems for food applications	Book Chapter	In *Encyclopedia of food chemistry*. ed. by Melton, B. L.; Shahidi, F.; Varelis, P. (Academic, Oxford), pp. 719–726, (2019)	Conceptualization of idea, writing and review [80%]
1	Food proteins as biomaterial for delivery functions	Book Chapter	In *Food proteins and peptides: emerging biofunctions, food and biomaterial applications*. ed. by Udenigwe, C. C. (RSC, London), pp. 97-126, (2021)	Conceptualization of idea, writing and review [65%]
2	Impact of succinylation on pea protein-curcumin interaction, polyelectrolyte complexation with chitosan, and gastrointestinal release of curcumin in loaded-biopolymer nano-complexes	Research article	Journal of Molecular Liquids, 325, 115248, (2021)	Conceptualization of idea, formal analysis, investigation, methodology, validation, visualization, writing, review, and editing [85%]
3	Molecular interactions of pea globulin, albumin and glutelin with curcumin: formation and gastric release mechanisms of curcumin-loaded bio-nanocomplexes	Research article	Food Biophysics, 17, pp. 10-25, (2022)	Conceptualization of idea, formal analysis, investigation, methodology, validation, visualization, writing, review, and editing [90%]
4	Molecular interaction of pea glutelin and	Research article	Journal of Agricultural and Food	Conceptualization of idea, formal

	lipophilic bioactive compounds: Structure-binding relationship and nano-/micro complexation		Chemistry, 71(12), pp. 4957-4969, (2023)	analysis, investigation, methodology, validation, visualization, writing, review, and editing [85%]
5	Curcumin–induced stabilization of protein–based nano-delivery vehicles reduces disruption of zwitterionic giant unilamellar vesicles	Research article	Molecules, 27(6), 1941, (2022)	Conceptualization of idea, formal analysis, investigation, methodology, validation, visualization, writing, review, and editing [85%]

The following first-authored article was also developed from this research but was not included in this thesis.

Article	Title of Publication	Type of Publication	Status of Publication	Candidate Contribution
1	Utilization of insect proteins to formulate nutraceutical delivery systems: Encapsulation and release of curcumin using mealworm protein-chitosan nano-complexes	Research article	International Journal of Biological Macromolecules, 151, pp 333-343 (2020)	Conceptualization of idea, writing and review [45%]

The candidate presented the following research, which is part of this thesis, at the scientific conferences listed below.

Abstract	Title of Presentation	Conference	Candidate's contribution
1	Curcumin-loaded protein and protein-chitosan nanocomplexes reduce rupturing of giant unilamellar vesicles compared to hollow nanoparticles: Preliminary investigation into bio-nano interaction	Canadian Lipids and Proteins Conference, 2022	Conceptualization of idea, formal analysis, investigation, methodology, validation, visualization, writing, review, and editing [85%]
2	Interaction of pea globulin, albumin and glutelin with curcumin and the formation of pepsin resistant and thermo-stabilized well-ordered spherical bio-nanocomplexes for oral delivery	American Oil Chemists Society Annual Meeting & Expo, 2021	Conceptualization of idea, formal analysis, investigation, methodology, validation, visualization, writing, review, and editing [90%]
3	Pea protein acylation and impacts on interaction, physicochemical properties, and the delivery of curcumin	American Oil Chemists Society Annual Meeting & Expo, 2020	Conceptualization of idea, formal analysis, investigation, methodology, validation, visualization, writing, review, and editing [85%]

.

Signed by: ……. Date: …….

Prof. Chibuike C. Udenigwe

(Primary Supervisor)

Signed by:……. Date: ……

Prof. André Beauchemin

(Co-supervisor)

ACKNOWLEDGEMENTS

I thank God almighty for his infinite grace, love, and guidance throughout this PhD journey and for making my lifelong ambition an accomplished one.

My principal supervisor, Professor Chibuike Udenigwe, deserves the deepest gratitude for having recognised my talent in my despondent state when I most needed a chance to pursue graduate studies. In 2015, I was shortlisted for the award of Presidential Special Scholarship Scheme for Innovation and Development (PRESSID) by the office of the Nigerian president through the National University Commission (NUC). This prestigious scholarship was instituted to train outstanding 100 First Class graduates to the top 25 Universities in the world. The scholars would act as a catalyst for technological and economic advancement in the country. Unfortunately, the scholarship was later canceled four months after publishing the names of beneficiaries due to change in government. I was devasted and in 2017, I requested for an opportunity in Prof. Udenigwe's lab, and he accepted to supervise and fund my study through the NSERC discovery grant. I thank you for your patience and advice throughout my research. I also wish to thank my co-supervisor, Prof. André Beauchemin for his guidance and almost instantaneous feedbacks. I am grateful to my thesis advisory committee, Dr. Corrie daCosta, Prof. Paul Mayer and Prof. Apollinaire Tsopmo for the advice and guidance. I cannot over emphasize the enormous help from both present and past lab members of Udenigwe's lab and the four students I supervised to completion under the direction of my supervisor. They comprise one Masters' student who is a Shastri intern visiting from India, and three undergraduate interns including a UOttawa research assistant, UROP student and Mitacs summer intern.

I wish to specially thank my parents Mr. and Mrs. Godwin Okagu for their financial and moral support. I cannot overemphasize the enormous love, care and encouragement from my lovely

children, Andre, Hailmary, Mia and Krista Okagu. Thank you all for believing in me and for being my source of strength and motivation.

Finally, I wish to thank the University of Ottawa for their financial support having awarded me Teaching Assistant, Research Assistant, International doctoral scholarship, admission scholarship, Tito Scaiano Scholarship 2020 and 2021, Navan Lions Club Science Scholarship 2019 and 2021, and Association of Professors of the University of Ottawa Student Award 2022.

ABSTRACT

Bioactive compounds, such as curcumin, lutein, coenzyme Q10, β-carotene, cholecalciferol, astaxanthin, and β-sitosterol, have antioxidant and anti-inflammatory properties that promote health, but their low solubility, fast metabolism, and degradation have made it difficult to fully harness their potential. Encapsulation techniques, such as nano and microencapsulation using food-based biopolymers, have been employed to address these challenges. However, research efforts in protein-based delivery have mainly focused on encapsulation without considering structural, physicochemical, and matrix compatibility, which is tedious, unsustainable, and not cost-effective. Hence, this thesis reports the structural basis of guest-host interaction in the gastrointestinal delivery of lipophilic bioactive compounds using protein-based vehicles.

This research employed fluorescence quenching techniques to estimate the influence of protein modification, fractionation and ionic strength on the nature and strength of interactions between protein and bioactive compounds. Morphological examination was carried out with transmission electron microscopy, confocal and widefield fluorescence microscopy whereas the sizes of the nano and micro-complexes was measured with dynamic light scattering techniques. Thermal stability was measured with differential scanning calorimetry and functional group characterization done with Fourier Transform infrared spectroscopy. Encapsulation efficiency was estimated by UV-Visible spectroscopy whereas *in vitro* bioactive compound release study was carried out in simulated salivary, gastric and intestinal fluids. Cytotoxicity assessment was estimated by calcein leakage assay.

The study showed that protein modification affects the strength of protein-curcumin interaction and encapsulation efficiency. Pea protein succinylation increased electrostatic interaction with chitosan but decreased protein-curcumin interaction. Pea glutelin, albumin and globulin fractions

showed different binding strengths with curcumin and the protein hydrophobicity and encapsulation efficiency correlated positively with the binding strength. The study also investigated the impact of bioactive compound lipophilicity and physiological ionic strength on the interaction between protein and bioactive compound. Lipophilicity influenced the strength of protein-bioactive compound interaction, while ionic strength changed the mode of interaction from static to static-dynamic quenching. The morphology of the nano and micro complexes formed with protein varied depending on the nature of encapsulated bioactive compound. Finally, bio-nano interaction involving giant unilamellar vesicles and curcumin-loaded pea protein of various surface functionalities as model biomembrane and nanoparticles respectively, was investigated. The result showed that while the protein/chitosan shell stabilizes bioactive compounds from degradation, the bioactive compound modulates their interaction with biomembrane.

Overall, this work has demonstrated that for a rational design of protein-based nano/micro-encapsulation system, it is essential to consider the influence of the structural and physicochemical properties of proteins and bioactive compounds, stabilizing intermolecular forces, ionic strength of the environment, lipophilicity of the bioactive compounds, mechanism of release and modulation of cytotoxicity by bioactive compound. For instance, in high ionic strength solution, the stoichiometric ratio between protein carrier and bioactive compounds influences the stability of the complex. Balancing the intermolecular forces in the shell and core of bilayer complexes is essential for the stability of nanocomplexes and the presence of bioactive compound stabilizes the macromolecular carrier to minimal biomembrane disruption.

PUBLICATION DETAILS

This is to acknowledge that the following book chapters and original research articles published in or submitted to international peer reviewed journals and presented in scientific conferences were used in formulating this thesis. The publications are listed in ascending order of year of publication or submission.

Original Research Articles

Okagu, O. D.; Jin, J.; Udenigwe, C. C. Impact of Succinylation on Pea Protein-Curcumin Interaction, Polyelectrolyte Complexation with Chitosan, and Gastrointestinal Release of Curcumin in Loaded-Biopolymer Nano-Complexes. *J. Mol. Liq.* **2021**, *325*, 115248.

Okagu, O. D.; Udenigwe, C. C. Molecular Interactions of Pea Globulin, Albumin and Glutelin with Curcumin: Formation and Gastric Release Mechanisms of Curcumin-loaded Bio-nanocomplexes. *Food Biophys.* **2022**, *17*, 10-25.

Okagu, O. D.; Abioye, R. O.; Udenigwe, C. C. Curcumin-Induced Stabilization of Protein-Based Nano-Delivery Vehicles Reduces Disruption of Zwitterionic Giant Unilamellar Vesicles. *Molecules.* **2022**, *27(6)*, 1941.

Okagu, O. D.; Abioye, R. O.; Udenigwe, C. C. Molecular Interaction of Pea Glutelin and Lipophilic Bioactive Compounds: 1. Structure-Binding Relationship and Nano / Micro Complexation. **2022**, (Submitted).

Okagu, O. D.; Abioye, R. O.; Udenigwe, C. C. Molecular Interaction of Pea Glutelin and Lipophilic Bioactive Compounds: 2. Effect of Nano/Micro Complexation on Model Biomembrane. **2022**, (Submitted).

Book Chapter

Okagu, O. D.; Wang, B.; Acquah, C.; Udenigwe, C. C. Protein-based nanodelivery systems for food applications. In *Encyclopedia of food chemistry*. ed. by Melton, B. L.; Shahidi, F.; Varelis, P. *Academic Press, Oxford, United Kingdom*. **2019**, 719–726.

Okagu, O. D.; Wang, B.; Udenigwe, C. C. Food proteins as biomaterial for delivery functions. in *Food proteins and peptides: emerging biofunctions, food and biomaterial applications*. ed. by Udenigwe C. C. *RSC, London*. **2021**, 97-126.

DEDICATIONS

TO MY LOVELY CHILDREN, ANDRE, HAILMARY, MIA AND KRISTA OKAGU

TABLE OF CONTENTS

ABBREVIATIONS

AFC: alternative force choice

AFM: atomic force microscopy

ANOVA: analysis of variance

ANS: 8-anilo-1-naphthalenesulfonic acid

As: astaxanthin

AsASF: astaxanthin-alkaline-soluble pea protein complex

ASF: alkaline-soluble pea glutelin protein fraction

BSA: bovine serum albumin

BSEs: backscattered electrons

CASF: curcumin-loaded alkaline-soluble pea protein fraction

CD: circular dichroism

Ch: cholecalciferol

ChASF: cholecalciferol-alkaline-soluble pea protein complex

CHI: chitosan

CLSM: confocal laser scanning microscopy

CSSF: curcumin-loaded salt-soluble pea protein fraction

CuASF: curcumin-alkaline-soluble pea protein complex

CUR/PPI/CHI: curcumin-native pea protein-chitosan complex

CUR/PPI: curcumin-native pea protein complex

CUR/SPPI/CHI: curcumin-succinylated pea protein-chitosan complex

CUR/SSPI: curcumin-succinylated pea protein complex

CUR: curcumin

CWSF: curcumin-loaded water-soluble pea protein fraction

DHA: docosahexaenoic acid

DLS: dynamic light scattering

DMSO: dimethyl sulfoxide

DOPC: 1,2-dioleoyl-sn-glycero-3-phosphocholine

DSC: differential scanning calorimetry

E_{CUR}: encapsulated curcumin

EDTA: Ethylenediaminetetraacetic acid

EE: encapsulation efficiency

Ems: electron microscopes

Eq: equation

ESF: ethanol-soluble pea prolamin fraction

f: accessible fluorophore fraction

F: fluorescence intensity of the protein in the presence of quencher

F_0: fluorescence intensity of the protein in the absence of quencher

FTIR: fourier-transform infrared spectroscopy

GRAS: generally recognized as safe

GUV: giant unilamellar vesicle

H_0: surface hydrophobicity

K: effective quenching constant for the accessible fluorophores

K_A: binding constant

K_D: Stern-Volmer quenching constant

K_Q: biomolecular quenching rate constant

lGUV: calcein-loaded giant unilamellar vesicles

MW: molecular weight

n: number of binding sites

NMR: nuclear magnetic resonance

O/W/W: oil-in-water-in-water emulsion

PDI: polydispersity index

PPI/CHI: hollow pea protein-chitosan complex

PPI: native pea protein isolate

Q: quencher

Q_{10}: coenzyme Q_{10}

Q_{10}ASF: coenzyme Q_{10}-alkaline-soluble pea protein complex

SDS-PAGE: sodium dodecyl sulfate-polyacrylamide gel electrophoresis

SEM: scanning electron microscopy

SEs: secondary electrons

SGF: simulated gastric fluid

SIF: simulated intestinal fluid

SPPI/CHI: hollow succinylated pea protein-chitosan complex

SPPI: succinylated pea protein isolate

SSF: salt-soluble pea globulin protein fraction (Chapter three)

SSF: simulated salivary fluid (Chapter two)

t_0: lifetime of protein fluorophore

TEM: transmission electron microscopy

Tg: glass transition temperature

W/W: water-in-water emulsion

WPI: whey protein isolate

WSF: water-soluble pea albumin protein fraction

XRD: X-ray diffraction

βCa: β-carotene

βCaASF: β-carotene-alkaline-soluble pea protein complex

βSi: β-sitosterol

βSiASF: β-sitosterol-alkaline-soluble pea protein complex

λ_{em}: emission wavelength

λ_{ex}: excitation wavelength

LIST OF SCHEMES

LIST OF FIGURES

LIST OF TABLES

CHAPTER ONE

INTRODUCTION

SECTION 1.1

Food Proteins as Biomaterial for Delivery Functions

Ogadimma D. Okagu, Bo Wang and Chibuike C. Udenigwe
in *Food proteins and peptides: emerging biofunctions, food and biomaterial applications*.
ed. by Udenigwe C. C. *RSC, London*. **2021**, 97-126.

https://doi.org/10.1039/9781839163425-00097

DECLARATION FOR THESIS SECTION 1.1

Food Proteins as Biomaterial for Delivery Functions

This is to declare that there is no conflict of interest associated with this work and the contribution of the candidate is as stated below:

Candidate's contribution	Conceptualization of idea, writing and review	65%

The following co-authors attest to the candidate's participation in a group publication as a component of his thesis and was active in the creation of this publication. The co-authors' permissions are as follows:

Name	Signature	Date
Bo Wang		22/11/2022
Chibuike C. Udenigwe		22/11/2022

1. INTRODUCTION

Functional foods are designed to add value beyond their normal nutrition and aid in improving wellness and human health through diet. They are mostly fortified and enriched with various bioactive compounds such as minerals, phytosterols, steroids, polyphenols, vitamins, probiotic bacteria, bioactive peptides, functional lipids, *etc.*[1] These bioactive compounds are mostly insoluble and unstable, and degrade during food processing, storage or in a gastrointestinal environment, which results in low bioavailability under physiological conditions. The design of food-grade materials for the encapsulation, protection and delivery of unstable, insoluble and non-bioavailable bioactive food compounds has attracted increasing attention in recent years.[1–4] They are fabricated based on the relationship between the physicochemical properties of the encapsulating agent and those of the bioactive compounds. Knowledge of their matrix compatibility, stability, solubility, interaction, bioaccessibility and bioavailability is essential for the rational design of a good delivery system.[5] Delivery vehicles are engineered to entrap bioactive compounds, protect them from oxidation and unfavorable pH, photochemical, chemical and enzymatic degradation and control their release at a specific rate and site.[6] They equally improve the solubility and bioavailability of the bioactive ingredient.[5,7]

Various food-grade materials such as lipids,[6,8] carbohydrates[9] and proteins[5,7] have been successfully employed in encapsulation techniques. Lipid-based delivery systems have recorded high encapsulation efficiencies, but lipids are highly sensitive to changes in pH and temperature and hence could induce irreversible aggregation and sedimentation.[9] Additionally, there are concerns over toxicity associated with burst release and risk of recrystallization and explosion. [6] Carbohydrate-based delivery systems face the challenge of α-amylase degradation in the salivary phase and also often encounter various chemical modifications to withstand gastric degradation.[10]

The fabrication of monodispersed carbohydrate-based delivery systems is often challenging owing to their high viscosity and a combination of amorphous and crystalline regions in their structure. [9] Protein-based delivery systems have been well researched and proven to be very promising. Proteins have inherent structural and physicochemical properties such as many well-arranged/ packed hydrophobic, hydrophilic, amphipathic and/or charged or neutral side-chain functional groups that can interact with and hence encapsulate, protect and deliver various nutraceutical and pharmaceutical bioactive compounds. [9] Proteins can adsorb and prevent aggregation on the surface of colloidal particles,[11] can form new structures such as fibers, tubes and spheres[12] and also its hydrolysate could act as antioxidants.[13] They also have gelation, emulsification and foaming properties that contribute to their diverse application in bioactive compound delivery.[1] Unlike carbohydrate-based systems, the absence of proteolytic enzymes enables proteins to protect the bioactive compound in the salivary phase. Proteins do not readily recrystallize or explode, making them a better candidate than lipid-based delivery systems.

This section discusses protein-based nano-and microencapsulation systems, their various fabrication techniques, physicochemical characterization, biochemical evaluation, biological assessment, applications, and challenges. It also highlights some research gaps that should be explored for the efficient and large-scale application of protein-based delivery systems.

2. PROTEIN-BASED DELIVERY SYSTEMS

Protein-based delivery systems can be classified based on the sources of the encapsulating protein agents. These include animal, plant and recombinant protein-based delivery systems which have been formulated for nano-and microencapsulation and delivery of bioactive compounds.

2.1. Animal Protein-based Delivery Systems

Animal-derived proteins have been reported to improve substantially the physicochemical and physiological activity of many unstable and non-bioavailable bioactive compounds. For instance, insect protein improved the solubility, bioaccessibility and membrane permeability of curcumin. [5] Likewise, gelatin modified with chitin ensured the protection and sustained release of tetrahydrocurcumin.[14] Chitosan–casein core–shell nanoparticles functionalized with l-arginine and l-lysine have been shown to have excellent stability and pH-responsive properties that allowed the encapsulation of both hydrophobic and hydrophilic bioactive compounds.[15] Micro- nalized chitosan casein core–shell and pH-responsive nanoparticles: fabrication, characterization and bioavailability enhancement of hydrophobic and hydrophilic bioactive compounds and nanostructures encapsulating riboflavin and quercetin were successfully fabricated from β lactoglobulin and the delivery system withstood several environmental conditions and ensured slow release of the bioactive agents.[16] Whey protein covalently crosslinked with citric acid improved the stability and antioxidant activity of curcumin.[17] Similarly, a milk proteins–curcumin-based delivery system increased the antioxidant, anticancer and antimicrobial properties of curcumin.[18]

2.2. Plant Protein-based Delivery Systems

Plant-based protein delivery systems are more sustainable or ‘green’ than their animal counterparts. The encapsulating materials have been fabricated from zein, soy protein and wheat

gliadins into nano-and microparticles, hydrogels, films and fibers.[1] Zein is an amphiphilic protein rich in α-helical conformation derived mainly from corn gluten meal. It can self-assemble into various mesostructures in different solvents and has demonstrated potential application in the delivery of nutraceutical compounds, especially hydrophobic bioactives.[19–21] Patel *et al.* reported improved photostability of curcumin encapsulated with zein nanoparticles and an encapsulation efficiency of 86.8%.[22] To improve the encapsulation efficiency further, complexation of zein with sodium caseinate was carried out and sustained release of curcumin from the stable zein–caseinate nanoparticles under gastric and intestinal conditions and an improved encapsulation efficiency of 95.55% were reported.[21] This is due to increased stability of the zein shell which degrades at high temperature, ionic strength and neutral pH. Also, complexation with sodium caseinate offers protection against enzymatic hydrolysis in the stomach. Zein-based delivery systems have also been used to deliver functional compounds such as micronutrients, antimicrobial compounds, essential oils, polyphenols, bioactive lipids and food coloring agents. [1]

Similar to zein, soy proteins have modifiable structural and functional properties that permit the encapsulation and delivery of nutraceuticals and drugs. The delivery vehicle is mainly fabricated by cold gelation coacervation and spray drying. [1] An emulsion gel prepared with soy protein by the cold gelation technique showed optimal thermal stability and successfully entrapped polyphenols within its matrix.[23] Soy protein gels modified into a double network of corn fiber gum–soy protein improved the efficiency of riboflavin release by hindering proteolysis in the gastric phase while promoting peptide cleavage in the intestinal phase.[24] They have ligand-binding properties and have been reported to form complexes with many bioactive compounds *via* hydrophobic, hydrogen bonding, electrostatic and van der Waals interactions. They have demonstrated potential applications in improving the stability, aqueous solubility and

bioavailability of both hydrophilic and hydrophobic bioactive compounds such as curcumin, resveratrol, grape polyphenols, cranberry polyphenols and vitamin B_{12}.[1]

Encapsulating systems derived from wheat gliadin and barley proteins have been reported for the delivery of nutraceutical ingredients. For instance, gliadin nanoparticle Pickering emulgels encapsulating β-carotene with better fluidity at low gliadin concentration and a stronger gel structure at high gliadin concentration were recently reported by Cheng *et al.* and it was found that the storage and thermal stability of β-carotene and also its bioaccessibility were significantly improved in the gliadin complex.[25] Curcumin-loaded gliadin–chitosan composite nanoparticles of high encapsulation efficiency were prepared by a combination of antisolvent precipitation and ionic crosslinking using different crosslinkers. The crosslinking agents improved the physicochemical properties of curcumin, with sodium phytate facilitating the best neuroprotective effect of the bioactive compound.[26] Wang *et al.* reported the microencapsulation of fish oil with barley protein prepared by pre-emulsification in the absence of any organic solvent or crosslinkers. The microcapsule had an encapsulation efficiency of 92.9–100.2% and protected the fish oil from oxidation.[27]

2.3. Recombinant Protein-based Delivery Systems

This type of protein-based delivery system is less common and involves the use of proteins biologically synthesized inside the host cells of living organisms. Proteins produced in this way are usually of high purity but face challenges of consumer acceptability and large-scale economic production. For instance, silk protein has been reported to be a promising encapsulating agent for bioactive compounds but large-scale production using conventional methods is not feasible.[2] Iron storage protein ferritins with cage-like structures are found in bacteria, plants and animals and have shown potential as a good delivery vehicle for curcumin. The curcumin-loaded ferritin complex

increased the stability and water solubility of curcumin.[28] This delivery system is specifically designed for high-value applications.

Protein-based delivery systems can also be classified according to the size of the loaded complexes, *viz.* nano-and microencapsulation systems.

3. PROTEIN ENCAPSULATION SYSTEMS

3.1. Protein-based Nanoencapsulation Systems

In protein-based nanoencapsulation systems, the bioactive compound is encapsulated in a protein matrix or protein–biopolymer complex within a size range of 1–100 nm (nanoscale). The size of the bioactive compound within a nanoscale complex greatly influences the rate of release, burst or sustained release, target specificity and nature of protein corona formed.[29] A nanoencapsulation system has a greater potential to encapsulate, protect, stabilize, and deliver bioactive compounds at a higher target specificity than microencapsulation systems.[10,30]

Protein-based nanoencapsulation systems have been fabricated from plant-and animal-based proteins owing to their unique functional and biological properties. They possess a modifiable feature that allows the fabrication of nanostructures such as nanotubes, nanogels, electrospun nanofibers, nanoparticles, hollow nanoparticles, nanopolyelectrolyte complexes and nanofibrillar complexes. They are advantageous owing to their amphiphilicity, surface activity, biocompatibility, availability, high nutritional properties, safety, antioxidant potential and emulsifying, film-forming, foaming and gelation properties.[31] Protein-based nanoencapsulation systems of different forms have been used to deliver bioactive food compounds efficiently to their preferred site in the body and the mechanism of release is mainly based on pH sensitivity, swelling or proteolytic degradation in a simulated physiological environment. [31] They are popularly

developed for their ability to improve the solubility and bioavailability of nutraceutical bioactive compounds and enhance their residence time and stability in the harsh gastrointestinal environment. Their small size increases their membrane permeability properties and they are easily absorbed by tissues and cells.[32,33]

Nanoencapsulation delivery systems of various forms have been fabricated from soy, whey, bovine serum albumin (BSA), egg albumin, zein, ovalbumin, lactoferrin–glycomacropeptide, β-lactoglobulin, gelatin, prolamine, β-lactalbumin and others for the delivery of various nutraceuticals such as curcumin, vitamin B_{12}, doxorubicin, vitamin D_3, lycopene, resveratrol, quercetin, metformin, 5-fluorouracil, riboflavin, caffeine, limonene, fish oil, metal nanoparticles, raspberry ketone, vitamins A and E, orange essential oil, β-carotene, rhodamine B, Congo Red, gallic acid and aceclofenac.[31]

Protein-based nanodelivery systems have been synthesized by emulsification, desolvation, nanoprecipitation, coacervation, polyelectrolyte complexation, salting out, self-assembly, nanospray drying, electrospraying and crosslinking methods.[34,35] The choice of encapsulation technique depends on the type of nanomaterial one wishes to produce, processing operation, amino acid composition, hydrophobicity, amphiphilicity, zeta potential and folding of the protein, in addition to the physicochemical properties of the bioactive molecule.

Designing a suitable protein-based nanoencapsulation system can be challenging owing to the complexity of determining a suitable protein for a given bioactive compound. This is mostly evaluated by studying the *in silico* structure–activity relationship, which does not consider the effects of temperature, aqueous environment, pH, ionic strength, viscosity and turbidity of the reaction mixture, or by performing protein–bioactive compound binding, which does not provide

all the information needed for efficient encapsulation. Obtaining the strength and nature of the interaction from binding studies (mostly performed) does not guarantee efficient delivery as binding does not necessarily translate to encapsulation efficiency or release potential. Also, the relationship between the type of protein, bioactive compound and fabrication conditions have not been thoroughly explored and could make it challenging to use a particular protein to design either nanoparticles, nanofibers, nanotubes or nanogels, *etc.* Also, due to the challenge of solubility and the necessity to ensure complete dissolution of both the encapsulating agent and the cargo, introduction of hazardous reagents is often unavoidable. Most nanoencapsulation systems are produced in the laboratory as there are limited cost-effective methods for large-scale Industrial production.

3.2. Protein-based Microencapsulation Systems

Protein-based microencapsulation is similar to nanoencapsulation but here both the encapsulating protein agent or coating material and the loaded biopolymer complexes are in the micro size range (10−6 m). The microencapsulation technique was first introduced by Bungen burg de Jon and Kan in 1931.[29] This technique is much older than nanoencapsulation and has been equally successfully applied to decrease the surface area-to- volume ratio of powdered food materials, enhance their storage and intestinal stability, prevent unwanted taste and texture, enhance the discharge properties of the bioactive compound, and increase bioavailability.[36] The smaller size of nanoencapsulation systems offers better encapsulation, protection, release, and permeability properties. For instance, nano-and microencapsulation of β-carotene with zein protein stabilized with glycerol by the electrospraying and spray drying technique, respectively, showed size-dependent release and absorption. This study clearly indicates the effect of the encapsulation technique on the size of nanoparticles as the same encapsulating agent and bioactive compound

gave rise to both nano-and microparticles. A higher encapsulation efficiency of 81% and better dissolution behavior were reported for the nanoencapsulated form obtained by electrospraying than the microencapsulated counterpart owing to the smaller size. Simulated *in vitro* gastrointestinal conditions showed a faster release of β-carotene from the nanoencapsulates and enhanced bioavailability and permeability compared with the microparticles. [37] Nanoparticles can form mixed micelles more quickly than microparticles during lipid digestion and hence preferentially favors the rate of release and bioavailability of the encapsulated bioactive agent.[38] Depending on the environmental conditions such as heat treatment and pH, Monteiro *et al.* reported micro-and nanoencapsulation systems using a mixture of two proteins, α-lactalbumin and lysozyme. They were found to be stable for 30 and 90 days at 25 and 4 °C, respectively.[39] Using similar fabrication techniques and proteins as in the nanoencapsulation systems, numerous microencapsulation systems have been developed and possess the ability to encapsulate various bioactive compounds. They face similar encapsulation challenges such as low solubility leading to the addition of non-friendly reagents, protein–bioactive compound compatibility and design, *etc.*[30]

4. FABRICATION TECHNIQUES FOR PROTEIN-BASED DELIVERY SYSTEMS

Protein-based delivery systems have been successfully fabricated by emulsification, desolvation, nanoprecipitation, coacervation, polyelectrolyte complexation, salting out, self-assembly, nanospray drying, electrospraying and crosslinking methods. The fabrication procedures in these techniques and their advantages and disadvantages were discussed in the preceding section.

4.1. Coacervation/Desolvation Techniques

Coacervation or desolvation techniques are commonly employed in both the nano-and microencapsulation of nutraceuticals. This approach is based on the differential solubility of proteins in various solvents as a function of the ionic strength, pH, polarity, dielectric constant, or

presence of electrolyte in the solvent. Protein solubility is reduced in the coacervation process by adding desolvation agents, leading to protein precipitation and hence phase separation. They could be simple or complex coacervates depending on whether a single or complex protein is used, respectively.[30] In complex coacervation, the electrostatic attraction between oppositely charged molecules is the major driving force in the phase separation into a protein-rich phase (coacervate) and a protein-poor phase of the solvent. The size of the micro-or nanoparticles is controlled by changing the processing conditions and stabilized with the help of a crosslinker such as glyoxal or glutaraldehyde.[40] The size of the micro-or nanoparticles depends on the processing conditions, pH, solvent, protein, nature of binding, folding, solubility, *etc.* For instance, acetone produced smaller albumin nanoparticles than ethanol. The pH prior to desolvation has been reported to be a major factor determining the particle size, as smaller particles were obtained at high pH whereas agglomeration was enhanced at high ionic strength owing to surface charge neutralization. An increase in protein concentration reduced the particle size of BSA owing to increased nucleation upon addition of antisolvent reagents.[41] For hydrophobic proteins, the protein solubility is enhanced by increasing the ionic strength of the solution, leading to smaller protein sizes.[42] Heating β-lactoglobulin before phase separation led to denaturation, which increased the solubility and hence produced smaller particles.[43] A major advantage of coacervation is the production of particles of desired sizes by regulating the processing conditions.[44] This technique has been reported to improve the stability of flavors, oils and vitamins compared with spray drying. It involves low-temperature conditions, has a high core loading level, higher encapsulation efficiency and better shell integrity and has demonstrated controlled-release potential.[30] Active agents with finite water solubility and pH can detrimentally affect the complex coacervation processes employed for micro-and nanoparticle fabrication. Variation of the atmospheric moisture content

could affect complex coacervates with a dry shell and could become plasticized at a relative humidity above 70%. Therefore, the ambient environmental conditions could considerably affect the release efficiency of complex coacervates.[45] Another major limitation of the coacervation technique is that it is applicable only to charged biopolymers.

4.2. Electrospraying

This electrohydrodynamic atomization technique involves the application of a high voltage to a solution of the protein, leading to the emission of a liquid jet stream through the nozzle, forming aerosolized liquid droplets containing the protein micro-or nanoparticles. This fabrication method is similar to electrospinning but instead of nanofibers, nanoparticles are formed. Dry nanoparticles are formed by the solvent evaporation that occurs during the flight of the droplets towards the grounded electrode. This technique has been employed for the production of elastin-like and gliadin peptide nanoparticles.[46,47] The advantage of this technique is that solid nanoparticles of high encapsulation efficiency are produced in a single step. By modifying the operating conditions such as voltage, flow rate and collector distance, the properties of the solution such as concentration, density, biopolymer type and viscosity or environmental conditions such as pressure and temperature, nanoparticles with various properties could be produced.[48]

4.3. Spray Drying

This technique is used to produce both protein micro-and nanoparticles by mechanical dehydration of a colloidal suspension through heating and solvent evaporation to produce powdered particles. The encapsulating agent and the bioactive compound are mixed to give a uniform dispersion, which is placed in a spray dryer. When the mixture passes through the spinning wheel or nozzle of the spray dryer, the hot chamber permits the atomization of the fluid and drying is achieved through a stream of hot air. This technique can operate in the temperature range 150–300 °C and

the particles are collected and separated in a cyclone.[49] The method is relatively simple and produces small particles at high yield and low cost. The solubility and stability of the bioactive compound are significantly improved. However, the high-temperature conditions associated with spray drying could result in denaturation of the protein or degradation of the bioactive compound. Spray drying is not effective in encapsulating volatile bioactive compounds. It sometimes produces heterogeneous particles in the nano and micro size ranges and with different shapes.[30] Nanoemulsions containing different wall materials of either maltodextrin or trehalose were stabilized by spray drying of whey protein. A high encapsulation efficiency of 97.1–98.9% and good emulsion properties and higher bulk density were reported.[50]

4.4. Homogenization

The most popular types of homogenization mostly employed in the encapsulation of bioactive compounds involve the use of a microchannel homogenizer, microfluidization, high-pressure homogenization, a high-shear mixer or a membrane homogenizer.[51,52] The high-shear mixer technique is mostly employed in the preparation of emulsion-based encapsulation systems from low to intermediate viscosity fluids to produce oil-in-water-in-water (O/W/W) or water-in-water (W/W) systems. It involves placing the encapsulation mixture in a container and on rapid rotation intense disruptive forces are generated that produce tiny droplets of lipids that are dispersed into the aqueous phase.[53] In high-pressure homogenization, small droplets of emulsion are produced as a result of the high shear stress generated by passing the O/W mixture through a narrow slit between the valves of the equipment. Microfluidization is a high-energy emulsification method in which a coarse O/W emulsion is produced from a mixture of water, oil and emulsifier by a high-shear mixer and passed through an interaction chamber using pneumatic pressure.[54] In a microchannel homogenizer, two immiscible liquids are forced into each other by passage through

a microporous glass membrane of uniform pore size. The interfacial tension between the oil and water phases, the pore diameter of the membrane, the applied pressure, the amount of emulsifier and the flow rate dictate the size of the droplets. This technique could be employed to produce droplets of a desired size by using the appropriate glass membrane.[55]

4.5. Extrusion and Co-extrusion

Both extrusion and co-extrusion have been employed in the encapsulation of bioactive compounds in a hard, dense and glassy structure by inducing gelation through the injection of a solution of bioactive compound into a solution of the encapsulating agent. Both techniques are usually performed under the same conditions except that in co-extrusion a concentric nozzle system is used. Equal-sized droplets are produced by breaking the laminar liquid jet using vibrational technology.[56] The co-extrusion technique produces reservoir-type particles of better structural integrity and offers more probiotic protection than extrusion. For instance, *Lactobacillus acidophilus* LA3 encapsulated by co-extrusion offered a better protective barrier for the probiotic in a simulated gastrointestinal environment than that with simple extrusion. *L. acidophilus* LA3 encapsulated with co-extrusion showed a viability of 6.2 log CFU g^{-1} compared with 5.3 log CFU g^{-1} when encapsulated with extrusion.[57] These techniques have the ability to protect bioactive compounds from oxidative degradation and evaporation and have been applied in the encapsulation of seed oils, probiotics and antioxidants.[30]

4.6. Cold-induced Gelation

This technique uses a combination of different steps to generate protein-based gels at ambient temperature. Initially, globular protein unfolding, and filament formation are induced in an environment with controlled ionic strength and pH by heating a solution of the protein above its thermal denaturation temperature. The solution of the denatured protein is then allowed to cool to

ambient temperature before mixing with the nutraceutical bioactive compound. Finally, the electrostatic repulsion in the denatured protein molecule is reduced by altering the pH or adding salt to cause association-induced encapsulation of the bioactive compound, which results in hydrogel production. This technique has been employed in the encapsulation of bioactive compounds with globular proteins obtained from soy and whey proteins.[58,59] The cold-induced gelation technique is advantageous especially in the encapsulation of temperature-sensitive bioactive compounds; however, it is limited mainly to globular proteins.

5. EVALUATION OF FOOD PROTEIN-BASED DELIVERY SYSTEMS

In the last several decades, much research work has been performed in both academia and industry to improve the performance of the delivery systems. Generally, there are two main aims in developing a delivery system: (1) to protect susceptible compounds during the manufacturing and application processes and storage using the wall materials and (2) to control and/or improve the release behavior of the encapsulated compounds after their ingestion. Because many delivery systems are specifically designed for their particular applications, wide ranges of core and wall materials and encapsulation techniques are used, which affect various physicochemical properties of the final particles.

5.1. Physical Characteristics

The application of a developed delivery system depends significantly on its physical characteristics such as morphology and structure, particle size and distribution, mechanical strength, thermal behavior and degree of crystallization. If the delivery system is further dehydrated to produce the final powder products, it is also important to determine the techno-functional characteristics such as flowability and reconstitution properties (if required). A wide range of analytical methods have been used for this purpose.

5.1.1. Morphology and Structure

Microscopy techniques are among the most widely used methods to observe and/or evaluate the morphology and structure of the delivery systems and optical, electron and fluorescence microscopy are commonly used (Table 1.1.1).

Table 1.1.1. The microscopical technique used to characterize the morphology and structure of the delivery system.

Microscopical technique	Particle size range (μm)	Advantage	Disadvantage	Reference
Optical microscopy	2-2,000	Ease-in-operation, low cost, accessibility	Less resolution than EM and cannot be used to characterize particles < 0.2 μm	[61,80,89,110].
Scanning electron microscopy	0.02-700	Reasonable complexity of sample preparation and operation, high resolution	Cannot differentiate compounds with different colors	[90,111–113].
Transmission electron microscopy	0.1-2	High resolution of the image	High complexity in sample preparation and high vacuum during the imaging might affect the sample morphology and structure	[64,114,115].
Atomic force microscopy	0.02-1.2	Three-dimensionally imaging the surface morphology and ease-in-operation	Small imaging scope	[69,71,116].

Confocal laser scanning microscopy	0.1-1,000	Differentiate the components using fluorescent dyes	Limited options of the dyes at some particular wavelengths.	[116–118].

Briefly, optical microscopy is the simplest method to monitor the formation of the delivery systems, and also the morphology and structure of the particles, with the advantages of ease of operation and low cost. However, it cannot be used when the size of the particles is below 200 nm owing to the limitations of the technique. As a result, various types of electron microscopes have been used.

5.1.1.1. Electron Microscopes (EMs). An EM uses electrons to image the sample and captures the images with dramatically higher resolution than in optical microscopy to reveal more detailed morphological and structural characteristics. The most widely used EM methods for the characterization of delivery systems are scanning electron microscopy (SEM) and transmission electron microscopy (TEM). Briefly, during EM imaging, backscattered electrons (BSEs), secondary electrons (SEs) and X-rays are the three signals generated and detected. Among these three signals, the SE signal measures the interaction of the primary beam close to the sample (a few nanometers). Therefore, the image produced usually has a fairly high resolution and it is also the most commonly used SEM imaging mode. On the other hand, BSE signals can provide images with a strong composition contrast. When it is used in combination with X-ray microanalysis, it is even possible to determine the chemical composition of the sample. Compared with SE and BSE signals, the X-ray signal can be used to capture an image within a larger interaction volume but gives a spatial resolution of the order of a few microns.

EM imaging requires the preparation of the sample prior to the observation. For example, dehydration (for liquid samples) and coating are the most common sample preparation methods

for liquid sample for SEM imaging: a few milligrams or drops of the sample are placed on an SEM grid, depending on the nature of the encapsulation system, followed by dehydration (if required). Subsequently, a gold or copper coating is sprayed on the surface of the sample to create high contrast. For example, in Nasri *et al.*'s study, a sardinelle protein isolate-based delivery system was developed and the spray-dried powder was mounted on the SEM grid, followed by sputter coating with a gold–palladium mixture.[60] The SEM images reported by Wang *et al.* can be referred to as a good example: A consistent coating of wall material surrounding the encapsulated fish oil could be visualized and no cracks on the encapsulation system were observed (Figure 1.1.1).[61]

Similarly to SEM, TEM also requires sample preparation before imaging. Negative staining, freeze-fracture and vitrification by plunge freezing are commonly used methods and each method can provide different morphological and structural details.[62] Among these three sample preparation methods, negative staining is most commonly used: a drop of sample is placed on a TEM grid (gold or copper of defined mesh size), followed by staining using a solution (*e.g.* uranyl acetate) to provide high contrast.[63] In Wei *et al.*'s study, coenzyme Q10 and resveratrol were co-encapsulated in a zein–propylene glycol alginate–rhamnolipid delivery system and the TEM image captured showed a uniform size of the nanoparticles.[64] Compared with the negative staining method, the freeze-fracture method can provide more information particularly relating to the internal structure of the particles.[65] After the sample has been located on the TEM grid, it is placed between two plates and further vitrified by rapid freezing using liquid propane or melting nitrogen. During cooling in a vacuum environment, the frozen sample is fractured along the areas with relatively weak molecular interactions. After further etching of the fractured plane, it is shadowed using a thin platinum/ carbon layer to provide a negative contrast of the fractured plane. Cryo-TEM, in which plunge freezing is involved, can be used to monitor the morphology and structure

characteristics of the sample as a direct investigation method. An advantage of cryo-TEM imaging is that it is performed with a vitrified and frozen hydrated state of the sample to reveal its internal structure, so it is close to the native state of the sample.[66]

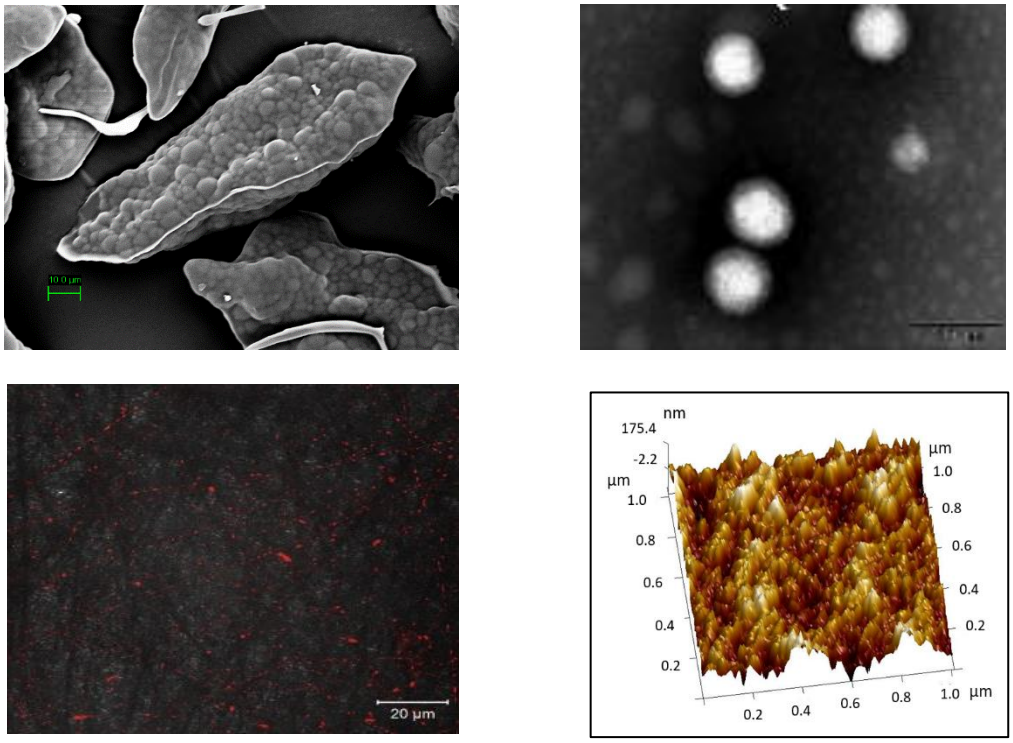

Figure 1.1.1. EM images of bioactive compounds encapsulated in the delivery system. (A) SEM image of fish oil in gelatin–sodium hexametaphosphate complex coacervates. Reproduced from ref. 61 with permission from Elsevier, Copyright 2014. (B) TEM image of zein–propylene glycol alginate–rhamnolipid complex nanoparticles in the presence or absence of resveratrol and coenzyme Q10. Reproduced from ref. 64 with permission from Elsevier, Copyright 2020. (C) CLSM image of high-oleic palm oil emulsion loaded in gelatin-based nanofibers. Reproduced from ref. 116 with permission from Elsevier, Copyright 2020. (D) AFM image of fish oil in gelatin–sodium hexametaphosphate complex coacervates. Reproduced from ref. 70 with permission from Elsevier, Copyright 2019.

Although EM imaging can provide an image with high resolution, it also has drawbacks. For example, EM imaging is performed under high-vacuum conditions to minimize the effect of radiation damage to the sample, which may alter some properties of the sample.

5.1.1.2. Confocal Laser Scanning Microscopy (CLSM). CLSM has commonly been applied to characterize delivery systems because it can be used to visualize the inner and outer structures simultaneously by carefully selecting the fluorescence dyes to stain different compounds in the delivery system. For example, in Shi and Lee's study, tributyrin was encapsulated in a whey protein isolate (WPI)-stabilized delivery system. The protein and oil components were stained with Nile Blue and Red, respectively, with excitation wavelengths of 633 and 488 nm, respectively, and the morphological structure of the reconstituted O/W emulsion droplet was successfully imaged by CLSM.[67] Similarly, Chen *et al.* used CLSM as an approach to characterize the core–shell structure of a zein-stabilized limonene system, with wall thickness between 27 and 50 nm. They even investigated the effect of zein participation on the thickness of the encapsulation system. Compared with sample preparation for EM imaging, the process for preparing samples for CLSM is simpler.[68] However, one of the major restrictions of this technique is its limited effective magnification.

5.1.1.3. Atomic Force Microscopy (AFM). Compared with SEM and CLSM, AFM is a relatively new technique mainly used to investigate the surface morphology and structures of nanoparticles. Images with a 3D configuration of the sample at the nanoscale can be captured by AFM at high resolution. Moreover, the surface mechanical properties of a single particle can be investigated during AFM imaging (see Section 5.1.3). The sample preparation for AFM imaging is straightforward since there is no need for straining or drying owing to its non-invasive nature.

Nejadmansouri *et al.* used a WPI-stabilized nanoemulsion to encapsulate fish oil with particle size <100 nm and the surface morphology of the nanodroplets was successfully detected by AFM.[69] In Wang *et al.*'s study, gelatin-based complex coacervates were used to develop a delivery system for fish oil at the microscale and AFM was used to study the surface morphology of the dehydrated particles, in combination with SEM imaging to reveal the overall structure. In this study, the surface roughness index of the particles was calculated and used to predict the shelf life of the microcapsule powder.[70] Similarly, Xia *et al.* hydrolyzed tuna oil using an enzymatic method and encapsulated the separated *ω*-3 concentrates in gelatin–sodium hexametaphosphate complex coacervates. Interestingly, the dehydrated microcapsules exhibited a dramatically improved oxidative index compared with encapsulated tuna oil and the smoother surface observed by AFM was found to be one of the key reasons for this unexpected improvement.[71]

However, AFM also exhibited some limitations: the interaction between the AFM tip and the surface of the encapsulation system may change the surface of the encapsulation system from its original state and the scale of the imagining is limited to the nanoscale.

5.1.2. Particle Size and Distribution

The particle size and distribution are one of the most important physical characteristics of a delivery system, because they significantly affect processing, handling and storage. The particle size and distribution in the liquid and dry samples can be determined by different methods and the choice of technique depends on the nature of the core and wall materials used.

Although the above-mentioned microscope methods can be used to determine the particle size of the encapsulation systems, dynamic light scattering (DLS) is becoming a preferred method, in which the light scattering intensity changes with changes in scattering angle, size of particles,

refractive indices of the particles and the medium used. Generally, the volume-surface (*D*[3,2]) and volume-weighted (*D*[4,3]) mean diameters are used to analyze the particles, calculated using the following equations:

$$D[3,2] = \frac{\sum d_i^3 n_i}{\sum d_i^2 n_i} \qquad (1.1)$$

$$D[4,3] = \frac{\sum d_i^4 n_i}{\sum d_i^3 n_i} \qquad (1.2)$$

where n_i is the number of particles with diameter d_i. To determine the particle size distribution, span is usually used, calculated using the equation:

$$Span = \frac{D_{90} - D_{10}}{D_{50}} \qquad (1.3)$$

where *D*50 is the diameter where half of the population lies below this value.

Similarly, 90% of the distribution lies below *D*90 and 10% of the population lies below *D*10, as Figure 1.1.2 shows.

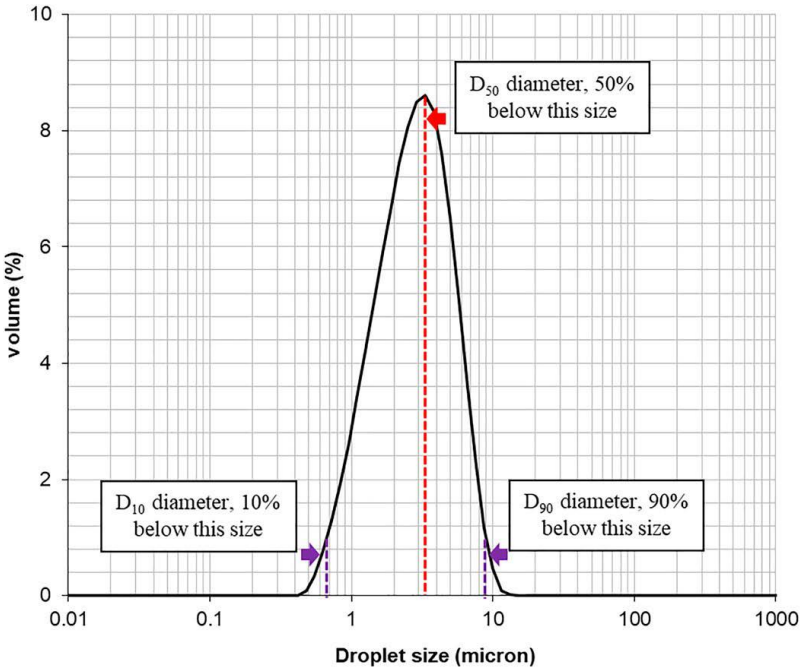

Figure 1.1.2. *D*10, *D*50 and *D*90 of a delivery system sample during DLS analysis. Partly adapted from data published in Wang *et al.* ref 119

The *Z*-average mean diameter, also known as the cumulant mean diameter, is also used to suggest the particle size of encapsulation systems. The *Z*-average mean diameter is the primary and most stable parameter obtained using the DLS technique. ISO 13321 and 22412 suggest it to be denoted the 'harmonic intensity averaged particle diameter'. The *Z*-average mean diameter of a particle, *DZ*, is calculated using the equation

$$D_z = \frac{\sum S_i}{\sum\left({}^{S_i}/_{D_i}\right)} \qquad (1.4)$$

where *Si* is the scattered intensity from particle *i* and *Di* is the diameter of particle *i*.

Similarly to span, the polydispersity index (PDI), also known as the heterogeneity index, is also a widely used term to suggest the degree of non-uniformity of particles size distribution. PDI is dimensionless and is calculated from a two-parameter fit to the correlation data (*i.e.* cumulants analysis). Generally, a sample with PDI >0.7 indicates that it has a very wide particle size distribution, and it is not suitable for DLS analysis, whereas a low PDI value (<0.05) suggests a highly monodisperse standard.

5.1.3. Mechanical Strength

Many delivery systems are finally dehydrated to produce a powder product to facilitate their applications, particularly for the fortification of food and nutraceutical products. For this purpose, these encapsulation systems should exhibit reasonably good mechanical strength to tolerate the shear during processing. Although the rheological behavior of the encapsulation system before dehydration or rehydrated dry encapsulates can be used by analyzing their resistance to shear, direct methods can provide more accurate and reliable results.

The classical method developed by Ohtsubo *et al.* used two compressed glass plates with a thin layer of dehydrated encapsulation system in between. The mechanical strength of the powder was

determined by the break of the particles when a certain force was applied by placing a given weight on the top plate.[72] Moreover, Yuliani *et al.* investigated the encapsulate extrudate using a three-point bend method and recorded the force required to break the sample. However, in these studies, the analysis was performed using multiple particles and the large ones broke before the small ones. Hence the mechanical strength data collected might not apply to all the particles.[73]

For this reason, the mechanical strength of an individual particle can be studied using AFM by compressing the sample on the grid with a probe that is connected with the data acquisition system. In Xia *et al.*'s study, the ω-3 concentrate made from enzymatic hydrolysis of ω-3 oils was encapsulated and compared with the entrapped ω-3 oils, and the microcapsule powder exhibited unexpected improved oxidative stability. Based on the measurement of the mechanical strength of a single particle, they found that the increased elasticity and more compact surface structure effectively retarded the permeation of oxygen during storage.[71] However, owing to the limited scope of AFM, it is difficult to assess an individual particle at the microscale. For this reason, Zhang developed the micromanipulation technique,[74] the principle of which is similar to that of AFM but at a larger scale.

5.1.4. Techno-functional Characteristics

For dehydrated delivery systems, techno-functional characteristics such as flowability and reconstitution properties are crucial for their application. Generally, powder flowability is a major challenge for industry because it is important to control the handling and transport of the powder in pipes and hoppers. The flowability of delivery systems is dependent on their physicochemical properties such as hydrophobic content on the surface, moisture content, particle size, heterogeneity of the particle size, surface roughness, *etc.*[75] Moreover, environmental stresses also affect the flowability of dehydrated delivery systems. For example, poor flowability is usually

observed at elevated temperature and relative humidity, which favors the glass transition phenomenon, finally leading a rubbery state of the wall material, which makes the powder sticky. Various methods have been developed to evaluate powder flowability.[75,76]

If the dehydrated delivery system needs to be reconstituted for some applications, it is worth investigating its reconstitution properties, which usually depend on some of its physicochemical properties such as chemical composition and particle size and distribution. Generally, powder reconstitution can be divided into four steps: wetting, sinking, dispersion and solubilization. The wetting step is the displacement of the solid/air interface by a solid/ water interface when the micro-and nanocapsule powder contact water. Wettability can be used to evaluate the ability of the powder to immerse without stirring.[77] The wettability of delivery systems is usually sensitive to several powder physicochemical parameters, particularly particle size: the smaller the particles, the longer is their wetting time, hence the poorer is the powder wettability. The surface composition also affects the wettability: an increase in the content of the hydrophobic component on the surface usually compromises the wettability.[78] The subsequent sinking step is the penetration of water into the powder, contributing to its swelling, and the dispersion step is the dissociation of the agglomerated particles into individual particles. In the dispersion step, the water-soluble components start to be solubilized. Finally, the solubilization step is the ability of powder to dissolve in water and lose its granular structure completely.[79]

*5.1.5. Glass Transition Temperature (*T*g) of Wall Materials*

The glass transition temperature (T_g) is defined as the midpoint temperature where a material changes its state from a ‘liquid rubbery’ to a ‘solid glassy’ state during heating/cooling. Generally, when the material is in its glassy state (storage temperature below T_g), motion of the molecules is minimized. Therefore, it is more stable. Once the material is in its rubbery state (storage

temperature above T_g), its molecular diffusion is faster, hence physicochemical reactions occur more readily. Thus, the information on the T_g of the wall material is helpful in determining the storage conditions and the stability during storage.

Differential scanning calorimetry (DSC) is a thermoanalytical technique that has been widely used to determine the T_g of wall materials. Briefly, DSC measures the heat flow difference between a test sample (sample in a sealed pan) and a reference (usually a sealed pan without sample), where the difference in the heat required to increase the temperature of the test sample and reference is recorded. It should be noted that during the heating/cooling, both sample and reference are controlled at nearly the same temperature and protective gas is usually used to avoid the reaction of the sample throughout the test. In Wang *et al.*'s study, anchovy oil was encapsulated in a whey protein isolate–agar gum–gellan gum system and DSC was used to confirm that the wall materials were in their glassy state during storage at room temperature. Moreover, the unchanged T_g of individual components of the delivery system confirmed that no chemical reaction occurred during the encapsulation, indicating the compatibility of the developed matrix (Figure 1.1.3).[80] In Gorska *et al.*'s study, retinyl palmitate was encapsulated in a β-lactoglobulin– carbohydrate system and it was suggested that the replacement of lactose with trehalose as the carbohydrate component significantly increased the T_g of the wall material, thus improving the stability of encapsulated retinyl palmitate.[81]

5.1.6. Degree of Crystallization

Generally, the crystalline or amorphous structure of the wall materials affects the flowability, dispersibility and permeability (*i.e.* absorbing moisture to form 'cake'). Thus, the degree of crystallization of the wall material can be used to design the encapsulate so as to meet the requirements of the application. From the storage perspective, an encapsulate with a crystalline

structure is preferred because the molecules are packed, which minimizes their interaction with external environmental factors. However, most of the biomolecules are in the partially crystalline state. Both X-ray diffraction (XRD) and nuclear magnetic resonance (NMR) spectroscopy have been used to determine the degree of crystallization of the material, with the former being more commonly used. In an XRD test, X-rays are used to analyze the orientation of molecules in a lattice structure. Based on the diffusion of X-rays through a crystal, the degree of crystallization can be determined. For example, Jiang *et al.* investigated the XRD pattern characteristics of encapsulated lemon essential oil in a grass carp collagen–chitosan system for food packaging material purposes. Based on the XRD analysis, they confirmed that the incorporation of lemon essential oil did not change the degree of crystallization of the grass carp collagen–chitosan system.[82] However, Valenzuela *et al.* reported a decreased degree of crystallization of quinoa protein–chitosan-based film after the introduction of sunflower oil.[83]

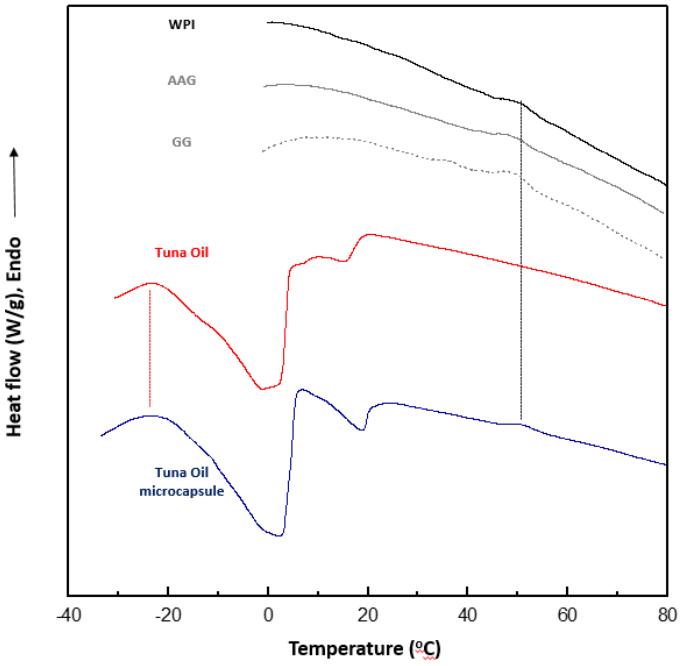

Figure 1.1.3. Thermal behavior of a developed delivery system and individual components. Adapted from ref. 80 with permission from Elsevier, Copyright 2019.

5.2. Chemical Characteristics

5.2.1. Total Active Content of Bioactive Compounds

The total active content of bioactive compounds, also termed the total active loading or payload, is the percentage of bioactive compound per gram of the encapsulation system. A higher active content of bioactive compounds suggests that a smaller quantity of wall materials is required for the delivery of the compounds at a specific dose. Hence both the fabrication cost of the encapsulate and its impact on applications are minimized. Generally, the active content of a bioactive compound in an encapsulate is calculated using the following equation:

$$A_c(\%) = {}^{M_A}/_{M_E} \times 100 \qquad (1.5)$$

where A_c is the active content of the bioactive compound and M_A and M_E are the weight of the bioactive compound and total encapsulates, respectively.

Generally, the entrapped bioactive compound in the encapsulate needs to be extracted to determine its quantity and the solvent needs to be selected based on the nature of the compounds and wall materials and the characteristics of the encapsulation system. After the bioactive compound has been extracted, its amount can be quantified using a wide range of analytical methods such as gravimetric, chromatographic and spectroscopic techniques, depending on the nature of the bioactive compound.

In Augustin *et al.*'s study, tuna oil was encapsulated in sodium caseinate–dextrose–maltodextrin Maillard reaction products and, in order to determine the total oil loading, the tuna oil was extracted by mixing the dehydrated microcapsule and petroleum ether in a ratio of 1 : 5 w/v at 60 °C with agitation for 15 min.[84] The amount of extracted tuna oil was determined gravimetrically based on the evaporation of the organic solvent. Similarly, Jafari's group reported the extraction of d-

limonene and fish oil using hexane from the delivery system with whey protein–pectin[85] and gelatin–gum Arabic[86] complexes, respectively, as the wall material, followed by gravimetric quantification of the extracted bioactive compounds.

However, for a delivery system with a compact structure, decomposition of the wall material may be required to release the oil into the organic solvent. In Xia *et al.*'s study, tuna oil was encapsulated in gelatin–sodium hexametaphosphate complex coacervates with compact structure. To extract the encapsulated oil using hexane, 1 M HCl was used to destabilize the wall material, followed by evaporation of organic solvent and gravimetric quantification of the tuna oil.[71] Similarly, Jafari's group used 1.2 M HCl to decompose the electrosprayed nanocapsule powder to release entrapped olive leaf phenolic compounds for the determination of total active content using HPLC.[87]

5.2.2. Surface Free Bioactive Compound

A surface free bioactive compound is a non-encapsulated compound that adsorbs on the surface of the final encapsulates. During storage and application, the surface free bioactive compound is readily degraded, which adversely affects the quality of the encapsulation system. The content of the surface free bioactive compound is usually calculated using the following equation:

$$A_s(\%) = {}^{M_S}/_{M_E} \times 100 \qquad (1.6)$$

where A_s is the content of the surface free bioactive compound and M_S and M_E are the weight of bioactive compound extracted from the surface and weight of total encapsulates, respectively.

Similarly to the determination of the total active content of bioactive compounds, the free bioactive compound at the surface of the encapsulation system needs to be extracted, and washing with a solvent is the most widely used strategy. Again, this solvent needs to be carefully selected to suit the active compounds, wall materials and characteristics of the encapsulation system. However, it

should be noted that the content of surface free bioactive compound is usually overestimated, because the entrapped bioactive compound close to the surface can also be extracted.

Based on total bioactive compounds and surface free bioactive compound, the encapsulation efficiency can be calculated using the following equation:

$$EE(\%) = \frac{(A_c - A_s)}{A_c} \times 100 \qquad (1.7)$$

where EE is the encapsulation efficiency and A_c and A_s are the content of total bioactive compounds and content of surface free bioactive compound, respectively. Generally, an ideal encapsulation system should exhibit a high total active content but a low content of surface free bioactive compound.

5.2.3. Stability

Mostly, bioactive compounds are encapsulated to improve their chemical stability and maintain their functionality against external environmental stresses such as oxygen and elevated temperature since the oxidative degradation of food, nutraceutical and pharmaceutical bioactive compounds is quite common. Briefly, during the storage and/or application of the encapsulation system, the encapsulated bioactive compound can be oxidized by free radicals, which are usually formed in a wide range of conditions such as enzyme–substrate reactions, elevated temperature during storage and/or application and environmental stresses such as light, transition metals, oxidants and other food components. The free radicals formed near the encapsulation system tend to permeate across the wall material and subsequently oxidize the encapsulated compounds. It is worth noting that in an encapsulation system where bioactive compounds are emulsified to micro- or even nanoscale particles, this oxidation reaction is exacerbated owing to the increased interfacial surface area compared with the bulk material. Although antioxidants and chelating agents can be

used to retard the formation and migration of free radicals to the encapsulation system, the chemical stability of the encapsulated bioactive needs to be monitored during storage.

The chemical stability of the entrapped core in an encapsulation system has been conventionally studied by measuring the quantity of oxidation by-products formed and/or the remaining core material after the extraction of the core material from encapsulation system during storage. Nowadays, this is still the basis of the shelf-life test in the food, nutraceutical and pharmaceutical industries. For example, in order to evaluate the chemical stability of ω-3 oils entrapped in microcapsule powder, the sample is stored under certain storage conditions. At a scheduled time point, the oil is usually extracted, followed by the application of standard oil characterization methods such as acid value, peroxide value, *p*-anisidine value and even fatty acid quantification by gas chromatography.[88,89] Although storage at elevated temperature is often used as an 'accelerated storage condition', this destructive method is still rather time consuming.[90] Depending on the oxidative susceptibility of the core material and protective effectiveness of the wall material, this oxidation test can take up to several weeks or even months.[91]

As oxygen is the critical component to induce oxidative degradation of encapsulated bioactive compounds, an effective indirect method for evaluating the oxidative stability of the dehydrated microencapsulation system is to monitor the quantity of oxygen in a sealed vessel at elevated temperature (*e.g.* Oxipres™). However, there is still concern that this 'accelerated oxidation' cannot model the real oxidative degradation of the core material. Hence it is usually used in combination with the conventional method.

Tikekar and Nitin developed a non-invasive and real-time spectroscopic method to monitor the interactions of hydroxyl radicals with the encapsulated core. Briefly, a hydroxyl radical-sensitive

dye, carboxy-H2DFFDA [5-(and 6-) carboxy-2′,7′-difluorodihydrofluorescein diacetate], was dispersed in the lipid phase and this lipid phase was further stabilized in an encapsulation system. During storage, the dye was converted from non-fluorescent to fluorescent form when it interacted with the hydroxyl radical.[92] Therefore, the increase in the fluorescence intensity of the encapsulation system can be used as an effective indicator to illustrate the migration of hydroxyl radicals across the wall materials.

5.2.4. Release Property/Bioavailability

To study the release property of entrapped bioactive compounds, an *in vitro* test is often used where a simulated gastrointestinal environment is employed and the release of the encapsulated core material from the encapsulation system is monitored. Generally, prolonged release of a bioactive compound is considered to be better than burst release and the protein-based encapsulation system can provide this property to the entrapped core material. For example, Silva *et al.* used a casein–whey protein mixture to develop a water-in-oil-in-water emulsion for the entrapment of grape seed oil. An *in vitro* digestion test suggested that the multiple emulsion produced was more gastric stable than the simple emulsion and the encapsulated grape seed oil was successfully released in the simulated intestinal environment.[93] Guedez Silva *et al.* encapsulated β-carotene in hydrogel filled with gelatin–starch–alginate to improve its oxidative stability during digestion.[94] An *in vitro* digestibility test suggested that the encapsulation system exhibited resistance to simulated oral and gastric fluids. Moreover, based on the introduction of native starch to this encapsulation system, β-carotene was well protected from oxygen, acidity, pro-oxidation and free radicals in the digesta. Based on the crosslinking of the protein wall material into a more stable form, the integrity of the bioactive particles could be further improved after their ingestion for controlled-release applications.[95]

Bioavailability refers to the portion of the bioactive compound that is absorbed in the body and available for the target tissue to perform its normal physiological applications.[96] Generally, an animal and/or human trial is required to confirm the bioavailability of the encapsulated bioactive compounds. Sun *et al.* used zein–caseinate nanoparticles to encapsulate dihydromyricetin with a particle size of ~206 nm. After a faster diffusion rate was observed in the encapsulated dihydromyricetin in the simulated gastric and intestinal fluids than with the non-encapsulated form, an *in vivo* trial was performed and the results suggested that the entrapped bioactive compound exhibited 1.95 times higher bioavailability in rats.[97] Similarly, in Ghasemi-Fard *et al.*'s study, infant formula was fortified with encapsulated docosahexaenoic acid (DHA) and the bioavailability of this encapsulated fatty acid was investigated, with liquid DHA oil as the control, in 60 healthy toddler subjects. Based on the analysis of the fatty acid level in blood and fecal samples, the encapsulated DHA exhibited significantly improved bioavailability.[98]

5.3. Sensory Profile

In the case where the developed delivery system is used as a functional ingredient for food application, its impact on the sensory profile of the fortified food products needs to be evaluated. There are three major types of sensory profile analysis method: discriminatory, affective and descriptive. The discriminatory test is used to determine if the sensory profile of the test sample is the same as that of the control sample, and common forms include the triangle test, duo–trio test, tetrad test and two-and three-alternative force choice (AFC) test. The affective test is used to determine the acceptance of the planned product by the target consumers. This test can be further categorized into qualitative (usually one-to- one interview) and quantitative (acceptance) tests. The descriptive method requires the participation of trained panelists to assess the complete sensory profile of a product both qualitatively and quantitatively. Generally, the odor and unpleasant flavor

of bioactive compounds can be significantly masked by the encapsulation system to promote their application. For example, green coffee oil was encapsulated in a whey protein-based delivery system by Rojas *et al.*[99] The freeze-dried powder was further used to fortify cookies. Based on the discriminatory test, no difference from cookies made with walnut oil was detected by the panelists.

Moreover, the texture of fortified food products might be affected by the encapsulation system, mainly depending on their particle size. In some studies, a general conclusion regarding the size of the encapsulation system for its detection and acceptance of the fortified food is reported. For example, Barrow *et al.* suggested that a microcapsule powder size >100 μm can be detected by the palate. However, this impact is rather delivery and food system specific.[100] Hinton reported that the size of detected microencapsulated flavor in fortified confectionery was 25 μm whereas Minifie indicated that those of detected particles in milk and dark chocolate were 65 and 35 μm, respectively.[101,102] Muthukumarasamy and Holley used extrusion and emulsion methods to encapsulate probiotic *Lactobacillus reuteri* in particles with different sizes. The extruded particles exhibited a microscale size whereas the emulsion-stabilized particles had a spherical morphology in the millimeter rage. However, neither of these two encapsulation systems affected the texture of the fortified food system.[103]

5.4. Nanotoxicity and Nanoecotoxicity Challenge

Food proteins are generally recognized as safe (GRAS) molecules, and so are protein-based encapsulation systems. However, when a protein-based encapsulation system is of nanoscale size, there are still concerns particularly regarding toxicity and ecotoxicity owing to the extremely small size attributes (size, structure, high surface-to-volume ratio and composition, *etc.*).[104,105] Briefly, nanoparticles can penetrate cellular membranes, biological barriers and tissues more efficiently than materials with a larger size at the microscale.[106] Hence some particularly designed

nanomaterials may damage cells, depending on their size, structure and composition.[107] Further, ecotoxicity may occur when nanomaterials are dispersed into the environment. For example, in the aquatic ecosystem, nanomaterials can accumulate in the fluvial sediments or remain suspended in the aqueous environment. A wide range of physical, chemical and biological transformations of aquatic organisms, including aggregation, oxidation, dissolution, bioreduction, biodegradation, photo-oxidation, surface degradation, interactions with macromolecules and deposition, have been reported following exposure to nanomaterials.[108] Hence the understanding of their impact on human health and the environment is important for the development of nanoencapsulation systems. However, there is still a lack of research in this field and most countries still do not have specific regulations aimed at assessing the risks associated with nanoencapsulated compounds.[109]

6. CONCLUSION

The structural, functional, physicochemical and biological properties of proteins have resulted in the emergence of protein-based delivery systems for nutraceutical bioactive compounds. This chapter describes various protein sources and fabrication and characterization techniques that have been employed in protein-based delivery with demonstrated potential application in the commercial production of encapsulated bioactive compounds. Advantages and disadvantages of various protein sources, effects of size in nano-and microencapsulation and various techniques for evaluating the quality of the delivery systems have been highlighted. Further research is necessary to address the limitations of large-scale economic production and also better characterization techniques are required in order to pinpoint accurately the location of bioactive compounds within a complex. The behavior of these delivery systems is usually studied under simulated salivary, gastric and intestinal conditions, which does not completely reflect *in vivo* biological behavior. This has been challenging owing to its complexity and ethical concerns. Also, the introduction of

toxic reagents for solubility purposes or to induce precipitation, aggregation, assembly or interaction is usually a challenge that needs to be addressed. Further, there is need for *in silico* techniques that can accurately predict bioactive compound–protein binding, encapsulation and release properties while considering the effects of environmental conditions such as pH, temperature, ionic strength and enzyme activity. This would reduce cumbersome laboratory screening for better proteins for encapsulating a given bioactive compound.

Reference

(1) Wan, Z. L.; Guo, J.; Yang, X. Q. Plant Protein-Based Delivery Systems for Bioactive Ingredients in Foods. *Food and Function*. **2015**, *6*(9), 2876-2889. https://doi.org/10.1039/c5fo00050e.

(2) Fathi, M.; Donsi, F.; McClements, D. J. Protein-Based Delivery Systems for the Nanoencapsulation of Food Ingredients. *Comprehensive Reviews in Food Science and Food Safety*. **2018**, *17*(4), 920-936. https://doi.org/10.1111/1541-4337.12360.

(3) Mcclements, D. J. Nanoscale Nutrient Delivery Systems for Food Applications: Improving Bioactive Dispersibility, Stability, and Bioavailability. *Journal of Food Science.* **2015**, *80* (7), N1602-N1611. https://doi.org/10.1111/1750-3841.12919.

(4) McClements, D. J.; Li, F.; Xiao, H. The Nutraceutical Bioavailability Classification Scheme: Classifying Nutraceuticals According to Factors Limiting Their Oral Bioavailability. *Annual Review of Food Science and Technology*. **2015**, *6*, 299-327. https://doi.org/10.1146/annurev-food-032814-014043.

(5) Okagu, O. D.; Verma, O.; McClements, D. J.; Udenigwe, C. C. Utilization of Insect Proteins to Formulate Nutraceutical Delivery Systems: Encapsulation and Release of Curcumin Using Mealworm Protein-Chitosan Nano-Complexes. *International Journal of Biological Macromolecules.* **2020**, *151*, 333-343. https://doi.org/10.1016/j.ijbiomac.2020.02.198.

(6) Fathi, M.; Mozafari, M. R.; Mohebbi, M. Nanoencapsulation of Food Ingredients Using Lipid Based Delivery Systems. *Trends in Food Science and Technology*. **2012**, *23*(1), 13-27. https://doi.org/10.1016/j.tifs.2011.08.003.

(7) Wang, F.; Yang, Y.; Ju, X.; Udenigwe, C. C.; He, R. Polyelectrolyte Complex Nanoparticles from Chitosan and Acylated Rapeseed Cruciferin Protein for Curcumin Delivery. *Journal of Agricultural and Food Chemistry.* **2018**, *66*(11), 2685-2693. https://doi.org/10.1021/acs.jafc.7b05083.

(8) Raikos, V.; Ranawana, V. Designing Emulsion Droplets of Foods and Beverages to Enhance Delivery of Lipophilic Bioactive Components – a Review of Recent Advances. *International Journal of Food Science and Technology*. **2017**, *52*(1), 68-80. https://doi.org/10.1111/ijfs.13272.

(9) Luo, Y. Perspectives on Important Considerations in Designing Nanoparticles for Oral Delivery Applications in Food. *Journal of Agriculture and Food Research.* **2020**, *2*, 100031. https://doi.org/10.1016/j.jafr.2020.100031.

(10) Fathi, M.; Martín, Á.; McClements, D. J. Nanoencapsulation of Food Ingredients Using Carbohydrate Based Delivery Systems. *Trends in Food Science and Technology*. **2014**, *39*(1), 18-39. https://doi.org/10.1016/j.tifs.2014.06.007.

(11) McClements, D. J.; Gumus, C. E. Natural Emulsifiers — Biosurfactants, Phospholipids, Biopolymers, and Colloidal Particles: Molecular and Physicochemical Basis of Functional Performance. *Advances in Colloid and Interface Science*. **2016**, *234*, 3-26. https://doi.org/10.1016/j.cis.2016.03.002.

(12) Mezzenga, R.; Fischer, P. The Self-Assembly, Aggregation and Phase Transitions of Food Protein Systems in One, Two and Three Dimensions. *Reports on Progress in Physics.* **2013**,*76*, 046601. https://doi.org/10.1088/0034-4885/76/4/046601.

(13) Samaranayaka, A. G. P.; Li-Chan, E. C. Y. Food-Derived Peptidic Antioxidants: A Review of Their Production, Assessment, and Potential Applications. *Journal of Functional Foods*. **2011**, *3*(4), 229-254. https://doi.org/10.1016/j.jff.2011.05.006.

(14) Uranga, J.; Etxabide, A.; Cabezudo, S.; de la Caba, K.; Guerrero, P. Valorization of Marine-Derived Biowaste to Develop Chitin/Fish Gelatin Products as Bioactive Carriers and Moisture Scavengers. *Science of the Total Environment.* **2020**, *706*, 135747. https://doi.org/10.1016/j.scitotenv.2019.135747.

(15) Du, Z.; Liu, J.; Zhang, H.; Chen, Y.; Wu, X.; Zhang, Y.; Li, X.; Zhang, T.; Xiao, H.; Liu, B. L-Arginine/l-Lysine Functionalized Chitosan-Casein Core-Shell and PH-Responsive Nanoparticles: Fabrication, Characterization and Bioavailability Enhancement of Hydrophobic and Hydrophilic Bioactive Compounds. *Food & Function.* **2020**, *11*, 4638-4647. https://doi.org/10.1039/d0fo00005a.

(16) Simões, L. S.; Abrunhosa, L.; Vicente, A. A.; Ramos, O. L. Suitability of β-Lactoglobulin Micro- and Nanostructures for Loading and Release of Bioactive Compounds. *Food Hydrocolloids.* **2020**, *101*, 105492. https://doi.org/10.1016/j.foodhyd.2019.105492.

(17) Mohammadian, M.; Moghadam, M.; Salami, M.; Emam-Djomeh, Z.; Alavi, F.; Momen, S.; Moosavi-Movahedi, A. A. Whey Protein Aggregates Formed by Non-Toxic Chemical Cross-Linking as Novel Carriers for Curcumin Delivery: Fabrication and Characterization. *Journal of Drug Delivery Science and Technology.* **2020**, *56*, 101531. https://doi.org/10.1016/j.jddst.2020.101531.

(18) Taha, S.; El-Sherbiny, I.; Enomoto, T.; Salem, A.; Nagai, E.; Askar, A.; Abady, G.; Abdel-Hamid, M. Improving the Functional Activities of Curcumin Using Milk Proteins as Nanocarriers. *Foods.* **2020**, *9*(8), 986. https://doi.org/10.3390/foods9080986.

(19) de Vries, A.; Nikiforidis, C. v.; Scholten, E. Natural Amphiphilic Proteins as Tri-Block Janus Particles: Self-Sorting into Thermo-Responsive Gels. *EPL.* **2014**, *107*, 58003. https://doi.org/10.1209/0295-5075/107/58003.

(20) Teng, M. J.; Wei, Y. S.; Hu, T. G.; Zhang, Y.; Feng, K.; Zong, M. H.; Wu, H. Citric Acid Cross-Linked Zein Microcapsule as an Efficient Intestine-Specific Oral Delivery System for Lipophilic Bioactive Compound. *Journal of Food Engineering.* **2020**, *281*, 109993. https://doi.org/10.1016/j.jfoodeng.2020.109993.

(21) Xue, J.; Zhang, Y.; Huang, G.; Liu, J.; Slavin, M.; Yu, L. (Lucy). Zein-Caseinate Composite Nanoparticles for Bioactive Delivery Using Curcumin as a Probe Compound. *Food Hydrocolloids.* **2018**, *83*, 25-35. https://doi.org/10.1016/j.foodhyd.2018.04.037.

(22) Patel, A.; Hu, Y.; Tiwari, J. K.; Velikov, K. P. Synthesis and Characterisation of Zein-Curcumin Colloidal Particles. *Soft Matter.* **2010**, *6*, 6192-6199. https://doi.org/10.1039/c0sm00800a.

(23) Muñoz-González, I.; Ruiz-Capillas, C.; Salvador, M.; Herrero, A. M. Emulsion Gels as Delivery Systems for Phenolic Compounds: Nutritional, Technological and Structural Properties. *Food Chemistry.* **2021**, *339*, 128049. https://doi.org/10.1016/j.foodchem.2020.128049.

(24) Yan, W.; Zhang, B.; Yadav, M. P.; Feng, L.; Yan, J.; Jia, X.; Yin, L. Corn Fiber Gum-Soybean Protein Isolate Double Network Hydrogel as Oral Delivery Vehicles for Thermosensitive Bioactive Compounds. *Food Hydrocolloids.* **2020**, *107*, 105865. https://doi.org/10.1016/j.foodhyd.2020.105865.

(25) Cheng, C.; Gao, Y.; Wu, Z.; Miao, J.; Gao, H.; Ma, L.; Zou, L.; Peng, S.; Liu, C.; Liu, W. Gliadin Nanoparticles Pickering Emulgels for β-Carotene Delivery: Effect of Particle Concentration on the Stability and Bioaccessibility. *Molecules.* **2020**, *25*(18), 4188. https://doi.org/10.3390/molecules25184188.

(26) Yang, S.; Liu, L.; Chen, H.; Wei, Y.; Dai, L.; Liu, J.; Yuan, F.; Mao, L.; Li, Z.; Chen, F.; Gao, Y. Impact of Different Crosslinking Agents on Functional Properties of Curcumin-Loaded Gliadin-Chitosan Composite Nanoparticles. *Food Hydrocolloids.* **2021**, *112*, 106258. https://doi.org/10.1016/j.foodhyd.2020.106258.

(27) Wang, R.; Tian, Z.; Chen, L. A Novel Process for Microencapsulation of Fish Oil with Barley Protein. *Food Research International.* **2011**, *44*(9), 2735-2741. https://doi.org/10.1016/j.foodres.2011.06.013.

(28) Chen, L.; Bai, G.; Yang, S.; Yang, R.; Zhao, G.; Xu, C.; Leung, W. Encapsulation of Curcumin in Recombinant Human H-Chain Ferritin Increases Its Water-Solubility and

Stability. *Food Research International.* **2014**, *62*, 1147-1153. https://doi.org/10.1016/j.foodres.2014.05.054.

(29) Suganya, V.; Anuradha, V. Microencapsulation and Nanoencapsulation: A Review. *International Journal of Pharmaceutical and Clinical Research.* **2017**, *9*(3), 233-239. https://doi.org/10.25258/ijpcr.v9i3.8324.

(30) de Souza Simões, L.; Madalena, D. A.; Pinheiro, A. C.; Teixeira, J. A.; Vicente, A. A.; Ramos, Ó. L. Micro- and Nano Bio-Based Delivery Systems for Food Applications: In Vitro Behavior. *Advances in Colloid and Interface Science*. **2017**, *243*, 23-45. https://doi.org/10.1016/j.cis.2017.02.010.

(31) Mohammadian, M.; Waly, M. I.; Moghadam, M.; Emam-Djomeh, Z.; Salami, M.; Moosavi-Movahedi, A. A. Nanostructured Food Proteins as Efficient Systems for the Encapsulation of Bioactive Compounds. *Food Science and Human Wellness*. **2020**, *9*(3), 199-213. https://doi.org/10.1016/j.fshw.2020.04.009.

(32) Shin, G. H.; Kim, J. T.; Park, H. J. Recent Developments in Nanoformulations of Lipophilic Functional Foods. *Trends in Food Science and Technology* **2015**, 46(1), 144-157. https://doi.org/10.1016/j.tifs.2015.07.005.

(33) Xu, H.; Shen, L.; Xu, L.; Yang, Y. Controlled Delivery of Hollow Corn Protein Nanoparticles via Non-Toxic Crosslinking: In Vivo and Drug Loading Study. *Biomedical Microdevices.* **2015,** *17*, 8. https://doi.org/10.1007/s10544-014-9926-5.

(34) Jahanshahi, M.; Babaei, Z. Protein Nanoparticle: A Unique System as Drug Delivery Vehicles. *African Journal of Biotechnology*. **2008**, *7*, 4926-4934. https://doi.org/10.5897/AJB08.081.

(35) Tarhini, M.; Greige-Gerges, H.; Elaissari, A. Protein-Based Nanoparticles: From Preparation to Encapsulation of Active Molecules. *International Journal of Pharmaceutics*. **2017**, *522*(1-2), 172-197. https://doi.org/10.1016/j.ijpharm.2017.01.067.

(36) Ayoub, A.; Sood, M.; Singh, J.; Bandral, J. D.; Gupta, N.; Bhat, A. Microencapsulation and Its Applications in Food Technology. *Journal of Pharmacology and Phytochemistry*. **2019**, *8*(3), 32-37.

(37) Mahalakshmi, L.; Leena, M. M.; Moses, J. A.; Anandharamakrishnan, C. Micro- and Nano-Encapsulation of β-Carotene in Zein Protein: Size-Dependent Release and Absorption Behavior. *Food & Function.* **2020**, *11*, 1647-1660. https://doi.org/10.1039/c9fo02088h.

(38) Chen, L.; Remondetto, G. E.; Subirade, M. Food Protein-Based Materials as Nutraceutical Delivery Systems. *Trends in Food Science and Technology*. **2006**, *17*(5), 272-283. https://doi.org/10.1016/j.tifs.2005.12.011.

(39) Monteiro, A. A.; Monteiro, M. R.; Pereira, R. N.; Diniz, R.; Costa, A. R.; Malcata, F. X.; Teixeira, J. A.; Teixeira, Á. V.; Oliveira, E. B.; Coimbra, J. S.; Vicente, A. A.; Ramos, Ó.

L. Design of Bio-Based Supramolecular Structures through Self-Assembly of α-Lactalbumin and Lysozyme. *Food Hydrocolloids.* **2016**, *58*, 60-74. https://doi.org/10.1016/j.foodhyd.2016.02.009.

(40) Langer, K.; Balthasar, S.; Vogel, V.; Dinauer, N.; von Briesen, H.; Schubert, D. Optimization of the Preparation Process for Human Serum Albumin (HSA) Nanoparticles. *International Journal of Pharmaceutics.* **2003**, *257*(1-2), 169-180. https://doi.org/10.1016/S0378-5173(03)00134-0.

(41) Wang, G.; Siggers, K.; Zhang, S.; Jiang, H.; Xu, Z.; Zernicke, R. F.; Matyas, J.; Uludağ, H. Preparation of BMP-2 Containing Bovine Serum Albumin (BSA) Nanoparticles Stabilized by Polymer Coating. *Pharmaceutical Research*. **2008**, 25, 2896-2909. https://doi.org/10.1007/s11095-008-9692-2.

(42) Irache, J. M.; Bergougnoux, L.; Ezpeleta, I.; Gueguen, J.; Orecchioni, A. M. Optimization and in Vitro Stability of Legumin Nanoparticles Obtained by a Coacervation Method. *International Journal of Pharmaceutics.* **1995**, *126*(1-2), 103-109. https://doi.org/10.1016/0378-5173(95)04103-6.

(43) Ko, S.; Gunasekaran, S. Preparation of Sub-100-Nm β-Lactoglobulin (BLG) Nanoparticles. *Journal of Microencapsulation.* **2006**, *23*(8), 887-898. https://doi.org/10.1080/02652040601035143.

(44) Wang, J.; Chen, S. H.; Xu, Z. C. Synthesis and Properties Research on the Nanocapsulated Capsaicin by Simple Coacervation Method. *Journal of Dispersion Science and Technology.* **2008**, *29*(5), 687-695. https://doi.org/10.1080/01932690701756651.

(45) Thies, C. Microcapsules. In *Encyclopedia of Food Sciences and Nutrition*. Ed. by Caballero, B. 2nd ed. Academic Press, Oxford, United Kingdom. **2003**, 3892-3903. https://doi.org/10.1016/b0-12-227055-x/01369-9.

(46) Gulfam, M.; Kim, J. E.; Lee, J. M.; Ku, B.; Chung, B. H.; Chung, B. G. Anticancer Drug-Loaded Gliadin Nanoparticles Induce Apoptosis in Breast Cancer Cells. *Langmuir.* **2012**, *28*(21), 8216-8223. https://doi.org/10.1021/la300691n.

(47) Wu, Y.; Mackay, J. A.; Mcdaniel, J. R.; Chilkoti, A.; Clark, R. L. Fabrication of Elastin-like Polypeptide Nanoparticles for Drug Delivery by Electrospraying. *Biomacromolecules.* **2009**, *10*(1), 19-24. https://doi.org/10.1021/bm801033f.

(48) Jafari, S. M.; McClements, D. J. Nanotechnology Approaches for Increasing Nutrient Bioavailability. In *Advances in Food and Nutrition Research*. Ed. by Toldrá, F. Academic Press, Oxford, United Kingdom. **2017**, *81*, 1-30. https://doi.org/10.1016/bs.afnr.2016.12.008.

(49) Matalanis, A.; Jones, O. G.; McClements, D. J. Structured Biopolymer-Based Delivery Systems for Encapsulation, Protection, and Release of Lipophilic Compounds. *Food Hydrocolloids.* **2011**, *25*(8), 1865-1880. https://doi.org/10.1016/j.foodhyd.2011.04.014.

(50) Teo, A.; Lam, Y.; Lee, S. J.; Goh, K. K. T. Spray Drying of Whey Protein Stabilized Nanoemulsions Containing Different Wall Materials – Maltodextrin or Trehalose. *Lwt-Food Science and Technology.* **2021**, *136* (P2), 110344. https://doi.org/10.1016/j.lwt.2020.110344.

(51) McClements, D. J. Nanoparticle- and Microparticle-Based Delivery Systems: Encapsulation, Protection and Release of Active Compounds; (1st ed.). CRC Press, Boca Raton, Florida, United States of America. **2014,** 1-572. https://doi.org/10.1201/b17280.

(52) Santana, R. C.; Perrechil, F. A.; Cunha, R. L. High- and Low-Energy Emulsifications for Food Applications: A Focus on Process Parameters. *Food Engineering Reviews* **2013**, *5*, 107-122. https://doi.org/10.1007/s12393-013-9065-4.

(53) Matalanis, A.; McClements, D. J. Hydrogel Microspheres for Encapsulation of Lipophilic Components: Optimization of Fabrication & Performance. *Food Hydrocolloids.* **2013**, *31*(1), 15-25. https://doi.org/10.1016/j.foodhyd.2012.09.012.

(54) Cheaburu-Yilmaz, C. N.; Karasulu, H. Y.; Yilmaz, O. Nanoscaled Dispersed Systems Used in Drug-Delivery Applications. In *Polymeric Nanomaterials in Nanotherapeutics*. Ed. by Vasile, C. Elsevier, Amsterdam, Netherlands. **2019**, 437-468. https://doi.org/10.1016/B978-0-12-813932-5.00013-3.

(55) Kandori, K. Applications of Microporous Glass Membranes. In *Food Processing*. Ed. by Gaonkar, A. G. Elsevier Science, Amsterdam, Netherlands, **1995**, 113-142. https://doi.org/10.1016/b978-044481500-2/50009-8.

(56) Whelehan, M.; Marison, I. W. Microencapsulation Using Vibrating Technology. *Journal of Microencapsulation*. **2011**, 28(8), 669-688. https://doi.org/10.3109/02652048.2011.586068.

(57) Silva, M. P.; Tulini, F. L.; Martins, E.; Penning, M.; Fávaro-Trindade, C. S.; Poncelet, D. Comparison of Extrusion and Co-Extrusion Encapsulation Techniques to Protect Lactobacillus Acidophilus LA3 in Simulated Gastrointestinal Fluids. *LWT - Food Science and Technology* **2018**, *89*, 392-399. https://doi.org/10.1016/j.lwt.2017.11.008.

(58) Sadeghi, S.; Madadlou, A.; Yarmand, M. Microemulsification-Cold Gelation of Whey Proteins for Nanoencapsulation of Date Palm Pit Extract. *Food Hydrocolloids.* **2014**, *35*, 590-596. https://doi.org/10.1016/j.foodhyd.2013.07.021.

(59) Zhang, J.; Liang, L.; Tian, Z.; Chen, L.; Subirade, M. Preparation and in Vitro Evaluation of Calcium-Induced Soy Protein Isolate Nanoparticles and Their Formation Mechanism Study. *Food Chemistry.* **2012**, *133*(2), 390-399. https://doi.org/10.1016/j.foodchem.2012.01.049.

(60) Nasri, R.; Taktak, W.; Hamdi, M.; ben Amor, N.; Kabadou, A.; Li, S.; Nasri, M. Sardinelle Protein Isolate as a Novel Material for Oil Microencapsulation: Novel Alternative for Fish by-Products Valorisation. *Materials Science and Engineering C.* **2020**, *116*, 111164. https://doi.org/10.1016/j.msec.2020.111164.

(61) Wang, B.; Adhikari, B.; Barrow, C. J. Optimisation of the Microencapsulation of Tuna Oil in Gelatin-Sodium Hexametaphosphate Using Complex Coacervation. *Food Chemistry.* **2014**, *158*, 358-365. https://doi.org/10.1016/j.foodchem.2014.02.135.

(62) Klang, V.; Matsko, N. B.; Valenta, C.; Hofer, F. Electron Microscopy of Nanoemulsions: An Essential Tool for Characterisation and Stability Assessment. *Micron*. **2012**, *43*(2-3), 85-103. https://doi.org/10.1016/j.micron.2011.07.014.

(63) Harris, J. R. Negative Staining across Holes: Application to Fibril and Tubular Structures. *Micron.* **2008**, *39* (2), 168-176. https://doi.org/10.1016/j.micron.2007.07.003.

(64) Wei, Y.; Yang, S.; Zhang, L.; Dai, L.; Tai, K.; Liu, J.; Mao, L.; Yuan, F.; Gao, Y.; Mackie, A. Fabrication, Characterization and in Vitro Digestion of Food Grade Complex Nanoparticles for Co-Delivery of Resveratrol and Coenzyme Q10. *Food Hydrocolloids.* **2020**, *105*, 105791. https://doi.org/10.1016/j.foodhyd.2020.105791.

(65) Severs, N. J.; Robenek, H. Chapter 11 Freeze-Fracture Cytochemistry in Cell Biology. *Methods in Cell Biology*. **2008**, *88*, 181-204. https://doi.org/10.1016/S0091-679X(08)00411-1.

(66) Hrubanova, K.; Nebesarova, J.; Ruzicka, F.; Krzyzanek, V. The Innovation of Cryo-SEM Freeze-Fracturing Methodology Demonstrated on High Pressure Frozen Biofilm. *Micron.* **2018**, *110*, 28-35. https://doi.org/10.1016/j.micron.2018.04.006.

(67) Shi, X.; Lee, Y. Encapsulation of Tributyrin with Whey Protein Isolate (WPI) by Spray-Drying with a Three-Fluid Nozzle. *Journal of Food Engineering.* **2020**, *281*, 109992. https://doi.org/https://doi.org/10.1016/j.jfoodeng.2020.109992.

(68) Chen, Y.; Shu, M.; Yao, X.; Wu, K.; Zhang, K.; He, Y.; Nishinari, K.; Phillips, G. O.; Yao, X.; Jiang, F. Effect of Zein-Based Microencapsules on the Release and Oxidation of Loaded Limonene. *Food Hydrocolloids.* **2018**, *84*, 330–336. https://doi.org/https://doi.org/10.1016/j.foodhyd.2018.05.049.

(69) Nejadmansouri, M.; Hosseini, S. M. H.; Niakosari, M.; Yousefi, G. H.; Golmakani, M. T. Physicochemical Properties and Storage Stability of Ultrasound-Mediated WPI-Stabilized Fish Oil Nanoemulsions. *Food Hydrocolloids.* **2016**, *61*, 801–811. https://doi.org/https://doi.org/10.1016/j.foodhyd.2016.07.011.

(70) Wang, B.; Adhikari, B.; Mathesh, M.; Yang, W.; Barrow, C. J. Anchovy Oil Microcapsule Powders Prepared Using Two-Step Complex Coacervation between Gelatin and Sodium Hexametaphosphate Followed by Spray Drying. *Powder Technology.* **2019**, *358*, 68–78. https://doi.org/https://doi.org/10.1016/j.powtec.2018.07.034.

(71) Xia, Q.; Wang, B.; Akanbi, T. O.; Li, R.; Yang, W.; Adhikari, B.; Barrow, C. J. Microencapsulation of Lipase Produced Omega-3 Concentrates Resulted in Complex Coacervates with Unexpectedly High Oxidative Stability. *Journal of Functional Foods* **2017**, *35*, 499–506. https://doi.org/https://doi.org/10.1016/j.jff.2017.06.017.

(72) Ohtsubo, T.; Tsuda, S.; Tsuji, K. A Study of the Physical Strength of Fenitrothion Microcapsules. *Polymer.* **1991**, *32* (13), 2395–2399. https://doi.org/https://doi.org/10.1016/0032-3861(91)90080-3.

(73) Yuliani, S.; Torley, P. J.; D'Arcy, B.; Nicholson, T.; Bhandari, B. Extrusion of Mixtures of Starch and D-Limonene Encapsulated with β-Cyclodextrin: Flavour Retention and Physical Properties. *Food Research International.* **2006**, *39* (3), 318–331. https://doi.org/https://doi.org/10.1016/j.foodres.2005.08.005.

(74) Zhang, Z. Mechanical Strength of Single Microcapsules Determined by a Novel Micromanipulation Technique. *Journal of Microencapsulation.* **1999**, *16* (1), 117–124. https://doi.org/10.1080/026520499289365.

(75) Fournaise, T.; Burgain, J.; Perroud, C.; Scher, J.; Gaiani, C.; Petit, J. Impact of Formulation on Reconstitution and Flowability of Spray-Dried Milk Powders. *Powder Technology.* **2020**, *372*, 107–116. https://doi.org/https://doi.org/10.1016/j.powtec.2020.05.085.

(76) Freeman, R. Measuring the Flow Properties of Consolidated, Conditioned and Aerated Powders — A Comparative Study Using a Powder Rheometer and a Rotational Shear Cell. *Powder Technology.* **2007**, *174* (1), 25–33. https://doi.org/https://doi.org/10.1016/j.powtec.2006.10.016.

(77) Schuck, P.; Dolivet, A.; Jeantet, R. Analytical Methods for Food and Dairy Powders; *John Wiley & Sons*, Ltd. **2012**, 1-228. https://doi.org/10.1002/9781118307397.

(78) Kim, E. H.-J.; Chen, X. D.; Pearce, D. Surface Characterization of Four Industrial Spray-Dried Dairy Powders in Relation to Chemical Composition, Structure and Wetting Property. *Colloids and Surfaces B: Biointerfaces.* **2002**, *26* (3), 197–212. https://doi.org/https://doi.org/10.1016/S0927-7765(01)00334-4.

(79) Mimouni, A.; Deeth, H. C.; Whittaker, A. K.; Gidley, M. J.; Bhandari, B. R. Investigation of the Microstructure of Milk Protein Concentrate Powders during Rehydration: Alterations during Storage. *Journal of Dairy Science.* **2010**, *93* (2), 463–472. https://doi.org/https://doi.org/10.3168/jds.2009-2369.

(80) Wang, B.; Adhikari, B.; Barrow, C. J. Highly Stable Spray Dried Tuna Oil Powders Encapsulated in Double Shells of Whey Protein Isolate-Agar Gum and Gellan Gum Complex Coacervates. *Powder Technology.* **2019**, *358*, 79–86. https://doi.org/https://doi.org/10.1016/j.powtec.2018.07.084.

(81) Górska, A.; Szulc, K.; Ostrowska-Ligęza, E.; Bryś, J.; Wirkowska-Wojdyła, M. Effect of Composition and Drying Method on Glass Transition Temperature, Water Sorption Characteristics and Surface Morphology of Newly Designed β-Lactoglobulin/Retinyl Palmitate/Disaccharides Systems. *Journal of Thermal Analysis and Calorimetry.* **2017**, *130* (1), 177–185. https://doi.org/10.1007/s10973-017-6392-3.

(82) Jiang, Y.; Lan, W.; Sameen, D. E.; Ahmed, S.; Qin, W.; Zhang, Q.; Chen, H.; Dai, J.; He, L.; Liu, Y. Preparation and Characterization of Grass Carp Collagen-Chitosan-Lemon Essential Oil Composite Films for Application as Food Packaging. *International Journal of Biological Macromolecules.* **2020**, *160*, 340–351. https://doi.org/https://doi.org/10.1016/j.ijbiomac.2020.05.202.

(83) Valenzuela, C.; Abugoch, L.; Tapia, C. Quinoa Protein–Chitosan–Sunflower Oil Edible Film: Mechanical, Barrier and Structural Properties. *LWT - Food Science and Technology.* **2013**, *50* (2), 531–537. https://doi.org/https://doi.org/10.1016/j.lwt.2012.08.010.

(84) Augustin, M. A.; Sanguansri, L.; Bode, O. Maillard Reaction Products as Encapsulants for Fish Oil Powders. *Journal of Food Science.* **2006**, *71* (2), E25–E32. https://doi.org/https://doi.org/10.1111/j.1365-2621.2006.tb08893.x.

(85) Ghasemi, S.; Jafari, S. M.; Assadpour, E.; Khomeiri, M. Nanoencapsulation of D-Limonene within Nanocarriers Produced by Pectin-Whey Protein Complexes. *Food Hydrocolloids.* **2018**, *77*, 152–162. https://doi.org/https://doi.org/10.1016/j.foodhyd.2017.09.030.

(86) Esfahani, R.; Jafari, S. M.; Jafarpour, A.; Dehnad, D. Loading of Fish Oil into Nanocarriers Prepared through Gelatin-Gum Arabic Complexation. *Food Hydrocolloids.* **2019**, *90*, 291–298. https://doi.org/https://doi.org/10.1016/j.foodhyd.2018.12.044.

(87) Soleimanifar, M.; Jafari, S. M.; Assadpour, E. Encapsulation of Olive Leaf Phenolics within Electrosprayed Whey Protein Nanoparticles; Production and Characterization. *Food Hydrocolloids.* **2020**, *101*, 105572. https://doi.org/https://doi.org/10.1016/j.foodhyd.2019.105572.

(88) Eratte, D.; Gengenbach, T. R.; Dowling, K.; Barrow, C. J.; Adhikari, B. Survival, Oxidative Stability, and Surface Characteristics of Spray Dried Co-Microcapsules Containing Omega-3 Fatty Acids and Probiotic Bacteria. *Drying Technology.* **2016**, *34* (16), 1926–1935. https://doi.org/10.1080/07373937.2016.1141782.

(89) Eratte, D.; Wang, B.; Dowling, K.; Barrow, Colin. J.; Adhikari, B. P. Complex Coacervation with Whey Protein Isolate and Gum Arabic for the Microencapsulation of Omega-3 Rich Tuna Oil. *Food & Function.* **2014**, *5* (11), 2743–2750. https://doi.org/10.1039/C4FO00296B.

(90) Xia, Q.; Akanbi, T. O.; Wang, B.; Li, R.; Yang, W.; Barrow, C. J. Investigating the Mechanism for the Enhanced Oxidation Stability of Microencapsulated Omega-3 Concentrates. *Marine Drugs* **2019**, *17* (3), 143. https://doi.org/10.3390/md17030143.

(91) Eratte, D.; Wang, B.; Dowling, K.; Barrow, C. J.; Adhikari, B. Survival and Fermentation Activity of Probiotic Bacteria and Oxidative Stability of Omega-3 Oil in Co-Microcapsules during Storage. *Journal of Functional Foods.* **2016**, *23*, 485–496. https://doi.org/https://doi.org/10.1016/j.jff.2016.03.005.

(92) Tikekar, R. v; Nitin, N. Effect of Physical State (Solid vs. Liquid) of Lipid Core on the Rate of Transport of Oxygen and Free Radicals in Solid Lipid Nanoparticles and Emulsion. *Soft Matter.* **2011**, *7* (18), 8149–8157. https://doi.org/10.1039/C1SM05031A.

(93) Silva, M.; Anh Bui, T. H.; Dharmadana, D.; Zisu, B.; Chandrapala, J. Ultrasound-Assisted Formation of Double Emulsions Stabilized by Casein-Whey Protein Mixtures. *Food Hydrocolloids.* **2020**, *109*, 106143. https://doi.org/https://doi.org/10.1016/j.foodhyd.2020.106143.

(94) Guedes Silva, K. C.; Feltre, G.; Dupas Hubinger, M.; Kawazoe Sato, A. C. Protection and Targeted Delivery of β-Carotene by Starch-Alginate-Gelatin Emulsion-Filled Hydrogels. *Journal of Food Engineering.* **2021**, *290*, 110205. https://doi.org/https://doi.org/10.1016/j.jfoodeng.2020.110205.

(95) Cho, Y. H.; Shim, H. K.; Park, J. Encapsulation of Fish Oil by an Enzymatic Gelation Process Using Transglutaminase Cross-Linked Proteins. *Journal of Food Science.* **2003**, *68* (9), 2717–2723. https://doi.org/https://doi.org/10.1111/j.1365-2621.2003.tb05794.x.

(96) Faridi Esfanjani, A.; Assadpour, E.; Jafari, S. M. Improving the Bioavailability of Phenolic Compounds by Loading Them within Lipid-Based Nanocarriers. *Trends in Food Science and Technology.* **2018**, *76*, 56-66. https://doi.org/10.1016/j.tifs.2018.04.002.

(97) Sun, C.-C.; Su, H.; Zheng, G.-D.; Wang, W.-J.; Yuan, E.; Zhang, Q.-F. Fabrication and Characterization of Dihydromyricetin Encapsulated Zein-Caseinate Nanoparticles and Its Bioavailability in Rat. *Food Chemistry.* **2020**, *330*, 127245. https://doi.org/https://doi.org/10.1016/j.foodchem.2020.127245.

(98) Fard, S. G.; Loh, S. P.; Turchini, G. M.; Wang, B.; Elliott, G.; Sinclair, A. J. Microencapsulated Tuna Oil Results in Higher Absorption of DHA in Toddlers. *Nutrients.* **2020**, *12* (1), 248. https://doi.org/10.3390/nu12010248.

(99) Rojas, V. M.; Inácio, A. G.; Martins Fernandes, I. P.; Leimann, F. V.; Gozzo, A. M.; Barros Fuchs, R. H.; Filipe Barreiro, M. F.; Barros, L.; Ferreira, I. C. F. R.; Coelho Tanamati, A. A.; Gonçalves, O. H. Whey Protein Supplement as a Source of Microencapsulated PUFA-Rich Vegetable Oils. *Food Bioscience.* **2020**, *37*, 100690. https://doi.org/https://doi.org/10.1016/j.fbio.2020.100690.

(100) Barrow, C. J.; Nolan, C.; Holub, B. J. Bioequivalence of Encapsulated and Microencapsulated Fish-Oil Supplementation. *Journal of Functional Foods.* **2009**, *1* (1), 38–43. https://doi.org/https://doi.org/10.1016/j.jff.2008.09.006.

(101) Pratt, C. D. *Twenty Years of Confectionery and Chocolate Progress; From the Proceedings of the 1947 to 1966 Annual Production Conferences of the Pennsylvania Manufacturing Confectioners' Association. Arranged by the Publications Editorial Committee of the P.M.C.A. Annual Production Conference Committee.* Westport, Conn., Avi Pub. Co., **1970**.

(102) Minifie, B. W. *Chocolate, Cocoa and Confectionery: Science and Technology*. Springer Dordrecht, Berlin, Germany. **1989,** 1-904. https://doi.org/10.1007/978-94-011-7924-9.

(103) Muthukumarasamy, P.; Holley, R. A. Microbiological and Sensory Quality of Dry Fermented Sausages Containing Alginate-Microencapsulated Lactobacillus Reuteri. *International Journal of Food Microbiology.* **2006**, *111* (2), 164–169. https://doi.org/https://doi.org/10.1016/j.ijfoodmicro.2006.04.036.

(104) Lead, J. R.; Batley, G. E.; Alvarez, P. J. J.; Croteau, M.-N.; Handy, R. D.; McLaughlin, M. J.; Judy, J. D.; Schirmer, K. Nanomaterials in the Environment: Behavior, Fate, Bioavailability, and Effects—An Updated Review. *Environmental Toxicology and Chemistry.* **2018**, *37* (8), 2029–2063. https://doi.org/https://doi.org/10.1002/etc.4147.

(105) Wang, Y.; Santos, A.; Evdokiou, A.; Losic, D. An Overview of Nanotoxicity and Nanomedicine Research: Principles, Progress and Implications for Cancer Therapy. *Journal of Materials Chemistry B.* **2015**, *3* (36), 7153–7172. https://doi.org/10.1039/C5TB00956A.

(106) Gidwani, M.; Singh, A. Nanoparticle Enabled Drug Delivery Across the Blood Brain Barrier: In Vivo and in Vitro Models, Opportunities and Challenges. *Current Pharmaceutical Biotechnology.* **2014**, *14* (14). https://doi.org/10.2174/1389201015666140508122558.

(107) Zhang, X.; Kitatani, K.; Toyoshima, M.; Ishibashi, M.; Usui, T.; Minato, J.; Egiz, M.; Shigeta, S.; Fox, T.; Deering, T.; Kester, M.; Yaegashi, N. Ceramide Nanoliposomes as a MLKL-Dependent, Necroptosis-Inducing, Chemotherapeutic Reagent in Ovarian Cancer. *Molecular Cancer Therapeutics.* **2018**, *17* (1), 50–59. https://doi.org/10.1158/1535-7163.MCT-17-0173.

(108) Rocha, T. L.; Gomes, T.; Sousa, V. S.; Mestre, N. C.; Bebianno, M. J. Ecotoxicological Impact of Engineered Nanomaterials in Bivalve Molluscs: An Overview. *Marine Environmental Research.* **2015**, *111*, 74–88. https://doi.org/https://doi.org/10.1016/j.marenvres.2015.06.013.

(109) Bazana, M. T.; Codevilla, C. F.; de Menezes, C. R. Nanoencapsulation of Bioactive Compounds: Challenges and Perspectives. *Current Opinion in Food Science.* **2019**, *26*, 47–56. https://doi.org/https://doi.org/10.1016/j.cofs.2019.03.005.

(110) Chen, Q.; McGillivray, D.; Wen, J.; Zhong, F.; Quek, S. Y. Co-Encapsulation of Fish Oil with Phytosterol Esters and Limonene by Milk Proteins. *Journal of Food Engineering.* **2013**, *117* (4), 505–512. https://doi.org/https://doi.org/10.1016/j.jfoodeng.2013.01.011.

(111) Kaasgaard, T.; Keller, D. Chitosan Coating Improves Retention and Redispersibility of Freeze-Dried Flavor Oil Emulsions. *Journal of Agricultural and Food Chemistry.* **2010**, *58* (4), 2446–2454. https://doi.org/10.1021/jf903464s.

(112) Zandi, M.; Mohebbi, M.; Varidi, M.; Ramezanian, N. Evaluation of Diacetyl Encapsulated Alginate–Whey Protein Microspheres Release Kinetics and Mechanism at Simulated

Mouth Conditions. *Food Research International.* **2014**, *56*, 211–217. https://doi.org/https://doi.org/10.1016/j.foodres.2013.11.035.

(113) Yang, Z.; Peng, Z.; Li, J.; Li, S.; Kong, L.; Li, P.; Wang, Q. Development and Evaluation of Novel Flavour Microcapsules Containing Vanilla Oil Using Complex Coacervation Approach. *Food Chemistry.* **2014**, *145*, 272–277. https://doi.org/https://doi.org/10.1016/j.foodchem.2013.08.074.

(114) Fieber, W.; Hafner, V.; Normand, V. Oil Droplet Size Determination in Complex Flavor Delivery Systems by Diffusion NMR Spectroscopy. *Journal of Colloid and Interface Science.* **2011**, *356* (2), 422–428. https://doi.org/https://doi.org/10.1016/j.jcis.2011.01.018.

(115) Gaber Ahmed, G. H.; Fernández-González, A.; Díaz García, M. E. Nano-Encapsulation of Grape and Apple Pomace Phenolic Extract in Chitosan and Soy Protein via Nanoemulsification. *Food Hydrocolloids.* **2020**, *108*, 105806. https://doi.org/https://doi.org/10.1016/j.foodhyd.2020.105806.

(116) Ricaurte, L.; Santagapita, P. R.; Díaz, L. E.; Quintanilla-Carvajal, M. X. Edible Gelatin-Based Nanofibres Loaded with Oil Encapsulating High-Oleic Palm Oil Emulsions. *Colloids Surfaces A: Physicochemical and Engineering Aspects.* **2020**, *595*, 124673. https://doi.org/https://doi.org/10.1016/j.colsurfa.2020.124673.

(117) Timilsena, Y. P.; Adhikari, R.; Barrow, C. J.; Adhikari, B. Digestion Behaviour of Chia Seed Oil Encapsulated in Chia Seed Protein-Gum Complex Coacervates. *Food Hydrocolloids.* **2017**, *66*, 71–81. https://doi.org/https://doi.org/10.1016/j.foodhyd.2016.12.017.

(118) Lv, P.; Wang, D.; Dai, L.; Wu, X.; Gao, Y.; Yuan, F. Pickering Emulsion Gels Stabilized by High Hydrostatic Pressure-Induced Whey Protein Isolate Gel Particles: Characterization and Encapsulation of Curcumin. *Food Research International.* **2020**, *132*, 109032. https://doi.org/https://doi.org/10.1016/j.foodres.2020.109032.

(119) Wang, B.; Vongsvivut, J.; Adhikari, B.; Barrow, C. J. Microencapsulation of Tuna Oil Fortified with the Multiple Lipophilic Ingredients Vitamins A, D3, E, K2, Curcumin and Coenzyme Q10. *Journal of Functional Foods.* **2015**, *19*, 893–901. https://doi.org/https://doi.org/10.1016/j.jff.2015.03.027.

SECTION 1.2

Binding, digestion and bioaccessibility of protein-based nanodelivery systems

Excerpt from

Protein-based nanodelivery systems for food applications

Ogadimma D. Okagu, Bo Wang, Caleb Acquah and Chibuike C. Udenigwe
In *Encyclopedia of food chemistry*. ed. By B.L. Melton, F. Shahidi, P. Varelis. *Academic Press, Oxford, United Kingdom*. **2019**, 719–726.

https://doi.org/10.1016/B978-0-08-100596-5.21864-7

DECLARATION FOR THESIS SECTION 1.2

Protein-based nanodelivery systems for food applications

This is a declaration that there are no conflicts of interest with this work, and the candidate's contribution is as follows:

Candidate's contribution	Conceptualization of idea, writing and review	80%

The following co-authors confirm that the candidate took part in a group publication that was part of his thesis and actively contributed to its creation. The following are the co-authors' permissions:

Name	Signature	Date
Bo Wang		22/11/2022
Caleb Acquah		22/11/2022
Chibuike C. Udenigwe		22/11/2022

1.2. BINDING, DIGESTION AND BIOACCESSIBILITY OF PROTEIN-BASED NANODELIVERY SYSTEMS

1. Binding and encapsulation

Various types of protein nanoparticles have been engineered from whey, gelatin, collagen, zein, casein,[1–6] β-lactoglobulin, lactoferrin,[7] potato protein,[8] soy protein,[9] fish protein,[10] and cruciferin.[11,12] The proteins can be employed in the food, pharmaceutical and medical industry as delivery vehicle for efficient capping, protection and release of bioactive compounds. Protein has inherent structural and physicochemical properties that enhance binding and hence encapsulation of molecules, ligands and ions. For instance, caseins spontaneously bind with calcium and calcium phosphate nanoparticles through their serine-phosphate residues. Alpha-lactalbumin easily binds calcium while lactoferrin is known to bind ferric ion.[13] β-Lactoglobulin can bind epigallocatechin,[14] vitamin D,[15] omega-3 fatty acid,[16] retinol,[13] and resveratrol.[17] The binding is usually facilitated by hydrophobic interaction, hydrogen bonding or van der Waals attraction. In a recent study, encapsulation and loading efficiency ranges of 68.1-72.0 and 5.4-6.2%, respectively with particle sizes of 217-227 nm was reported for acylated rapeseed cruciferin protein loaded with curcumin.[11] Stability study indicates increase in particle size and decrease in encapsulation efficiency with time due to the diffusion of curcumin out of the nanoparticle matrix. Moreover, casein-folic acid nanoparticles stabilized with cationic lysine and arginine, prepared by coacervation, had 95–97% yield and 40% encapsulation efficiency, with decreases in particle size, polydispersity index and zeta potential when compared with unstabilized casein nanoparticles.[6] Furthermore, the nanoparticles stabilized with lysine and arginine were reported to be stable for at least 48 h and 16 h, respectively. Affinity of bioactive compounds to the proteins is important in achieving high encapsulation efficiency, but this can also influence the release of the compounds

in vivo. Some examples of various types and properties of protein-based nanodelivery systems are presented in Table 1.2.1.

2. *In vitro* release studies

Protein has demonstrated efficient binding of bioactive compounds and there is need to consider the release of various encapsulated nutraceutical into the target regions of the human body. Protein nanoparticles digest rapidly and can permeate the mucus layer and epithelium cells of the intestine.[18] The small size of the nanoparticle can increase the bioavailability, chemical stability and absorption of bioactive compounds encapsulated within the matrix. The nanoparticle may release any encapsulated agent more rapidly during digestion in the gastrointestinal tract due to their small size and large surface area. Some studies reported efficient release of bioactive compounds encapsulated in protein nanodelivery systems as a result of inherent structural and physicochemical properties of proteins. For instance, casein can easily undergo proteolytic cleavage due to their open structures, a result of their high proline content and low contents of α-helix and β-sheet secondary structures. Moreover, acid-soluble calcium-phosphate bridging in casein can facilitate target-activated release mechanism for offloading encapsulated compounds in the stomach.[13] Likewise, bovine serum albumin binds small molecules in the blood and offloads them in their target locations.[19] Recently, *in vitro* release of curcumin from acylated rapeseed cruciferin protein nanoparticles was demonstrated in simulated gastric fluid (SGF) and intestinal fluid (SIF) within 6 h of exposure.[11] Initial burst release of about 70% in the first 2 h and sustained release of about 75% after 2 h was observed in the SIF. In the SGF treatment, only about 10% of curcumin was released in the first 1 h followed by slow and up to 25% release after 6 h. Acidic nature (pH 1.2) of the system compared to the isoelectric point of chitosan (pI 6.5) contributed to the slow curcumin release in the SGF. Burst release of curcumin in the SIF in the first 2 h at pH

6.8 was due to deprotonation of the amine group of chitosan giving rise to a weaker polysaccharide-protein interaction. A pH-dependent release of folic acid encapsulated with casein nanoparticles was demonstrated using a similar digestion model.[6] No folic acid was released in the SGF (pH 1.2) with pepsin action due to strong binding of the vitamin inside the protein network. Burst release was equally observed at 2 h followed by slow and sustained release in the SIF. This is likely because of the electrostatic repulsion between folic acid and casein at neutral pH.

The interactions can also depend on the protein type and complexity of the matrix. For instance, kinetics of *in vitro* release of curcumin from electrospun zein nanofibre into cell culture media showed initial burst release of about 80% between 5 to 20 h, followed by constant release of about 90% for the nanofibre loaded with 10 wt% curcumin.[20] The initial burst release is as a result of diffusion of curcumin adsorbed at the outer region of electrospun zein nanofiber, whereas the steady release after 20 h was due to slow diffusion of water molecules into the covered nanofiber, which limited the release of capped curcumin. Larger molecules have also been successfully released from protein nanoparticles. Stephansen et al. (2015) demonstrated the control release of insulin encapsulated with electrospun fish sarcoplasmic protein nanoparticles in simulated intestinal fluid. The encapsulating agent shielded insulin against chymotrypsin degradation, which is expected to enhance its bioavailable amount. In contrast, whey-protein-stabilized astaxanthin was resistant to pepsin, but trypsin digested the complex leading to the release of astaxanthin [1]. The rate, extent and trigger mechanism of release of protein-encapsulated components depends on protease activity, temperature, pH, dilution, and ionic strength of the gastrointestinal environment. These factors are critical especially when delivering sparingly water-soluble components with the goal of controlling their release within the mouth, stomach, or small intestine.[21]

3. Bioaccessibility and uptake studies

Protein-based nanomaterials do not only bind, encapsulate and protect bioactive compounds but also control their release, uptake and transport across cells thereby reducing the risk of toxicity associated with burst release. For instance, acylated cruciferin-chitosan nanoparticles loaded with curcumin had higher permeability coefficient in cultured Caco-2 intestinal cells, and lower effect on cell viability compared to free curcumin.[11] The latter may be due to the delayed release of curcumin from the curcumin nanoparticles, among other factors. Properties of the nanoparticles, e.g. surface charge, are critical to the bioaccessibility and uptake of protein-based nanoparticles. Akbari et al. (2017) demonstrated that uptake of negatively charged cruciferin/calcium nanoparticles by Caco-2 cells was far higher than that of positively charged cruciferin/chitosan nanoparticles. Uptake and transport of the nanoparticles was not affected by the mucus secreted by a Caco-2/HT29 cells co-culture, which demonstrate that they are potentially biostable. As demonstrated for cruciferin-curcumin,[11] an increase in cellular uptake of coumarin was recorded for the digested nanoparticles in simulated gastrointestinal fluids, and this was more with cruciferin/chitosan than cruciferin/calcium nanoparticles.[12] Likewise, Stephansen et al. (2015) reported the permeability of insulin encapsulated with electrospun fish sarcoplasmic protein nanoparticles across Caco-2 cells. The protein-based delivery agent was also found to be biocompatible, and insulin uptake in Caco-2 cell was pH-dependent. However, overall insulin transport was not affected by the increased release from the protein nanoparticles, and insulin binding and structural properties were not affected after cell permeation. Lastly, capping astaxanthin with whey protein isolate and polymerized whey protein enhanced its apparent permeability coefficient in Caco-2 cells by 10- and 16 folds, respectively.[1] If translated *in vivo*,

this observation can result in the use of lower amounts of bioactive compounds in food products to achieve beneficial health effects in humans.

4. Drawbacks of Protein-based Nanodelivery Systems

Protein-based nanoparticles have demonstrated efficient binding, encapsulation, protection and controlled release of bioactive compounds. However, there are drawbacks associated with protein nanomaterials. Allergenicity can occur in some individuals due to the ability of some proteins to elicit immune response. Proteins from egg, soybean, fish, cow's milk, etc. can be allergenic,[22] and this would impede their use for producing nanodelivery agents. Protein abundance, resistance to digestive enzymes, and processing may lead to allergenicity.[23] Furthermore, high specific surface area associated with the small size of nanoparticles could lead to adsorption of digestive or metabolic enzymes, which may consequently interfere with their normal gastrointestinal function.[24] Also, changes in thermodynamic environment after adsorption of some proteins to the nanoparticle surface can cause denaturation thereby affecting the activity of many digestive enzymes. As a result of the small size associated with nanoparticles, rapid digestion and burst release in the intestinal medium may also lead to adverse effects. Currently, there is no standardized analytical technique for assessing the potential toxicity of protein nanoparticles and further studies is required in this area.

Table 1.2.1. Types and properties of protein-based nanodelivery systems

Protein-based nanodelivery agent	Preparation technique	Bioactive compound encapsulated	Encapsulation efficiency (%)	Size range (nm)	PDI	Zeta potential (mV)	Loading ability	% Release in SIF	% Release in SGF	Transport across Caco-2 cells	Apparent permeability coefficient (cm/s)	Reference
Cruciferin	Cold gelation	Coumarin	n.d.	58-334	0.29-0.45	-14.3 to -33.0	n.d.	85	0	2-50%	$1.4x10^{-6}$ -$3.0x10^{-6}$	[12]
	Polyelectrolyte complexation	Curcumin	68.1-79.0	217.7-454.4	0.139-0.204	+15.3 to +18.6	5.4-6.2%	20-80	25	1.8%	$2.43x10^{-6}$ - $6.00x10^{-6}$	[11]
Casein	Coacervation	Folic acid	40	128-305	0.17-0.45	-9.4 to -17.6	23-31 μg/mg	60-90	0	n.d.	n.d.	[6]
Whey protein isolate	Emulsification-Evaporation	Astaxanthin	92.1 - 93.5	80.4-267	0.21-0.543	-19.3 to -35.0	1-5%	25-65	0-10	0.25-2.5 μg	$2.0x10^{-6}$ -$3.5x10^{-6}$	[1]
Fish sarcoplasmic protein	Electrospinning	Insulin	98.6	349-360	n.d.	n.d.	14	75	45	2-14%	$0.5x10^{-6}$ -$1.5x10^{-6}$	[10]
Zein	Electrohydrodynamic atomization	Curcumin	85-90	175-900	n.d.	n.d.	n.d.	n.d.	n.d.	n.d.	n.d.	[25]
Whey protein concentrate	Nanospray drying and electrospraying	Folic acid	80.8-83.9	n.d.	n.d.	n.d.	n.d.	n.d.	n.d.	n.d.	n.d.	[5]
n.d., data not available; PDI, polydispersity index												

SECTION 1.3. RESEARCH GAPS AND PROJECT NOVELTY

Several plant and animal-based nano and micro delivery protein vehicles have been fabricated from casein,[26–28] soy protein,[29] zein,[30–36] insect protein,[37] whey protein,[38–41] human serum albumin,[42] collagen/gelatin,[43] gliadin,[44] rapeseed cruciferin,[11] millet protein,[45] and β-lactoglobulin[46] for the gastrointestinal delivery of bioactive compounds such as curcumin. Current research is based on assessing various combinations of proteins and bioactive compounds that could produce stable encapsulation systems without prior knowledge of the structural, matrix and physicochemical compatibility. This method is tedious and not cost-effective. Unfortunately, limited information is available on the structural relationship between protein carrier and bioactive compounds, making it challenging to fabricate delivery systems that would ensure long-term stability, resistance to harsh gastric condition, and improved bioaccessibility and bioavailability. Polyelectrolyte complexation technique has gained increasing interest in the design of bilayer wall made up of polyelectrolytes for encapsulation and protection of bioactive compounds during gastrointestinal delivery. Promising gastric stability, encapsulation and release efficiency has been reported using this technique.[11,37] However, no study has investigated the impact of conflicting intermolecular forces in the complex that could lead to destabilization and degradation. For instance, the bioactive compound in the core of the complex mostly undergoes hydrophobic interaction with one of the polyelectrolytes while electrostatic forces stabilize the bilayer polyelectrolyte shell. Increasing electrostatic forces in the shell by increasing the negative or positive charge of the polyelectrolyte could reduce hydrophobic contact with the bioactive compound. Moreover, the impact of various structural modifications during polyelectrolyte encapsulation process, such as succinylation, on the physicochemical properties of protein, binding with bioactive compounds, encapsulation efficiency, stability and release has not been

emphasized. Hence, the first part of this thesis addresses these research gaps using curcumin, pea protein isolate, and chitosan as model bioactive compounds, negatively and positively charged polyelectrolyte to facilitate the rational design of protein-based delivery vehicles for bioactive compounds.

Curcumin is a bioactive compound found in turmeric, which has been reported to possess several health-promoting properties, such as anti-inflammatory, antioxidant and anticancer properties. However, curcumin has poor solubility and stability under physiological condition, which limits its bioavailability and effectiveness. The use of food proteins in the encapsulation of curcumin can overcome these limitations and enhance its protection and delivery to the target site. This is due to the structural and techno-functional properties of proteins having a wide range of side-chain functional groups, hydrophobic and hydrophilic regions, charged and uncharged groups, and amphipathic regions. These properties enable the binding of small molecules and hence enhance encapsulation, protection against environmental factors, such as heat, light, and oxygen, and improve the solubility and stability of curcumin. Additionally, protein encapsulation can improve the absorption and bioavailability of curcumin in the body. Several studies have reported the effectiveness of protein encapsulation in improving the functional properties of curcumin [26-46].

Chitosan is a natural biopolymer present in chitin. It is a desirable material for application in food protein-based nanoencapsulation due to its distinctive qualities, including biocompatibility, biodegradability, and antibacterial activity.[47] It is positively charged under acidic condition due to the protonation of its amine group and hence makes it an excellent candidate for stabilizing a negatively charged carrier such as pea protein. Therefore, electrostatic interaction between positively charged chitosan and negatively charged pea protein can protect bioactive compounds better in the presence of the acidic nature of gastric phase of digestion. Also, chitosan gels at acidic

pH which offers additional layer of protection of the shell and bioactive compound during gastric digestion leading to increased amount of curcumin reaching the intestinal phase and hence, possibility of improved bioavailability.

Pea protein is abundant, affordable, safe, sustainable, highly digestible and has a well-balanced essential amino acid composition. It has low allergenicity and possess interesting structural and techno-functional properties such as emulsifying and gelling effect that can promote the encapsulation of nutraceutical compounds.[48,49] It contains four major classes of storage proteins, which are water-soluble albumin, salt-soluble globulin, ethanol-soluble prolamin and alkaline-soluble glutelin fractions. These proteins have varying structural and physicochemical properties, such as folding pattern, charge, hydrophobicity, and solubility, different from the parent whole pea protein isolate.[48,50] There is a dearth of information on how a given bioactive compound would respond to such diverse physical, chemical and structural properties which would either promote or hinder binding, encapsulation, biostability in the gastric digestion phase, and release. This information is essential in the design of specific protein-based delivery agents for a given bioactive compound. The second part of this thesis seeks to fill this gap.

Protein hydrophobicity is an important parameter that influences protein-bioactive compound interaction. However, there is limited information on how physiologically relevant parameters such as ionic strength impact surface hydrophobicity of protein and its binding with bioactive compounds. Additionally, the effect of bioactive compound lipophilicity at various ionic strength on its interaction with protein has not been well-emphasized. Also, it is not clear how the nature of bioactive compound dictates the nano or micro morphology of protein-bioactive complexes. This information is crucial in producing protein-bioactive complexes that would withstand the ionic nature of the gastrointestinal tract. The third research chapter focuses on this area.

There is lack of knowledge regarding how food-based protein nanodelivery systems interact with the biomembrane. Concerns exist that modifications to the structural and physicochemical characteristics of proteins during conversion to nanoparticles that support their use in food formulation may cause unintended physiological reactions. This is conceivable given that adverse nanoparticle-membrane interactions may occur and affect cellular uptake efficiency, exocytosis, and endocytosis mechanisms, as well as transepithelial and permeation capabilities. When administered orally, the potential effects of the interaction on the liver, gut microbiota, and muscle systems include inflammation, nanoparticle accumulation, decreased protein digestibility, and serious adverse effects on the gastrointestinal cell membrane, as well as alteration of the structural integrity of the protein nanoparticles.[24,51–53] The last chapter of this project will address bio-nano interaction.

SECTION 1.4. RESEARCH QUESTIONS

Based on research gaps highlighted in **section 1.3**, the following research questions helped shape the main idea of this study:

- Does the strength of protein-curcumin interaction translate to encapsulation efficiency and stability of complex? What is the effect on release profile of curcumin?
- How does structural modification of protein by succinylation, which is intended to improve its negative charge, affect hydrophobicity and interaction with curcumin?
- In curcumin-loaded protein-chitosan bilayer complex, how do we strike a balance between the electrostatic interaction between negatively charged protein and chitosan and hydrophobic interaction between curcumin and protein to ensure stability of the complex?
- How would different structural and physicochemical properties of water-soluble albumin, salt-soluble globulin, ethanol-soluble prolamin and alkaline-soluble glutelin fractions

derived from pea protein influence its interaction with curcumin? What is the significance of the nature of interaction in designing delivery vehicles for specific bioactive compounds?

- How do we ensure that protein-bioactive compound complex does not dissociate under the ionic strength of the gastrointestinal tract before reaching their intended location in the body?
- Does lipophilicity of bioactive compounds influence the choice of their protein-based delivery vehicles?
- Will changes in the physicochemical and structural properties of proteins after conversion to nanoparticle affect biocompatibility and safety especially with regards to interaction with biomembrane?

SECTION 1.5. AIM OF THE STUDY

The aim of this thesis is to understand the structural basis of guest-host interaction in the gastrointestinal delivery of lipophilic bioactive compounds.

1.5.1. Specific Objectives

The specific objectives are:

- To understand the nature and strength of pea protein–curcumin interaction and the impact of protein succinylation on binding, stability, encapsulation efficiency, and gastrointestinal release profile.
- To understand how diverse structural and physicochemical properties of pea glutelin, albumin and globulin influence their interaction with curcumin, physicochemical

properties of their complexes, biostability in the gastric digestion phase, and *in vitro* curcumin bioaccessibility.

- To study the influence of some physiological relevant parameters such as ionic strength and lipophilicity on protein-bioactive compound interaction, morphology, and stability of their complexes.
- To assess the influence of the physicochemical properties of different well-characterized hollow and nutraceutical-loaded food protein nanoparticles on the interaction occurring at the bio-nano interface using giant unilamellar vesicles as model bio membrane.

SECTION 1.6. SIGNIFICANCE OF THE STUDY

This study provided in-depth information on the types of interactions and binding forces that stabilise protein-bioactive compound complexes, and demonstrated how binding strength correlates with encapsulation effectiveness, sustained release, gastric stability, and long-term storage capacity. The thesis covered the stability and physicochemical characteristics of loaded curcumin-protein complexes, as well as polyelectrolyte complexes with chitosan, and the effects of succinylation on the structural alteration of pea protein and its interaction with curcumin. The second aspect of this research uncovered the binding strength of curcumin with various protein fractions and the behaviour of curcumin-loaded protein complexes under gastric condition in the presence and absence of enzyme. The third aspect of this research complements currently available binding data used in the encapsulation of bioactive compounds to prevent undesirable interactions with the carrier food matrix and to ensure appropriate stoichiometry in the selection of protein-bioactive compound combinations for improved binding, encapsulation efficiency, and release profile. Likewise, it will help alleviate difficulties associated with the complex nature of the gastrointestinal tract with varying ionic strengths. This can affect the binding of proteins and

bioactive compounds and thus the stability and integrity of the delivery system during oral administration. The final study provides the first proof of the implications of interactions at the bio-nano interface for food protein-based nanodelivery systems. These overall findings of the study will facilitate the development of delivery systems that safely interact with biological membranes, guarantee the guest compound protection against degradation, and enable its sustained release at the intended site in the body.

SECTION 1.7. THESIS LAYOUT

The chapters of this thesis addressed the various research objectives comprehensively as follows.

Chapter two addressed the first objective by investigating the impact of succinylation on pea protein-curcumin interaction, polyelectrolyte complexation with chitosan and gastrointestinal release of curcumin in the loaded-biopolymer nano-complexes.

Chapter three focused on the second objective and investigated the molecular interactions of pea protein-derived globulin, albumin and glutelin fractions with curcumin, and the formation and gastric release mechanisms of curcumin-loaded bio-nanocomplexes. Data obtained in this study were compared with those of whole pea in chapter one for the role of the individual fraction in the encapsulation efficiency of pea protein and for the design of structurally compatible protein-bioactive compound delivery systems.

Chapter four investigated the role of ionic strength, a physiologically relevant parameter, in the mode and strength of protein-bioactive compound interaction, and stabilization or destabilization of the complexes during gastrointestinal delivery of nutraceuticals. It also focused on understanding the influence of bioactive compound lipophilicity on their interaction with protein and morphological properties of the complex.

The final goal was addressed in **Chapter five** by examining how the physicochemical, structural, and morphological properties of nano and microparticles of protein-bioactive compound delivery system that demonstrated potential application in functional food formulation could cause unintended physiological response.

The conclusion is given in **Chapter six**, along with a summary of the major discoveries from this study and suggestions for further investigation.

Reference

(1) Shen, X.; Zhao, C.; Lu, J.; Guo, M. Physicochemical Properties of Whey-Protein-Stabilized Astaxanthin Nanodispersion and Its Transport via a Caco-2 Monolayer. *J Agric Food Chemistry.* **2018**, *66* (6), 1472–1478. https://doi.org/10.1021/acs.jafc.7b05284.

(2) Gomez-Guillen, M. C.; Gimenez, B.; Lopez-Caballero, M. E.; Montero, M. P. Functional and Bioactive Properties of Collagen and Gelatin from Alternative Sources: A Review. *Food Hydrocolloids.* **2011**, *25* (8), 1813–1827. https://doi.org/10.1016/j.foodhyd.2011.02.007.

(3) Livney, Y. D. Nanostructured Delivery Systems in Food: Latest Developments and Potential Future Directions. *Current Opinion in Food Science.* **2015**, *3*, 125–135. https://doi.org/10.1016/j.cofs.2015.06.010.

(4) Raikos, V.; Ranawana, V. Designing Emulsion Droplets of Foods and Beverages to Enhance Delivery of Lipophilic Bioactive Components – a Review of Recent Advances. *International Journal of Food Science and Technology*. **2017**, pp 68–80. https://doi.org/10.1111/ijfs.13272.

(5) Pérez-Masiá, R.; López-Nicolás, R.; Periago, M. J.; Ros, G.; Lagaron, J. M.; López-Rubio, A. Encapsulation of Folic Acid in Food Hydrocolloids through Nanospray Drying and Electrospraying for Nutraceutical Applications. *Food Chemistry*. **2015**, pp 124–133. https://doi.org/10.1016/j.foodchem.2014.07.051.

(6) Penalva, R.; Esparza, I.; Agüeros, M.; Gonzalez-Navarro, C. J.; Gonzalez-Ferrero, C.; Irache, J. M. Casein Nanoparticles as Carriers for the Oral Delivery of Folic Acid. *Food Hydrocolloids.* **2015**, *44*, 399–406. https://doi.org/10.1016/j.foodhyd.2014.10.004.

(7) Chapeau, A. L.; Tavares, G. M.; Hamon, P.; Croguennec, T.; Poncelet, D.; Bouhallab, S. Spontaneous Co-Assembly of Lactoferrin and β-Lactoglobulin as a Promising Biocarrier for Vitamin B9. *Food Hydrocolloids.* **2016**, *57*, 280–290. https://doi.org/10.1016/j.foodhyd.2016.02.003.

(8) David, S.; Livney, Y. D. Potato Protein Based Nanovehicles for Health Promoting Hydrophobic Bioactives in Clear Beverages. *Food Hydrocolloids.* **2016**, *57*, 229–235. https://doi.org/10.1016/j.foodhyd.2016.01.027.

(9) Lee, H.; Yildiz, G.; dos Santos, L. C.; Jiang, S.; Andrade, J. E.; Engeseth, N. J.; Feng, H. Soy Protein Nano-Aggregates with Improved Functional Properties Prepared by Sequential PH Treatment and Ultrasonication. *Food Hydrocolloids.* **2016**, *55*, 200–209. https://doi.org/10.1016/j.foodhyd.2015.11.022.

(10) Stephansen, K.; García-Díaz, M.; Jessen, F.; Chronakis, I. S.; Nielsen, H. M. Bioactive Protein-Based Nanofibers Interact with Intestinal Biological Components Resulting in Transepithelial Permeation of a Therapeutic Protein. *International Journal of Pharmaceutics*. **2015**, pp 58–66. https://doi.org/10.1016/j.ijpharm.2015.08.076.

(11) Wang, F.; Yang, Y.; Ju, X.; Udenigwe, C. C.; He, R. Polyelectrolyte Complex Nanoparticles from Chitosan and Acylated Rapeseed Cruciferin Protein for Curcumin Delivery. *Journal of Agricultural Food Chemistry.* **2018**, *66*(11), 2685-2693. acs.jafc.7b05083. https://doi.org/10.1021/acs.jafc.7b05083.

(12) Akbari, A.; Lavasanifar, A.; Wu, J. Interaction of Cruciferin-Based Nanoparticles with Caco-2 Cells and Caco-2/HT29-MTX Co-Cultures. *Acta Biomaterialia.* **2017**, *64*, 249–258. https://doi.org/10.1016/j.actbio.2017.10.017.

(13) Fox, P. F.; McSweeney, P. L. H. Advanced Dairy Chemistry: Volume 1: Proteins, Parts A\&B: Protein. *Advanced Dairy Chemistry*. **2003,** 1-674.

(14) Livney, Y. D. Milk Proteins as Vehicles for Bioactives. *Current Opinion in Colloid & Interface Science.* **2010**, *15* (1–2), 73–83. https://doi.org/10.1016/j.cocis.2009.11.002.

(15) Forrest, S. A.; Yada, R. Y.; Rousseau, D. Interactions of Vitamin D3with Bovine β-Lactoglobulin A and β-Casein. *Journal of Agricultural Food Chemistry.* **2005**, *53* (20), 8003–8009. https://doi.org/10.1021/jf050661l.

(16) Zimet, P.; Livney, Y. D. Beta-Lactoglobulin and Its Nanocomplexes with Pectin as Vehicles for ω-3 Polyunsaturated Fatty Acids. *Food Hydrocolloids.* **2009**, *23* (4), 1120–1126. https://doi.org/10.1016/j.foodhyd.2008.10.008.

(17) Liang, L.; Tajmir-Riahi, H. a; Subirade, M. Interaction of Beta-Lactoglobulin with Resveratrol and Its Biological Implications. *Biomacromolecules.* **2008**, *9* (1), 50–56. https://doi.org/10.1021/bm700728k.

(18) McClements, D. J. Encapsulation, Protection, and Delivery of Bioactive Proteins and Peptides Using Nanoparticle and Microparticle Systems: A Review. *Advances in Colloid and Interface Science*. 2018, pp 1–22. https://doi.org/10.1016/j.cis.2018.02.002.

(19) Li, J.; Yao, P. Self-Assembly of Ibuprofen and Bovine Serum Albumin-Dextran Conjugates Leading to Effective Loading of the Drug. *Langmuir.* **2009**, *25* (11), 6385–6391. https://doi.org/10.1021/la804288u.

(20) Brahatheeswaran, D.; Mathew, A.; Aswathy, R. G.; Nagaoka, Y.; Venugopal, K.; Yoshida, Y.; Maekawa, T.; Sakthikumar, D. Hybrid Fluorescent Curcumin Loaded Zein Electrospun Nanofibrous Scaffold for Biomedical Applications. *Biomedical Materials.* **2012**, *7* (4), 045001. https://doi.org/10.1088/1748-6041/7/4/045001.

(21) McClements, D. J.; Rao, J. Food-Grade Nanoemulsions: Formulation, Fabrication, Properties, Performance, Biological Fate, and Potential Toxicity. *Critical Reviews in Food Science and Nutrition.* **2011**, *51* (4), 285–330. https://doi.org/10.1080/10408398.2011.559558.

(22) Hefle, S. L.; Nordlee, J. A.; Taylor, S. L. Allergenic Foods. *Critical Reviews in Food Science and Nutrition.* **1996**, *36* (Supplement), 69S-89S. https://doi.org/10.1080/10408399609527760.

(23) Bannon, G. A. What Makes a Food Protein an Allergen? *Current Allergy and Asthma Reports.* **2004**, *4* (1), 43–46. https://doi.org/10.1007/s11882-004-0042-0.

(24) McClements, D. J.; Xiao, H. Is Nano Safe in Foods? Establishing the Factors Impacting the Gastrointestinal Fate and Toxicity of Organic and Inorganic Food-Grade Nanoparticles. *npj Science of Food*. **2017**, *1*(1), 1-13. https://doi.org/10.1038/s41538-017-0005-1.

(25) Gomez-Estaca, J.; Balaguer, M. P.; Gavara, R.; Hernandez-Munoz, P. Formation of Zein Nanoparticles by Electrohydrodynamic Atomization: Effect of the Main Processing Variables and Suitability for Encapsulating the Food Coloring and Active Ingredient Curcumin. *Food Hydrocolloids.* **2012**, *28* (1), 82–91. https://doi.org/10.1016/j.foodhyd.2011.11.013.

(26) Ghayour, N.; Hosseini, S. M. H.; Eskandari, M. H.; Esteghlal, S.; Nekoei, A. R.; Hashemi Gahruie, H.; Tatar, M.; Naghibalhossaini, F. Nanoencapsulation of Quercetin and Curcumin in Casein-Based Delivery Systems. *Food Hydrocolloids.* **2019**, 87, 394-403. https://doi.org/10.1016/j.foodhyd.2018.08.031.

(27) K. Purushothaman, B.; Harsha S, M.; Maheswari, P. U.; Sheriffa Begum, K. M. M. Magnetic Assisted Curcumin Drug Delivery Using Folate Receptor Targeted Hybrid Casein-Calcium Ferrite Nanocarrier. *Journal of Drug Delivery Science and Technology.* **2019**, *52*, 509-520. https://doi.org/10.1016/j.jddst.2019.05.010.

(28) Esmaili, M.; Ghaffari, S. M.; Moosavi-Movahedi, Z.; Atri, M. S.; Sharifizadeh, A.; Farhadi, M.; Yousefi, R.; Chobert, J. M.; Haertlé, T.; Moosavi-Movahedi, A. A. Beta Casein-Micelle as a Nano Vehicle for Solubility Enhancement of Curcumin; Food Industry Application. *LWT - Food Science and Technology.* **2011**, *44*, 2166-2172. https://doi.org/10.1016/j.lwt.2011.05.023.

(29) Tapal, A.; Tiku, P. K. Complexation of Curcumin with Soy Protein Isolate and Its Implications on Solubility and Stability of Curcumin. *Food Chemistry.* **2012,** *130*, 960-965. https://doi.org/10.1016/j.foodchem.2011.08.025.

(30) Alehosseini, A.; Gómez-Mascaraque, L. G.; Martínez-Sanz, M.; López-Rubio, A. Electrospun Curcumin-Loaded Protein Nanofiber Mats as Active/Bioactive Coatings for Food Packaging Applications. *Food Hydrocolloids.* **2019**, *87*, 758-771. https://doi.org/10.1016/j.foodhyd.2018.08.056.

(31) Dai, L.; Wei, Y.; Sun, C.; Mao, L.; McClements, D. J.; Gao, Y. Development of Protein-Polysaccharide-Surfactant Ternary Complex Particles as Delivery Vehicles for Curcumin. *Food Hydrocolloids.* **2018**, *85*, 75-85. https://doi.org/10.1016/j.foodhyd.2018.06.052.

(32) Sun, C.; Xu, C.; Mao, L.; Wang, D.; Yang, J.; Gao, Y. Preparation, Characterization and Stability of Curcumin-Loaded Zein-Shellac Composite Colloidal Particles. *Food Chemistry.* **2017**, *228*, 656-667. https://doi.org/10.1016/j.foodchem.2017.02.001.

(33) Hu, S.; Wang, T.; Fernandez, M. L.; Luo, Y. Development of Tannic Acid Cross-Linked Hollow Zein Nanoparticles as Potential Oral Delivery Vehicles for Curcumin. *Food Hydrocolloids.* **2016**, **61**, 821-831. https://doi.org/10.1016/j.foodhyd.2016.07.006.

(34) Wang, H.; Hao, L.; Wang, P.; Chen, M.; Jiang, S.; Jiang, S. Release Kinetics and Antibacterial Activity of Curcumin Loaded Zein Fibers. *Food Hydrocolloids.* **2017**, *63*, 437-446. https://doi.org/10.1016/j.foodhyd.2016.09.028.

(35) Xue, J.; Zhang, Y.; Huang, G.; Liu, J.; Slavin, M.; Yu, L. (Lucy). Zein-Caseinate Composite Nanoparticles for Bioactive Delivery Using Curcumin as a Probe Compound. *Food Hydrocolloids.* **2018**, *83*, 25-35. https://doi.org/10.1016/j.foodhyd.2018.04.037.

(36) Liu, Q.; Jing, Y.; Han, C.; Zhang, H.; Tian, Y. Encapsulation of Curcumin in Zein/ Caseinate/Sodium Alginate Nanoparticles with Improved Physicochemical and Controlled Release Properties. *Food Hydrocolloids.* **2019**, *93*, 432-442. https://doi.org/10.1016/j.foodhyd.2019.02.003.

(37) Okagu, O. D.; Verma, O.; McClements, D. J.; Udenigwe, C. C. Utilization of Insect Proteins to Formulate Nutraceutical Delivery Systems: Encapsulation and Release of Curcumin Using Mealworm Protein-Chitosan Nano-Complexes. *International Journal of Biological Macromolecules.* **2020**, *151*, 333-343. https://doi.org/10.1016/j.ijbiomac.2020.02.198.

(38) Mohammadian, M.; Salami, M.; Alavi, F.; Momen, S.; Emam-Djomeh, Z.; Moosavi-Movahedi, A. A. Fabrication and Characterization of Curcumin-Loaded Complex Coacervates Made of Gum Arabic and Whey Protein Nanofibrils. *Food Biophysics.* **2019**, pp. 1-12. https://doi.org/10.1007/s11483-019-09591-1.

(39) Mohammadian, M.; Salami, M.; Momen, S.; Alavi, F.; Emam-Djomeh, Z. Fabrication of Curcumin-Loaded Whey Protein Microgels: Structural Properties, Antioxidant Activity, and in Vitro Release Behavior. *LWT - Food Science and Technology.* **2019**, 103, 94-100. https://doi.org/10.1016/j.lwt.2018.12.076.

(40) Mohammadian, M.; Salami, M.; Momen, S.; Alavi, F.; Emam-Djomeh, Z.; Moosavi-Movahedi, A. A. Enhancing the Aqueous Solubility of Curcumin at Acidic Condition

through the Complexation with Whey Protein Nanofibrils. *Food Hydrocolloids.* **2019**, *87*, 902-914. https://doi.org/10.1016/j.foodhyd.2018.09.001.

(41) Pan, Y.; Xie, Q. T.; Zhu, J.; Li, X. M.; Meng, R.; Zhang, B.; Chen, H. Q.; Jin, Z. Y. Study on the Fabrication and in Vitro Digestion Behavior of Curcumin-Loaded Emulsions Stabilized by Succinylated Whey Protein Hydrolysates. *Food Chemistry.* **2019**, *287*, 76-84. https://doi.org/10.1016/j.foodchem.2019.02.047.

(42) Song, Z.; Lu, Y.; Zhang, X.; Wang, H.; Han, J.; Dong, C. Novel Curcumin-Loaded Human Serum Albumin Nanoparticles Surface Functionalized with Folate: Characterization and in Vitro/Vivo Evaluation. *Drug Design, Development and Therapy.* **2016**, *10*, 2643-2649. https://doi.org/10.2147/DDDT.S112039.

(43) Zuanon, L. A. C.; Malacrida, C. R.; Telis, V. R. N. Effect of Ultrasound on the Stability of Turmeric Oleoresin Microencapsulated in Gelatin-Collagen Matrices. *Journal of Food Process Engineering.* **2017**, *40*(2), e12360. https://doi.org/10.1111/jfpe.12360.

(44) Mathew, M. S.; Vinod, K.; Jayaram, P. S.; Jayasree, R. S.; Joseph, K. Improved Bioavailability of Curcumin in Gliadin-Protected Gold Quantum Cluster for Targeted Delivery. *ACS Omega.* **2019**, *4*(10), 14169-14178. https://doi.org/10.1021/acsomega.9b00917.

(45) Wang, L.; Gulati, P.; Santra, D.; Rose, D.; Zhang, Y. Nanoparticles Prepared by Proso Millet Protein as Novel Curcumin Delivery System. *Food Chemistry.* **2018**, *240*, 1039-1046. https://doi.org/10.1016/j.foodchem.2017.08.036.

(46) Mirpoor, S. F.; Hosseini, S. M. H.; Yousefi, G. H. Mixed Biopolymer Nanocomplexes Conferred Physicochemical Stability and Sustained Release Behavior to Introduced Curcumin. *Food Hydrocolloids* **2017**, *71*, 216-224. https://doi.org/10.1016/j.foodhyd.2017.05.021.

(47) Bakshi, P. S.; Selvakumar, D.; Kadirvelu, K.; Kumar, N. S. Chitosan as an Environment Friendly Biomaterial – a Review on Recent Modifications and Applications. *International Journal of Biological Macromolecules.* **2020**, **150**, 1072-1083. https://doi.org/10.1016/j.ijbiomac.2019.10.113.

(48) Lu, Z. X.; He, J. F.; Zhang, Y. C.; Bing, D. J. Composition, Physicochemical Properties of Pea Protein and Its Application in Functional Foods. *Critical Reviews in Food Science and Nutrition*. **2019**, *60*(15), 2593-2605. https://doi.org/10.1080/10408398.2019.1651248.

(49) Tömösközi, S.; Lásztity, R.; Haraszi, R.; Baticz, O. Isolation and Study of the Functional Properties of Pea Proteins. *Nahrung – Food.* **2001**, *45*(6), 399-401. https://doi.org/10.1002/1521-3803(20011001)45:6<399::AID-FOOD399>3.0.CO;2-0.

(50) Adebiyi, A. P.; Aluko, R. E. Functional Properties of Protein Fractions Obtained from Commercial Yellow Field Pea (Pisum Sativum L.) Seed Protein Isolate. *Food Chemistry.* **2011**, *128*(4), 902-908. https://doi.org/10.1016/j.foodchem.2011.03.116.

(51) Wong, C. Y.; Al-Salami, H.; Dass, C. R. Cellular Assays and Applied Technologies for Characterisation of Orally Administered Protein Nanoparticles: A Systematic Review. *Journal of Drug Targeting*. **2020**, *28*(6), 585-599. https://doi.org/10.1080/1061186X.2020.1726356.

(52) Yang, L.; Li, M.; Sun, Y.; Zhang, L. A Cell-Penetrating Peptide Conjugated Carboxymethyl-β-Cyclodextrin to Improve Intestinal Absorption of Insulin. *International Journal of Biological Macromolecules.* **2018**, *111,* 685-695. https://doi.org/10.1016/j.ijbiomac.2018.01.077.

(53) Hirano, A.; Uda, K.; Maeda, Y.; Akasaka, T.; Shiraki, K. One-Dimensional Protein-Based Nanoparticles Induce Lipid Bilayer Disruption: Carbon Nanotube Conjugates and Amyloid Fibrils. *Langmuir*. **2010**, *26* (22), 17256-17259. https://doi.org/10.1021/la103615b.

CHAPTER TWO

IMPACT OF PROTEIN MODIFICATION ON POLYELECTROLYTE COMPLEX-BASED DELIVERY SYSTEMS AND THE NATURE OF STABILIZING INTERMOLECULAR FORCES

Impact of succinylation on pea protein-curcumin interaction, polyelectrolyte complexation with chitosan, and gastrointestinal release of curcumin in loaded-biopolymer nano-complexes

Ogadimma D. Okagu, Jian Jin, Chibuike C. Udenigwe

Journal of Molecular Liquids **2021**, *325*, 115248. https://doi.org/10.1016/j.molliq.2020.115248.

DECLARATION FOR THESIS CHAPTER TWO

Impact of succinylation on pea protein-curcumin interaction, polyelectrolyte complexation with chitosan, and gastrointestinal release of curcumin in loaded-biopolymer nano-complexes

This is to declare that there is no conflict of interest associated with this work and the contribution of the candidate is as stated below:

Candidate's contribution	Conceptualization of idea, formal analysis, investigation, methodology, validation, visualization, writing, review, and editing	85%

The following co-authors attest to the candidate's participation in a group publication as a component of his thesis and was active in the creation of this publication. The co-authors' permissions are as follows:

Name	Signature	Date
Jian Jin		22/11/2022
Chibuike C. Udenigwe		22/11/2022

Abstract

The influence of pea protein succinylation on the nature and strength of interaction with curcumin for a potential role in encapsulation and gastrointestinal delivery was investigated. Succinylation neutralized the positive charge on lysine residue and increased the effective negative charge on the protein from -34.4 ± 0.2 to -59.9 ± 0.9 mV with corresponding decrease in surface hydrophobicity and binding with curcumin. The binding constants (K) of 6.9 (± 0.21) × 10^4 M^{-1} and 4.2 (±0.05) × 10^4 M^{-1} were obtained for the native protein-curcumin (CUR/PPI) and succinylated protein-curcumin (CUR/SPPI) interactions, respectively. These values increased to 14.5 (± 0.64) × 10^4 M^{-1} and 187.9 (± 12.40) × 10^4 M^{-1} for curcumin-native pea protein-chitosan (CUR/PPI/CHI) and curcumin-succinylated protein-chitosan complexes (CUR/SPPI/CHI), respectively. Incorporation of chitosan to the protein-curcumin complex favoured static interaction. Transmission electron microscopy and dynamic light scattering confirmed the formation of spherical nano-complexes within the size range of 100-194.5 nm. FTIR showed that curcumin was stabilized more in the native protein complex than in the succinylated form. Polyelectrolyte complexation with chitosan by electrostatic interaction stabilized the succinylated protein-curcumin complex. The encapsulation efficiency decreased with a decrease in protein hydrophobicity and binding as a result of succinylation, from 34.65 ± 0.10% in CUR/PPI to 24.92 ± 0.03% in CUR/SPPI and from 85.01 ± 1.43 in CUR/PPI/CHI to 62.05 ± 2.95% in CUR/SPPI/CHI nano-complex. Although polyelectrolyte biopolymers enhance curcumin-loaded complex stability at the gastric phase, the release profile demonstrated that pea protein isolate effectively encapsulated and released curcumin without protein modification or incorporation of chitosan.

Keywords: Pea protein; plant-based protein; succinylation; curcumin; chitosan; polymeric nanoparticles; encapsulation; molecular interaction; nanodelivery; bioaccessibility

1. Introduction

Yellow peas (*Pisum sativum L*) are leguminous grains cultivated around the world as food.[1,2] The protein powder isolated from pea seeds is rich in albumin, globulin, glutelin, and prolamin,[3] which have emulsifying, gelling, and structural properties that could enhance the binding, encapsulation, and release of small bioactive molecules.[4] Pea proteins are used as a functional ingredient in the food industry globally due to their high digestibility, low allergenicity, and high nutritional quality being an important source of indispensable amino acids.[4,5] Furthermore, pea proteins are readily available, safe, and affordable; hence, they are considered a sustainable source of food protein.[4] Therefore, the application of pea protein in the delivery of bioactive compounds could confer additional nutritional and health benefits.

Protein succinylation is useful in the fabrication of polyelectrolyte complexes for the encapsulation and release of functional ingredients by increasing the negative charge on the protein to ensure stronger electrostatic interaction with positively charged polyelectrolytes.[6] Pea proteins are rich in lysine [7] and succinylation will neutralize the positive charge of lysine and introduce the negative charge on the carboxylic group of succinic anhydride, thereby increasing the effective negative charge on the protein (Scheme 2.1).[8] Also, the addition of succinyl moiety (Mw 100 Da) introduces a relatively large group compared to the case of acetylation and methylation. This is expected to have a significant effect on protein structure and function especially with respect to encapsulation, protection, and controlled release of bioactive compounds. Hence, bioactive compounds encapsulated with succinylated proteins could be stabilized more by positively charged polyelectrolytes in the acidic environment of the stomach.

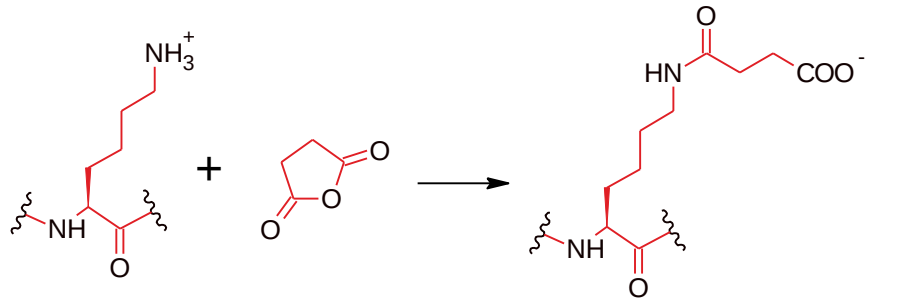

Protein lysyl residue
(Effective charge, +1)

Protein succinylated lysyl residue
(Effective charge, -1)

Scheme 2.1. Succinylation of lysine residue of proteins.

Curcumin is a hydrophobic bioactive compound derived from a plant, *Curcuma longa*. It has been shown to have anti-cancer, anti-inflammatory, antimicrobial, and antioxidant properties, and could be used in the management of arthritis, metabolic syndrome, muscle soreness, anxiety, and hyperlipidemia.[9] However, curcumin has poor bioavailability due to its low aqueous solubility, rapid clearance, and rapid metabolism under physiological conditions.[10] Among various approaches for improving curcumin bioavailability, encapsulation technology involving biopolymer complexes has been promising.[6,11–15] Recent study has shown that the encapsulation efficiency and size of curcumin loaded in alginate microspheres by water-in-oil emulsion could vary on alginate concentration and has high swelling induced release properties.[16] The potential of using pH sensitive injectable curcumin-loaded smart polymeric micelles of release efficiency above 90% and with reduced photo-degradative effect has been achieved through curcumin encapsulation.[17] Curcumin-loaded polysaccharides-based polyelectrolyte complexes of high encapsulation and release efficiency have demonstrated sustained release and shown to withstand the harsh gastrointestinal environment.[18]

Polyelectrolyte complexes of protein and chitosan have demonstrated strong potential in the encapsulation of curcumin to ensure stability, solubility, bioaccessibility, and bioavailability.[6,11]

However, a rational design of the encapsulating agents for long-term storage and improved curcumin bioavailability has been challenging due to limited information on the nature of interaction and binding forces stabilizing the complexes. For the first time, we are reporting the influence of structural modification by succinylation on the physicochemical properties of pea protein and their interaction with curcumin as well as the stability and physicochemical properties of the loaded curcumin-protein complexes and polyelectrolyte complexes with chitosan. This study equally demonstrated the need to strike a balance between the hydrophobic interaction that drives curcumin-protein binding in the core and electrostatic interaction during polyelectrolyte complexation with chitosan at the surface of the biopolymer nano-complexes, and investigated their combined effects on the stability, controlled release and bioaccessibility of curcumin in vitro.

2. Materials and methods

2.1. Materials

Chitosan (medium molecular weight), curcumin (Cur, ≥ 94% purity), 8-anilo-1-naphthalenesulfonic acid (ANS), ethanol, tris(hydroxymethyl)aminomethane (Tris-base), and succinic acid anhydride were purchased from MilliporeSigma Chemical Co., Ltd. (St. Louis, MO, USA). Yellow pea seeds were generously donated by Pulse Canada (Manitoba, Canada). All reagents are of analytical grade and used without further purification. Milli-Q water with a resistivity of 18.2 MΩcm at 25 °C and total organic carbon level ≤ 5 ppb was obtained from a commercial water-purification system (Advantage A10 Q-POD Milli-Q Water System).

2.2. Pea protein isolate preparation

Pea protein isolate (PPI) was extracted from yellow pea (*Pisum sativum*) using a previously reported technique.[3] Briefly, the yellow pea seeds were dehulled, ground, and sieved to obtain

powdered flour. The flour (200 g) was extracted with NaOH solution (2 L, 0.05 M) at pH 12.7 after stirring for 4 h. The mixture was centrifuged at 5600 × g for 30 min at room temperature. The supernatant was collected and acidified with HCl (1 M) to a pH of 4.5 to precipitate PPI, which was separated after centrifugation for 30 min, then washed once with Milli-Q water and adjusted to pH 7. The sample was freeze-dried to obtain the PPI powder. Total protein content of PPI was determined by Lowry assay using the Bio-Rad protein assay kits and a bovine serum albumin standard calibration curve.

2.3. Pea protein succinylation

Succinylated pea protein isolate (SPPI) was prepared using a previously reported method.[6] A solution of PPI was prepared in water (100 mL, 2% w/v), pH adjusted to 11 with NaOH (0.5 M) and heated to 38 °C while stirring for 45 min. Approximately 4 mL of succinic acid anhydride (0.5 M) was added slowly and pH maintained at 10.5 with NaOH (1 M). The solution was stirred for 4 h, dialyzed against deionized water (molecular weight cut-off of 3.5 kDa) at 4 °C for 48 h and freeze-dried. The powdered sample was stored at -20 °C.

2.4. Surface hydrophobicity of SPPI and PPI

The surface hydrophobicity of the pea protein isolate and the succinylated form was determined using ANS assay.[11] Briefly, ANS solution (8 mM) and protein stock solution (5 mg/mL) were prepared separately in sodium phosphate buffer solution (0.1 M, pH 7.2). Dilute solutions of the protein (1.0, 0.75, 0.5, 0.25, and 0.125 mg/mL) were prepared in the sodium phosphate buffer through serial dilution and each solution (200 μL) was mixed with 5 μL of ANS. Fluorescence intensity was measured at the excitation and emission wavelengths of 390 and 470 nm, respectively using a Spark multimode microplate reader (Tecan, Stockholm, Sweden). The surface

hydrophobicity was calculated as the slope of the fluorescence intensity vs. protein concentration plot.

2.5. Protein-curcumin interactions by fluorescence spectroscopy

The interaction of pea protein isolate and the succinylated form with curcumin, in the absence or presence of chitosan, was investigated by fluorescence quenching technique using Varian Cary Eclipse (Agilent, Santa Clara, CA, USA) based on a previously reported method.[11,19,20] A stock solution of curcumin (2.7 mM) was prepared in ethanol followed by serial dilution to concentrations of 1 mM in ethanol/Tris-HCl buffer (60:40%), 0.5 mM in ethanol buffer (30:70%) and concentration range of 0-200 μM in Tris-HCl buffer at pH 7.4. Solutions of PPI and SPPI (0.25 mg/mL) were prepared in Tris-HCl and mixed with an equal volume of the various concentrations of curcumin to obtain a final protein concentration of 0.125 mg/mL and curcumin concentrations of 0-100 μM. Fluorescence spectra were recorded at λ_{ex} 280 nm (Trp) and λ_{em} from 300-500 nm. Similarly, the interaction of curcumin with protein was investigated in the presence of chitosan. All measurements were carried out in triplicate and the intensity at 334 nm (tryptophan) was used to calculate the binding parameters as previously reported.[11,19,20]

If the quenching reaction between curcumin and PPI or SPPI obeys Eq. 2.1, the binding constant K_A and number of binding sites for curcumin, *n* could be determined graphically from the intercept and slope respectively of a plot of $\log\left[\frac{F_o-F}{F}\right]$ vs. $log[Q]$.

$$\log\left[\frac{F_o - F}{F}\right] = logK_A + nlog[Q] \qquad 2.1$$

[Q] is the molar concentration of the quencher (curcumin), and F and F_0 are the fluorescence intensity with and without curcumin, respectively.

The modified Stern-Volmer equation (Eq. 2.2) was used to estimate the accessible fluorophore fraction (*f*) and the Stern-Volmer quenching constant *K* from the intercept and slope of a plot of $\frac{F_o}{F_o-F}$ vs. $\frac{1}{[Q]}$ (Eq. 2.2).

$$\frac{F_o}{F_o - F} = \frac{1}{fK[Q]} + \frac{1}{f} \qquad 2.2$$

The Stern-Volmer equation (Eq. 2.3) was used to estimate the biomolecular quenching rate constant (K_Q) from a slope of $\frac{F_o}{F}$ vs. $[Q]$ (Eq. 2.3) plot.

$$\frac{F_o}{F} = 1 + K_Q t_o[Q] = 1 + K_D[Q] \qquad 2.3$$

Here, K_D is the Stern-Volmer quenching constant while t_o is the lifetime of the protein fluorophore in the absence of curcumin, usually in the order of 10^{-9} seconds.[11,19,20]

2.5.1. Fluorescence stability of the protein-curcumin complex

The fluorescence intensity of PPI or SPPI (0.25 mg/mL, 1 mL) mixed with curcumin solution (100 μM, 1 mL) was monitored in a fluorescence spectrophotometer at different intervals (0, 0.5, 1, 1.5, 2, 3, 4, 5, 6, 7 h). Each scan was taken after shaking and triplicate spectra were recorded.

2.6. Circular dichroism (CD) Spectroscopy

The CD spectra of the native pea protein, succinylated form and their polyelectrolyte complexes with chitosan were measured at concentration of 0.25 mg/mL in water instead of buffer to eliminate charge interference. The spectra were scanned at a wavelength range of 185–260 nm with Jasco J-715 Circular Dichroism (CD) spectrometer (Jasco Corp., Tokyo, Japan) using quartz cuvette with a path length of 0.01 cm at 25°C in nitrogen gas. Three scans were recorded at a scan rate of 50 nm/min and a bandwidth of 1 nm and averaged to obtain the final spectrum. Using a mean residue

molecular weight of 110 g/mol, mean residue ellipticity ($degcm^2dmol^{-1}$) was obtained. Water blank spectrum was subtracted from the average spectra of the samples and smoothened to obtain the corrected spectra. The secondary structure fractions were calculated from the mean residue ellipticity at wavelengths 185–260 nm using CD Pro software installed with CONTIN/LL method.

2.7. Thermal stability of PPI, SPPI and their curcumin/chitosan complexes

The thermal stability of PPI, SPPI and the biopolymer nano-complexes was investigated using differential scanning calorimetry (DSC Q2000, TA instruments, USA). Samples (1.5-6 mg) were separately sealed in a clean pre-weighed Tzero Aluminum Hermetic pan, then purged with pure nitrogen gas at a flow rate of 20 mL/min and the thermogram recorded from 25-250°C at a scan rate of 10°C/min. An empty pan was used as a reference. The transition enthalpies (J/g) were evaluated using Origin 9 software (OriginLab Corporation, Northampton, Massachusetts, USA) from the area of integrated peak or dip of the plot of $\frac{heat\ flow\ (\frac{mJ}{s})}{weight\ of\ sample\ (mg)}\ vs\ time\ (s)$.

2.8. Preparation of protein nanoparticle and curcumin encapsulation

2.8.1. Solution preparation

Curcumin (1 mg/mL) and chitosan (2.5 mg/mL) were prepared in ethanol and acetic acid (1%) respectively, while the protein samples, SPPI and PPI (5 mg/mL), were prepared in Milli-Q water. The solutions of chitosan and protein were stirred for 6 h using a magnetic stirrer (Cimarec, ThermoFisher Scientific, Waltham, MA USA) in separate flasks and centrifuged at 40,000 × g for 30 min using Sorvall LYNX 4000 superspeed centrifuge (ThermoFisher Scientific, Waltham, MA USA). The supernatants were collected by vacuum filtration (Whatman filter paper number 50, pore size 2.7 μm) and degassed with Polylab vacuum desiccator to remove impurities and air

bubbles from the solution. Curcumin solutions were protected from light by wrapping containers with aluminum foil.

2.8.2. Synthesis of curcumin-loaded protein nano-complexes

The preparation of CUR/PPI and CUR/SPPI nano-complexes was carried out following a previously reported method[11] with minor modifications. The solution of curcumin (10 mL, 1 mg/mL) was added dropwise separately into PPI and SPPI solutions (100 mL). The reactions were stirred (320 rpm) and monitored for 5 h until a steady negative zeta-potential was obtained. Low aqueous solubility of curcumin led to the generation of nanoparticles, which were recovered by centrifugation at 40,000 × g for 20 min. The residues were washed twice with deionized water, freeze-dried and the powdered samples stored at -20 °C.

2.8.3. Synthesis of PPI/CHI and SPPI/CHI hollow nano-complexes

The protein-chitosan hollow nano-complexes (i.e., not loaded with curcumin) were prepared by the dropwise addition of chitosan solution (50 mL, 2.5 mg/mL) to the various protein solutions (100 mL) until a steady positive zeta potential was maintained. The solutions were stirred for 5 h and the precipitate recovered by centrifugation at 40,000 × g for 20 min, washed twice with deionized water and lyophilized. The powdered particles were stored in -20 °C before analysis.

2.8.4. Synthesis of CUR/PPI/CHI and CUR/SPPI/CHI nano-complexes

The curcumin-loaded protein-chitosan nano-complexes were prepared by the electrostatic deposition method[6,11] through dropwise addition of chitosan solution (50 mL, 2.5 mg/mL) into the solution of curcumin-protein complexes (100 mL protein, 10mL CUR) prepared in section 2.8.2, with stirring (320 rpm) for additional 5 h. The biopolymer nano-complexes formed were recovered

by centrifugation at 40,000 × g, washed twice with deionized water and freeze-dried. The resulting powders were stored at -20 °C before analysis.

2.9. Characterization of the biopolymer nano-complexes

2.9.1. Measurement of particles size, zeta potential, and polydispersity

The average particle size, zeta potential, and polydispersity of the various biopolymer nano-complexes were determined with Nano-ZS Zetasizer (Malvern Instruments Ltd., Malvern, UK). Dilute solutions of the nano-complexes (refractive index 1.450, absorption 0.001) were prepared and analyzed in Milli-Q water (pH 7, refractive index 1.330, viscosity 0.8872 cP and dielectric constant 78.5) to avoid multiple scattering effects. Triplicate analysis was performed at 25 °C using the Smoluchowski model at F(ka) 1.50 and backscattered angle of 173°.

2.9.2. Determination of particle morphology

The morphology of the freshly prepared colloidal solution of the freeze-dried nano-complexes was determined with a transmission electron microscope (JEM-2100F Field Emission Electron Microscope, JEOL, Tokyo, Japan). The particles were dispersed in aqueous ethanol by ultrasonication for 10 min and Aa drop of various colloidal solution was placed on a carbon film 300 mesh, copper grid and left for 1 h to dry. Before this, glow-discharge was performed on the grids for 50 s using the Gatan Solarus Advanced Plasma System.

2.9.3. Fourier transform infrared spectroscopy (FTIR) analysis

The functional group and non-covalent bond interaction of the biopolymer nano-complexes were investigated with an infrared spectrometer (Nicolet 6700 FTIR, ThermoFisher Scientific,

Waltham, MA USA). The FTIR spectra were recorded in absorbance mode from 4000 to 400 cm^{-1} after background subtraction.

2.10. Encapsulation efficiency

Curcumin encapsulation efficiency was determined by UV-Vis spectrophotometer (Spark multimode microplate reader, Tecan, Stockholm, Sweden) as previously reported [6,11] with slight modification. First, the calibration curve (R^2 = 0.996) of various concentrations of curcumin (0-10 μg/mL) in ethanol was prepared at the excitation wavelength of 425 nm.[11] The biopolymer complexes containing curcumin were dispersed in ethanol, vortexed for 30 s and then centrifuged at 5,000 × g for 10 min. Absorbance measurement of the supernatant was performed at λ_{max} 425 nm to estimate the concentration of curcumin and encapsulation efficiency was estimated from Eq. 2.4.

$$\text{EE}\ (\%) = \frac{E_{CUR}}{\text{C}} \times 100 \qquad 2.4$$

E_{CUR} is the encapsulated curcumin (mg) and C is the curcumin input (mg).

2.11. Kinetic release profile of curcumin and membrane permeability studies

In vitro kinetic release profile of curcumin and its membrane permeability were studied for the free curcumin and protein/chitosan biopolymer nano-complexes in simulated salivary fluid (SSF), gastric fluid (SGF) and intestinal fluid (SIF) as previously reported.[11,14] The SSF, SGF, and SIF electrolytes were prepared according to the consensus protocol.[21]

2.11.1 Oral phase

The powdered curcumin-loaded nano-complexes and free curcumin (2 mg in each case) were dispersed separately in SSF (pH 7). $CaCl_2$ (25 μL, 0.3 M) and salivary α-amylase (1500 U/mL)

were added to attain an enzyme concentration of 75 U/mL in the total volume of 10 mL. The mixture was poured into a dialysis tube (3.5 kD molecular weight cut-off) and placed into a flask containing the releasing media [200 mL SSF (50% ethanol)], free of enzyme and $CaCl_2$. The mixture was incubated for 2 min at 37 °C followed by absorbance reading of the releasing media at 425 nm.

2.11.2 Gastric phase

SGF electrolyte (10 mL) containing $CaCl_2$ (5 μL, 0.3 M) and pepsin (1.6 mL, 2500 U/mL) were mixed with an oral phase containing the various samples of free curcumin and curcumin-loaded nano-complexes in a dialysis bag. The pH was adjusted to 1.2 with HCl (1 M) and the sample added into a flask containing 200 mL of SGF releasing media (50 % ethanol) free of enzyme and $CaCl_2$, and incubated for 2 h at 37 °C while shaking at 120 rpm. Aliquots (1 mL) of the releasing media were withdrawn every 30 min for absorbance reading at 425 nm and replaced with the exact volume of fresh SGF releasing media.

2.11.3. Small intestinal phase

After 2 h of incubation in the SGF, the content in the dialysis bag was mixed with SIF (20 mL) containing pancreatin solution (5 mL, 800 U/mL), fresh bile (2.5 mL, 160 mM) and $CaCl_2$ (40 μL, 0.3 M), and transferred into a flask containing 200 mL of SIF releasing medium (50% ethanol) free of enzyme and $CaCl_2$. The mixture was incubated at 37 °C for 4 h while shaking at 120 rpm. The cumulative curcumin released into the media was estimated using a similar procedure as in SGF. For the three stages of stimulated digestion, the amount of curcumin released was quantified by determining the excitation scan of curcumin and plotting a calibration curve (Figure S2.1 a&b).

2.12. Statistical analysis

The results were presented as mean ± standard deviation obtained from triplicate measurements and analyzed by one-way analysis of variance (ANOVA) using Origin 9 software (OriginLab Corporation, Northampton, Massachusetts, USA). Tukey's test was used to analyze group mean differences and values at $p < 0.05$ were considered significantly different.

3. Results and discussion

3.1. Effect of succinylation on pea protein surface hydrophobicity

The binding affinity of curcumin to proteins majorly depends on the surface hydrophobicity of the protein. Their interaction decreases with a decrease in protein hydrophobicity. In fact, curcumin has been suggested as a potential probe for assessing the hydrophobicity of proteins.[22] Based on this phenomenon, the impact of succinylation on the surface hydrophobicity of pea protein isolate was investigated. Succinylation decreased the surface hydrophobicity of the pea protein by nearly 3 folds (Figure S2.2). Nonetheless, the values for PPI and SPPI were within the range of surface hydrophobicity reported for isolated wheat and soy proteins,[23] bovine serum albumin, and insect proteins,[11] which have been used to encapsulate curcumin. Thus, the surface hydrophobicity data suggest possible curcumin binding to both the native and succinylated pea proteins, albeit to different extents, and hence their potential application in the encapsulation and delivery of curcumin.

3.2. Binding parameters for curcumin-protein interaction

The excitation scan of the proteins showed a dominant peak of tryptophan at 280 nm (Figure S2.3). The fluorescence emission properties of the protein would depend on the environment of this residue (apolar or aqueous) and their interaction with specific biomolecules known as the

quencher.[24] The intensity of the fluorescence and maximum emission wavelength of tryptophan may change on interaction with curcumin due to physical or chemical processes, such as molecular rearrangement, direct quenching, excited-state reaction, and energy transfer. These processes may lead to changes in secondary structure and conformation of the protein,[19,20,25,26] which consequently reveal the strength of the binding and accessibility of curcumin to protein pockets containing the tryptophan residue.[27]

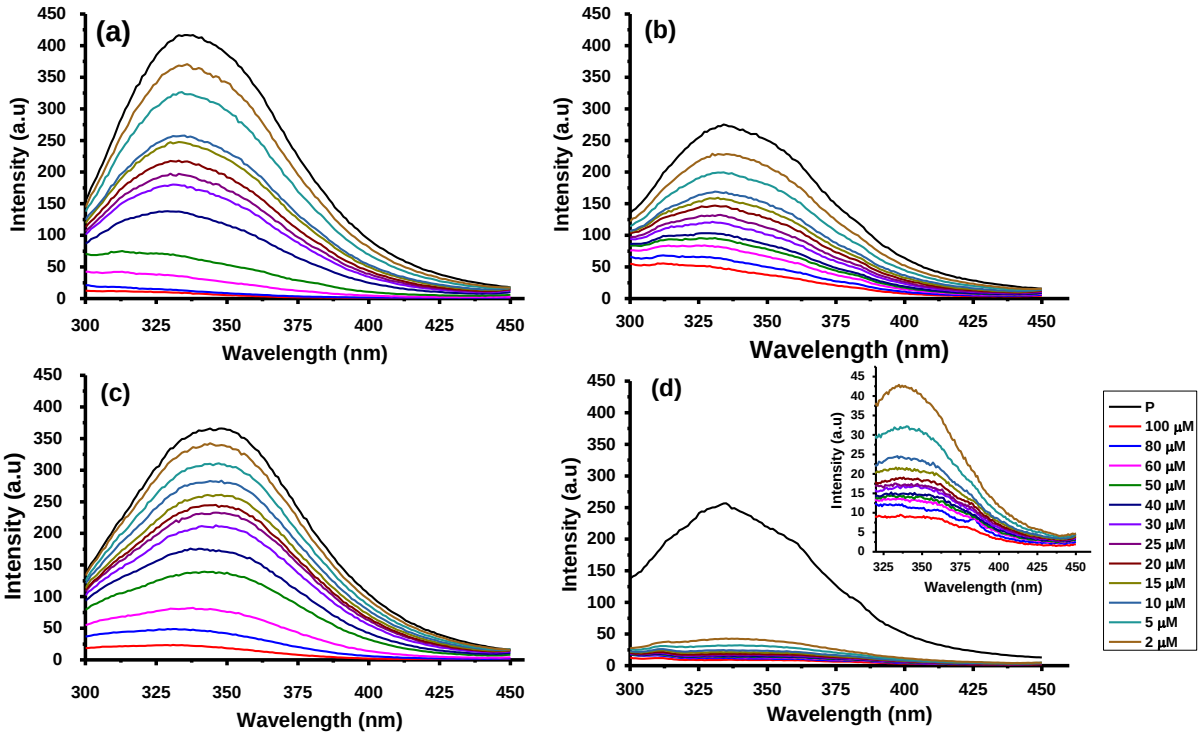

*P represents the intrinsic Trp fluorescence of (a) PPI, (b) PPI/CHI, (c) SPPI and (d) SPPI/CHI in the absence of curcumin.

Figure 2.1. Fluorescence emission spectra of the (a) curcumin-native pea protein, (b) curcumin-native pea protein-chitosan, (c) curcumin-succinylated pea protein, and (d) curcumin-succinylated protein-chitosan interactions.

On succinylation, the fluorescence intensity of the native protein decreased, and the emission wavelength maxima experienced a red shift (Figure 2.1a & c). These changes were due to structural alteration upon protein modification.[28] Addition of chitosan to the native and modified protein or increase in the concentration of curcumin loaded on both proteins in the presence and absence of chitosan, decreased the fluorescence intensity (Figure 2.1a-d). This decrease was because the protein-chitosan, curcumin-protein and curcumin-protein-chitosan complex formation induced conformational changes on the protein structure.[19] The magnitude of decrease in fluorescence intensity with increasing concentration of curcumin was higher in the native protein-curcumin compared to the modified protein. This could be attributed to stronger hydrophobic interaction leading to stronger binding, as depicted by their *K* values (Figure 2.1a & c, Table 2.1). An opposite effect was observed in the presence of chitosan due to stronger electrostatic interaction between the modified protein and chitosan, which restored the net hydrophobicity and improved protein-curcumin binding (Figure 2.1b & d, Table 2.1).[29] The wavelength of maximum fluorescence emission remained constant on increasing the concentration of curcumin, which suggests that the tryptophan residue was not exposed to changes in polarity,[19,20] solvent effect, and hydrogen bonding.[30] This indicates that the tryptophan residue was buried in the hydrophobic pocket of the protein and could be the site of interaction of the pea protein with curcumin. This was further corroborated by the emission λ_{max} at 334 nm for native protein-curcumin, native protein-curcumin-chitosan and succinylated protein-curcumin-chitosan, as well as the small value of accessible fluorophore fraction (Table 2.1), which quantifies the interaction occurring in the hydrophobic core of proteins. However, the emission λ_{max} at 344 nm for succinylated protein-curcumin suggests that the tryptophan residue or hydrophobic core of the protein was exposed upon succinylation and could have contributed to the low binding, thus influencing curcumin

encapsulation (Table 2.1).[24,31,32] Therefore, the native pea protein and the succinylated form with chitosan have the potential of improving the stability and solubility of Curcumin.[33]

Table 2.1. Binding parameters and encapsulation efficiency of the pea protein-curcumin nano-complexes.

Complexes	K ($\times 10^4$ M^{-1})	K_D ($\times 10^4$ M^{-1})	K_Q ($\times 10^{13}$ $M^{-1}S^{-1}$)	n	f	EE (%)
CUR/PPI	6.9 ± 0.21^{c}	4.6 ± 0.01^{b}	4.6 ± 0.01^{b}	1.00 ± 0.01^{a}	0.92 ± 0.01^{b}	34.65 ± 0.10^{d}
CUR/SPPI	4.2 ± 0.05^{d}	2.5 ± 0.03^{d}	2.5 ± 0.03^{d}	0.95 ± 0.04^{a}	0.83 ± 0.00^{c}	24.92 ± 0.03^{e}
CUR/PPI/CHI	14.5 ± 0.64^{b}	4.4 ± 0.01^{c}	4.4 ± 0.01^{c}	0.71 ± 0.01^{b}	0.71 ± 0.00^{d}	85.01 ± 1.43^{a}
CUR/SPPI/CHI	187.9 ± 12.40^{a}	18.0 ± 0.03^{a}	18.0 ± 0.03^{a}	0.54 ± 0.06^{c}	0.95 ± 0.00^{a}	62.05 ± 2.95^{b}
CUR/CHI	n.d.	n.d.	n.d.	n.d.	n.d.	41.88 ± 0.06^{c}

The superscriptsMean values with different letters (a-e) in a column indicates that the mean values are significantly different ($P < 0.05$).
Abbreviations: PPI, pea protein isolate; SPPI, succinylated pea protein; CUR, curcumin; CUR/SPPI, curcumin-succinylated pea protein complex; CUR/PPI, curcumin-pea protein complex; CUR/SPPI/CHI, curcumin-succinylated pea protein-chitosan complex; CUR/PPI/CHI, curcumin-pea protein-chitosan complex; CUR/CHI, curcumin-chitosan complex K, binding constant; n, substantive binding pockets of IP for curcumin; KD, Stern-Volmer quenching constant; KQ, biomolecular quenching rate constant; f, accessible fluorophore fraction; EE, encapsulation efficiency; n.d., not determined.

If fluorescence quenching is directly related to curcumin binding to the protein, the Trp peak intensity at 334 nm can be extracted and plotted as $\frac{F_o}{F_o - F}$ vs. $\frac{1}{[Q]}$ (Figure 2.2a & 2.3b, Figure 2.3a & 2.3b, Eq. 2.2) for the determination of the association constant, *K*. Chitosan-protein-curcumin complexes showed stronger binding affinity similar to well-known ligand-protein complexes.[34] However, the protein-curcumin complexes demonstrate moderate binding as shown in the K values (Table 2.1). This could be attributed to improved hydrophobicity and stability of the protein-chitosan complex by electrostatic interaction, which in turn increased the interaction between the protein and curcumin.[29] These values are comparable with that reported for curcumin binding to other proteins determined by fluorescence spectrophotometry.[11,19,20]

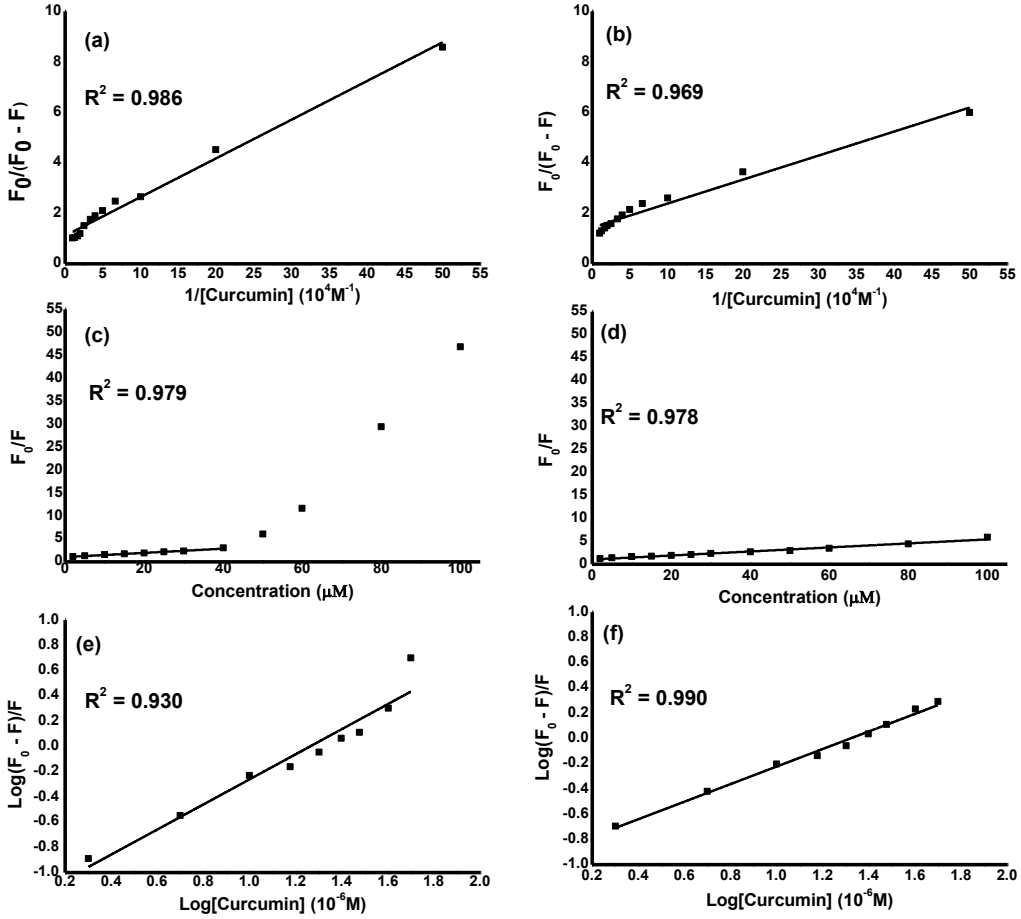

Figure 2.2. Plots of $F_0/(F_0-F)$ vs. 1/[Curcumin] for (a) CUR/PPI and (b) CUR/PPI/CHI complex for binding constant (*K*) determination. Stern-Volmer plots for quenching constant determination of (c) curcumin-PPI, and (d) curcumin-PPI-chitosan binding. Plots of $\log(F_0 - F)/F$ vs. log[Curcumin] for the determination of the number of bound curcumin (*n*) in the (e) CUR/PPI and (f) CUR/PPI/CHI complexes.

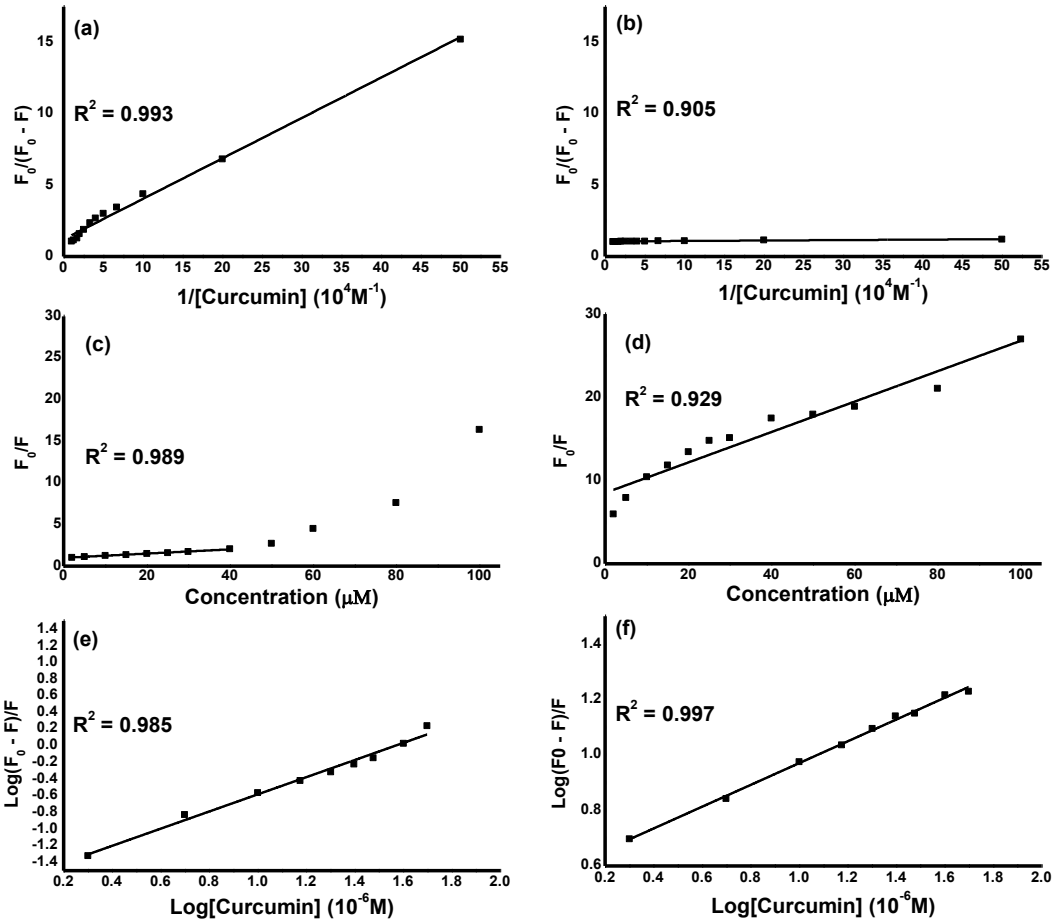

Figure 2.3. Plots of $F_0/(F_0\text{-}F)$ vs. 1/[Curcumin] for (a) CUR/SPPI and (b) CUR/SPPI/CHI complex for binding constant (*K*) determination. Stern-Volmer plots for quenching constant determination of (c) curcumin-SPPI, and (d) curcumin-SPPI-chitosan binding. Plots of $\log(F_0 - F)/F$ vs. log[Curcumin] for the determination of the number of bound curcumin (*n*) in the (e) CUR/SPPI and (f) CUR/SPPI/CHI complexes.

The presence of static and dynamic quenching was investigated through a plot of $\frac{F_o}{F}$ vs. $[Q]$ (Figure 2.2c & 2.2d, Figure 2.3c & 2.3d, Eq. 2.3). Interestingly, native pea protein-curcumin and succinylated protein-curcumin showed static quenching (linear plot) at low curcumin concentrations and dynamic quenching above 40 μM. However, the incorporation of chitosan

favoured mainly static interaction. This could be another reason for the higher binding affinity of the protein to curcumin in the presence of chitosan (Table 2.1). The biomolecular quenching rate constant (K_Q) values, which were higher than the value (2×10^{10} $M^{-1}S^{-1}$) reported as maximum static quenching for ligand-macromolecule interaction, is an indication that binding was mainly static leading to the formation of non-fluorescent complexes.[35] Both K_Q and Stern-Volmer quenching constant (K_D) increased on the incorporation of chitosan to the succinylated form (Table 2.1). This increase was due to the predominantly static interaction in the complex (Figure 2.3d), and stronger electrostatic interaction between the highly negatively charged succinylated pea protein and the positively charged chitosan (Table 2.2), which increases hydrophobicity. This result indicates that even though succinylation decreased hydrophobicity (Figure S2.2), electrostatic interaction with chitosan restored the hydrophobicity of the protein within the complex. The K_Q and K_D values are consistent with the range of values reported for curcumin-protein interaction.[11,19,20]

The number of curcumin molecule bound per protein (*n*) was estimated from Figure 2.2e & 2.2f, 2.3e & 2.3f, and Eq. (2.1), and data presented in Table 2.1. The *n* values, which decreased in the presence of chitosan, showed approximately one curcumin molecule per protein molecule binding. The decrease in *n* values can be attributed to electrostatic interaction between chitosan and protein, which could have blocked some accessible binding pocket of curcumin. As expected, an increase in negative charge on the protein by succinylation (Table 2.2) would increase electrostatic interaction with chitosan giving rise to about 50% decrease in *n* value of curcumin-succinylated protein-chitosan complex. These values are comparable with those reported for curcumin-protein binding.[11,19,20]

Table 2.2. Dynamic light scattering data, transition temperatures and enthalpies of the redispersed freeze-dried particles.

Complexes	Size (nm)	PDI	Zeta potential (mV)	Transition temperature (°C)	Transition enthalpy (J/g)
PPI/CHI hollow	151.5 ± 7.7^{bc}	0.50 ± 0.04^{a}	+40.8 ± 2.0^{b}	157.4	84.42
SPPI/CHI hollow	176.3 ± 10.0^{ab}	0.26 ± 0.01^{bcd}	+20.3 ± 1.9^{c}	136.3, 145.0, 171.7	0.89, 4.55, 101.76
CUR/PPI	165.6 ± 11.0^{abc}	0.49 ± 0.06^{a}	-46.8 ± 0.4^{f}	135.9, 152.5, 158.3, 233.0	5.20, 2.45, 2.85, 95.12
CUR/SPPI	159.9 ± 1.1^{abc}	0.23 ± 0.00^{cd}	-53.9 ± 0.4^{g}	167.1, 213.9	22.63, 2.49
CUR/PPI/CHI	194.5 ± 7.6^{a}	0.42 ± 0.03^{abc}	+20.9 ± 0.3^{c}	154.3, 234.3	3.91, 69.08
CUR/SPPI/CHI	183.3 ± 0.6^{ab}	0.16 ± 0.01^{d}	+12.8 ± 0.9^{d}	150.9, 158.7, 193.5	0.28, 0.70, 10.02
CUR/CHI	152.0 ± 7.6^{bc}	0.47 ± 0.11^{ab}	+39.5 ± 1.3^{b}	n.d.	n.d.
PPI	107.9 ± 1.4^{d}	0.27 ± 0.01^{bcd}	-34.4 ± 0.2^{e}	137.0, 158.2, 161.2	2.45, 0.76, 8.45
SPPI	130.5 ± 1.1^{cd}	0.27 ± 0.01^{bcd}	-59.9 ± 0.9^{h}	158.1	136.32
CHI	131.7 ± 12.2^{cd}	0.40 ± 0.02^{abc}	+63.2 ± 0.8^{a}	n.d.	n.d.

The superscripts with different letters (a-h) in a column indicates that the mean values are significantly different ($P < 0.05$).
n.d., not determined.Mean values with different letters in a column are significantly different ($P < 0.05$)
Abbreviations: PPI, pea protein isolate; SPPI, succinylated pea protein; CUR, curcumin; CHI, chitosan; CUR/SPPI, curcumin-succinylated pea protein nano-complex; CUR/PPI, curcumin-pea protein nano-complex; CUR/SPPI/CHI, curcumin-succinylated pea protein-chitosan nano-complex; CUR/PPI/CHI, curcumin-pea protein-chitosan nano-complex; CUR/CHI, curcumin-chitosan nano-complex; SPPI/CHI hollow, succinylated pea protein-chitosan shell; PPI/CHI hollow, native pea protein-chitosan shell; n.d., not determined.

3.3. Stability of the protein-curcumin interactions

The stability of the curcumin-protein binding in solution was investigated by fluorescence spectrophotometry. The spectra (Figure S2.4) showed fluctuations in fluorescence intensity over time, which is peculiar to the dynamic binding behaviour. This could be attributed to conformational changes because of the association of protein and curcumin or dissociation of the complex in solution over time. The magnitude of increase in fluorescence intensity of the native pea protein-curcumin complex appeared higher than that of the modified protein-curcumin. This is probably due to unfavourable binding (Table 2.1) leading to faster rate of complex decomposition. These observations support the dynamic binding observed in the plot of

$\frac{F_0}{F}$ Vs curcumin concentration (Figs. 2.2c & 2.3c) and justify the need for chitosan incorporation, which promoted mostly static binding. A similar dynamic binding behaviour was reported for insect protein-curcumin, although addition of chitosan did not favour static binding.[11] This is probably due to different structural properties or weaker electrostatic interaction in the moderately anionic protein compared to the highly anionic native and modified pea proteins used in our study.

3.4. Protein conformation

The effect of succinylation and electrostatic interaction with chitosan on protein conformation was investigated by circular dichroism. As shown in Table 2.3, succinylation significantly favoured the formation of both regular and distorted α-helix while decreasing the proportion of regular and distorted β-strand. Unlike native pea protein, the changes in the protein secondary structure caused by succinylation considerably influenced the protein-chitosan interaction. This could be attributed to strong electrostatic interaction formed between the highly negatively charged SPPI and the positively charged chitosan. The conformational changes in protein due to succinylation influenced its hydrophobicity (Figure S2.2) and interaction with curcumin (Table 2.1), which could affect encapsulation and release behaviour.

Table 2.3. Effect of succinylation and interaction with chitosan on the secondary structure of pea protein.

Secondary structure fractions (%)						
Samples	Regular α-helix	Distorted α-helix	Regular β-strand	Distorted β-strand	Turn	Unordered
PPI	0.3	3.7	28.5	14.3	21.6	31.6
SPPI	8.8	10.4	17.5	10.8	22.2	30.4
PPI/CHI	0.3	4.1	28.4	14.3	21.9	31.1
SPPI/CHI	10.4	8.4	19.5	10.6	21.1	30.0
PPI, pea protein isolate; SPPI, succinylated pea protein; PPI/CHI, native pea protein-chitosan complex; SPPI/CHI, succinylated pea protein-chitosan complex.						

3.5. Thermal stability of the complexes

Some of the major criteria in the application of protein for the encapsulation of bioactive compounds are favourable molecular interactions between the ligand and protein, and stability of the complex. The latter is very important especially in food processing and storage. Thus, the thermal stability of the proteins and biopolymer complexes of curcumin was investigated. Differential scanning calorimetric thermograms (Figure S2.5, Table 2.2) showed that succinylation modified the thermostability of the protein by merging the three transition temperatures in PPI into one broad peak, which could improve the thermal stability of the lowest peak at 137°C. The interaction of the native and modified proteins with curcumin or chitosan and on the coating with chitosan, to form curcumin-protein, protein-chitosan and curcumin-protein-chitosan, increased the thermal stability of the protein as observed from their transition temperatures and enthalpies (Table 2.2). The transition enthalpy of the native protein is generally lower than that of the succinylated form and the complexes formed with curcumin or chitosan. This indicates that the native protein is more prone to denaturation than the modified one, and interaction with curcumin or chitosan conferred additional stability. This could be due to the hydrophobic interaction in curcumin-protein complexes and electrostatic interactions in protein-chitosan or curcumin-protein-chitosan complexes, which increased hydrophobic interaction and hence the stability of the complexes.[29,36] This result is consistent with that reported for curcumin-gliadin,[37] insect protein-curcumin, and insect protein-curcumin-chitosan complexes.[11] Overall, pea protein stabilized with either chitosan or curcumin could be more resistant to changes in temperature.

3.6. Encapsulation and physicochemical properties of the biopolymer nano-complexes

3.6.1. Encapsulation efficiency

The encapsulation efficiency of various nano-complexes was estimated from Eq. 2.4 and presented in Table 2.1. Encapsulation efficiency decreased on protein succinylation due to a decrease in surface hydrophobicity (Figure S2.2) leading to a decrease in the binding affinity of the protein to curcumin (Table 2.1). Coating with chitosan significantly improved the encapsulation efficiency of both the native and succinylated proteins probably due to increased binding affinity and stability as noted from the K, K_D and K_Q values (Table 2.1), as well as increased hydrophobicity induced by electrostatic interaction between the protein and chitosan.[29] Interestingly, chitosan demonstrated encapsulation potential independently and this may have contributed to the increased encapsulation efficiency of the chitosan-coated complexes. The encapsulation efficiency is consistent with that reported for curcumin encapsulated with cruciferin-chitosan complex,[6] sunflower protein,[38] zein-sodium caseinate-sodium alginate complex,[13] zein-caseinate complex[14] and tannic acid crossed-linked hollow zein complex.[15]

3.6.2. Physicochemical properties of the biopolymer nano-complexes

The size, polydispersity and zeta potential of the nano-complexes were investigated during synthesis (Table S2.1) and after freeze-drying (Table 2.2) by electrophoresis and dynamic light scattering. Protein succinylation had no significant effect ($P < 0.05$) on the size of the various nano-complexes as shown for PPI vs. SPPI, PPI/CHI vs. SPPI/CHI, CUR/PPI vs. CUR/SPPI, and CUR/PPI/CHI vs. CUR/SPPI/CHI. This suggests that succinylation did not lead to protein degradation, agglomeration or aggregation. The particles are mainly homogenous within a size range of 100-195 nm with the chitosan-coated complexes showing larger diameters due to the

presence of an additional layer of a macromolecule. The presence of curcumin in the loaded chitosan, native or succinylated protein nanocomplexes led to increase in size of the particles compared to free protein or chitosan solution. These values are comparable with that reported for curcumin-zein-caseinate nano-complexes (187 nm),[14] curcumin-zein-caseinate-alginate nano-complexes (185-288),[13] curcumin-sunflower protein complex (194 nm),[38] insect protein-curcumin (176.6 nm) and insect protein-curcumin-chitosan complexes (161.2 nm).[11] The zeta potential values showed that all the curcumin-protein complexes were negatively charged due to the negative charge on the protein. The strength of this charge significantly increased after succinylation due to the neutralization of the positive charge of lysine (Scheme 2.1), a major amino acid in pea proteins.[7,8] This increase in negative charge of SPPI facilitated stronger electrostatic interaction with the positively charge chitosan. The positive charge on the curcumin-protein-chitosan complex indicated effective coating and stabilization of the complex with the cationic chitosan.

3.6.3. Morphological characterization of the nano-complexes

The morphology of the hollowed protein-chitosan and curcumin-loaded complexes were investigated by transmission electron microscopy. As shown in Figure 2.4. Both curcumin-loaded protein (Figure 2.4b & 2.4e) and curcumin-protein-chitosan complexes (Figure 2.4c & 2.4f) showed predominantly spherical nano-structures, whereas the hollow protein-chitosan complex images (Figure 2.4a & 2.4d) displayed several pores formed by electrostatic interaction, which suggests that pore formation could be the mechanism for curcumin encapsulation.[11] Like the particle size, succinylation of pea protein did not cause any significant change to the morphology of the nano-complexes. The size range of the particles is consistent with that obtained from dynamic light scattering (Table 2.2 & Table S2.1) with curcumin-protein-chitosan complex having

larger particle size than curcumin-protein complex due to additional layer of chitosan. The similar shape of curcumin-loaded complexes has been reported for insect protein-curcumin[11] and zein-caseinate-sodium alginate complexes.[13]

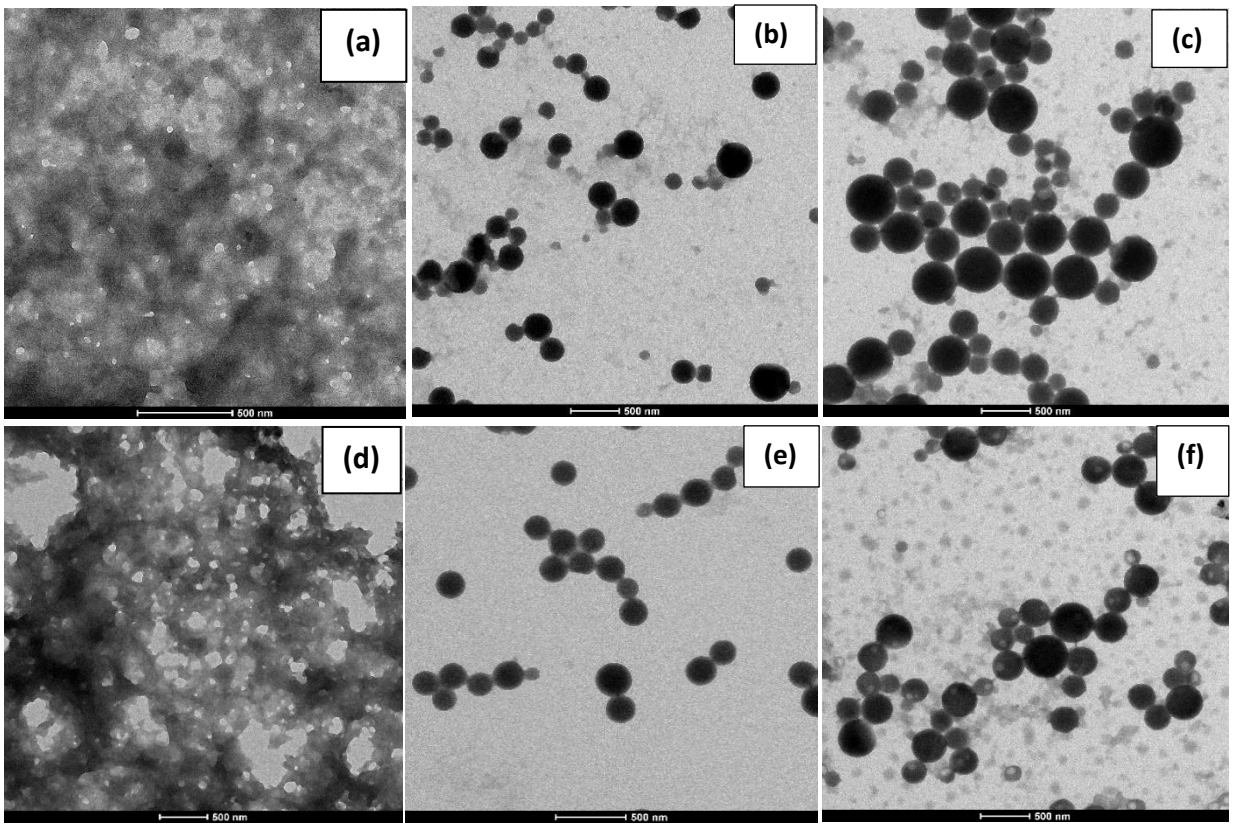

Figure 2.4. Transmission electron microscopy images of freshly prepared colloidalfreeze-dried and redispersed particles of (a) PPI/CHI hollow, (b) CUR/PPI, (c) CUR/PPI/CHI, (d)SPPI/CHI hollow, (e)CUR/SPPI, and (f) CUR/SPPI/CHI.

3.6.4. Functional group characterization of the nano-complexes

The impact of encapsulation, hydrogen bonding, electrostatic, covalent, and hydrophobic interaction on the functional group of pea proteins, curcumin, and chitosan was investigated by Fourier transformed infrared spectroscopy. The FTIR spectrum of curcumin (Figure 2.5a) displayed prominent peaks at 3509, 1503 and 1628 cm^{-1}, which are characteristics of -OH stretching vibrations of phenolic compounds, stretching vibration of C–C in aromatic ring system

and C=O stretching vibration of enol group, respectively. The peaks observed at 1273 and 1426 cm^{-1} are peculiar to the C–O stretching vibrations of alcohol and C–H bending vibration of alkane, whereas those in the region of 1022 to 961 cm^{-1} are as a result of C–O stretching vibrations in ester and carboxylic acid. The peaks observed at 857 and 805 cm^{-1} are consistent with the out-of-plane bending mode of meta- and para-substituted aromatic systems.[6,39] As shown in Figure 2.5b & 2.5c, succinylation did not cause any apparent modification in the FTIR spectra of the protein as the functional groups involved in succinylation are already inherent in the protein. The FTIR spectra of the protein-chitosan complexes (Figure 2.5e & 2.5f) retained almost all the prominent peaks of the proteins (Figure 2.5b & 2.5c) and chitosan (Figure 2.5d), suggesting that the interaction was mainly electrostatic.[12] The various spectra shifts observed in CUR/PPI, and CUR/SPPI compared to the individual CUR, PPI and SPPI could be attributed to the effect of hydrophobic interaction between protein core and curcumin while the shifts observed in PPI/CHI and SPPI/CHI compared to the individual proteins and chitosan could be attributed to strong electrostatic interaction between highly negatively charged protein and strongly positively charged chitosan (Table 2.2).[40] The FTIR spectra further collaborate the need of establishing a balance to ensure that the hydrophobic interaction between curcumin and protein does not disrupt strong electrostatic interaction between protein and chitosan and vice versa in the curcumin-protein-chitosan complexes. The spectra of native protein-curcumin (Figure 2.5g) and native protein-curcumin-chitosan (Figure 2.5i) showed decreased intensity or disappearance of prominent peaks of curcumin, suggesting that the bioactive compound was buried in the hydrophobic core of the protein, which decreased its molecular vibration. This supports the finding from fluorescence quenching that curcumin mainly binds in the hydrophobic pocket of the protein where the tryptophan residue is protected from changes in polarity. Similar behaviour has been reported for

insect protein-curcumin[11] and ovalbumin-curcumin complexes.[41] FTIR spectrum of the succinylated protein-curcumin nano-complex (Figure 2.5h) showed almost all the peaks of curcumin indicating that curcumin was not well encapsulated in the complex. This was probably because of the decreased protein hydrophobicity (Figure S2.2) leading to weak binding (Table 2.1). Coating the succinylated protein with chitosan (Figure 2.5j) buried these functional groups, suggesting favourable interaction because of restored hydrophobicity, well-organized protein structure, and increased binding as demonstrated from the binding parameters (Table 2.1). Overall, hydrophobic interaction occurring in the core of the protein, and electrostatic interaction between the protein and chitosan played major roles in stabilizing the complex.

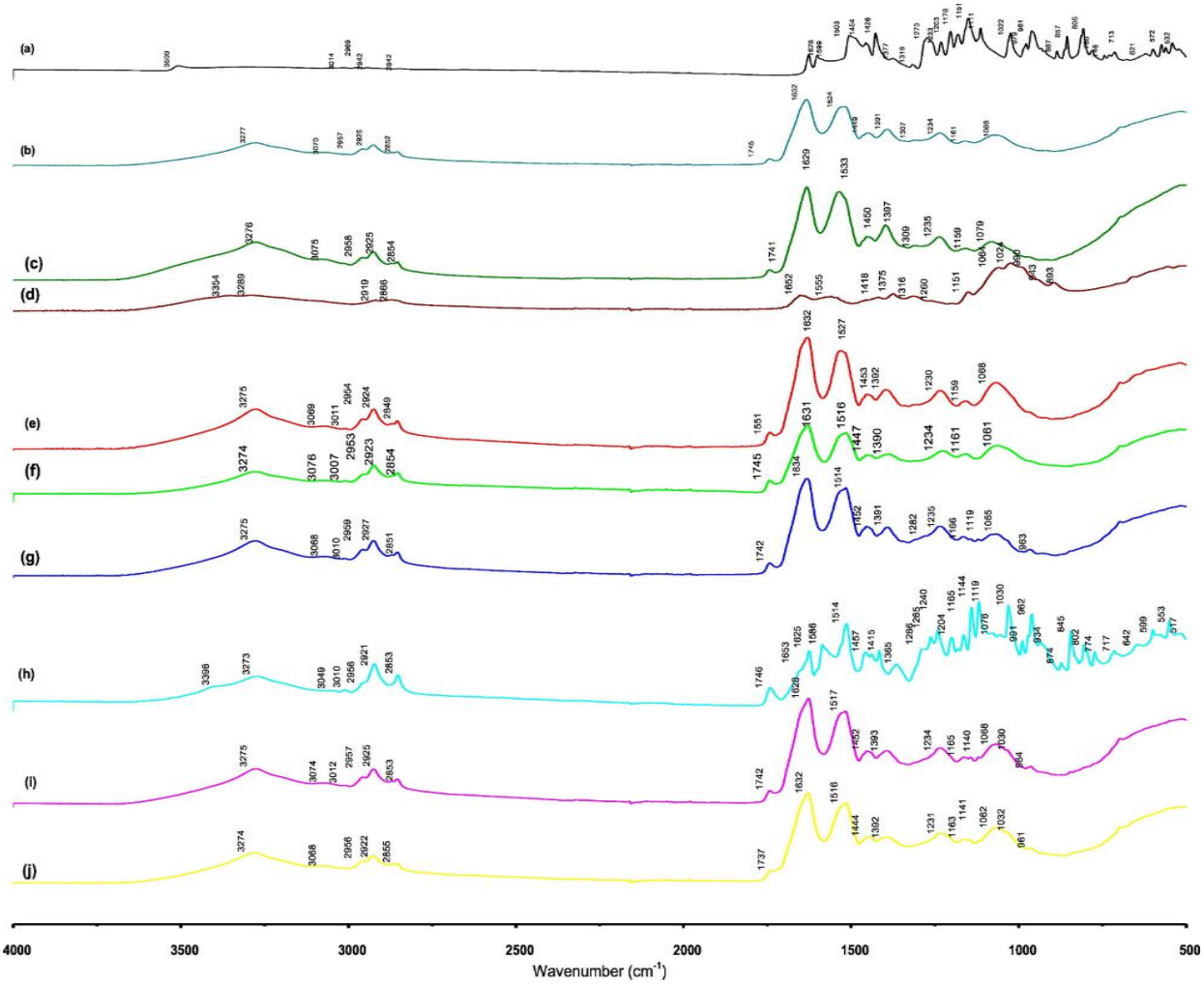

Figure 2.5. Fourier transformed infra-red spectra of (a) curcumin, (b) PPI, (c) SPPI, (d) CHI, (e) PPI/CHI, (f) SPPI/CHI, (g) CUR/PPI, (h) CUR/SPPI, (i) CUR/PPI/CHI, and (j) CUR/SPPI/CHI

3.76. In-vitro curcumin release from the complexes

The low aqueous solubility of curcumin and rapid degradation under physiological conditions have necessitated its encapsulation with proteins followed by chitosan coating to ensure the stability of the complex in the gastric phase. The release, membrane permeability, bioaccessibility, and cellular uptake of curcumin are crucial for its food, pharmaceutical, and medical applications. For this reason, the *in-vitro* curcumin release was investigated using a simulated oral/salivary, gastric, and intestinal fluid model to assess the effect of pea protein succinylation on gastrointestinal stability of the nano-complexes (Figure 2.6).

At the end of the oral phase, 1.25%, 12.76% and 0.29 % of curcumin was released from the free curcumin, CUR/PPI and CUR/SPPI, respectively, while 21.10%, 20.85% and 0.89 % was released from the CUR/PPI/CHI, CUR/SPPI/CHI and CUR/CHI complexes, respectively. The low values observed for free curcumin was due to its low solubility. The low values for CUR/SPPI and CUR/CHI were because of low hydrophobic interaction in CUR/SPPI due to the impact of succinylation (leading to the low curcumin solubility in the complex) and the absence of hydrophobic core in chitosan leading to low solubility of curcumin in the CUR/CHI complex. Higher values observed for CUR/PPI, CUR/PPI/CHI and CUR/SPPI/CHI were due to the increased solubility of curcumin because of favourable interaction occurring in the hydrophobic core of the protein (Table 2.1). Also, the isoelectric point of chitosan is close to 7 (the pH of salivary fluid), which might have decreased electrostatic interaction with the protein. Additionally, chitosan is less viscous at neutral pH and offers minimal protection by gelling effect unlike in acidic condition.

At the end of gastric digestion, 1.83%, 14.98% and 11.23% of curcumin was released from the free curcumin, CUR/PPI and CUR/SPPI, respectively, while 8.34%, 7% and 12.98% were released from the CUR/PPI/CHI, CUR/SPPI/CHI, and CUR/CHI complexes, respectively. The low values observed for CUR/PPI/CHI and CUR/SPPI/CHI were as a result of the increased positive charge on chitosan under the acidic gastric phase due to amine group protonation leading to stronger electrostatic interaction with the protein.[6,11] Also, chitosan is highly viscous at acidic pH and therefore, strengthens the curcumin-protein complexes through gelling effect thereby preventing the access of pepsin to the cleavage sites. This engineered behavior of curcumin-protein-chitosan ensures that a large amount of curcumin reaches the intestinal phase.

At the end of the small intestinal phase, the bioaccessibility of curcumin in free curcumin, CUR/PPI and CUR/SPPI were 9.89%, 64.10% and 12.52%, respectively, while those of CUR/PPI/CHI, CUR/SPPI/CHI and CUR/CHI were 62.69%, 57.73% and 16.66%, respectively. Unfavourable binding between succinylated protein and curcumin (Table 2.1) may be responsible for the low bioaccessibility of curcumin in the CUR/SPPI complex. There was no significant difference ($p < 0.05$) between the bioaccessible curcumin in the CUR/PPI, CUR/PPI/CHI and CUR/SPPI/CHI complexes. This was because CUR/PPI/CHI and CUR/SPPI/CHI stabilized the complex more during the gastric phase at approximately the same extent at which CUR/PPI stabilized its complex during the oral phase. Therefore, about the same amount of curcumin reached the small intestinal phase for these three complexes. Overall, the amount of curcumin released in the small intestinal phase was much higher than that observed in the oral and gastric phase. This is attributable to the presence of bile salts, which possess hydrophobic interior in the micelles that could solubilize curcumin.[42] Also, in the small intestine, chitosan losses its charge due to amine group deprotonation at pH 7, leading to a weak protein-chitosan interaction and,

consequently, dissociation of the complex.[6,11,43] The bioaccessibility of curcumin in the native pea protein and native or succinylated pea protein-chitosan complexes as observed in this study were significantly higher than those reported for whey protein-gum Arabic (33%),[12] zein-sodium caseinate-sodium alginate (17%),[13] zein-caseinate (10.6%)[14] and tannic acid crossed-linked hollow zein complexes (10-15%).[15] Therefore, native and succinylated pea proteins and their chitosan complexes have tremendous potential for future development as delivery vehicles for curcumin.

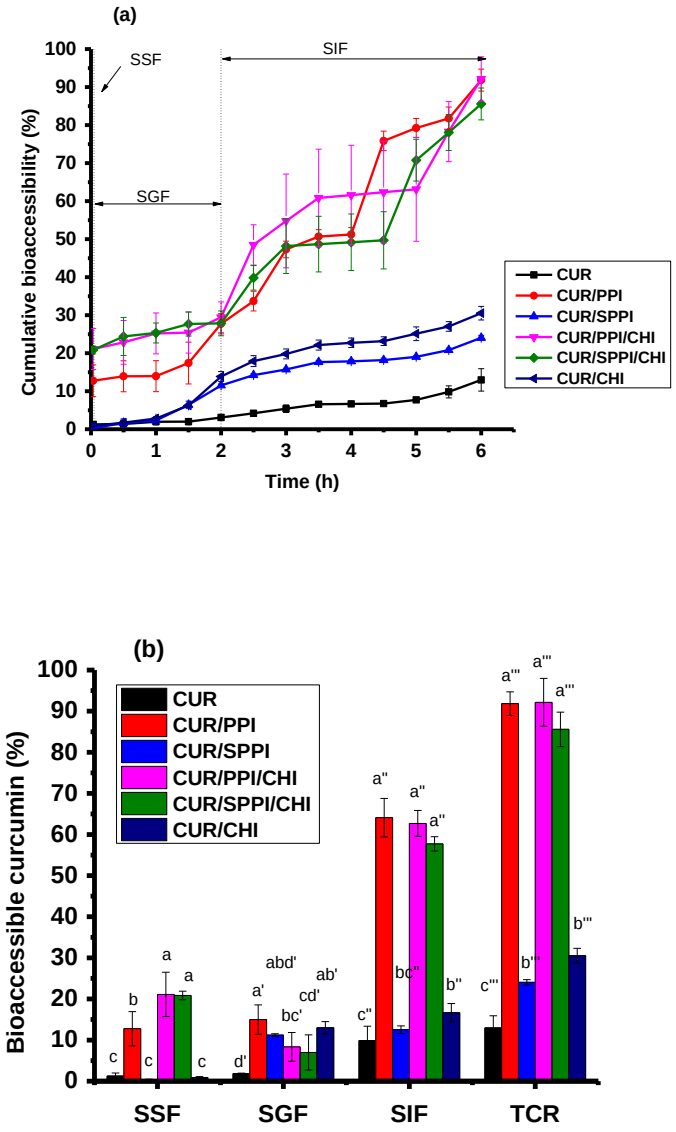

Figure 2.6. (a) Cumulative bioaccessibility profile of curcumin in free, CUR/PPI, CUR/SPPI, CUR/PPI/CHI, CUR/SPPI/CHI, and CUR/CHI complex forms under simulated salivary (SSF), gastric (SGF) and intestinal fluids (SIF). (b) Total bioaccessible curcumin at the various stages of the simulated salivary, gastric, and intestinal conditions.

4. Conclusion

This study demonstrated that curcumin-loaded biopolymer nano-complexes could be fabricated from native and succinylated pea proteins and their chitosan complexes. Succinylation increased the negative charge on the protein favouring electrostatic interaction with chitosan; however, it decreased its surface hydrophobicity hindering hydrophobic contact. Hydrophobic interaction between curcumin and the core of the protein increased the solubility and stability of curcumin. Hence, striking a balance during succinylation to ensure an increase in negative charge with little or no effect on the protein hydrophobicity is essential for curcumin encapsulation with the polyelectrolyte complex. The binding of curcumin to either the native pea protein or the succinylated protein showed some degree of dynamic binding whereas the incorporation of chitosan favoured static binding. The electrostatic interaction between the succinylated protein and chitosan restored the protein hydrophobicity and ensured stronger binding of curcumin. The stronger binding led to the highest encapsulation efficiency of curcumin in the native protein-chitosan complex. Compared to native protein-curcumin, there was a low curcumin release from succinylated protein-curcumin because of unfavourable binding and weaker stabilization occurring in the latter. Native pea protein-curcumin complex reduced the release of curcumin in the salivary phase more effectively than the complexes stabilized with chitosan whereas the latter showed better protection in the gastric phase. These behaviours culminated in the equivalent amount of curcumin reaching the intestinal phase and hence similar bioaccessibility for the two

complexes. Therefore, our study demonstrated that pea protein isolate could effectively encapsulate and release substantial amount of curcumin in a simulated gastrointestinal system, without protein modification by succinylation or polyelectrolyte complexation with chitosan.

Acknowledgements

This project was supported by the Natural Sciences and Engineering Research Council of Canada (NSERC) through the Discovery Grant Program (RGPIN-2018-06839) and the University of Ottawa through the University Research Chair Program Funds.

Reference

(1) Sun, X. D.; Arntfield, S. D. Gelation Properties of Salt-Extracted Pea Protein Induced by Heat Treatment. *Food Research International*. **2010**, *43*(2), 509-515. https://doi.org/10.1016/j.foodres.2009.09.039.

(2) Maninder, K.; Sandhu, K. S.; Singh, N. Comparative Study of the Functional, Thermal and Pasting Properties of Flours from Different Field Pea (Pisum Sativum L.) and Pigeon Pea (Cajanus Cajan L.) Cultivars. *Food Chemistry.* **2007**, *104*(1), 259-267. https://doi.org/10.1016/j.foodchem.2006.11.037.

(3) Adebiyi, A. P.; Aluko, R. E. Functional Properties of Protein Fractions Obtained from Commercial Yellow Field Pea (Pisum Sativum L.) Seed Protein Isolate. *Food Chemistry.* **2011,** *128*(4), 902-908. https://doi.org/10.1016/j.foodchem.2011.03.116.

(4) Lu, Z. X.; He, J. F.; Zhang, Y. C.; Bing, D. J. Composition, Physicochemical Properties of Pea Protein and Its Application in Functional Foods. *Critical Reviews in Food Science and Nutrition*. **2019**, 1-13. https://doi.org/10.1080/10408398.2019.1651248.

(5) Tömösközi, S.; Lásztity, R.; Haraszi, R.; Baticz, O. Isolation and Study of the Functional Properties of Pea Proteins. *Nahrung – Food.* **2001**, *45*(6), 399-401. https://doi.org/10.1002/1521-3803(20011001)45:6<399::AID-FOOD399>3.0.CO;2-0.

(6) Wang, F.; Yang, Y.; Ju, X.; Udenigwe, C. C.; He, R. Polyelectrolyte Complex Nanoparticles from Chitosan and Acylated Rapeseed Cruciferin Protein for Curcumin Delivery. *Journal of Agricultural and Food Chemistry.* **2018**, *66*(11), 2685-2693. https://doi.org/10.1021/acs.jafc.7b05083.

(7) Leterme, P.; Monmart, T.; Baudart, E. Amino Acid Composition of Pea (Pisum Sativum) Proteins and Protein Profile of Pea Flour. *Journal of the Science of Food and Agriculture.* **1990**, *53*(1), 107-110. https://doi.org/10.1002/jsfa.2740530112.

(8) Gudiksen, K. L.; Gitlin, I.; Moustakas, D. T.; Whitesides, G. M. Increasing the Net Charge and Decreasing the Hydrophobicity of Bovine Carbonic Anhydrase Decreases the Rate of Denaturation with Sodium Dodecyl Sulfate. *Biophysical Journal.* **2006**, *91*(1), 298-310. https://doi.org/10.1529/biophysj.106.081547.

(9) Hewlings, S.; Kalman, D. Curcumin: A Review of Its' Effects on Human Health. *Foods.* **2017**, *6*(10), 92. https://doi.org/10.3390/foods6100092.

(10) Anand, P.; Kunnumakkara, A. B.; Newman, R. A.; Aggarwal, B. B. Bioavailability of Curcumin: Problems and Promises. *Molecular Pharmaceutics*. **2007**, *4*(6), 807-818. https://doi.org/10.1021/mp700113r.

(11) Okagu, O. D.; Verma, O.; McClements, D. J.; Udenigwe, C. C. Utilization of Insect Proteins to Formulate Nutraceutical Delivery Systems: Encapsulation and Release of Curcumin Using Mealworm Protein-Chitosan Nano-Complexes. *International Journal of Biological Macromolecules.* **2020**, *151*, 333-343. https://doi.org/10.1016/j.ijbiomac.2020.02.198.

(12) Mohammadian, M.; Salami, M.; Alavi, F.; Momen, S.; Emam-Djomeh, Z.; Moosavi-Movahedi, A. A. Fabrication and Characterization of Curcumin-Loaded Complex Coacervates Made of Gum Arabic and Whey Protein Nanofibrils. *Food Biophysics.* **2019**, *14*(4), 425-436. https://doi.org/10.1007/s11483-019-09591-1.

(13) Liu, Q.; Jing, Y.; Han, C.; Zhang, H.; Tian, Y. Encapsulation of Curcumin in Zein/ Caseinate/Sodium Alginate Nanoparticles with Improved Physicochemical and Controlled Release Properties. *Food Hydrocolloids.* **2019**, *93*, 432-442. https://doi.org/10.1016/j.foodhyd.2019.02.003.

(14) Xue, J.; Zhang, Y.; Huang, G.; Liu, J.; Slavin, M.; Yu, L. (Lucy). Zein-Caseinate Composite Nanoparticles for Bioactive Delivery Using Curcumin as a Probe Compound. *Food Hydrocolloids.* **2018**, *83*, 25-35. https://doi.org/10.1016/j.foodhyd.2018.04.037.

(15) Hu, S.; Wang, T.; Fernandez, M. L.; Luo, Y. Development of Tannic Acid Cross-Linked Hollow Zein Nanoparticles as Potential Oral Delivery Vehicles for Curcumin. *Food Hydrocolloids.* **2016**, *61*, 821-831. https://doi.org/10.1016/j.foodhyd.2016.07.006.

(16) Thanh Uyen, N. T.; Abdul Hamid, Z. A.; Thi, L. A.; Ahmad, N. B. Synthesis and Characterization of Curcumin Loaded Alginate Microspheres for Drug Delivery. *Journal of Drug Delivery Science and Technology.* **2020**, *58*, 101796. https://doi.org/10.1016/j.jddst.2020.101796.

(17) Iurciuc-Tincu, C. E.; Cretan, M. S.; Purcar, V.; Popa, M.; Daraba, O. M.; Atanase, L. I.; Ochiuz, L. Drug Delivery System Based on PH-Sensitive Biocompatible Poly(2-Vinyl Pyridine)-b-Poly(Ethylene Oxide) Nanomicelles Loaded with Curcumin and 5-

Fluorouracil. *Polymers (Basel).* **2020**, *12*(7), 1450. https://doi.org/10.3390/polym12071450.

(18) Iurciuc-Tincu, C. E.; Atanase, L. I.; Ochiuz, L.; Jérôme, C.; Sol, V.; Martin, P.; Popa, M. Curcumin-Loaded Polysaccharides-Based Complex Particles Obtained by Polyelectrolyte Complexation and Ionic Gelation. I-Particles Obtaining and Characterization. *International Journal of Biological Macromolecules.* **2020**, *147*, 629-642. https://doi.org/10.1016/j.ijbiomac.2019.12.247.

(19) Bourassa, P.; Bariyanga, J.; Tajmir-Riahi, H. A. Binding Sites of Resveratrol, Genistein, and Curcumin with Milk α- And β-Caseins. *Journal of Physical Chemistry B.* **2013**, *117*(5), 1287-1295. https://doi.org/10.1021/jp3114557.

(20) Kanakis, C. D.; Tarantilis, P. A.; Polissiou, M. G.; Tajmir-Riahi, H. A. Probing the Binding Sites of Resveratrol, Genistein, and Curcumin with Milk β -Lactoglobulin. *Journal of Biomolecular Structure and Dynamics.* **2013**, *31*(12), 1455-1466. https://doi.org/10.1080/07391102.2012.742461.

(21) Minekus, M.; Alminger, M.; Alvito, P.; Ballance, S.; Bohn, T.; Bourlieu, C.; Carrière, F.; Boutrou, R.; Corredig, M.; Dupont, D.; Dufour, C.; Egger, L.; Golding, M.; Karakaya, S.; Kirkhus, B.; Le Feunteun, S.; Lesmes, U.; MacIerzanka, A.; MacKie, A.; Marze, S.; McClements, D. J.; Ménard, O.; Recio, I.; Santos, C. N.; Singh, R. P.; Vegarud, G. E.; Wickham, M. S. J.; Weitschies, W.; Brodkorb, A. A Standardised Static in Vitro Digestion Method Suitable for Food-an International Consensus. *Food & Function.* **2014**, *5*(6), 1113-1124. https://doi.org/10.1039/c3fo60702j.

(22) Sneharani, A. H. Curcumin as a Tool to Assess the Surface Hydrophobicity of Proteins. *Spectroscopy Letters.* **2016**, *49*(9), 568-572. https://doi.org/10.1080/00387010.2016.1223697.

(23) Konieczny, P.; Uchman, W. Comparative characterization of surface hydrophobicity and other physico-chemical properties of selected protein prepartions. *Electronic Journal of Polish Agricultural Universities*. **2002**, *5*(2).

(24) Liang, L.; Tajmir-Riahi, H. A.; Subirade, M. Interaction of β-Lactoglobulin with Resveratrol and Its Biological Implications. *Biomacromolecules.* **2008**, *9*(1), 50-56. https://doi.org/10.1021/bm700728k.

(25) Tayeh, N.; Rungassamy, T.; Albani, J. R. Fluorescence Spectral Resolution of Tryptophan Residues in Bovine and Human Serum Albumins. *Journal of Pharmaceutical and Biomedical Analysis.* **2009**, *50*(2), 107-116. https://doi.org/10.1016/j.jpba.2009.03.015.

(26) Mohammadi, F.; Bordbar, A. K.; Mohammadi, K.; Divsalar, A.; Saboury, A. A. Circular Dichroism and Fluorescence Spectroscopic Study on the Interaction of Bisdemethoxycurcumin and Diacetylbisdemethoxycurcumin with Human Serum Albumin. *Canadian Journal of Chemistry.* **2010**, *88*(2), 155-163. https://doi.org/10.1139/V09-169.

(27) Mohammadi, F.; Moeeni, M. Study on the Interactions of Trans-Resveratrol and Curcumin with Bovine α-Lactalbumin by Spectroscopic Analysis and Molecular Docking. *Materials Science and Engineering C.* **2015**, *50*, 358-366. https://doi.org/10.1016/j.msec.2015.02.007.

(28) Moafian, Z.; Khoshaman, K.; Oryan, A.; Kurganov, B. I.; Yousefi, R. Protective Effects of Acetylation on the Pathological Reactions of the Lens Crystallins with Homocysteine Thiolactone. *PloS One.* **2016**, *11*(10), e0164139. https://doi.org/10.1371/journal.pone.0164139.

(29) Miklavžin, A.; Cegnar, M.; Kerč, J.; Kristl, J. Effect of Surface Hydrophobicity of Therapeutic Protein Loaded in Polyelectrolyte Nanoparticles on Transepithelial Permeability. *Acta Pharmaceutica.* **2018**, 68(3), 275-293. https://doi.org/10.2478/acph-2018-0032.

(30) Yang, J. T.; Wu, C. S. C.; Martinez, H. M. Calculation of Protein Conformation from Circular Dichroism. *Methods in Enzymology.* **1986**, *130*, 208-269. https://doi.org/10.1016/0076-6879(86)30013-2.

(31) Mandeville, J. S.; Froehlich, E.; Tajmir-Riahi, H. A. Study of Curcumin and Genistein Interactions with Human Serum Albumin. *Journal of Pharmaceutical and Biomedical Analysis.* **2009**, *49*(2), 468-474. https://doi.org/10.1016/j.jpba.2008.11.035.

(32) Sułkowska, A. Interaction of Drugs with Bovine and Human Serum Albumin. *Journal of Molecular Structure.* **2002**, 614(1-3), 227-232. https://doi.org/10.1016/S0022-2860(02)00256-9.

(33) Tapal, A.; Tiku, P. K. Complexation of Curcumin with Soy Protein Isolate and Its Implications on Solubility and Stability of Curcumin. *Food Chemistry.* **2012**, *130*(4), 960-965. https://doi.org/10.1016/j.foodchem.2011.08.025.

(34) Kratochwil, N. A.; Huber, W.; Müller, F.; Kansy, M.; Gerber, P. R. Predicting Plasma Protein Binding of Drugs: A New Approach. *Biochemical Pharmacology.* **2002**, *64*(9), 1355-1374. https://doi.org/10.1016/S0006-2952(02)01074-2.

(35) Ware, W. R. Oxygen Quenching of Fluorescence in Solution: An Experimental Study of the Diffusion Process. *Journal of Physical Chemistry.* **1962**, *66*(3), 455-458. https://doi.org/10.1021/j100809a020.

(36) Schellman, J. A. Temperature, Stability, and the Hydrophobic Interaction. *Biophysical Journal.* **1997**, *73*(6), 2960-2964. https://doi.org/10.1016/S0006-3495(97)78324-3.

(37) Mathew, M. S.; Vinod, K.; Jayaram, P. S.; Jayasree, R. S.; Joseph, K. Improved Bioavailability of Curcumin in Gliadin-Protected Gold Quantum Cluster for Targeted Delivery. *ACS Omega.* **2019**, *4*(10), 14169-14178. https://doi.org/10.1021/acsomega.9b00917.

(38) Sneharani, A. H. Curcumin–Sunflower Protein Nanoparticles—A Potential Antiinflammatory Agent. *Journal of Food Biochemistry.* **2019**, *43*(8), e12909. https://doi.org/10.1111/jfbc.12909.

(39) Pecora, T. M. G.; Cianciolo, S.; Catalfo, A.; De Guidi, G.; Ruozi, B.; Cristiano, M. C.; Paolino, D.; Graziano, A. C. E.; Fresta, M.; Pignatello, R. Preparation, Characterization and Photostability Assessment of Curcumin Microencapsulated within Methacrylic Copolymers. *Journal of Drug Delivery Science and Technology.* **2016**, *33*, 88-97. https://doi.org/10.1016/j.jddst.2016.03.013.

(40) Taha, S.; El-Sherbiny, I.; Enomoto, T.; Salem, A.; Nagai, E.; Askar, A.; Abady, G.; Abdel-Hamid, M. Improving the Functional Activities of Curcumin Using Milk Proteins as Nanocarriers. *Foods.* **2020**, *9*(8), 986. https://doi.org/10.3390/foods9080986.

(41) Liu, Y.; Ying, D.; Cai, Y.; Le, X. Improved Antioxidant Activity and Physicochemical Properties of Curcumin by Adding Ovalbumin and Its Structural Characterization. *Food Hydrocolloids.* **2017**, *72*, 304-311. https://doi.org/10.1016/j.foodhyd.2017.06.007.

(42) Tian, C.; Asghar, S.; Wu, Y.; Chen, Z.; Jin, X.; Yin, L.; Huang, L.; Ping, Q.; Xiao, Y. Improving Intestinal Absorption and Oral Bioavailability of Curcumin via Taurocholic Acid-Modified Nanostructured Lipid Carriers. *International Journal of Nanomedicine.* **2017**, *12*, 7897. https://doi.org/10.2147/IJN.S145988.

(43) Okagu, O. D.; Wang, B.; Acquah, C.; Udenigwe, C. C. Protein-Based Nanodelivery Systems for Food Applications. In *Encyclopedia of Food Chemistry*; Melton, L., Shahidi, F., Varelis, P., Eds.; Academic Press, Oxford, United Kingdom. **2019**, 719–726. https://doi.org/https://doi.org/10.1016/B978-0-08-100596-5.21864-7.

SUPPLEMENTARY INFORMATION

Impact of succinylation on pea protein-curcumin interaction, polyelectrolyte complexation with chitosan, and gastrointestinal release of curcumin in loaded-biopolymer nano-complexes

Ogadimma D. Okagu, Jian Jin, Chibuike C. Udenigwe

Journal of Molecular Liquids **2021**, *325*, 115248. https://doi.org/10.1016/j.molliq.2020.115248.

Table S2.1. Zeta potential, mean diameter and polydispersity index of the colloidal solutions monitored during synthesis

Complexes	Size (nm)	PDI	Zeta potential (mV)
PPI/CHI hollow	105.6 ± 8.6^{d}	0.16 ± 0.00^{cd}	$+42.8 \pm 0.2^{b}$
SPPI/CHI hollow	232.5 ± 6.7^{a}	0.09 ± 0.04^{d}	$+22.3 \pm 1.6^{d}$
CUR/PPI	114.7 ± 1.3^{cd}	0.32 ± 0.02^{b}	-27.8 ± 0.1^{e}
CUR/SPPI	126.3 ± 3.3^{cd}	0.27 ± 0.01^{bc}	-37.2 ± 0.4^{f}
CUR/PPI/CHI	65.1 ± 4.5^{e}	0.63 ± 0.04^{a}	$+37.2 \pm 0.4^{c}$
CUR/SPPI/CHI	164.3 ± 5.0^{b}	0.27 ± 0.04^{bc}	$+37.4 \pm 0.6^{c}$
CUR/CHI	149.9 ± 14.1^{bc}	0.30 ± 0.03^{bc}	$+52.0 \pm 0.4^{a}$

Mean values that are not connected with the same superscript in a column are significantly different ($P < 0.05$)

Abbreviations: PPI, pea protein isolate; SPPI, succinylated pea protein; CUR, curcumin; CHI, chitosan; CUR/SPPI, curcumin-succinylated pea protein nano-complex; CUR/PPI, curcumin-pea protein nano-complex; CUR/SPPI/CHI, curcumin-succinylated pea protein-chitosan nano-complex; CUR/PPI/CHI, curcumin-pea protein-chitosan nano-complex; CUR/CHI, curcumin-chitosan nano-complex; SPPI/CHI hollow, succinylated pea protein-chitosan shell; PPI/CHI hollow, native pea protein-chitosan shell.

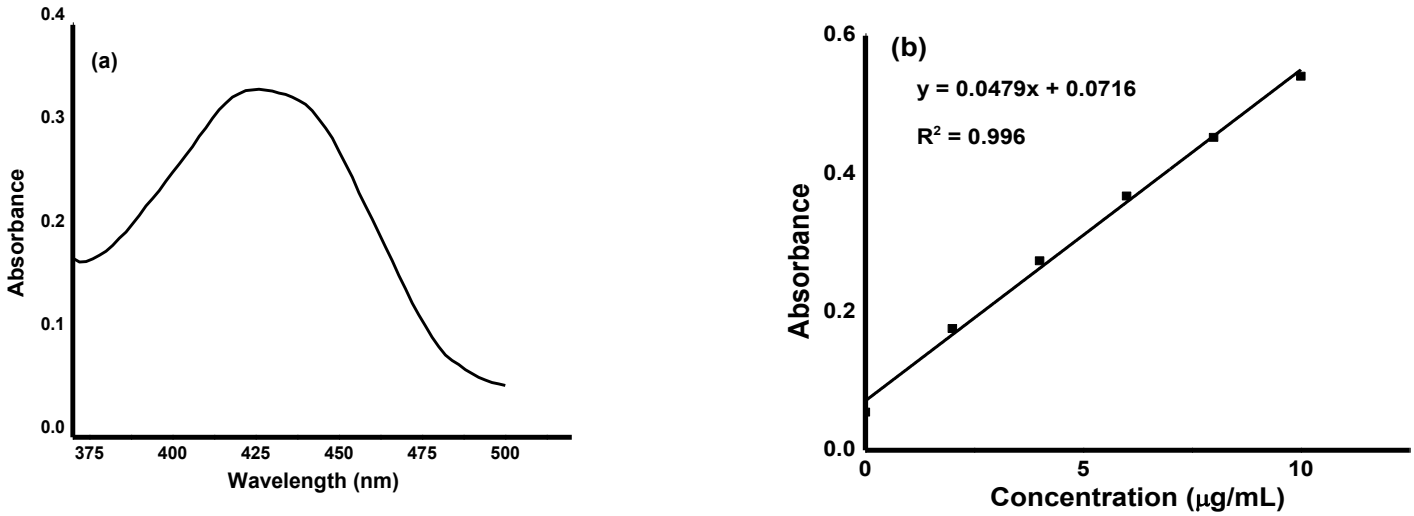

Figure S2.1. (a) Excitation scan and (b) calibration curve of curcumin

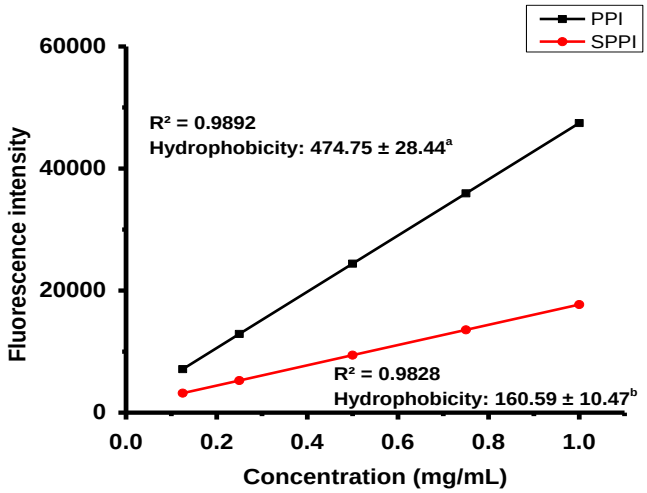

Mean values with different superscripts indicate a significant difference ($P < 0.05$)

Figure S2.2. Determination of surface hydrophobicity of PPI and SPPI through a plot of fluorescence intensity against the concentration

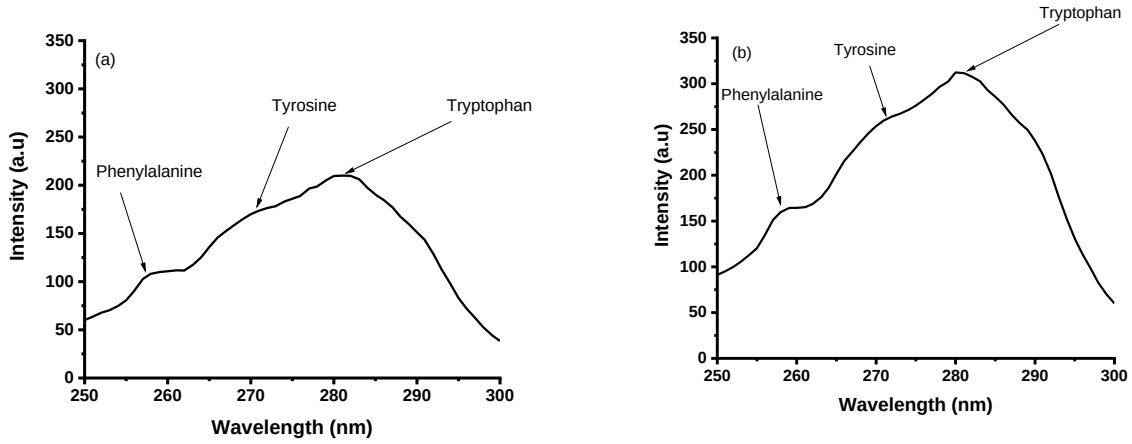

Figure S2.3. Excitation scan of (a) PPI and (b) SPPI solution

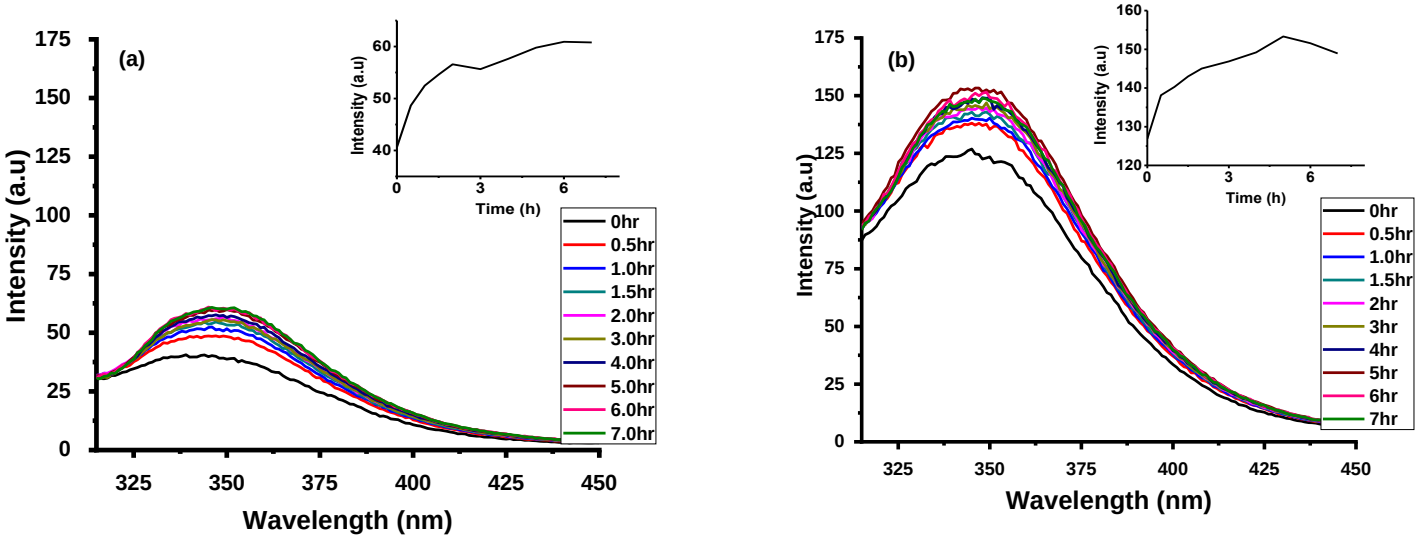

Figure S2.4. Stability of (a) PPI-curcumin and (b) SPPI-curcumin interaction

Figure S2.5. Differential scanning calorimetric thermograms of (a) PPI (b) SPPI (c) PPI/CHI (d) SPPI/CHI (e) CUR/PPI (f) CUR/SPPI (g) CUR/PPI/CHI and (h) CUR/SPPI/CHI

CHAPTER THREE

INFLUENCE OF STRUCTURAL PROPERTIES OF PEA PROTEIN FRACTIONS ON THEIR INTERACTION WITH BIOACTIVE COMPOUNDS: ENCAPSULATION AND GASTRIC RELEASE MECHANISMS

Molecular Interactions of Pea Globulin, Albumin and Glutelin with Curcumin: Formation and Gastric Release Mechanisms of Curcumin-loaded Bio-nanocomplexes

Ogadimma D. Okagu, Chibuike C. Udenigwe

Food Biophysics **2022**, *17*(1), 10-25. https://doi.org/10.1007/s11483-021-09697-5

DECLARATION FOR THESIS CHAPTER THREE

Molecular Interactions of Pea Globulin, Albumin and Glutelin with Curcumin: Formation and Gastric Release Mechanisms of Curcumin-loaded Bio-nanocomplexes

This is to declare that there is no conflict of interest associated with this work and the contribution of the candidate is as stated below:

Candidate's contribution	Conceptualization of idea, formal analysis, investigation, methodology, validation, visualization, writing, review, and editing	90%

The following co-author attest to the candidate's participation in a group publication as a component of his thesis and was active in the creation of this publication. The co-author's permission is as follows:

Name	Signature	Date
Chibuike C. Udenigwe		22/11/2022

Abstract

The impact of structural and physicochemical properties of pea globulin, glutelin and albumin on their interaction with curcumin for their functional role in the gastrointestinal delivery of curcumin was investigated. The binding constant K for curcumin binding with the alkaline-soluble glutelin, salt-soluble globulin and water-soluble albumin fractions was determined by tryptophan fluorescence quenching analysis to be $2.2\pm0.11\times10^4\ M^{-1}$, $2.6\pm0.03\times10^4\ M^{-1}$ and $1.3\pm0.15\times10^4\ M^{-1}$, respectively. Encapsulation efficiency was consistent with the strength of protein-curcumin binding, which consequently depends on the protein surface hydrophobicity. Differential scanning calorimetry showed improved thermostability of the protein on curcumin encapsulation whereas TEM revealed the formation of well-ordered spherical nanocomplexes with hydrodynamic diameters of 100-270 nm, consistent with dynamic light scattering results. FTIR spectroscopy showed prominent spectral shifts of the individual proteins or curcumin in the complex due to intermolecular interactions. The curcumin-loaded alkaline-soluble glutelin and water-soluble albumin protein complexes demonstrated better curcumin protection in the gastric fluid than curcumin- loaded -salt-soluble globulin protein complex and released curcumin by pepsin-dependent mechanism whereas the latter released curcumin by salt-dependent mechanism. Although, alkaline-soluble and water-soluble protein fractions showed comparable stability of curcumin in their loaded-complexes under physiological condition, the former could have better potential in the encapsulation and delivery of curcumin due to their higher hydrophobicity, stronger interaction with curcumin and formation of a more homogenous nanocomplexes. Overall, isolated pea glutelin, albumin and globulin could be a potential candidate for curcumin encapsulation and delivery as demonstrated from the gastric stability of their various complexes, hence ensuring that curcumin reaching the intestinal phase are of physiologically relevant amount.

Keywords: protein fractions; curcumin; molecular interaction; nanoencapsulation; biostability; bioaccessibility

1. Introduction

The nature and strength of protein–bioactive compound interaction is essential for a rational design of delivery vehicles for nutraceuticals.[1–3] The physicochemical properties of the bioactive compound and protein, such as solubility, charge, hydrophobicity, folding pattern, etc., could dictate the nature of this interaction, and hence food matrix compatibility, nanoparticle formation, encapsulation efficiency and release mechanism. Pea protein isolate, which contains four major classes of storage proteins, namely globulin, albumin, glutelin and prolamin with different physicochemical properties,[4,5] was used as a model to study the influence of fraction-based properties on binding with water-insoluble bioactive compound (curcumin) and the nature of nanoparticle formation, thermal and gastric stabilization, and mechanism of release. Pea globulin is soluble in concentrated salt solution and comprises of trimeric 7S vicilin (150-180 kDa) and hexameric quaternary 11S legumin (300-400 kDa) in the ratio of ~1:2.[6,7] The six subunits of 11S legumin are well-arranged into acidic (α-subunit, ~40 kDa) and basic (β-subunit, ~20 kDa) subunits linked by disulfide bonds such that the hydrophilic residues are exposed at the surface to interact with water and the hydrophobic residue are buried in the protein core.[8,9] Vicilin contains heterogeneous glycosylated polypeptides with a hydrophilic surface lacking disulfide linkages due to the absence of cysteine residues.[6,10] Unlike legumin, α, β and γ subunits of vicilin are held together by hydrophobic interaction rather than covalent disulfide bond. Depending on the ionic strength, vicilin can form a hexamer through reversible aggregation.[10] Beta sheet-type secondary structure dominate both legumin and vicilin.[11] A third class of globulin known as convicilin, which possesses distinct amino acid profile and little carbohydrate, has been isolated from pea seeds. The

native form of convicilin has a molecular weight of ~290 kDa consisting of four 71 kDa subunits and displays about 80% sequence homology with vicilin but differs by possessing one cysteine residue and highly negatively charged N-terminal extension region due to the abundance of aspartate residues.[12] Pea albumin is water soluble and found in the soluble cytosol fraction of cotyledon cells where they play metabolic as well as enzymatic roles and aid in seed germination.[13,14] Two classes of albumin (PA1a and PA1b) with molecular weight of about 6 kDa and 4 kDa and high cysteine content have been reported.[15] In another study, dimeric pea albumin with a molecular weight of ~50 kDa was reported to have a tightly folded, non-helical and globular structure that is resistant to trypsin hydrolysis and denaturation. Each subunit (PA2a and PA2b) has a molecular weight of ~26 kDa and the native dimeric form does not have intermolecular disulfide bonding. The subunits are each made up of four close-knit structural domains with free sulfhydryl groups, which cause polymerization through disulfide interchange under alkaline condition.[16,17] Pea glutelin is rich in hydrophobic residues and soluble in dilute alkaline or acid, detergents, reducing or chaotropic agents. Compared to globulin, glutelin is characterized by high methionine and cysteine contents and are of high nutritional value and protein quality.[18] Prolamin is an ethanol soluble plant storage protein with high glutamine and proline content. It is present in small amount in peas. There is limited information on the structural properties of pea glutelin and prolamin.

Curcumin is a hydrophobic nutraceutical compound extracted from *Curcuma longa* plants. It is commonly used in food coloring, cosmetics, food flavoring and as herbal supplement.[19] It has demonstrated strong antioxidant, antimicrobial, anti-inflammatory, antimutagenic and anticancer properties.[20] However, its low bioavailability due to its rapid degradation in aqueous environment, low solubility and rapid metabolism limits its food, biopharmaceutical and biomedical

application.[21] Various micro- and nanoencapsulation technologies have effectively improved the stability, solubility, bioaccessibility and bioavailability of curcumin. Proteins have been in the frontline and modified in various ways with cationic and anionic polysaccharides to ensure strong curcumin binding, high encapsulation, and loading and release efficiencies as well as to improve the stability of protein-curcumin complexes during gastric digestion.[1,2,22–27] The first step usually involves understanding the nature and strength of curcumin-protein binding and the possible effect on the stability of the protein, accessibility, bioavailability and membrane permeability of released curcumin.[1,2]

Our previous study demonstrated that pea protein isolate with or without modification by succinylation binds with curcumin resulting in reasonable encapsulation efficiency and release [2]. However, there is a dearth of information on how differences in the structural properties of individual native protein fractions influence their interaction with curcumin, physicochemical properties of their complexes, biostability in the gastric digestion phase and curcumin bioaccessibility. This information is crucial in the design of protein-based nanodelivery systems for specific water-insoluble bioactive compounds. For the first time, we investigated the nature and strength of interaction of pea globulin, albumin and glutelin fractions with curcumin. Prolamin fraction was excluded in the study due to low yield and solubility challenges. We further investigated the structural properties of the three fractions in relation to the physicochemical properties and biostability of their curcumin-loaded nanocomplexes against pepsin in the gastric phase, and role in gastrointestinal delivery of curcumin.

2. Materials and Methods

2.1. Materials

All reagents were of analytical grade and used without further purification. Sodium hydroxide pellet, HCl and GelCode™ Blue Safe Protein Stain were purchase from Fisher Scientific Inc. (Ottawa, ON, Canada). Lowry reagent and Precision Plus Protein™ Dual Xtra Standards were purchased from BioRad (Mississauga, ON, Canada). Ethanol, curcumin (≥ 94 % purity), tris(hydroxymethyl)aminomethane (Tris-base), 8-anilo-1-naphthalenesulfonic acid (ANS) and pepsin (≥250 units/mg solid) from porcine were purchase from MilliporeSigma Chemical Co., Ltd. (St. Louis, MO, USA). Pulse Canada (Manitoba, Canada) generously donated the yellow pea seeds used in this study. Milli-Q water was obtained from a commercial water-purification system (Advantage A10 Q-POD Milli-Q Water System) with a total organic carbon level ≤ 5 ppb and resistivity of 18.2 MΩcm at 25°C.

2.2. Extraction of pea protein isolate (PPI)

Extraction of pea protein isolate from yellow pea seeds was carried out according to previously reported techniques.[2,4] Briefly, yellow pea seeds were dehulled, ground and sieved into fine powder, and 200 g of the powder was extracted with 2 L of NaOH solution (0.05 M) at pH 12.7 after stirring for 4 h. The mixture was centrifuged at room temperature at 5600 × g for 30 min using Sorvall LYNX 4000 Superspeed centrifuge (ThermoFisher Scientific, Waltham, MA USA) and supernatant separated and acidified with HCl (1 M) to pH 4.5 while stirring at 320 rpm with a magnetic stirrer (Cimarec, ThermoFisher Scientific, Waltham, MA USA). The resulting precipitate was separated from the solution by centrifugation for 30 min, washed with Milli-Q water twice and adjusted to pH 7.0 with NaOH (1 M). The viscous solution was frozen at -80°C

and lyophilized with Labconco freeze-dryer (Labconco corporation, Kansas, MO, USA) at a vacuum pressure of 0.02 mbar and collector temperature of -51°C. The resulting powder was used as the pea protein isolate (PPI).

2.3. Isolation of albumin, globulin, glutelin and prolamin fractions

Protein fractions were isolated from pea protein isolate following a previously reported method with some modifications.[4] Briefly, sequential extraction of albumin (WSF) and globulin (SSF) fractions from PPI (45 g) was carried out with NaCl solution (2%, 600 mL) followed by extraction of prolamin fraction (ESF) from the residue with ethanol (70%, 600 mL) and finally glutelin fraction (ASF) with NaOH (0.02 M, 600 mL). In each case, the mixture was stirred for 3 h, centrifuged at 20,500 × g for 30 min and supernatant collected. The protein fractions were re-extracted twice from the residue, centrifuged and the supernatants pooled, and filtered. The supernatant containing ESF and SSF were dialyzed against deionized water for 48 h at 4°C while changing the dialysate frequently with deionized water. The retentate from the salt soluble fraction was centrifuged to separate the salt soluble globulin from water soluble albumin (WSF). The supernatant from ASF was adjusted to pH 4.8 with 6 M HCl, allowed to rest for 1 h, centrifuged, and the precipitate collected, washed, adjusted to pH 7 and centrifuged again. All the fractions were freeze-dried and stored in -20°C. Total protein content was determined by Lowry assay using a standard calibration curve of bovine serum albumin and Bio-Rad protein assay kits. Sodium dodecyl sulfate-polyacrylamide gel electrophoresis was used to confirm the protein profile of the fractions (supplementary material).

2.4. Determination of surface hydrophobicity (H0)

Surface hydrophobicity of the pea protein fractions was assessed using a previously reported method with slight modification 1,2. Solution of the samples (1.0, 0.75, 0.5, 0.25, and 0.125

mg/mL) and ANS (8 mM) was prepared in sodium phosphate buffer (0.1 M, pH 7.2). The protein solution (200 µL) was mixed with ANS (5 µL) and the fluorescence intensity measured at the λ_{ex} 390 nm and λ_{em} 470 nm using Spark multimode microplate reader (Tecan, Stockholm, Sweden). Slope of the graph of fluorescence intensity against protein concentration was calculated as H_0.

2.5. Fluorescence quenching study of curcumin-protein interaction

Fluorescence quenching technique using Varian Cary Eclipse (Agilent, Santa Clara, CA, USA) was used in studying the interaction of curcumin with three pea protein fractions as reported previously.[1,2,28,29] Curcumin stock solution (2.7 mM) was prepared in ethanol and diluted to 1 mM in ethanol/water (60/40%) from which 500 µM was prepared in 30/70% ethanol/water and diluted to a concentration range of 0-200 µM in water. Protein fractions (0.25 mg/mL) were prepared in water and mixed with equal volume of various concentration of curcumin, resulting in final curcumin concentration of 0, 2, 5, 10, 15, 20, 25, 30, 40, 50, 60, 80 and 100 µM, and protein concentration of 0.125 mg/mL Fluorescence excitation scan was first performed to determine tryptophan excitation wavelength (280 nm) followed by fluorescence emission scan from 300-450 nm. Triplicate measurements were performed, and tryptophan fluorescence intensity was used in calculating the binding parameters.[1,2,28–31]

If one assumes that tryptophan quenching was because of protein-curcumin binding, Stern-Volmer equation can be used to estimate binding parameters and determine the nature and strength of the binding. Stern-Volmer quenching constant K_D and biomolecular quenching rate constant (K_Q) can be calculated from the slope of a graph of $\frac{F_o}{F}$ vs. $[Q]$ of the Stern-Volmer equation (Eq. 3.1).

$$\frac{F_o}{F} = 1 + K_Q t_o[Q] = 1 + K_D[Q] \qquad 3.1$$

F_0 and F are fluorescence intensity of the protein in the absence and presence of the quencher, curcumin, respectively, and [Q] is the curcumin concentration in molarity unit and t_0 is the fluorophore lifetime in the absence of the quencher, usually in the order of 10^{-9} seconds. [1,2,28,29]

The accessible fluorophore fraction (*f*) could be estimated from the intercept of the modified Stern-Volmer equation by plotting $\frac{F_o}{F_o-F}$ vs. $\frac{1}{[Q]}$ (Eq. 3.2).

$$\frac{F_o}{F_o - F} = \frac{1}{fK[Q]} + \frac{1}{f} \qquad 3.2$$

K is the effective quenching constant for the accessible fluorophores and can be estimated from the slope which is equal to $\frac{1}{fK}$.

The number of binding sites *n* for curcumin could be estimated graphically (Eq. 3.3) from the slope of a plot of $\log\left[\frac{F_o-F}{F}\right]$ vs. $log[Q]$ [28]

$$\log\left[\frac{F_o - F}{F}\right] = logK_A + nlog[Q] \qquad 3.3$$

2.6. Effect of curcumin-protein binding on the thermal stability of the protein

The impact of curcumin-protein complexation on the thermal stability of the protein fractions was studied using differential scanning calorimetry (DSC Q2000, TA instrument, USA). The freeze-dried powdered samples (0.3-6 mg) were separately placed into a pre-weighed Tzero Aluminum Hermetic pan and empty pan was used as reference. The thermogram was recorded from 25-250°C in a nitrogen atmosphere at a flow rate of 20 mL/min and a scan rate of 10 °C/min. Transition enthalpies were calculated from the area of the integrated peak or dip of a plot of

$\frac{heat\ flow\ (\frac{mJ}{s})}{weight\ of\ sample\ (mg)}\ vs.time\ (s)$ using Origin 9 software (OriginLab Corporation, Northampton, Massachusetts, USA).

2.7. Synthesis of protein-curcumin complexes and calculation of encapsulation efficiency

2.7.1. Solution preparation for protein-curcumin complexation

The solutions of the pea protein fraction (1 mg/mL) were prepared in Milli-Q water, stirred for 6 h with a magnetic stirrer (Cimarec ThermoFisher Scientific, Waltham, MA USA) and centrifuged at 7200 × *g* for 20 min. The supernatant was collected, vacuum filtered with Whatman filter paper number 50, pore size 2.7 µm and degassed with Polylab vacuum desiccator to remove impurities and air bubbles from the solution. Curcumin solution (1 mg/mL) was prepared in ethanol and protected from light with aluminum foil.

2.7.2. Synthesis of protein-curcumin nanocomplexes

The synthesis of protein-curcumin nanocomplexes was carried out according to previously reported method with slight modification.[1,2] Briefly, curcumin solution in ethanol (1 mg/mL, 10 mL) was added dropwise to solutions of the pea protein fractions (1 mg/mL, 40 mL) in a separate flask covered with aluminum foil and stirred at 320 rpm for 6 h. The mixture was centrifuged at 7200 × g for 20 min and residue washed twice with water, frozen at -80°C and lyophilized to obtain the powdered samples of CASF, CSSF and CWSF. The fractions were stored in -20°C freezer prior to analysis.

2.8. Physicochemical characterization of the curcumin-loaded nanocomplexes

2.8.1. Dynamic light scattering

Dynamic light scattering technique was used to determine the average particle size, polydispersity and zeta potential of the protein fractions and their curcumin-loaded complexes using Nano-ZS Zetasizer (Malvern Instruments Ltd., Malvern, UK). To reduce multiple scattering effect, dilute solution of the samples (refractive index 1.450, absorption 0.001) was prepared and analyzed in Milli-Q water (pH 7, refractive index 1.330, viscosity 0.8872 cP and dielectric constant 78.5). The dynamic light scattering effect was analyzed with Smoluchowski model at F(ka) 1.50 and backscattered angle of 173° at 25 °C from triplicate measurements.

2.8.2. Morphological analysis

Morphology of freshly prepared colloidal solution of the nanoparticles was analyzed with a transmission electron microscope (JEM-2100F Field Emission Electron Microscope, JEOL, Tokyo, Japan). A drop of colloidal solution of each sample was placed on a carbon film 300-mesh copper grid activated by glow-discharge for 50 s using the Gatan Solarus Advanced Plasma System and allowed to air-dry for 1 h. Images of the curcumin-protein nanocomplexes at different magnifications were acquired.

2.8.3. Functional group characterization by Fourier Transformed Infrared Spectroscopy (FTIR) Analysis

Functional group characterization on the freeze-dried solid samples (2-5 mg) was investigated by FTIR spectroscopy (Nicolet 6700 FTIR, ThermoFisher Scientific, Waltham, MA USA). The FTIR spectra of the samples were recorded from 4000 to 400 cm^{-1} in absorbance mode after background subtraction.

2.9. Determination of encapsulation efficiency

Encapsulation efficiency of the pea protein fractions for curcumin was investigated by UV-Vis spectrophotometer (Spark multimode microplate reader, Tecan, Stockholm, Sweden) using a recently reported method[1,2] with some modification. The curcumin-loaded nanocomplexes of the protein fractions were dispersed in ethanol (2-3 µg/mL), vortexed for 30 s and centrifuged at 7000 × g for 10 min. Absorbance of the supernatant was measured at λ_{max} 425 nm [1,2] and the concentration of curcumin in the matrix estimated from the calibration curve of curcumin in ethanol (R^2 = 998). Encapsulation efficiency was determined using Eq. 3.4.

$$\text{EE } (\%) = \frac{E_{CUR}}{\text{C}} \times 100 \qquad 3.4$$

EE is the encapsulation efficiency (%), E_{CUR} is the weight of encapsulated curcumin (mg) and *C* is the amount of curcumin added during the complexation process (mg).

2.10. Pepsin resistibility study, kinetic release profile and membrane permeability of curcumin

Resistibility of the curcumin-loaded biopolymer nanocomplexes against pepsin degradation, kinetic release profile, membrane permeability of curcumin and effect of ionic strength were investigated as previously reported[1,2,23,26] with slight modification as the digestion process did not go through salivary and intestinal digestion phases. Simulated gastric fluid (SGF) was prepared according to the standardized static *in vitro* digestion protocol.[32] Briefly, SGF electrolyte (20 mL), containing pepsin (1.6 mL, 2500 U/mL), $CaCl_2$ (5 µL, 0.3 M) and protein fraction (1.2-4 mg), was transferred into a dialysis membrane (MW cutoff of 3.5 kDa). Thereafter, pH was adjusted to 1.2 with HCl (1 M) before placing the mixture into a 500-mL flask containing 200 mL of releasing media (SGF electrolyte containing 50% ethanol, without enzyme and $CaCl_2$). The mixture was

incubated at 37°C while shaking at 70 rpm. Aliquots (3 mL) were withdrawn from the releasing media after 0, 0.5, 1.0, 1.5, 2.0, 2.5, 3.0, 3.5, and 4.0 h, absorbance measured at λ_{max} 424 nm (curcumin), and same volume of fresh releasing medium added. In a similar way, the effect of physiological (gastric) ionic strength on the nanocomplex release profile was investigated in the absence of pepsin. All measurements were carried out in triplicate and the amount of curcumin released was quantified from the calibration of curve.

2.11. Statistical analysis

Statistical comparison between the means of triplicate measurements of the various samples were analyzed by one-way analysis of variance (ANOVA) using Origin 9 software (OriginLab Corporation, Northampton, Massachusetts, USA). Data were analyzed using the Tukey's test and group mean differences and values at $p < 0.05$ were considered significantly different.

3. Results and Discussion

3.1. Surface hydrophobicity of the protein fractions

Surface hydrophobicity of proteins influences the nature of binding and stability of complexes formed with water insoluble nutraceuticals, such as curcumin[1,2,33] and could hence impact the release of the bioactive compound. For this reason, the surface hydrophobicity of three pea protein fractions were investigated by ANS assay. The ethanol-soluble prolamin fraction was excluded from further analysis due to its low yield and poor protein profile, which may be because of its co-extraction with polyphenols and poor aqueous solubility.[4] The alkaline soluble fraction had significantly higher H_0 (522.75±17.95) followed by the salt soluble (427.04±5.56) and water soluble fractions (328.96±3.28, $p < 0.05$), as previously reported at neutral pH for protein fractions from commercial PPI.[4] The high H_0 of glutelin was due to its high content of hydrophobic amino

acid residues, e.g., tryptophan, leucine, valine and alanine.[34] Conversely, the lower H_0 of the other fractions could be attributed to the high content of hydrophilic residues, e.g., glutamic acid, aspartic acid, arginine and lysine in albumin[35] and hydrophilic glycosylated polypeptides of vicilin[6,10] and convicilin[9] of globulin, which enhance protein-water interaction.[9,36] Overall, H_0 of the protein fractions are within the range of values reported for whole PPI,[2] insect protein and bovine serum albumin,[1] which have shown reasonable binding with curcumin and demonstrated gastric stability and effective release properties.

3.2. Protein-curcumin interaction and the estimation of binding parameters

Fluorescence quenching technique was employed in studying protein-curcumin binding by monitoring the behavior of tryptophan residue (λ_{exc} 280) of the proteins within the fluorescence emission wavelength of 300-450 nm as it interacts with various concentration of curcumin. The nature of the environment of tryptophan residue (apolar or aqueous) and their binding with some biomolecules could impact their fluorescence intensity and maximum emission wavelength.[37] This is due to chemical or physical processes such energy transfer, excited-state reaction, molecular rearrangement and/or direct quenching that influence the protein secondary structure and conformation. The effect of protein-curcumin binding on fluorescence emission intensity and maximum emission wavelength of tryptophan can be measured and used to estimate the accessibility of curcumin to the tryptophan residue and calculate the various binding parameters for such interaction.[1,2,28,29,38–40]

The tryptophan fluorescence intensity of the three pea protein fractions decreased on addition of curcumin and the effect is more pronounced with increase in curcumin concentration (Figure 3.1). This is because of changes in protein structure and conformation induced by the formation of less

fluorescent protein-curcumin complex. The magnitude of the decrease in tryptophan fluorescence with increasing curcumin concentration is more evident in curcumin-glutelin followed by curcumin-globulin and then curcumin-albumin complex. This could be because of increased hydrophobic interaction in CASF and CSSF compared to CWSF in line with their surface hydrophobicity (Table 3.1). The hydrophobicity of the protein is one of the major driving force for protein-curcumin binding and could significantly trigger changes in protein conformation, which consequently affect tryptophan fluorescence.[1,2,28,33,41] At various concentrations of curcumin, the wavelength at maximum fluorescent intensity was nearly constant at 335 nm for the salt-soluble and alkaline soluble fractions (Figure 3.1a&b), an indication that the tryptophan residue is protected from changes in solvent effect, hydrogen bonding[42] and polarity.[28,29] The fluorescence emission wavelength (λ_{em}) at 335 nm is characteristic of interaction at the hydrophobic core of protein and is probably the site of the protein-curcumin interaction; this could account for the stronger binding and higher encapsulation efficiency observed in these two protein fractions (Table 3.1). The λ_{em} of WSF experiences a redshift from 343 to 350 nm upon binding with curcumin and the shift become more apparent at higher curcumin concentration (Figure 3.1c). Fluorescence emission wavelength of binding within a range of 340 to 350 nm and fluctuation in λ_{em} upon binding is characteristic of exposed tryptophan residue or hydrophobic core. The location of the tryptophan residue or exposure of the hydrophobic core in addition to the observed lower surface hydrophobicity of WSF could be responsible for the lower binding and encapsulation efficiency (Table 3.1).[1,2,37,43,44] Hence, alkaline, and salt-soluble pea protein fraction binds strongly with curcumin and showed better encapsulation efficiency, thus demonstrating greater potential in improving the stability, solubility and bioaccessibility of curcumin than water-soluble fraction.[1,2]

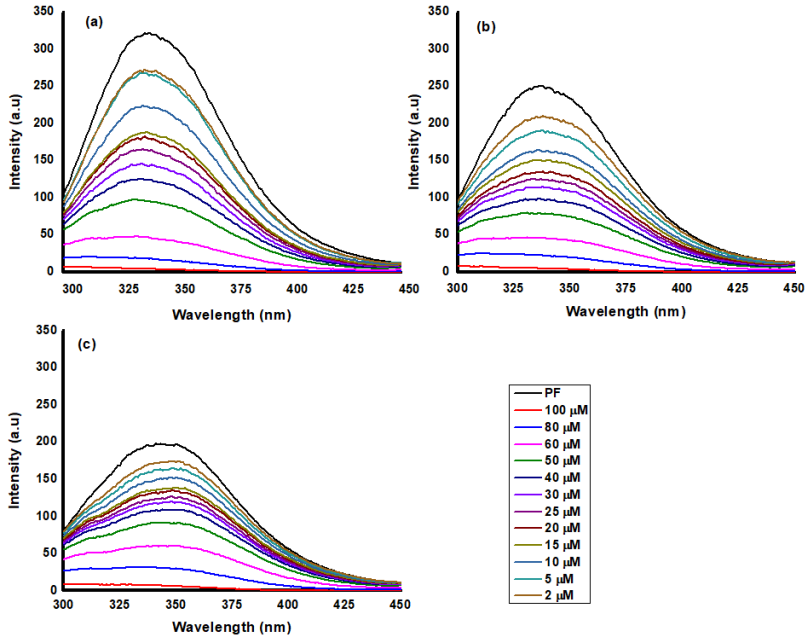

Figure 3.1. Fluorescence emission spectra of the (a) curcumin-alkaline soluble protein fraction (ASF), (b) curcumin-salt soluble protein fraction (SSF), and (c) curcumin-water soluble protein fraction (WSF) colloidal complexes. PF is the fluorescence intensity of ASF in (a), SSF in (b), and WSF in (c).

Table 3.1. Protein-curcumin binding parameters and encapsulation efficiency

Complexes	K ($\times 10^4$ M^{-1})	K_D ($\times 10^4$ M^{-1})	K_Q ($\times 10^{13}$ $M^{-1}S^{-1}$)	n	f	Encapsulation efficiency (%)
CASF	2.2±0.11^a	4.1±0.06^a	4.1±0.06^a	0.98±0.01^a	1.39±0.03^{ab}	95.07±1.11^a
CSSF	2.6±0.03^a	3.5±0.14^a	3.5±0.14^a	0.72±0.01^b	1.25±0.01^b	71.40±0.98^b
CWSF	1.3±0.15^b	1.9±0.05^b	1.9±0.05^b	0.62±0.02^c	1.45±0.06^a	43.18±0.60^c

Mean values with different letters in a column are significantly different ($P < 0.05$).

Abbreviations: CASF, alkaline soluble fraction-curcumin complex; CSSF, salt soluble fraction-curcumin complex; CWSF, water soluble fraction-curcumin complex.; K, effective quenching constant for the accessible fluorophores; n, substantive binding pockets of the various fractions for curcumin; K_D, Stern-Volmer quenching constant; K_Q, biomolecular quenching rate constant; and f, accessible fluorophore fraction.

The nature of protein-curcumin binding, the biomolecular quenching rate constant K_Q and Stern-Volmer quenching constant K_D were determined from Eq. 3.1 and results presented in Figure 3.2 and Table 3.1. The various pea protein fractions showed static quenching behavior at low curcumin concentration (linear curve) and dynamic quenching above 50 µM (Figure 3.2). This indicates that the rate of dissociation of the protein-curcumin complex at low concentrations of curcumin is lower than that at higher concentrations. Protein-curcumin association reaction is more favorable than dissociation of the complex at low curcumin concentration. Therefore, the stability of the complex is more guaranteed at lower curcumin concentration; hence, an optimum stoichiometric ratio of protein-to-curcumin will be essential for the design of a stable protein-based delivery vehicle for curcumin. The estimated K_Q and K_D for CASF and CSSF (Table 3.1) are comparable and significantly higher than that of CWSF. This could be also linked to the lower surface hydrophobicity of WSF and the environment of the tryptophan residue. Moreover, the lower molecular weight of WSF as observed from the SDS-PAGE (Figure S3.1) indicates less functional groups available to interact with curcumin and, consequently, could have decreased the strength of protein-curcumin binding. Since the K_Q values are higher than 2×10^{10} $M^{-1}S^{-1}$ reported as maximum static quenching for ligand-macromolecule interaction, the binding of curcumin with the three pea protein fractions is predominantly static and led to the formation of less fluorescent biopolymer complexes.[45,46] The value of K_D and K_Q is comparable with those previously reported for protein-curcumin binding.[1,2,28,29]

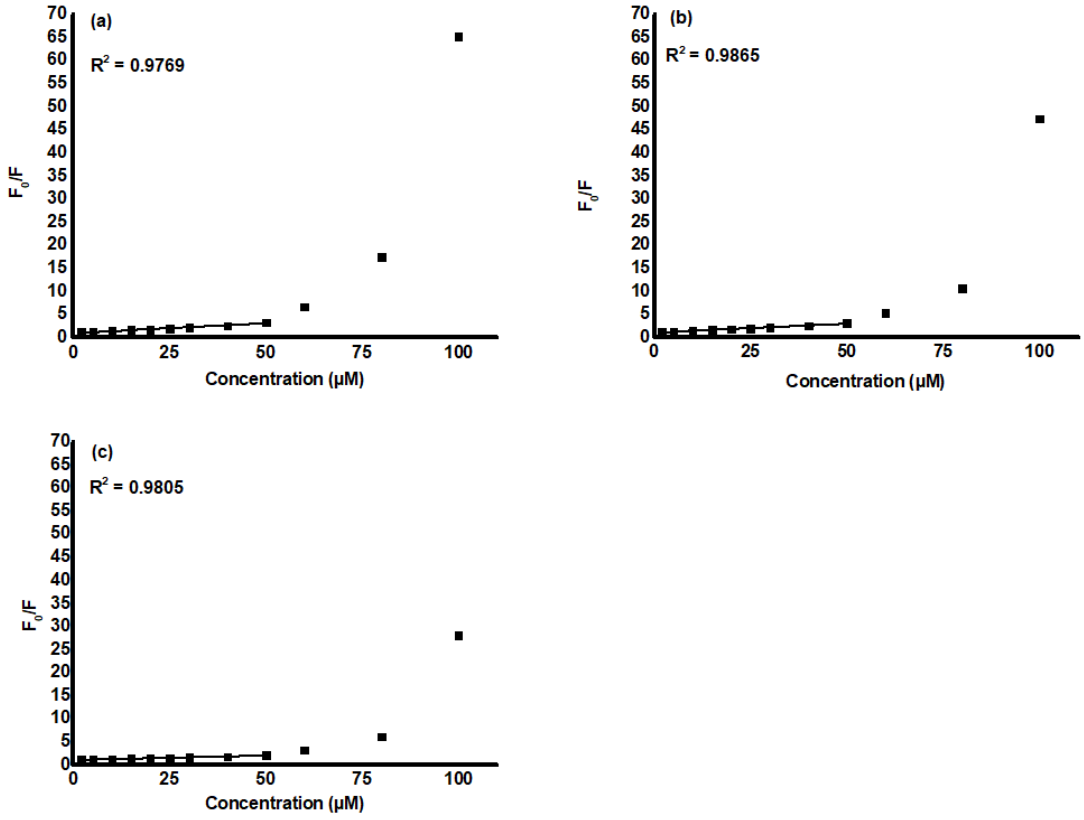

Figure 3.2. Stern-Volmer plots for quenching constant determination of (a) ASF-curcumin, (b) SSF-curcumin, and (c) WSF-curcumin binding.

The effective quenching constant *K* for the accessible fluorophores (Figure 3.3, Table 3.1) was determined by assuming that tryptophan fluorescence quenching is as a result of protein-curcumin binding. This parameter is commonly employed in measuring the strength of protein-ligand binding *via* fluorescence quenching technique. There is no significant difference between the values of *K* for CASF and CSSF but CWSF showed lower binding affinity, which could be as a result of its lower hydrophobicity, position of the tryptophan residue relative to the protein surface, or nature of the interaction. The *K* values of the three pea protein fractions for curcumin are within the range of those classified as moderate interaction and comparable to previously reported protein-curcumin binding as determined by fluorescence spectrophotometry.[1,2,28,29]

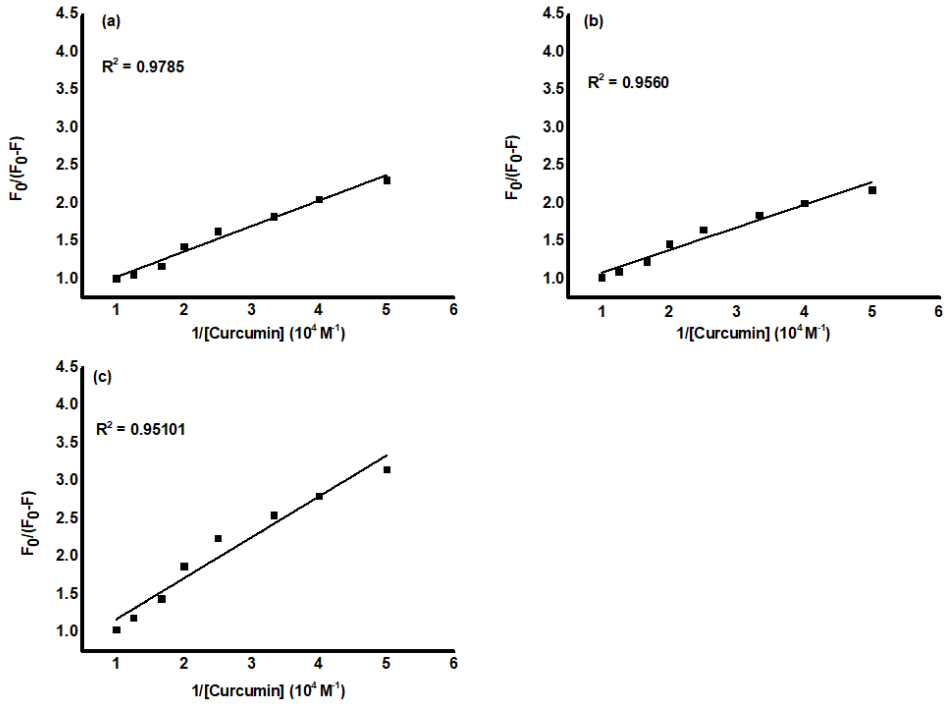

Figure 3.3. Plots of $F_0/(F_0-F)$ vs. 1/[Curcumin] for determination of accessible fluorophore fractions (*f*) and effective quenching constant (*K*) for the accessible fluorophores in (a) CASF (b) CSSF and (c) CWSF complexes

Accessible fluorophore fraction and number of binding sites for curcumin in the protein was estimated from Eqs. 3.2 and 3.3, respectively. The value of *n* estimated from the linear region (static binding, Table 3.1, Figure 3.4) showed that CASF has the highest bound curcumin per protein followed by CSSF and then CWSF, which is consistent with the trend of their encapsulation efficiency (Table 3.1). The number of accessible fluorophore fraction (Table 3.1, Figure 3.3) in CWSF is higher than that of CASF and CSSF and corroborates the fluorescent emission wavelength range of WSF. The estimated *n* and *f* are similar to previously reported values for curcumin-protein binding.[1,2,28,29]

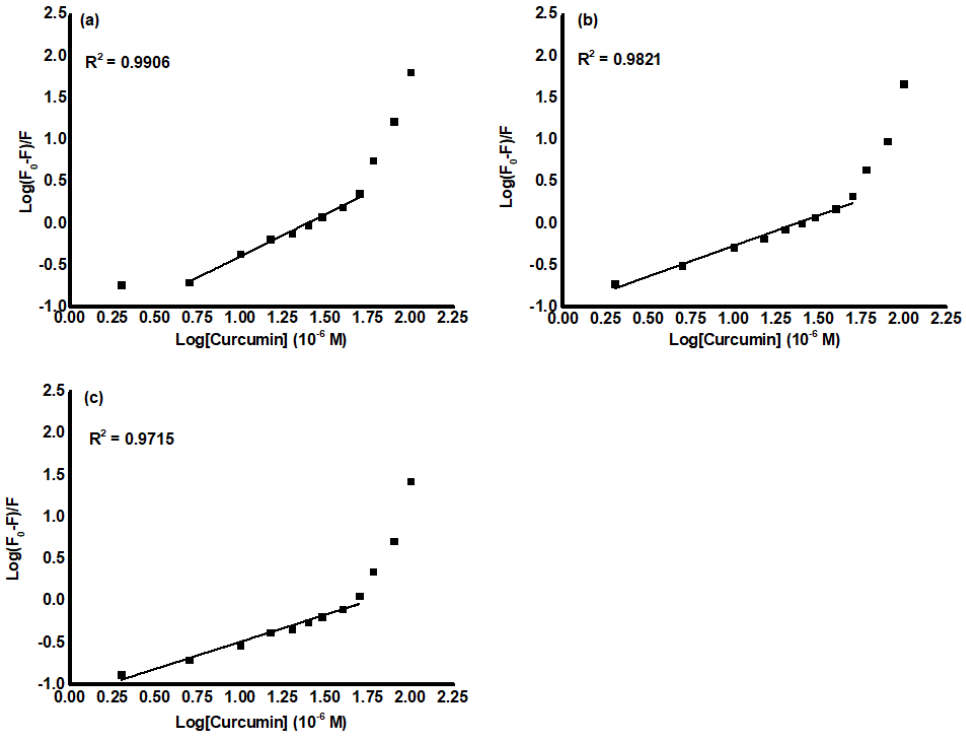

Figure 3.4. Plots of log(F_0 - F)/F vs. log[Curcumin] for the determination of the number of bound curcumin (*n*) in the (a) CASF, (b) CSSF, and (c) CWSF complexes.

3.3. Thermal stability of the complexes as determined from differential scanning calorimetry

The influence of protein-curcumin interaction on the stability of the protein and complexes was investigated using freeze-dried protein-curcumin complexes (Figure 3.5, Table 3.2). This information is essential in ascertaining protein response to changes in temperature and the optimum storage condition for the biopolymer nanocomplexes. The three protein fractions showed a single endothermic peak at lower temperature region but the protein-curcumin complexes showed up to 4 endothermic peaks at higher temperatures. The peaks in the protein-curcumin complexes could be attributed to conformational changes in the protein as result of binding with curcumin. The increase in transition temperature of the complexes indicates favorable interaction and improved thermal stability. In a previous study, the interaction of curcumin with insect

protein,[1] whole pea protein,[2] and gliadin,[47] improved the thermal stability of the protein. From Table 3.2, the transition enthalpies of alkaline and salt soluble fractions were lower than one or more transition enthalpies in the curcumin-loaded complexes, CASF and CSSF. Thus, it is thermodynamically more feasible to denature the protein fractions, even at lower temperature, than their complexes with curcumin. The transition enthalpy of CWSF was lower than that of the protein WSF even though the transition temperature of CWSF is higher. This indicates that, at higher temperature, it was easier to degrade CWSF and does not necessarily mean than the protein was more stable than the complex. Therefore, protein-curcumin complexes are more resistant to changes in temperature than the free protein forms.

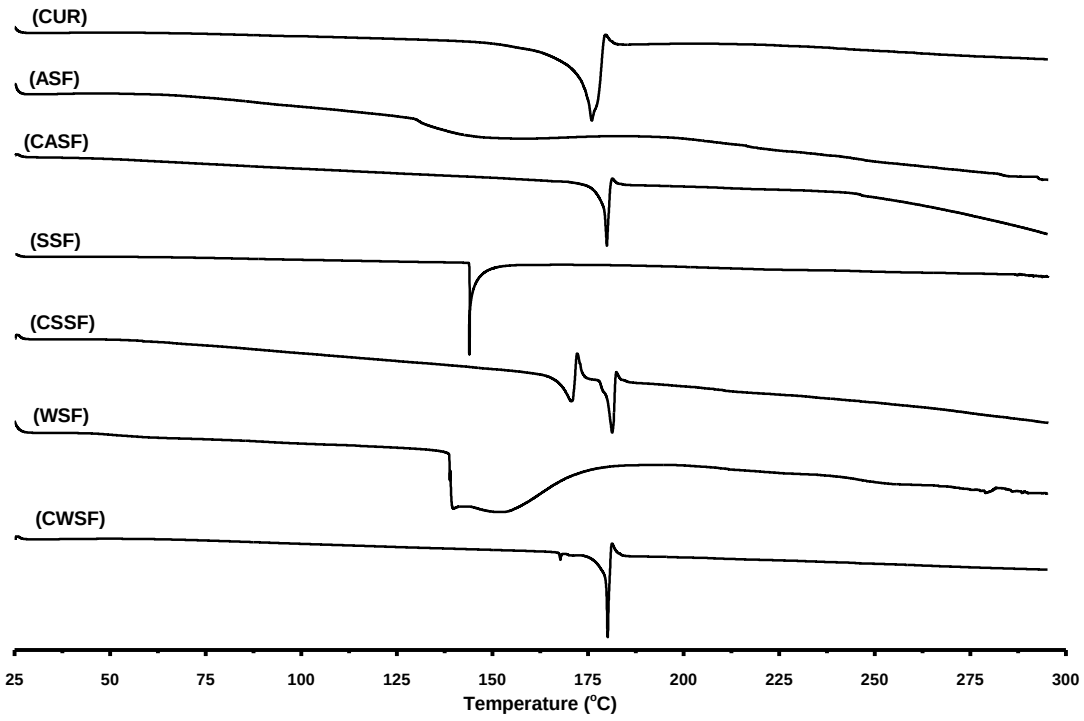

Figure 3.5. Differential scanning calorimetric thermograms of the various protein fractions and curcumin-loaded protein complexes.

Table 3.2. Dynamic light scattering data of the colloidal solution of the nanocomplexes, and the transition temperatures and enthalpies of the freeze-dried particles.

Complexes	Size (nm)	PDI	Zeta potential (mV)	Transition temperatures (°C)	Transition enthalpies (J/g)
ASF	69.6 ± 0.5^{e}	0.48 ± 0.01^{bc}	-42.9 ± 1.03^{f}	146.3	99.5
SSF	97.5 ± 1.3^{d}	0.34 ± 0.00^{de}	-35.9 ± 0.91^{e}	144.2	94.7
WSF	153.2 ± 0.4^{c}	0.28 ± 0.01^{e}	-32.1 ± 0.35^{a}	152.0	234.4
CASF	267.4 ± 7.2^{a}	0.52 ± 0.03^{b}	-19.7 ± 0.26^{c}	180.1, 181.5	134.7,6.6
CSSF	111.1 ± 5.7^{d}	0.42 ± 0.02^{cd}	-12.5 ± 0.29^{b}	171.1, 171.9, 180.8, 182.5	104.1, 39.8, 133.8, 13.2
CWSF	216.3 ± 5.4^{b}	0.63 ± 0.02^{a}	-7.8 ± 0.82^{a}	167.8, 180.5, 181.6	3.6, 94.1, 8.0

Mean values with different superscript in a column are significantly different ($P < 0.05$)
Abbreviations: ASF, alkaline soluble fractions; CASF, alkaline soluble fraction-curcumin complex; SSF, salt soluble fraction; CSSF, salt soluble fraction-curcumin complex; WSF, water soluble fraction; CWSF, water soluble fraction-curcumin complex.

3.4. Encapsulation potential of pea protein fractions and physicochemical properties of curcumin-loaded nano-complexes

3.4.1. Encapsulation efficiency

The potential of encapsulating curcumin with the individual pea protein fractions was derived from Eq. 3.4 and data presented in Table 3.1. The alkaline-soluble fraction had higher encapsulation efficiency followed by salt-soluble fraction and finally water-soluble fraction. This result is in line with their surface hydrophobicity and interaction with curcumin as demonstrated from K, K_D and K_Q (Table 3.1). The result shows that higher surface hydrophobicity of the protein promoted the interaction with curcumin, and the strength of this binding dictated the encapsulation efficiency. The encapsulation efficiencies of the three protein fractions are higher than that of the

unfractionated pea protein, which showed encapsulation efficiency of 34% and increased to 85% upon incorporation of chitosan.[2] In fact, ASF alone had an encapsulation efficiency of 95%. This indicates that the mixture of proteins in PPI interfered with their ability to encapsulate curcumin effectively, hence the need for protein fractionation. Encapsulation efficiency reported for the pea protein fractions are similar to some other curcumin-loaded protein complexes, including sunflower protein-curcumin (60-93%),[48] soy protein isolate-curcumin (89-98%),[49] insect protein-curcumin (37-47%),[1] curcumin-gliadin (80-85%) [50] and walnut protein isolate-curcumin (~61.5%) complexes.[51]

3.4.2. Particle characteristics of protein fractions and curcumin-loaded complexes

Average particle size, polydispersity index and zeta potential of the three pea protein fractions and their curcumin-loaded complexes was investigated by electrophoretic light scattering (Table 3.2). Hollow pea protein fractions had smaller particle sizes than their curcumin-loaded complexes, which indicates that curcumin encapsulation increased the size of protein nanoparticles. The protein nanoparticles and their curcumin complexes were moderately homogenous except CWSF, which could be because of unfavorable interaction between water-soluble protein and hydrophobic curcumin resulting in the formation of particles of various sizes (Tables 3.1 & 3.2, Figure 3.6a-f). The pea protein fractions had high negative zeta potential, which decreased after curcumin encapsulation. This is contrary to the effect observed for curcumin-loaded zein nanoparticles where incorporation of curcumin increased the negative charge on the protein.[24] The discrepancy could be attributed to differences in intermolecular interactions. CWSF had a lower negative zeta potential compared to other curcumin-loaded complexes, which indicates poor stability and corroborates the low binding to curcumin and low encapsulation efficiency. Zeta potential and

particle sizes of the nanoparticles fall within the range of values reported for some other curcumin-loaded protein complexes.[2,23,24,26,27]

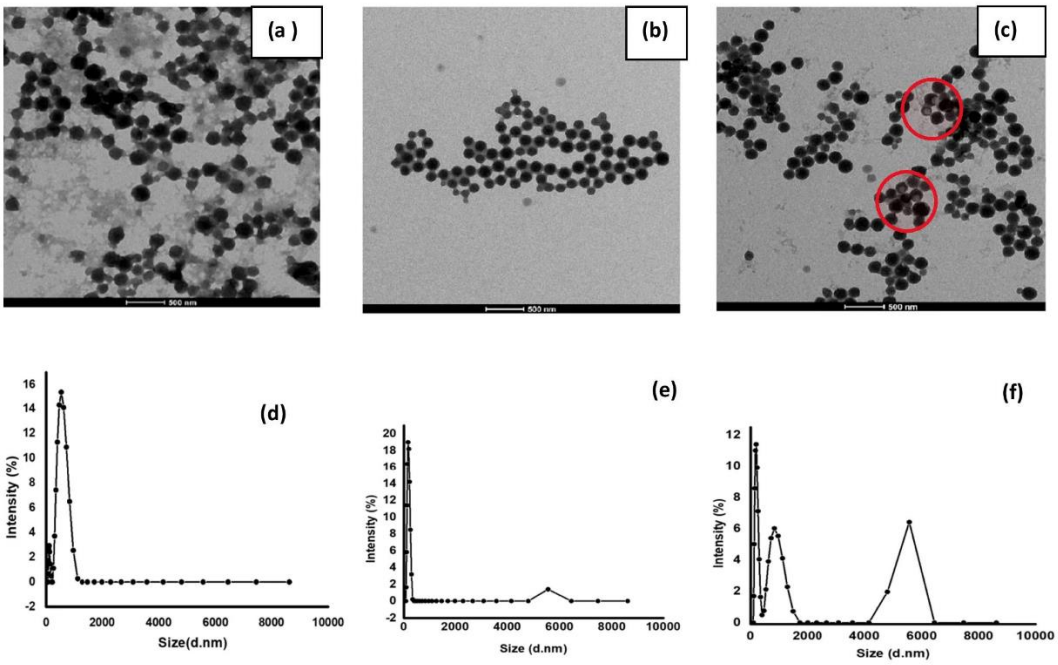

Figure 3.6. Transmission electron microscopy images of the colloidal solution of (a) CASF, (b) CSSF, and (c) CWSF complexes and particle size distribution of (d) CASF, (e) CSSF, and (f) CWSF complexes.

3.4.3. Nanostructures of the curcumin-loaded protein nanocomplexes

Morphology of the curcumin-loaded protein nanocomplexes was investigated by transmission electron microscopy and the images acquired at a magnification of 500 nm are shown in Figure 3.6a-c. All the various curcumin-protein complexes had similar well-ordered spherical morphology and smooth surfaces in the size range of 100-230 nm. Larger and smaller particles were formed from alkaline-soluble and salt-soluble fractions, respectively. The particles were slightly smaller than sizes derived from electrophoretic light scattering (Table 3.2), which is

expected as DLS measures the hydrodynamic diameter.[24] Particles of CSSF (Figure 3.6b) seem to be held together better than those of CASF and CWSF, which could be due to intermolecular forces. The core of each spherical nanoparticle appears darker than the surface, indicating the encapsulation of curcumin in the core with proteins on the surface. Curcumin was not effectively encapsulated in all CWSF particles as highlighted in the image showing spherical nanoparticles with empty or partially filled core (Figure 3.6c). This could be attributed to unfavorable binding and supports the low encapsulation efficiency.

3.4.4. Functional groups of the curcumin-protein nanocomplexes

The nature and impact of intermolecular interactions on the functional groups of the protein fractions and curcumin within the complexes was investigated by Fourier-transform infrared spectroscopy. As shown in Figure 3.7, FTIR spectrum of curcumin showed a broad peak at 3500 cm^{-1}, which is characteristic of the stretching vibration of hydroxyl groups (O-H). This peak shifted to 3396 and 3404 cm^{-1} in CSSF and CWSF, respectively and this is likely as a result of hydrogen bonding interaction between the protein and curcumin. The protein spectra also showed broad peak of O-H group at 3273-3280 cm^{-1} and a sharp peak around 1630 and 1450 cm^{-1}, which are characteristics of carboxyl (-COO-) symmetrical stretching vibrations.[52] The peaks around 1504 and 1628 cm^{-1} in curcumin can be assigned to C-C stretching vibration of the aromatic system and C=O stretching vibration of enol group, respectively. The peaks at 1273 and 1427 cm-1 are characteristics of stretching vibration of C-O of alcohol and bending vibration of C-H of alkanes, whereas the peaks located within the region of 1026-957 are peculiar to C-O stretching vibrations in carboxylic acids and esters. The peaks within 854 to 804 could be as a result of out-of-plane bending mode of meta- and para-substituted aromatic systems.[23,53] Multiple stretching vibration peaks within the region of 2839-3199 cm^{-1} in both curcumin and protein fractions can be assigned

to the hydrophobic C-H group. The spectra shifts observed in this region for the curcumin-loaded protein complexes confirm that hydrophobic interaction played a role in curcumin-protein binding. Peaks within the range of 1400-1700 cm^{-1} in the protein fraction and curcumin-loaded complexes can be assigned to amide I and II bonds[54] and spectral shifts observed in curcumin-loaded complexes were as a result of intermolecular interactions. The intensity of the O-H group of curcumin increased while the hydrophobic C-H group (2839-3199 cm^{-1}) in the protein decreased after curcumin encapsulation, indicating a decrease in surface hydrophobicity and increase in solubility of the curcumin-loaded protein nanocomplexes.[24] Most of the prominent peaks of the proteins and curcumin appeared in the complexes suggesting that the interaction is mainly non-covalent and therefore guarantees the structural integrity of curcumin within the complex is preserved.

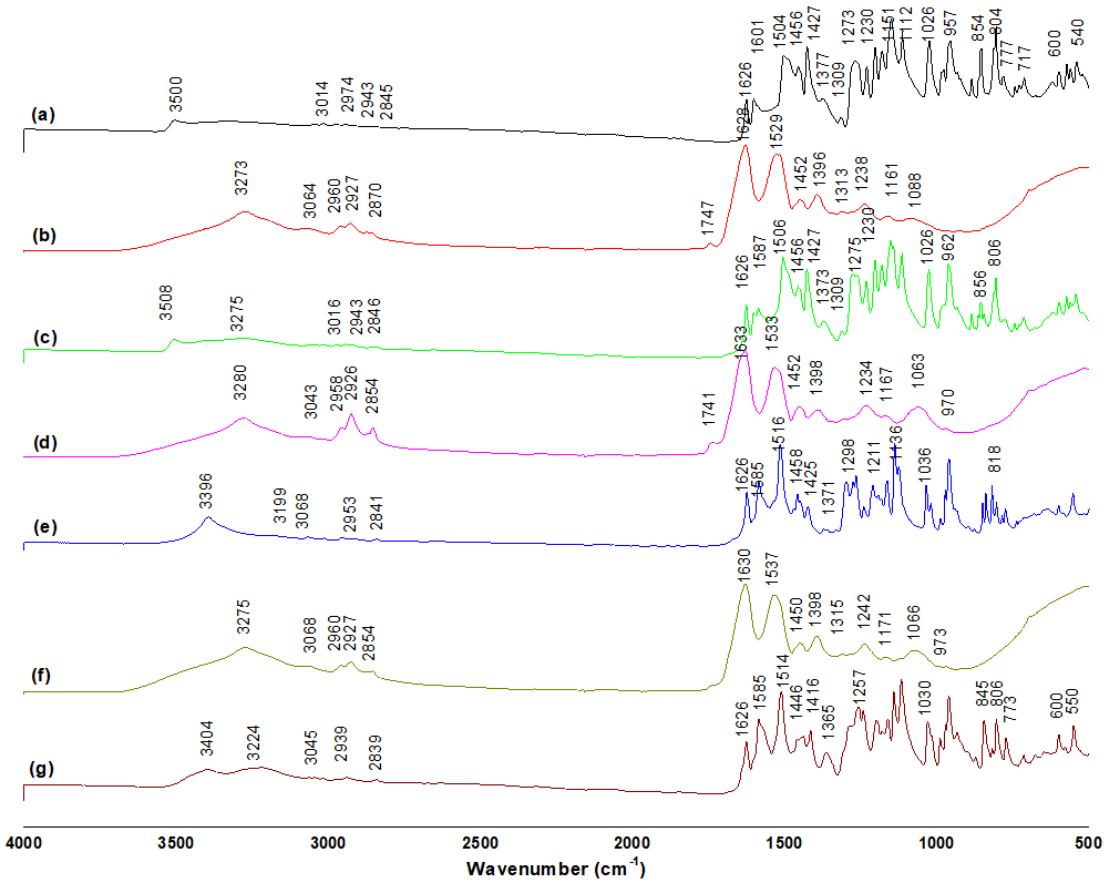

Figure 3.7. Fourier transformed infrared spectra of (a) curcumin (b) ASF (c) CASF (d) SSF (e) CSSF (f) WSF and (g) CWSF.

3.5. Effect of ionic strength of gastric fluid and resistance against pepsin degradation

Stability of the curcumin-loaded protein complexes in gastric fluid in the presence and absence of pepsin is presented in Figure 3.8 a & b. Curcumin encapsulated with alkaline-soluble and water-soluble fractions showed better stability against pepsin degradation or the gastric ionic condition as observed from the smaller amounts of curcumin released after 2 h of gastric phase treatments. For CASF, the amounts of curcumin released after 2 h were 7.5 and 0% in the presence and absence of pepsin, respectively. This is because of strong curcumin-ASF binding (Table 3.1) resulting from the high protein surface hydrophobicity, which limits the accessibility of pepsin to the protein network or dissolution in gastric fluid. Moreover, 8.3% and 2.0% of curcumin were released from CWSF after 2 h with and without pepsin, respectively. The low amount of curcumin released from CWSF could be because of the tight folding, non-helical and globular structure of albumin, which was previously reported to be resistant to pepsin, pancreatin[35] and trypsin degradation.[16] Conversely, solubility of globulin fraction (SSF) in concentrated salt solution resulted in dissolution of the curcumin-protein complex under the ionic strength of the gastric fluid. This enabled the accessibility of pepsin to the various protein cleavage sites and, consequently, higher curcumin release (Figure 3.8). Since there was no significant difference between the amount of curcumin released from CSSF (17.9% and 17.1% in the presence and absence of pepsin, respectively), the release mechanism was mainly because of dissolution of the complex in the gastric fluid rather than enzymatic disintegration of the complex. Unencapsulated curcumin showed comparable curcumin release under the two tested conditions.

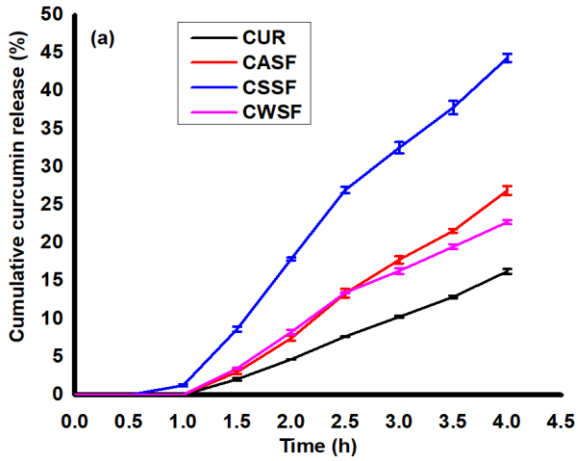
(a)
CUR
CASF
CSSF
CWSF
Cumulative curcumin release (%)
Time (h)

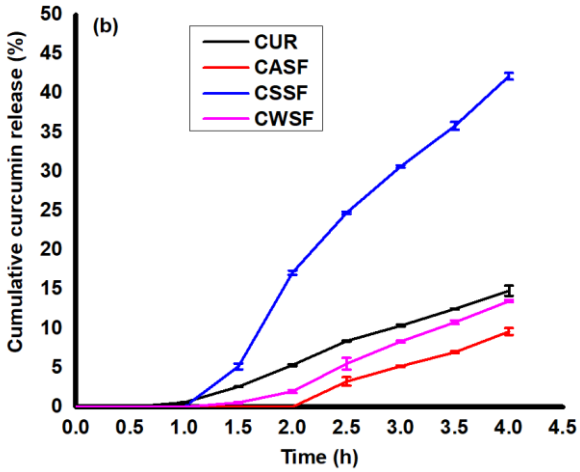
(b)
CUR
CASF
CSSF
CWSF
Cumulative curcumin release (%)
Time (h)

(c)

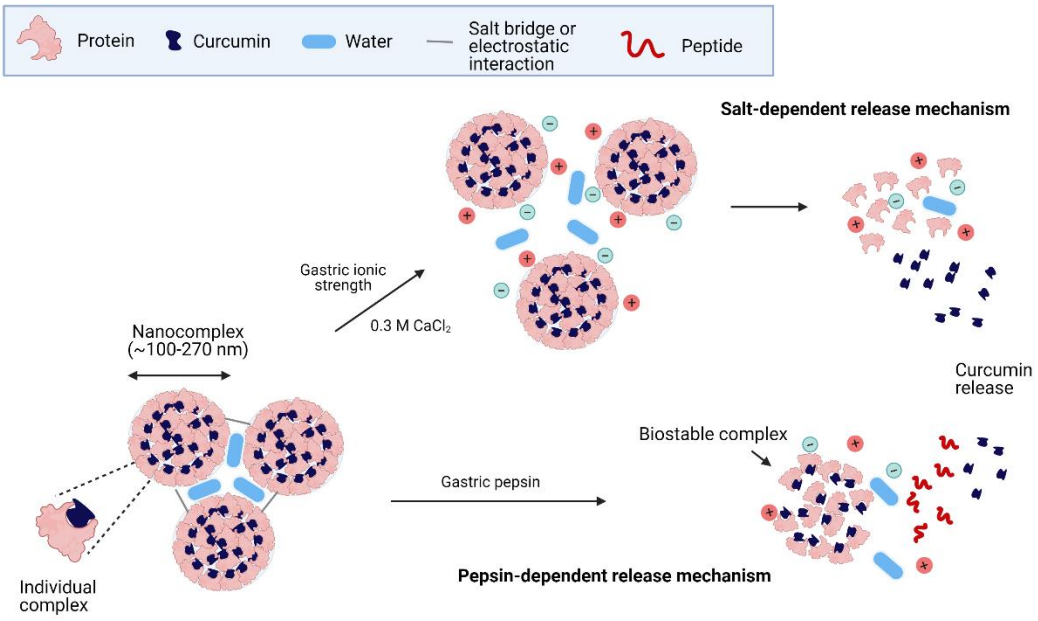
Protein
Curcumin
Water
Salt bridge or electrostatic interaction
Peptide
Salt-dependent release mechanism
Gastric ionic strength
0.3 M CaCl2
Nanocomplex (~100-270 nm)
Curcumin release
Biostable complex
Gastric pepsin
Individual complex
Pepsin-dependent release mechanism

Figure 3.8. Kinetic release profile of curcumin from the various complexes under simulated gastric fluid in the (a) presence and (b) absence of pepsin. (c) Schematic representation of the salt-dependent (CSSF) and pepsin-dependent (CWSF and CASF) curcumin release from the protein nanocomplexes in the gastric digestion phase. Presence of salt decreases electrostatic energy between protein molecules within the nanocomplex leading to increased aqueous solubility and curcumin dissociation/release. Pepsin-resistant complex results in less curcumin release, thus providing more biostable nanocomplexes to the intestinal phase. Image created with Biorender.

Overall, pepsin-dependent release of curcumin was estimated by comparing the kinetic release profiles in the presence and absence of pepsin and were found to be 7.5, 0.8 and 6.3% for CASF, CSSF and CWSF respectively. The result enabled the postulation of two release mechanisms of curcumin encapsulated in the matrix of protein nanoparticles under gastric condition; salt-dependent and pepsin-dependent release. These release mechanisms depend on the structural properties of the protein such as solubility (salt-soluble protein, SSF), strength of the curcumin-protein binding (as demonstrated in CASF), and access of pepsin to the protein network (CWSF). As shown in the schematic representation (Figure 3.8c), salt-dependent release of curcumin demonstrated by CSSF involves the screening out of charge-charge interactions between protein nanoparticles by salt ions, thus decreasing surface tension, preventing aggregation and precipitation, and increasing protein denaturation, solubility and consequently curcumin release. The interaction of salt ions with the protein shell after disintegration of the electrostatic interaction increased protein solubility and decreased hydrophobic contact between the protein shell and curcumin core. TEM images (Figure 3.6c) further corroborate the schematic representation and, as shown from the effect of gastric ionic strength, the CSSF protein nanoparticles are held together by strong electrostatic interaction, which are distorted in the presence of salt ions. The second

mechanism (Figure 3.8c) demonstrated by CASF and CWSF involves pepsin degradation of the protein shell network encapsulating curcumin leading to the release of curcumin. Amount of curcumin released depends on access of pepsin to the protein cleavage sites, which depends on the strength of protein-curcumin binding (CASF) or protein folding and conformation (CWSF). Unlike CSSF, the low amount of curcumin released under gastric ionic strength indicates that the particle-particle interaction shown in the TEM images of CASF and CWSF (Figure 3.6a & c) is mainly due to other forces (e.g. hydrophobic, Van der Waals, etc.) rather than electrostatic interaction. Thus, the nature of interaction forces holding CASF and CWSF compared to CSSF could be responsible for their different nanoparticle arrangements.

This study shows that nanoencapsulation using the protein fractions improved curcumin solubility as observed from the higher release from the loaded-complexes compared to free curcumin in the presence of pepsin. Without the enzyme, CASF and CWSF complexes protected curcumin and reduced its release compared to free curcumin while higher amount of curcumin was released from CSSF because of its high solubility. Similar total gastric release amounts have been reported for curcumin complexes with native and modified whole pea protein (1.8-13%),[2] and insect protein (3.7-18.1%).[1] However, our study is the first to provide evidence of enzyme-dependent and salt-dependent curcumin release mechanisms that rely mostly on the nature of the proteins. Low release of curcumin from the complexes after 2 h of gastric digestion would ensure that more curcumin is delivered to the intestinal phase for absorption and increased bioavailability.

4.0. Conclusion

The nature of binding of three pea protein fractions with curcumin was investigated and the curcumin-loaded complexes of the protein characterized by spectroscopic and microscopic techniques. The results show that surface hydrophobicity of the protein is essential for its binding

with curcumin while the strength of this interaction dictates the encapsulation efficiency and stability of the complex in the gastric phase of digestion. The solubility and structural properties of the protein plays a key role in its binding, encapsulation efficiency and curcumin protection in the gastric phase. Interaction of protein with curcumin induced a structural change in the protein and improved its thermal stability. Transmission electron microscopy showed a successful synthesis of well-ordered spherical nanocomplexes of curcumin. Taken together, antisolvent precipitation technique resulted in the fabrication of thermostable pepsin-resistant and spherical nanocomplexes of curcumin-protein fractions. The curcumin-pea protein fraction complex released curcumin during gastric digestion through two different mechanisms; salt-dependent mechanism as observed from curcumin-loaded salt-soluble fractions and pepsin-dependent mechanism for the curcumin complex of water and alkaline-soluble pea protein fractions. The high encapsulation efficiency, stability in gastric fluid and resistant to pepsin degradation suggest the potential application of this complexes in the gastrointestinal delivery of curcumin.

Acknowledgements

This research was funded through the Discovery Grant Program (RGPIN-2018-06839) of the Natural Sciences and Engineering Research Council of Canada (NSERC) and the University Research Chair Program Funds from the University of Ottawa.

Reference

(1) Okagu, O. D.; Verma, O.; McClements, D. J.; Udenigwe, C. C. Utilization of Insect Proteins to Formulate Nutraceutical Delivery Systems: Encapsulation and Release of Curcumin Using Mealworm Protein-Chitosan Nano-Complexes. *International Journal of Biological Macromolecules.* **2020**, *151*, 333-343. https://doi.org/10.1016/j.ijbiomac.2020.02.198.

(2) Okagu, O. D.; Jin, J.; Udenigwe, C. C. Impact of Succinylation on Pea Protein-Curcumin Interaction, Polyelectrolyte Complexation with Chitosan, and Gastrointestinal Release of

Curcumin in Loaded-Biopolymer Nano-Complexes. *Journal of Molecular Liquids.* **2020**, *325*, 115248. https://doi.org/10.1016/j.molliq.2020.115248.

(3) Okagu, O. D.; Wang, B.; Udenigwe, C. C. CHAPTER 4 Food Proteins as Biomaterial for Delivery Functions; in *Food proteins and peptides: emerging biofunctions, food and biomaterial applications*. ed. by C.C. By, Udenigwe (RSC, London, 2021), 97-126. https://doi.org/10.1039/9781839163425-00097.

(4) Adebiyi, A. P.; Aluko, R. E. Functional Properties of Protein Fractions Obtained from Commercial Yellow Field Pea (Pisum Sativum L.) Seed Protein Isolate. *Food Chemistry.* **2011**, *128*(4), 902-908. https://doi.org/10.1016/j.foodchem.2011.03.116.

(5) Lu, Z. X.; He, J. F.; Zhang, Y. C.; Bing, D. J. Composition, Physicochemical Properties of Pea Protein and Its Application in Functional Foods. *Critical Reviews in Food Science and Nutrition*. **2020**, *60*(15), 2593-2605. https://doi.org/10.1080/10408398.2019.1651248.

(6) O'Kane, F. E.; Happe, R. P.; Vereijken, J. M.; Gruppen, H.; Van Boekel, M. A. J. S. Characterization of Pea Vicilin. 2. Consequences of Compositional Heterogeneity on Heat-Induced Gelation Behavior. *Journal of Agricultural and Food Chemistry*. **2004**, *52*(10), 3149-3154. https://doi.org/10.1021/jf035105a.

(7) Mertens, C.; Dehon, L.; Bourgeois, A.; Verhaeghe-Cartrysse, C.; Blecker, C. Agronomical Factors Influencing the Legumin/Vicilin Ratio in Pea (Pisum Sativum L.) Seeds. *Journal of the Science of Food Agriculture*. **2012**, *92*(8), 1591-1596. https://doi.org/10.1002/jsfa.4738.

(8) Barac, M.; Cabrilo, S.; Pesic, M.; Stanojevic, S.; Zilic, S.; Macej, O.; Ristic, N. Profile and Functional Properties of Seed Proteins from Six Pea (Pisum Sativum) Genotypes. *International Journal of Molecular Sciences.* **2010**, *11*(12), 4973-4990. https://doi.org/10.3390/ijms11124973.

(9) Reinkensmeier, A.; Bußler, S.; Schlüter, O.; Rohn, S.; Rawel, H. M. Characterization of Individual Proteins in Pea Protein Isolates and Air Classified Samples. *Food Research International*. **2015**, *76*, 160-167. https://doi.org/10.1016/j.foodres.2015.05.009.

(10) Shewry, P. R.; Napier, J. A.; Tatham, A. S. Seed Storage Proteins: Structures and Biosynthesis. *Plant Cell*. **1995**, *7*(7), 945. https://doi.org/10.1105/tpc.7.7.945.

(11) Sikorski, Z. E. *Chemical and Functional Properties of Food Proteins*; 1st edn. (CRC Press, Boca Raton, Florida, USA). **2001**, 407-436. https://doi.org/10.1201/9781482279047.

(12) Croy, R. R.; Gatehouse, J. A.; Tyler, M.; Boulter, D. The Purification and Characterization of a Third Storage Protein (Convicilin) from the Seeds of Pea (Pisum Sativum L.). *Biochemical Journal.* **1980**, *191*(2), 509-516. https://doi.org/10.1042/bj1910509.

(13) McCarthy, N. A.; Kennedy, D.; Hogan, S. A.; Kelly, P. M.; Thapa, K.; Murphy, K. M.; Fenelon, M. A. Emulsification Properties of Pea Protein Isolate Using Homogenization, Microfluidization and Ultrasonication. *Food Research International*. **2016**, *89*, 415-421. https://doi.org/10.1016/j.foodres.2016.07.024.

(14) Croy, R. R.; Hoque, M. S.; Gatehouse, J. A.; Boulter, D. The Major Albumin Proteins from Pea (Pisum Sativum L). Purification and Some Properties. *Biochemical Journal.* **1984**, *218*(3), 795-803. https://doi.org/10.1042/bj2180795.

(15) Higgins, T. J. V.; Chandler, P. M.; Randall, P. J.; Spencer, D.; Beach, L. R.; Blagrove, R. J.; Kortt, A. A.; Inglis, A. S. Gene Structure, Protein Structure, and Regulation of the Synthesis of a Sulfur-Rich Protein in Pea Seeds. *Journal of Biological Chemistry*. **1986**, *261*(24), 11124-11130. https://doi.org/10.1016/s0021-9258(18)67357-0.

(16) Gruen, L. C.; Guthrie, R. E.; Blagrove, R. J. Structure of a Major Pea Seed Albumin: Implication of a Free Sulphydryl Group. *Journal of the Science of Food and Agriclture.* **1987**, *41*(2), 167-178. https://doi.org/10.1002/jsfa.2740410210.

(17) Higgins, T. J. V.; Beach, L. R.; Spencer, D.; Chandler, P. M.; Randall, P. J.; Blagrove, R. J.; Kortt, A. A.; Guthrie, R. E. CDNA and Protein Sequence of a Major Pea Seed Albumin (PA 2 : Mr≈26 000). *Plant Molecular Biology*. **1987**, *8*(1), 37-45. https://doi.org/10.1007/BF00016432.

(18) Singh, U.; Jambunathan, R. Distribution of Seed Protein Fractions and Amino Acids in Different Anatomical Parts of Chickpea (Cicer Arietinum L.) and Pigeonpea (Cajanus Cajan L.). *Qualitas Plantarum Plant Foods for Human Nutrition.* **1982**, *31*(4), 347-354. https://doi.org/10.1007/BF01094046.

(19) Majeed, S. *The State of the Curcumin Market*. Natural Products Insider. Nat. Prod. Insid. https://www.naturalproductsinsider.com/herbs-botanicals/state-curcumin-market. Accessed 12 Aug 2021 (**2015**)

(20) Hewlings, S.; Kalman, D. Curcumin: A Review of Its' Effects on Human Health. *Foods* **2017**, *6*(10), 92. https://doi.org/10.3390/foods6100092.

(21) Anand, P.; Kunnumakkara, A. B.; Newman, R. A.; Aggarwal, B. B. Bioavailability of Curcumin: Problems and Promises. *Molecular Pharmaceutics*. **2007**, *4*(6), 807-818. https://doi.org/10.1021/mp700113r.

(22) Okagu, O. D.; Wang, B.; Acquah, C.; Udenigwe, C. C. Protein-Based Nanodelivery Systems for Food Applications. In *Encyclopedia of Food Chemistry*; Melton, L., Shahidi, F., Varelis, P., Eds.; Academic Press, Oxford, United Kingdom. **2019**, 719–726. https://doi.org/https://doi.org/10.1016/B978-0-08-100596-5.21864-7.

(23) Wang, F.; Yang, Y.; Ju, X.; Udenigwe, C. C.; He, R. Polyelectrolyte Complex Nanoparticles from Chitosan and Acylated Rapeseed Cruciferin Protein for Curcumin Delivery. *Jorunal of Agricultural and Food Chemistry.* **2018**, *66*(11), 2685-2693. https://doi.org/10.1021/acs.jafc.7b05083.

(24) Liu, Q.; Jing, Y.; Han, C.; Zhang, H.; Tian, Y. Encapsulation of Curcumin in Zein/ Caseinate/Sodium Alginate Nanoparticles with Improved Physicochemical and Controlled Release Properties. *Food Hydrocolloids.* **2019**, *93*, 432-442. https://doi.org/10.1016/j.foodhyd.2019.02.003.

(25) Mohammadian, M.; Salami, M.; Alavi, F.; Momen, S.; Emam-Djomeh, Z.; Moosavi-Movahedi, A. A. Fabrication and Characterization of Curcumin-Loaded Complex Coacervates Made of Gum Arabic and Whey Protein Nanofibrils. *Food Biophysics.* **2019**, *14*(4), 425-436. https://doi.org/10.1007/s11483-019-09591-1.

(26) Xue, J.; Zhang, Y.; Huang, G.; Liu, J.; Slavin, M.; Yu, L. (Lucy). Zein-Caseinate Composite Nanoparticles for Bioactive Delivery Using Curcumin as a Probe Compound. *Food Hydrocolloids.* **2018**, *83*, 25-35. https://doi.org/10.1016/j.foodhyd.2018.04.037.

(27) Hu, S.; Wang, T.; Fernandez, M. L.; Luo, Y. Development of Tannic Acid Cross-Linked Hollow Zein Nanoparticles as Potential Oral Delivery Vehicles for Curcumin. *Food Hydrocolloids.* **2016**, *61*, 821-831. https://doi.org/10.1016/j.foodhyd.2016.07.006.

(28) Bourassa, P.; Bariyanga, J.; Tajmir-Riahi, H. A. Binding Sites of Resveratrol, Genistein, and Curcumin with Milk α- And β-Caseins. *Journal of Physical Chemistry B.* **2013**, *117*(5), 1287-1295. https://doi.org/10.1021/jp3114557.

(29) Kanakis, C. D.; Tarantilis, P. A.; Polissiou, M. G.; Tajmir-Riahi, H. A. Probing the Binding Sites of Resveratrol, Genistein, and Curcumin with Milk β -Lactoglobulin. *Journal of Biomolecular Structure and Dynamics.* **2013**, *31*(12), 1455-1466. https://doi.org/10.1080/07391102.2012.742461.

(30) Zhang, Y.; Zhong, Q. Binding between Bixin and Whey Protein at PH 7.4 Studied by Spectroscopy and Isothermal Titration Calorimetry. *Journal of Agricultural and Food Chemistry.* **2012**, *60* (7), 1880-1886. https://doi.org/10.1021/jf2050262.

(31) Zhang, Y.; Zhong, Q. Effects of Thermal Denaturation on Binding between Bixin and Whey Protein. *Journal of Agricultural and Food Chemistry*. **2012**, *60* (30), 7526-7531. https://doi.org/10.1021/jf3021656.

(32) Minekus, M.; Alminger, M.; Alvito, P.; Ballance, S.; Bohn, T.; Bourlieu, C.; Carrière, F.; Boutrou, R.; Corredig, M.; Dupont, D.; Dufour, C.; Egger, L.; Golding, M.; Karakaya, S.; Kirkhus, B.; Le Feunteun, S.; Lesmes, U.; MacIerzanka, A.; MacKie, A.; Marze, S.; McClements, D. J.; Ménard, O.; Recio, I.; Santos, C. N.; Singh, R. P.; Vegarud, G. E.; Wickham, M. S. J.; Weitschies, W.; Brodkorb, A. A Standardised Static in Vitro Digestion Method Suitable for Food-an International Consensus. *Food & Function.* **2014**, *5*(6), 1113-1124. https://doi.org/10.1039/c3fo60702j.

(33) Mirzaee, F.; Hosseinzadeh, L.; Ashrafi-Kooshk, M. R.; Esmaeili, S.; Ghobadi, S.; Farzaei, M. H.; Zad-Bari, M. R.; Khodarahmi, R. Diverse Effects of Different "Protein-Based" Vehicles on the Stability and Bioavailability of Curcumin: Spectroscopic Evaluation of the Antioxidant Activity and Cytotoxicity In Vitro. *Protein & Peptide Letters.* **2018**, *26*(2), 132-147. https://doi.org/10.2174/0929866525666181114152242.

(34) Wen, T.-N.; Luthe, D. S. Biochemical Characterization of Rice Glutelin. *Plant Physiology.* **1985**, *78*(1), 172-177. https://doi.org/10.1104/pp.78.1.172.

(35) Rubio, L. A.; Pérez, A.; Ruiz, R.; Guzmán, M. Á.; Aranda-Olmedo, I.; Clemente, A. Characterization of Pea (Pisum Sativum) Seed Protein Fractions. *Journal of the Science of Food and Agriculture.* **2014**, *94*(2), 280-287. https://doi.org/10.1002/jsfa.6250.

(36) Mundi, S.; Aluko, R. E. Physicochemical and Functional Properties of Kidney Bean Albumin and Globulin Protein Fractions. *Food Research International*. **2012**, *48*(1), 299-306. https://doi.org/10.1016/j.foodres.2012.04.006.

(37) Liang, L.; Tajmir-Riahi, H. A.; Subirade, M. Interaction of β-Lactoglobulin with Resveratrol and Its Biological Implications. *Biomacromolecules.* **2008**, *9*(1), 50-56. https://doi.org/10.1021/bm700728k.

(38) Tayeh, N.; Rungassamy, T.; Albani, J. R. Fluorescence Spectral Resolution of Tryptophan Residues in Bovine and Human Serum Albumins. *Journal of Pharmaceutical and Biomedical Analysis.* **2009**, *50*(2), 107-116. https://doi.org/10.1016/j.jpba.2009.03.015.

(39) Mohammadi, F.; Bordbar, A. K.; Mohammadi, K.; Divsalar, A.; Saboury, A. A. Circular Dichroism and Fluorescence Spectroscopic Study on the Interaction of Bisdemethoxycurcumin and Diacetylbisdemethoxycurcumin with Human Serum Albumin. *Canadian Journal of Chemistry.* **2010**, *88*(2), 155-163. https://doi.org/10.1139/V09-169.

(40) Mohammadi, F.; Moeeni, M. Study on the Interactions of Trans-Resveratrol and Curcumin with Bovine α-Lactalbumin by Spectroscopic Analysis and Molecular Docking. *Materials Science and Engineering C.* **2015**, *50*, 358-366. https://doi.org/10.1016/j.msec.2015.02.007.

(41) Moafian, Z.; Khoshaman, K.; Oryan, A.; Kurganov, B. I.; Yousefi, R. Protective Effects of Acetylation on the Pathological Reactions of the Lens Crystallins with Homocysteine Thiolactone. *PLoS One.* **2016**, *11*(10), e0164139. https://doi.org/10.1371/journal.pone.0164139.

(42) Yang, J. T.; Wu, C. S. C.; Martinez, H. M. Calculation of Protein Conformation from Circular Dichroism. *Methods in Enzymology.* **1986**, *130*, 208-269. https://doi.org/10.1016/0076-6879(86)30013-2.

(43) Mandeville, J. S.; Froehlich, E.; Tajmir-Riahi, H. A. Study of Curcumin and Genistein Interactions with Human Serum Albumin. *Journal of Pharmceutical and Biomedical Analysis.* **2009**, 49(2), 468-474. https://doi.org/10.1016/j.jpba.2008.11.035.

(44) Sułkowska, A. Interaction of Drugs with Bovine and Human Serum Albumin. *Journal of Molecular Structure*. **2002**, *614*(1-3), 227-232. https://doi.org/10.1016/S0022-2860(02)00256-9.

(45) Ware, W. R. Oxygen Quenching of Fluorescence in Solution: An Experimental Study of the Diffusion Process. *Journal of Physical Chemistry* **1962**, *66*(3), 455-458. https://doi.org/10.1021/j100809a020.

(46) Jiang, M.; Xie, M. X.; Zheng, D.; Liu, Y.; Li, X. Y.; Chen, X. Spectroscopic Studies on the Interaction of Cinnamic Acid and Its Hydroxyl Derivatives with Human Serum Albumin. *Journal of Molecular Structure.* **2004**, *692*(1-3), 71-80. https://doi.org/10.1016/j.molstruc.2004.01.003.

(47) Mathew, M. S.; Vinod, K.; Jayaram, P. S.; Jayasree, R. S.; Joseph, K. Improved Bioavailability of Curcumin in Gliadin-Protected Gold Quantum Cluster for Targeted Delivery. *ACS Omega.* **2019**, *4*(10), 14169-14178. https://doi.org/10.1021/acsomega.9b00917.

(48) Sneharani, A. H. Curcumin–Sunflower Protein Nanoparticles—A Potential Antiinflammatory Agent. *Journal of Food Biochemistry.* **2019**, *43*(8), e12909. https://doi.org/10.1111/jfbc.12909.

(49) Chen, F. P.; Liu, L. L.; Tang, C. H. Spray-Drying Microencapsulation of Curcumin Nanocomplexes with Soy Protein Isolate: Encapsulation, Water Dispersion, Bioaccessibility and Bioactivities of Curcumin. *Food Hydrocolloids.* **2020**, *105*, 105821. https://doi.org/10.1016/j.foodhyd.2020.105821.

(50) Akman, P. K.; Bozkurt, F.; Balubaid, M.; Yilmaz, M. T. Fabrication of Curcumin-Loaded Gliadin Electrospun Nanofibrous Structures and Bioactive Properties. *Fibers and Polymers.* **2019**, *20*(6), 1187-1199. https://doi.org/10.1007/s12221-019-8950-8.

(51) Asadi, M.; Salami, M.; Hajikhani, M.; Emam-Djomeh, Z.; Aghakhani, A.; Ghasemi, A. Electrospray Production of Curcumin-Walnut Protein Nanoparticles. *Food Biophysics.* **2021**, *16*(1), 15-26. https://doi.org/10.1007/s11483-020-09637-9.

(52) Zhao, W.; Yuan, P.; She, X.; Xia, Y.; Komarneni, S.; Xi, K.; Che, Y.; Yao, X.; Yang, D. Sustainable Seaweed-Based One-Dimensional (1D) Nanofibers as High-Performance Electrocatalysts for Fuel Cells. *Journal of Material Chemistry A.* **2015**, *3*(27), 14188-14194. https://doi.org/10.1039/c5ta03199k.

(53) Pecora, T. M. G.; Cianciolo, S.; Catalfo, A.; De Guidi, G.; Ruozi, B.; Cristiano, M. C.; Paolino, D.; Graziano, A. C. E.; Fresta, M.; Pignatello, R. Preparation, Characterization and Photostability Assessment of Curcumin Microencapsulated within Methacrylic Copolymers. *Journal of Drug Delivery Science and Technology.* **2016**, *33*, 88-97. https://doi.org/10.1016/j.jddst.2016.03.013.

(54) Farrell, J.; Wickham, E. D.; Unruh, J. J.; Qi, P. X.; Hoagland, P. D. Secondary Structural Studies of Bovine Caseins: Temperature Dependence of β-Casein Structure as Analyzed by Circular Dichroism and FTIR Spectroscopy and Correlation with Micellization. *Food Hydrocolloids*. **2001**, *15*(4-6), 341-354. https://doi.org/10.1016/S0268-005X(01)00080-7.

SUPPLEMENTARY INFORMATION

Molecular Interactions of Pea Globulin, Albumin and Glutelin with Curcumin: Formation and Gastric Release Mechanisms of Curcumin-loaded Bio-nanocomplexes

Ogadimma D. Okagu, Chibuike C. Udenigwe

Food Biophysics **2022**, *17*(1), 10-25. https://doi.org/10.1007/s11483-021-09697-5

S1. Materials and Methods

S1.1 Sodium dodecyl sulfate-polyacrylamide gel electrophoresis (SDS-PAGE) profiles of the protein fractions

The SDS-PAGE profile of the protein fractions under reducing condition was analyzed in a 6 - 18% gradient gel (w/v, pH 8.8) and 5% stacking gel (w/v, pH 6.8). A solution of the fractions (7 mg/mL) was prepared in water and equal volume was mixed with sample buffer containing β-mercaptoethanol (5%, v/v), SDS (2%, m/v), 62.5 mM Tris-HCl (pH 6.8), glycerol (20%, v/v), and bromophenol blue (0.5%, m/v). The mixture was heated at 95°C for 10 min while stirring at 300 rpm (Thermomixer, Eppendorf AG, Hamburg, Germany), allowed to cool and centrifuged at 7000 × g for 10 min. Aliquots of the supernatant and standard protein molecular weight marker (10 µL) were loaded into the gel and electrophoresis performed at 150 V for 1.5 h using BioRad Mini PROTEAN Tetra System (BioRad Inc., Mississauga, ON, Canada). The gel was stained with Coomassie Brilliant Blue R-250 staining solution (Bio-Rad Inc., Mississauga, ON, Canada) and destained with solution of water-methanol-acetic acid (50/40/10%). Thereafter, the gel image was acquired with BioRad Imaging System (BioRad Inc., Mississauga, ON, Canada).

S2. Results and Discussion

S2.1. Protein profile of the fractions

The molecular weight profile of PPI and the various fractions were analyzed by reducing SDS-PAGE. As depicted in Figure S3.1, PPI displayed several polypeptide bands with prominent ones

at 15, 20, 25, 30, 37, 50, 70, 85 and 90 kDa, with the 20-kDa band being in highest proportion. The alkaline-soluble fraction displayed similar polypeptide fractions as PPI with slight differences in the intensity of the bands. This could be because PPI was extracted under alkaline condition and therefore the alkaline soluble fraction retained some of the original proteins of PPI. Similar result was reported for commercial PPI and their associated fractions.[1] The salt-soluble fraction showed smeared polypeptide bands in the low molecular weight region of 10 to 37 kDa, with more intense bands observed below 20 kDa. The resulting polypeptides could be because of the disintegration of the disulfide bonds holding the six subunit of 11S legumin,[2,3] breaking of the hydrophobic interaction in vicilin thereby releasing the α, β and γ subunits,[4] or denaturation of convicilin. Water-soluble fraction showed polypeptide bands at 10-17, 25-30 and 75-80 kDa. The bands could be resulting from the disintegration of dimeric pea albumin to each subunit, PA2a and PA2b.[5,6] The difference in the polypeptide band pattern between globulin and albumin indicates that both proteins could be separated by dialysis. Therefore, different protein fractions of reasonable purity could be isolated using different solvent systems.

S2.2. Yield of the pea protein fractions

As presented in Table S3.1, yield of the three protein fractions in different extraction solvents per 45 g pea protein isolate was expressed as percentage ratio of the freeze-dried fractions to the original. Water soluble albumin (40.8%) predominate followed by alkaline soluble glutelin (24.8%), salt soluble globulin (5.0%) and ethanol soluble prolamin (0.12%). This result differs from previously reported pattern for commercial pea protein fractions where glutelin fractions was the major fraction (87.5%) followed by water soluble fraction (7.0%), salt soluble fraction (2.47%) and ethanol soluble fraction (1.52%).[1] The discrepancy could be because of variation in the protein extraction processes, or other genetic and environmental factors.[2,7,8] Protein contents of ASF, SSF

and WSF were high and similar (Table S3.1); however, prolamin fraction had a low protein content of 9.1%. The protein contents of ASF, SSF and WSF are in good agreement with those reported for commercial PPI.[1] The prolamin fraction was excluded from further analysis due to its low yield and poor protein profile, which may be because of its co-extraction with polyphenols and poor aqueous solubility.[1]

Table S3.1. Yield and protein content of the various pea protein fractions

Protein fractions	Protein yield (g/45 g PPI)	Protein content (%)
ASF	11.14 ± 0.15^{b}	88.52 ± 1.36^{a}
SSF	2.26 ± 0.04^{c}	84.68 ± 1.26^{a}
WSF	18.36 ± 2.02^{a}	88.60 ± 0.46^{a}
Mean values with different letters in a column are significantly different ($P < 0.05$) Abbreviations: ASF, alkaline soluble fraction; SSF, salt soluble fraction; WSF, water soluble fraction.		

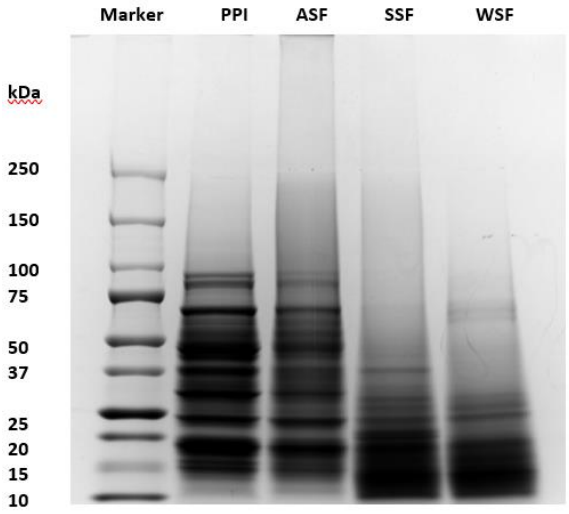

Figure S3.1. SDS-PAGE of PPI and the various protein fractions.

References

(1) Adebiyi, A. P.; Aluko, R. E. Functional Properties of Protein Fractions Obtained from Commercial Yellow Field Pea (Pisum Sativum L.) Seed Protein Isolate. *Food Chemistry*. **2011**, *128*(4), 902-908. https://doi.org/10.1016/j.foodchem.2011.03.116.

(2) Barac, M.; Cabrilo, S.; Pesic, M.; Stanojevic, S.; Zilic, S.; Macej, O.; Ristic, N. Profile and Functional Properties of Seed Proteins from Six Pea (Pisum Sativum) Genotypes. *International Journal of Molecular Sciences.* **2010**, *11*(12), 4973-4990. https://doi.org/10.3390/ijms11124973.

(3) Reinkensmeier, A.; Bußler, S.; Schlüter, O.; Rohn, S.; Rawel, H. M. Characterization of Individual Proteins in Pea Protein Isolates and Air Classified Samples. *Food Research International*. **2015**, *76*, 160-167. https://doi.org/10.1016/j.foodres.2015.05.009.

(4) Shewry, P. R.; Napier, J. A.; Tatham, A. S. Seed Storage Proteins: Structures and Biosynthesis. *Plant Cell*. **1995**, *7*(7), 945. https://doi.org/10.1105/tpc.7.7.945.

(5) Gruen, L. C.; Guthrie, R. E.; Blagrove, R. J. Structure of a Major Pea Seed Albumin: Implication of a Free Sulphydryl Group. *Journal of the Science of Food and Agriculture*. **1987**, *41*(2), 167-178. https://doi.org/10.1002/jsfa.2740410210.

(6) Higgins, T. J. V.; Beach, L. R.; Spencer, D.; Chandler, P. M.; Randall, P. J.; Blagrove, R. J.; Kortt, A. A.; Guthrie, R. E. CDNA and Protein Sequence of a Major Pea Seed Albumin (PA 2 : Mr≈26 000). *Plant Molecular Biology*. **1987**, *8*(1), 37-45. https://doi.org/10.1007/BF00016432.

(7) Wang, N.; Hatcher, D. W.; Gawalko, E. J. Effect of Variety and Processing on Nutrients and Certain Anti-Nutrients in Field Peas (Pisum Sativum). *Food Chemistry*. **2008**, *111*(1), 132-138. https://doi.org/10.1016/j.foodchem.2008.03.047.

(8) Hood-Niefer, S. D.; Warkentin, T. D.; Chibbar, R. N.; Vandenberg, A.; Tyler, R. T. Effect of Genotype and Environment on the Concentrations of Starch and Protein in, and the Physicochemical Properties of Starch from, Field Pea and Fababean. *Journal of the Science of Food and Agriculture*. **2012**, *92*(1), 141-150. https://doi.org/10.1002/jsfa.4552.

CHAPTER FOUR

IMPACT OF IONIC STRENGTH AND LIPOPHILICITY ON MOLECULAR INTERACTION OF PROTEINS WITH BIOACTIVE COMPOUNDS: STRUCTURE-BINDING RELATIONSHIP

Molecular Interaction of Pea Glutelin and Lipophilic Bioactive Compounds: Structure-Binding Relationship and Nano-/Micro Complexation

Ogadimma D. Okagu, Raliat O. Abioye, Chibuike C. Udenigwe

Journal of Agricultural and Food Chemistry **2023**, 71(12), 4957–4969.
https://doi.org/10.1021/acs.jafc.3c00047

DECLARATION FOR THESIS CHAPTER FOUR

Molecular Interaction of Pea Glutelin and Lipophilic Bioactive Compounds: Structure-Binding Relationship, Nano/Micro Complexation and Effect on Model Biomembrane

This is to declare that there is no conflict of interest associated with this work and the contribution of the candidate is as stated below:

Candidate's contribution	Conceptualization of idea, formal analysis, investigation, methodology, validation, visualization, writing, review, and editing	85%

The following co-authors attest to the candidate's active and leading participation in this research which constitute part of his thesis and has been published in Journal of Agricultural and Food Chemistry. The co-author's permission is as follows:

Name	Signature	Date
Raliat O. Abioye		22/11/2022
Chibuike C. Udenigwe		22/11/2022

Abstract

This study investigated the impact of ionic strength and lipophilicity of bioactive compounds on their interaction with alkaline-soluble pea glutelin fraction (ASF). Stern-Volmer quenching constant, K_D of 8.9±0.10, 5.3±0.06, 4.0±0.01, 1.1±0.00, 0.9±0.02 and 0.1±0.00 ($\times 10^4$ M^{-1}) was observed for curcumin-ASF (CuASF), astaxanthin-ASF (AsASF), cholecalciferol-ASF (ChASF), β-carotene-ASF (βCaASF), coenzyme Q_{10}-ASF (Q_{10}ASF) and β-sitosterol-ASF (βSiASF) complexes, respectively. Ionic strength increase did not significantly change K_D, the effective quenching constant K, and bimolecular quenching rate constant K_Q. However, it changed the mode of interaction of cholecalciferol, β-carotene, coenzyme Q_{10} and β-sitosterol from static to static-dynamic quenching. TEM showed that the morphology formed with protein (spherical nano-complexes, micro-aggregates, or fibre-like particles) differed amongst the compounds. Leakage assay, dynamic light scattering, and fluorescence microscopy showed that the complexes bind on the surface of calcein-loaded giant unilamellar vesicles. The favourable binding of CuASF, AsASF, ChASF and βCaASF complexes provides stable matrices for formulating protein-based delivery systems.

Keywords: curcumin, coenzyme Q_{10}, β-carotene, cholecalciferol, astaxanthin, β-sitosterol, alkaline-soluble glutelin, plant protein, biomolecular interactions, giant unilamellar vesicles, ionic strength, lipophilicity, fluorescence quenching

1. Introduction

Lipophilic bioactive compounds, such as curcumin, lutein, coenzyme Q_{10}, β-carotene, cholecalciferol, astaxanthin, and β-sitosterol, are widely known to promote health through their antioxidant, anticancer, antidiabetic, cardioprotective, anti-inflammatory and neuroprotective properties.[1–3] However, their rapid photo, chemical and gastric degradation, fast metabolic rate, relatively short half-life under physiological condition, and low water-solubility lead to low bioaccessibility and bioavailability and hence limit their food and pharmaceutical applications.[4–13] To mitigate these challenges, food protein-based encapsulation systems have been developed from native and succinylated pea protein,[4,11] pea protein fractions,[14] β-lactoglobulin,[12] insect protein,[5] whey protein,[8–10] rapeseed cruciferin,[15] gliadin,[16] zein,[7,17,18] soy,[8,19] casein,[8] and millet protein.[20] These encapsulation systems have been applied in the stabilization, protection, and release of the lipophilic nutraceuticals and hence enhancement of their bioavailability. Protein-based delivery vehicles have gained wider application in this area than those of lipids and carbohydrates due to the inherent physicochemical and structural properties of proteins, such as well-organized hydrophobic, hydrophilic, amphipathic, charged, and neutral amino acid side chains that can interact with various hydrophilic and lipophilic nutraceuticals via different intermolecular forces. Moreover, protein offers better protection of bioactive compounds in the salivary phase than carbohydrates due to the absence of proteolytic enzymes and eliminates the challenges of recrystallization and explosion associated with lipid-based formulation.[21]

Understanding the nature, mode, and strength of interaction between the lipophilic bioactive compounds and protein carriers is essential in the rational design of protein-based encapsulation systems with improved stability, high aqueous solubility, encapsulation efficiency, sustained and controlled release of the bioactive compounds as well as industrial scalability.[4,5,14,21] Tryptophan

fluorescence quenching technique is a widely employed method of investigating the mode and binding strength of protein-bioactive compound interactions.[22–24] Recently, this technique was used to demonstrate that surface hydrophobicity, structural and physicochemical properties of protein influence their interaction with bioactive compounds as well as how the overall nature and strength of the interaction translate to loading, encapsulation efficiency, gastrointestinal stability, and release profile.[4,5,14] However, there is limited information on the impact of some key physiologically relevant parameters encountered during oral administration, such as ionic strength, on hydrophobicity of the protein carriers and protein-bioactive compound interaction. In addition, there is a dearth of information on the effect of bioactive compound lipophilicity on their strength and nature of interaction with protein carriers, especially for established lipophilic nutraceuticals such as curcumin, coenzyme Q_{10}, β-carotene, cholecalciferol, astaxanthin, and β-sitosterol. This information would complement existing binding data employed in the encapsulation of bioactive compounds to prevent undesirable interactions with the carrier food matrix and ensure appropriate stoichiometry in the choice of protein-bioactive compound combinations for improved binding, encapsulation efficiency and release profile. It would equally help mitigate the difficulty associated with the complex nature of the gastrointestinal track with varying ionic strengths that could affect protein-bioactive compound binding and hence the stability and integrity of delivery systems during oral administration.

Development of efficient encapsulation systems is often accompanied with cytotoxicity assessment because the same parameters that promote binding, encapsulation, stability, and release could trigger unwanted physiological responses due to changes in the structural and physicochemical properties of protein or bioactive compounds. One commonly used method investigates the interaction occurring at the bio-nano/micro interface involving nano/micro

particles and model membranes such as giant unilamellar vesicles. This information is essential as undesirable interaction could negatively affect cell viability, efficacy of uptake, endocytosis, exocytosis mechanisms, permeation and transepithelial capacity. The overall outcome of this interaction could decrease protein digestibility and bioactive compound absorption, increase nano/microparticle accumulation and inflammation, or cause considerable side effects in the muscles, liver, and gut microbiota.[25–29]

In our previous study, alkaline-soluble pea glutelin fraction (ASF) demonstrated higher hydrophobicity than water-soluble albumin and salt-soluble globulin fractions, which translated to higher binding strength and encapsulation efficiency of curcumin, and pepsin-resistance of the nano-complexes formed.[14] Hence, ASF was employed as model protein to understand its interaction with structurally diverse bioactive compounds (Figure 4.1) of varying degree of lipophilicity. The objectives of this study were to (1) evaluate the binding of pea glutelin fraction with six lipophilic bioactive compounds (curcumin, coenzyme Q_{10}, β-carotene, cholecalciferol, astaxanthin, and β-sitosterol); (2) investigate the influence of lipophilicity of the compounds on protein interaction at various ionic strength; (3) characterize the protein-bioactive compound complexes with dynamic light scattering and transmission electron microscopy; and (4) investigate how bioactive compounds modulates the interaction of protein carrier with giant unilamellar vesicles using calcein leakage assay and widefield fluorescence microscopy.

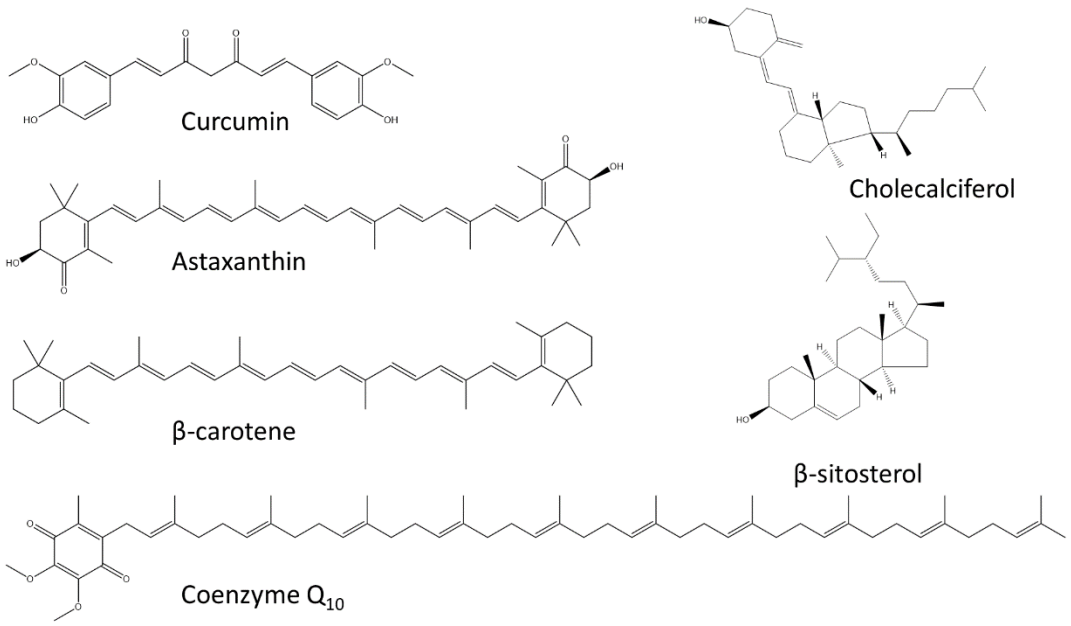

Figure 4.1: Chemical structure of various lipophilic bioactive compounds.

2. Materials and methods

2.1. Chemicals and Reagents

Curcumin (≥94%), coenzyme Q_{10} (≥98%), β-carotene (≥93%), cholecalciferol (≥97%), astaxanthin (≥98%), β-sitosterol (≥95%), 1,2-dioleoyl-sn-glycero-3-phosphocholine (≥99%), chloroform (≥99.5%), dimethyl sulfoxide (≥99.9%), ethanol, calcein, 1,2-dioleoyl-sn-glycero-3 phosphoethanolamine-N-(lissamine rhodamine B sulfonyl) (ammonium salt) (≥99%), and 8-anilo-1-naphthalenesulfonic acid (ANS) were purchased from MilliporeSigma Chemical Co. (St. Louis, MO, USA). Tris-EDTA (99.4–100.6%), sodium chloride (≥99.0%), Tris(hydroxymethyl)aminomethane (Tris-base, ≥ 100.1%), and sodium hydroxide (≥98%) were purchased from Fisher Scientific (Toronto, ON, Canada). Triton X-100 was bought from VWR (Mississauga, ON, Canada). Pulse Canada (Manitoba, Canada) generously donated the yellow pea

seed. Milli-Q water was dispensed from water-purification system (Advantage A10 Q-POD Milli-Q Water System) with resistivity of 18.2 MΩcm and total organic carbon level ≤ 5 ppb at 25 °C. All chemical reagents were of analytical grade and no further purification was performed.

2.2. Pea Protein Isolate Extraction

Pea protein isolate was extracted by isoelectric precipitation method as previously reported.[4,14] Briefly, dehulled yellow pea seeds were ground, sieved and the powder extracted with NaOH solution (0.05 M, 2 L, pH 12.7) to a final concentration of 100 g/L. The solution was stirred for 4 h in a magnetic stirrer (Cimarec, ThermoFisher Scientific, Waltham, MA USA) and centrifuged with Sorvall LYNX 4000 Superspeed centrifuge (Cimarec, ThermoFisher Scientific, Waltham, MA USA) under room temperature condition for 30 min at 5600 × g. The supernatant was adjusted to pH 4.5 using HCl (1 M) and the precipitate formed separated after centrifugation for 30 min, washed twice with Milli-Q water and pH adjusted to 7.0 with NaOH (1 M). The viscous solution was lyophilized with Labconco freeze dryer (Labconco corporation, Kansas, MO, USA) after freezing at −80 °C for 24 h. The total protein content of the resulting powder determined from Lowry assay has been previously reported as 96.1%.[29]

2.3. Isolation of Glutelin Fraction

Alkaline-soluble glutelin fraction (ASF) was extracted from the pea protein isolate after sequential extraction of water-soluble albumin, salt-soluble globulin and ethanol-soluble prolamin fractions as previously reported.[14,30] Briefly, albumin and globulin were extracted from pea protein isolate (45 g) using NaCl solution (2 %, 600 mL) and separated by dialysis. Prolamin fraction was extracted with ethanol (70%, 600 mL) from the residue obtain after albumin and globulin extraction and, finally, glutelin fraction was extracted using NaOH (0.02 M, 600 mL). In each step,

the mixture was stirred for 3 h and centrifuged for 30 min at 20,500 × g. Each extraction was carried out twice, centrifuged and the supernatants pooled. The supernatant of the glutelin fraction was adjusted to pH 4.8, allowed to stand for 1 h, centrifuged, and the precipitate collected, washed and the pH adjusted to 7 before centrifugation. The final precipitate of the alkaline-soluble glutelin fraction was lyophilized and stored in -20ºC. The total protein content of the glutelin fraction determined by Lowry assay has been previously reported as 88.52%.[14]

2.4. Surface hydrophobicity (H_0)

The surface hydrophobicity of alkaline-soluble pea protein isolate was determined as previously reported with some modifications; this time at 0, 0.1 and 150 mM NaCl to determine the effect of ionic strength. Protein solutions at various ionic strength were prepared in sodium phosphate buffer (0.1 M, pH 7.2) to a final concentration of 1.0, 0.75, 0.5, 0.25, 0.125 and 0.0 mg/mL. Each concentration at a given ionic strength (200 μL) was mixed with ANS (8 mM, 5μL) prepared in the same buffer in a black flat bottom Greiner 96-well microplate and fluorescence intensity measured at an excitation and emission wavelengths of 390 and 470 nm, respectively in a Spark multimode microplate reader (Tecan, Stockholm, Sweden). Surface hydrophobicity was calculated as a slope of fluorescence intensity vs. protein concentration.

2.5. Determination of bioactive compound lipophilicity

The lipophilicity of curcumin, coenzyme Q_{10}, β-carotene, cholecalciferol, astaxanthin, and β-sitosterol was determined using ALOGPS 2.1 program[31] by uploading the canonical SMILES of the various bioactive compounds in the web server (http://www.vcclab.org/web/alogps/). The result obtained was further corroborated with that from ChemDraw version 21.0.0, (https://perkinelmerinformatics.com/products/research/chemdraw).

2.6. Fluorescence quenching study of bioactive compounds interaction with alkaline soluble pea protein fraction

The interaction of the six lipophilic bioactive compounds with the glutelin fraction of pea protein isolate was investigated by fluorescence quenching technique using Varian Cary Eclipse (Agilent, Santa Clara, CA, USA) as previously reported with some modifications.[4,5,14,22,24] Solutions of curcumin, cholecalciferol, β-carotene and β-sitosterol were prepared in ethanol-water (50% ethanol) whereas that of astaxanthin and coenzyme Q_{10} were prepared in DMSO-water (70% DMSO) to a bioactive compound concentration range of 0-200 μM. Three sets of these solutions were made at NaCl concentration of 0, 0.1 and 150 mM. Equal volume of each lipophilic compound concentration was mixed with pea glutelin fraction (0.25 mg/mL) prepared at the corresponding ionic strength resulting in a final protein concentration of 0.125 mg/mL and bioactive compound concentration of 0, 2, 5, 10, 15, 20, 25, 30, 40, 50, 60, 80, and 100 μM. The final concentration of ethanol and DMSO in their respective solutions were 25 and 35 % respectively. The mixture in cuvette was shaken for 10 s and equilibrated for 3 min before fluorescence measurement. The spectrofluorometer was first zeroed with ethanol-water (25% ethanol) or DMSO-water (35% DMSO) at various ionic strength before fluorescence emission scan was performed from 300 to 450 nm at excitation wavelength of tryptophan (280 nm). Measurements were performed in triplicate and the binding parameters estimated from the tryptophan fluorescence intensity.[4,5,14,22,24,32,33]

The tryptophan fluorescence intensity of a protein is a function of the protein concentration. Hence, the decrease in fluorescence intensity because of binding of bioactive compound to form a non-fluorescence complex could be employed in estimating the strength and nature of the interaction. Stern-Volmer equation can employ the changes in tryptophan fluorescence intensity to measure

the binding parameters. Stern-Volmer equation (Eq. 4.1) can be used to estimate the Stern Volmer quenching constant K_D and biomolecular quenching rate constant, K_Q from the slope of a plot of $\frac{F_o}{F}$ vs. $[Q]$.

$$\frac{F_o}{F} = 1 + K_Q t_o[Q] = 1 + K_D[Q] \quad 4.1$$

F and F_0 are the fluorescence intensity of the protein with and without the quencher, respectively. The quenchers in the present study are curcumin, coenzyme Q_{10}, β-carotene, cholecalciferol, astaxanthin, and β-sitosterol. [Q] represents the various concentrations of the quencher while t_0, which is usually in the order of 10^{-9} s, is the lifetime of the fluorophore in the absence of the quencher.[4,5,14,22,24]

The modified Stern-Volmer equation (Eq. 4.2) could be used to estimate the accessible fluorophore fraction *(f)* and the effective quenching constant for the accessible fluorophores, *K*, from the intercept ($\frac{1}{f}$) and slope ($\frac{1}{fK}$) of a plot of $\frac{F_o}{F_o - F}$ vs. $\frac{1}{[Q]}$.

$$\frac{F_o}{F_o - F} = \frac{1}{fK[Q]} + \frac{1}{f} \quad 4.2$$

The substantive binding site *n* for the various bioactive compounds on the protein could be determined graphically from the slope of a graph of $\log\left[\frac{F_o - F}{F}\right]$ vs. $log[Q]$ (Eq. 4.3).[4,5,14,22,24]

$$\log\left[\frac{F_o - F}{F}\right] = logK_A + nlog[Q] \quad 4.3$$

K_A is the binding constant.

2.7. Transmission electron microscopy

Morphological analysis of the various complexes of pea glutelin with curcumin, coenzyme Q_{10}, β-carotene, cholecalciferol, astaxanthin, and β-sitosterol was performed with transmission electron microscopy technique. First, protein solution in water (1 mg/mL) was prepared, centrifuged at 7200 ×g, filtered with Whatman filter paper number 50, and degassed (Polylab vacuum desiccator) to remove impurities and air bubbles. Colloidal solutions of the complexes were prepared by mixing equal volume of each lipophilic compound (1 mg/mL) prepared either in ethanol (curcumin, β-carotene, cholecalciferol, and β-sitosterol) or DMSO (coenzyme Q_{10}, and astaxanthin) with solution of protein and stirred at 320 rpm for 4 h. A drop of each sample (10 µL) was added on a 300-mesh Formvar-carbon coated copper grid, allowed to dry and images acquired at different magnifications with JEM-1400Flash Electron Microscope (JOEL, Tokyo, Japan) at an accelerating voltage of 120 kV.

2.8. Interaction of protein-bioactive compound complexes with calcein-loaded GUV

2.8.1. Synthesis of Protein-Bioactive Compound Complexes

The complexes of the alkaline-soluble pea protein fraction and each of the six lipophilic bioactive compounds were prepared by anti-solvent precipitation method as previously reported with slight modifications.[4,29] The solution (1 mg/mL, 0.5 mL) of curcumin, β-carotene, cholecalciferol, and β-sitosterol prepared in ethanol, and coenzyme Q_{10} and astaxanthin prepared in DMSO was added dropwise to solutions of the glutelin fraction (5 mg/mL, 2 mL) in six flasks placed on a magnetic stirrer while stirring at 320 × g for 5 h until a steady negative zeta potential was attained. The various flaks were covered with aluminium foil to protect the bioactive compounds from photodegradation. The complexes were separated from the solvent by centrifugation at 7500 × g

for 30 min using an Eppendorf 5430R centrifuge (Eppendorf, Mississauga, ON, Canada). The residues were washed with Milli-Q water twice and redispersed in water (5 mL) for dynamic light scattering and light microscopic analysis, or in leakage buffer (10 mM Tris, 150 mM NaCl, 1 mM EDTA, pH 7.5) for the calcein-loaded GUV leakage assay.

2.8.2. Synthesis of hollow and calcein-loaded zwitterionic giant unilamellar vesicles

The preparation of hollow and calcein-loaded zwitterionic GUV was carried out using a previously reported technique,[29,34] with some modifications. Lipid solution of 1,2-dioleoyl-snglycero-3-phosphocholine (7.2 mg/mL) prepared in chloroform in a 50-mL centrifuge tube, protected with aluminum foil, was dried under a stream of nitrogen for 4 h, followed by vacuum drying for an extra 12 h. A solution of calcein at a concentration in which it undergoes self-quenching (70 mM, 12 mL) was prepared in leakage buffer and pH adjusted to 7.5 with NaOH (0.2 M). This solution (9 mL) was used to rehydrate the dried film to a final lipid concentration of 2 mg/mL, vortexed for 1 min, sonicated at 30 ºC for 1 h and subjected to five freeze/thaw cycles each comprising of 3 min in liquid N_2, 5 min in water bath (60 ºC) and 1 min vortex mixing. The calcein-loaded GUV was separated from the free calcein by size exclusion column (sephadex G-50) using a leakage buffer for equilibration and elution. The eluted calcein-loaded GUV was used for the leakage assay and was placed in 4 ºC for maximum of 72 h.

Fluorescence-labeled hollow and calcein-loaded GUV were prepared in a similar way for microscopic visualization of the nature of interaction of protein-bioactive compound complexes with calcein-loaded GUV. This time, a mixture of 1,2-dioleoyl-snglycero-3-phosphocholine (18 mg) and 1,2-dioleoyl-sn-glycero-3 phosphoethanolamine-N- (lissamine rhodamine B sulfonyl) (ammonium salt) (1 mg) was dissolved in chloroform.

2.8.3. Zwitterionic GUV leakage assay

Fluorescence spectroscopic technique using Varian Cary Eclipse (Agilent, Santa Clara, CA, USA) was employed to study the impact of interaction of the various complexes of the protein-bioactive compounds on the structural integrity of the calcein-loaded GUV as previously demonstrated.[29,34] Leakage buffer (pH 7.4) consisting of EDTA (1 mM), NaCl (150 mM) and Tris-base (10 mM) was prepared in Milli-Q water. Equal volume of solutions of the redispersed complexes of the protein-bioactive compound complexes in leakage buffer and calcein-loaded GUV (diluted two-fold with leakage buffer) was mixed in a cuvette to a final complex concentration of 0.8–80 µg/mL. Fluorescence emission scan (500 to 625 nm) was performed at excitation wavelength of calcein (495 nm) and slit width of 2.5 nm, after the equipment was zeroed with the leakage buffer. The baseline fluorescence intensity (F_0) of the calcein-loaded GUV was measured in the absence of the protein-bioactive compound complexes and was monitored for 10 min to ensure peak stabilization. After interaction of calcein-loaded GUV with various concentrations of the protein-bioactive compound complexes, fluorescence intensity (F) was measured. The mixture of equal volume of Triton X-100 (10%) with calcein-loaded GUV was assumed to cause 100% calcein leakage to produce the maximum fluorescence intensity (F_M). The percentage zwitterionic GUV leakage induced by the interaction of the various protein-bioactive compound complexes was estimated from (Eq. 4.4).

$$\%Leakage = \frac{(F - F_0)}{(F_M - F_0)} \times 100 \quad (4.4)$$

2.8.4. Widefield fluorescence microscopy

Widefield fluorescence microscopy was used to visualize the impact of interaction of the protein-bioactive compound complexes on the calcein-loaded GUV as reported previously.[29] Various

solutions of the complexes (150 µL, 0.16 mg/mL) or 10% Triton X-100 (150 µL) were mixed with calcein-loaded GUV solution, vortexed for 1 min, and allowed to stand for 15 min before mounting on glass microscope slides. All solutions were prepared in leakage buffer and the hollow and calcein-loaded GUV visualized before and after interaction with the various protein complexes of the lipophilic compounds. Visualization was done separately in the rhodamine B (λex 540, λem 625) and calcein (λex 494, λem 517) channels, with the Axio Imager 2 fluorescence microscope equipped with an Axiocam 506 monochromatic camera (Carl Zeiss, Oberkochen, Germany). The images acquired were processed and optimized with Zen 2.3 pro and 3.4 software (Carl Zeiss, Oberkochen, Germany).

2.8.5. Dynamic light scattering measurements

The particle size, zeta potential and polydispersity index of the various colloidal dispersions of the protein complexes of the lipophilic bioactive compounds as well as the empty and calcein-loaded GUV before and after interaction with the complexes were investigated by dynamic light scattering technique, using Nano-ZS Zetasizer (Malvern Instrument Ltd., Malvern, UK) as previously reported.[29] The same composition of the calcein-loaded GUV-bioactive compound complex mixtures used for widefield microscopy was analyzed in triplicate using Smoluchowski model at refractive index of 1.450, F(ka) 1.50, absorption of 0.001 and backscattered angle of 173◦ at 25 ◦C.

2.9. Statistical Analysis

The mean values of the data generated from triplicate measurements in the fluorescence quenching study, leakage assay and dynamic light scattering were analyzed by one-way analysis of variance,

using the Turkey's test and group mean differences, in Origin 9 software (OriginLab Corporation, Northampton, MA, USA). Values at $p < 0.05$ were considered to be significantly different.

3. Results and discussion

3.1. Effect of Ionic Strength on the Surface Hydrophobicity of ASF

The surface hydrophobicity of alkaline soluble pea protein fraction was previously reported to be significantly greater than those of the water-soluble albumin and salt-soluble globulin fractions.[14,30] The higher surface hydrophobicity resulted in better encapsulation efficiency of the lipophilic bioactive compound curcumin and offered better gastric protection and release profile.[14] Hence, it is crucial to understand the influence of some physiologically relevant parameters on the surface hydrophobicity of protein and its subsequent binding to bioactive compounds. The present study focused on understanding how ionic strength, a key physiological parameter, influences the surface hydrophobicity of ASF and hence its interaction with different bioactive compounds of varying lipophilicity. The surface hydrophobicity of ASF at zero ionic strength was greater than those at 0.1 and 150 mM NaCl, although there was neither any particular pattern nor significant difference between the surface hydrophobicity estimated at the three different conditions (Figure 4.2). A similar trend has equally been reported in the solubility curve of pea protein at different ionic strength and pH. At neutral pH, the hydrophobicity of pea protein at zero ionic strength was greater than those of higher ionic strength but no pattern was observed at various ionic concentrations.[35] At higher ionic strength, hydrophobic residues are buried towards the protein core while polar residues are exposed to aqueous environment. This process leads to decrease in interfacial energy and hence increase in protein solubility.[36] The effect of ionic strength on hydrophobicity is usually more pronounced at acidic pH. A previous study has reported an increase in solubility of pea protein at pH 4.5 from 3.25% at zero ionic strength to 80.75% at 0.9 M NaCl.[35]

Unlike salt-soluble pea globulin,[36] alkaline-soluble glutelin showed irregular hydrophobicity pattern at varying ionic strength at neutral pH, which could be attributed to their different structural and physicochemical properties.

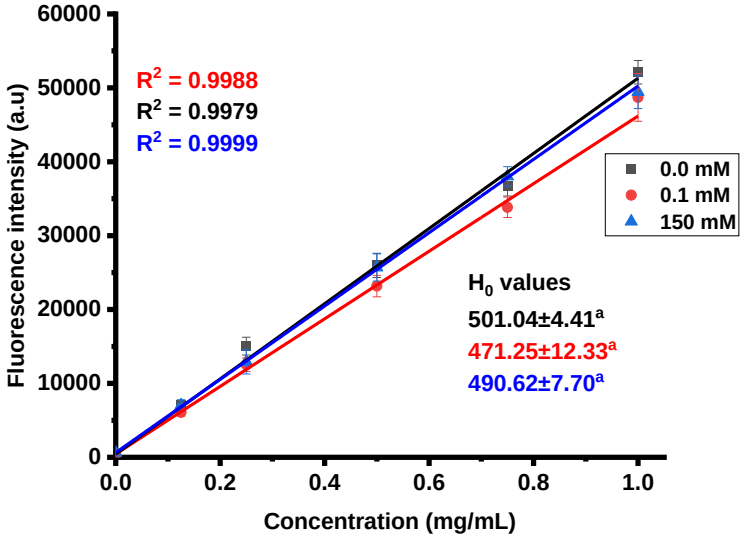

Figure 4.2. Surface hydrophobicity plot of ASF at various ionic strength.

Mean values with same superscript are not significantly different at $P < 0.05$.

3.2. Protein-lipophilic bioactive compounds interaction at different ionic environment

The presence of tryptophan residues in the alkaline-soluble pea protein fraction, which fluorescence at excitation wavelength of 280 nm, enables the estimation of the protein-bioactive compound interactions by fluorescence quenching technique.[14] The interaction of bioactive compounds in the vicinity of this fluorophore induces changes in fluorescence intensity and emission wavelength because of changes in the local environment. This effect changes protein secondary structure and conformation and could be induced by physical or chemical processes, such as collision quenching, molecular rearrangement, excited state reaction, ground state

complexation, and/or energy transfer. The magnitude of this effect is proportional to the concentration of the interacting bioactive compounds. By monitoring the behaviour of tryptophan fluorescence intensity and emission wavelength after interaction of various concentrations of the lipophilic compounds, the nature and strength of the interaction could be estimated by calculating the binding constants, accessible fluorophore fractions and the number of binding sites in the protein.[4,5,14,22,24]

The fluorescence emission spectra of ASF in the presence and absence of various concentrations of lipophilic bioactive compounds at 0, 0.1 and 150 mM NaCl are shown in Figures 4.3, 4.4 and 4.5, respectively. At the various ionic strengths, all the lipophilic bioactive compounds decreased the tryptophan fluorescence intensity at increasing concentration. The fluorescence quenching is because of binding of the small molecules, including curcumin, astaxanthin, cholecalciferol, β-carotene, coenzyme Q_{10} and β-sitosterol, which altered the microenvironment of the tryptophan residue to form less fluorescent complexes and caused changes in protein conformation and structure. This effect is more pronounce with less lipophilic bioactive compounds such as curcumin, astaxanthin and cholecalciferol (Table 4.1 and 4.2), which reached a plateau at 100 μM of the ligands, indicating greater binding affinity compared to β-carotene, coenzyme Q_{10} and β-sitosterol.

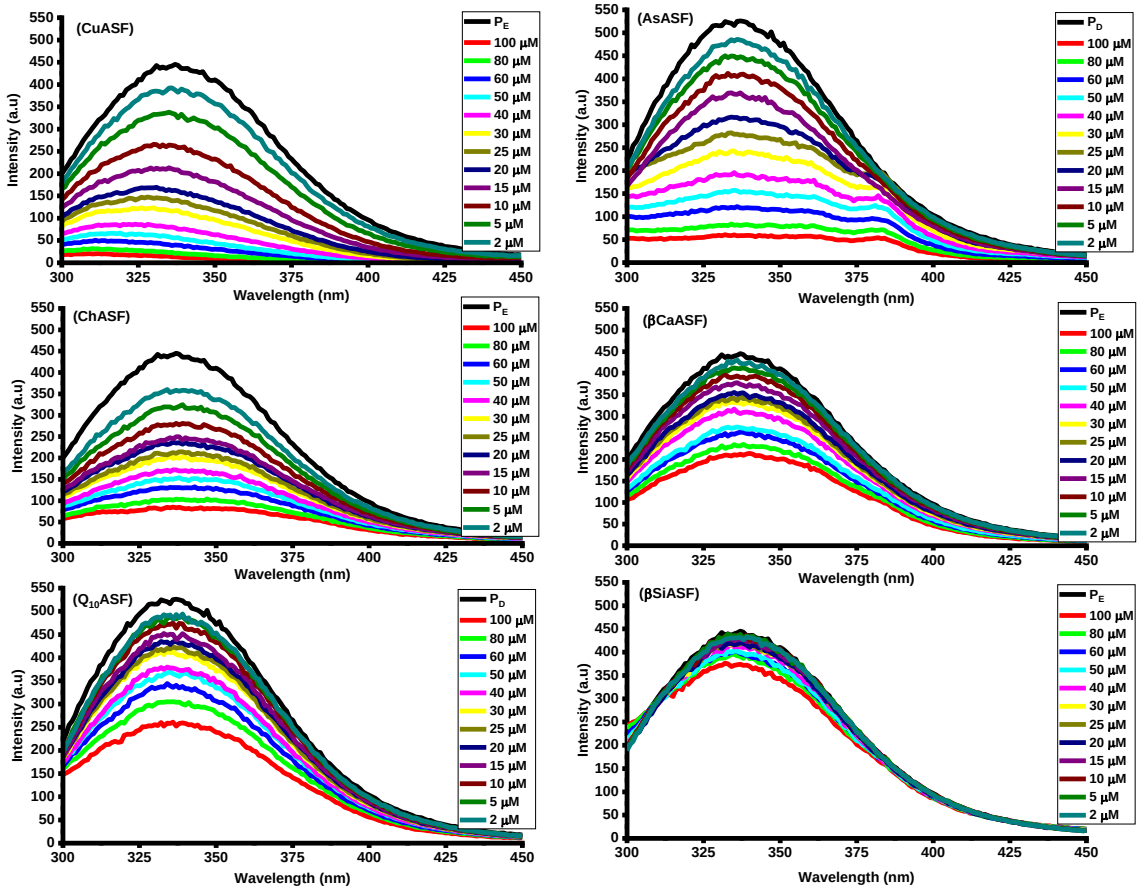

Figure 4.3. Fluorescence emission spectra of the curcumin-ASF, astaxanthin-ASF, cholecalciferol-ASF, β-carotene-ASF, co-enzyme Q10-ASF and β-sitosterol-ASF complexes at zero NaCl concentration depicting the impact of the interaction of the various bioactive lipophilic compounds on the fluorescence spectra of ASF.

P_E and P_D represent baseline fluorescence intensity of ASF in 25% ethanol and 35% DMSO respectively.

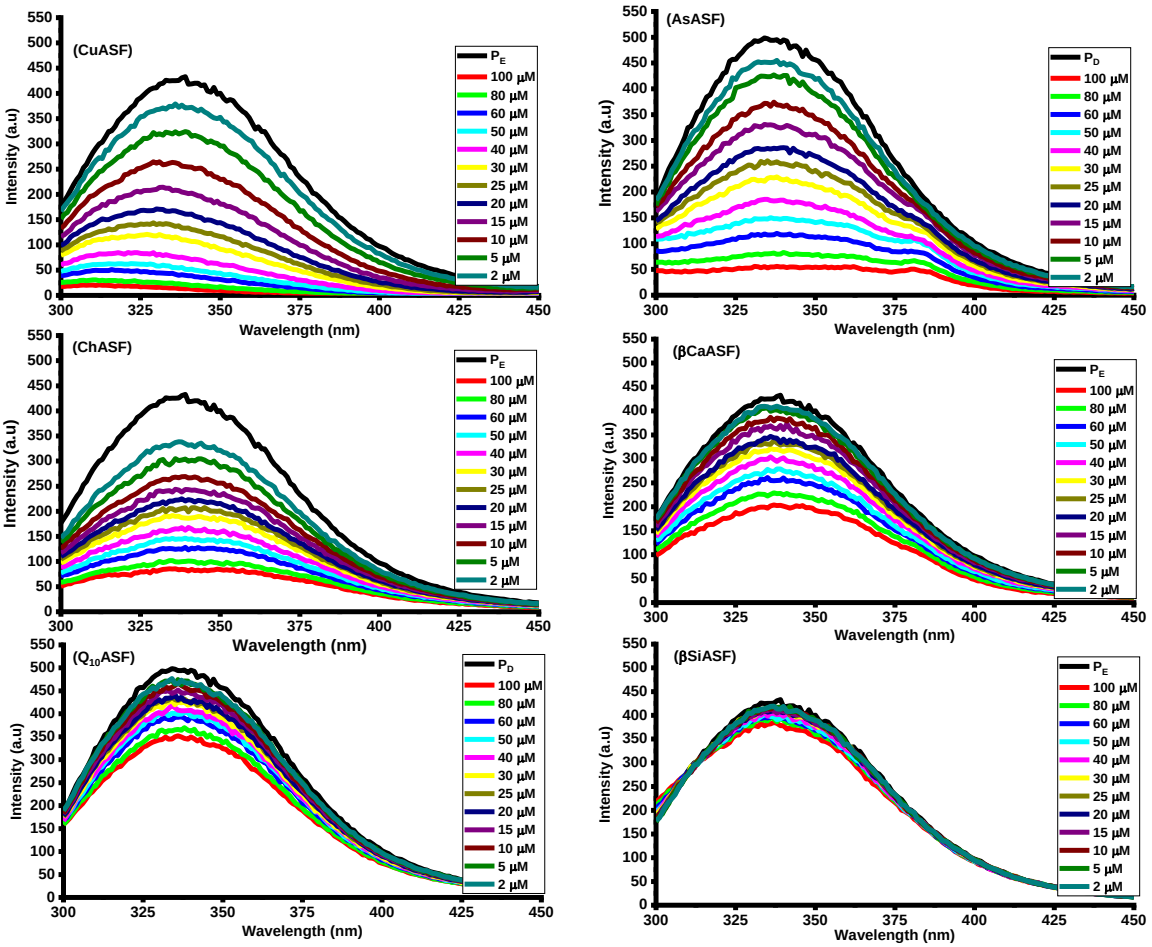

Figure 4.4. Fluorescence emission spectra of the curcumin-ASF, astaxanthin-ASF, cholecalciferol-ASF, β-carotene-ASF, co-enzyme Q10-ASF and β-sitosterol-ASF complexes at 0.1 mM NaCl concentration depicting the impact of the interaction of the various bioactive lipophilic compounds on the fluorescence spectra of ASF.

P_E and P_D represent baseline fluorescence intensity of ASF in 25% ethanol and 35% DMSO respectively.

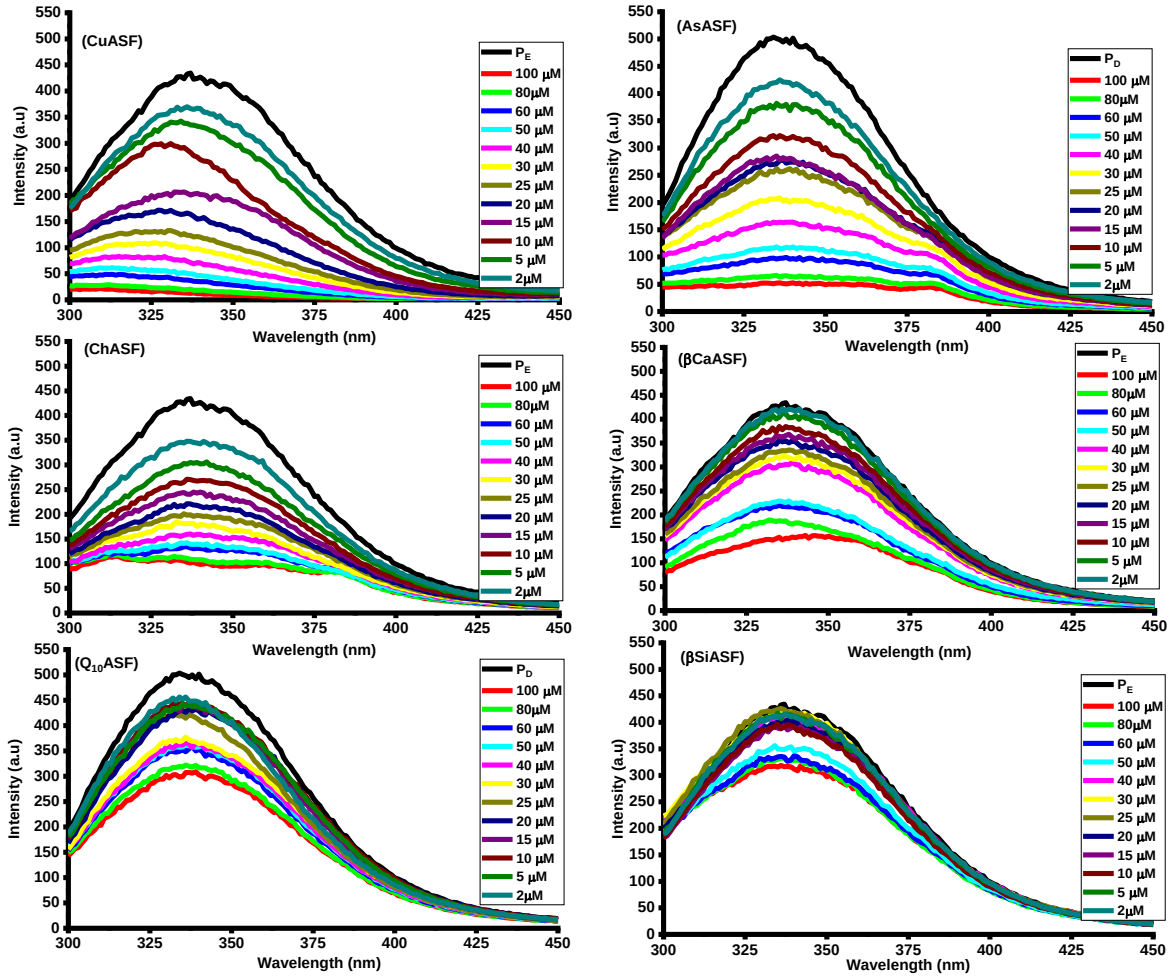

Figure 4.5. Fluorescence emission spectra of the curcumin-ASF, astaxanthin-ASF, cholecalciferol-ASF, β-carotene-ASF, co-enzyme Q10-ASF and β-sitosterol-ASF complexes at 150 mM NaCl concentration depicting the impact of the interaction of the various bioactive lipophilic compounds on the fluorescence spectra of ASF.

P_E and P_D represent baseline fluorescence intensity of ASF in 25% ethanol and 35% DMSO respectively.

The fluorescence emission spectra of ASF after interaction with curcumin showed better peak separation indicating stronger interaction compared to the overlapping peaks of β-sitosterol. This result indicates that although lipophilicity and hydrophilicity of the bioactive compounds plays

key roles in their interaction with ASF, moderate rather than higher lipophilicity is essential for stronger binding. It equally ensures that the bioactive compounds are soluble and stoichiometrically available for interaction in an aqueous environment. This is evident in Table 4.1 and 4.2 as the binding parameters of β-sitosterol could not be determined at 150 μM NaCl due to precipitation. ASF interaction with curcumin resulted in a hypsochromic shift of the maximum emission wavelength, which is more pronounced at higher ionic strength. This is an indication that the tryptophan residue is buried in the protein core.[37,38] The interaction of astaxanthin, cholecalciferol, β-carotene, coenzyme Q_{10} and β-sitosterol did not cause any significant effect on the maximum emission wavelength of ASF, which shows that the tryptophan residue is hidden from changes in polarity of the environment, hydrogen bonding, and effect of solvent.[4,14,22,24] The maximum emission wavelength of ASF at 335 nm, further corroborate that the lipophilic bioactive compounds were probably interacting in the vicinity of tryptophan residue buried in the hydrophobic core hidden from the hydrophilic aqueous environment of the solvent.[14,37] Interestingly, this result indicates that traces of ethanol and DMSO in the solvent had negligible impact on tryptophan residue and protein conformation. These solvents were inevitable due to the extremely low solubility of the lipophilic bioactive compounds in water or buffer.

Table 4.1. Bioactive compound lipophilicity

Bioactive compounds	LogP (ChemDraw)	LogP (ALogPs)
Curcumin	2.56	3.62
Astaxanthin	6.57	7.40
Cholecalciferol	7.03	7.98
β-Carotene	10.68	9.72
Coenzyme	ND	9.94
β-Sitosterol	8.14	7.27
LogP is the logarithm of the partition coefficient. Positive value indicates lipophilicity and the greater the value, the more lipophilic the bioactive compounds. Negative value would indicate hydrophilicity.		

Table 4.2. Binding parameters of interaction of alkaline soluble pea protein with lipophilic bioactive compounds at different NaCl concentrations.

Zero ionic strength					
Complexes	K ($\times 10^4$ M^{-1})	K_D ($\times 10^4$ M^{-1})	K_Q ($\times 10^{13}$ $M^{-1}S^{-1}$)	n	f
Curcumin-ASF	$6.3\pm0.38^{a,b}$	8.9 ± 0.10^{b}	8.9 ± 0.10^{b}	$1.25\pm0.01^{a,b}$	$1.09\pm0.02^{a,b}$
Astaxanthin-ASF	5.0 ± 0.25^{c}	5.3 ± 0.06^{d}	5.3 ± 0.06^{d}	$1.18\pm0.01^{a,b}$	$0.81\pm0.01^{b,c,d,e}$
Cholecalciferol-ASF	4.9 ± 0.11^{c}	4.0 ± 0.01^{e}	4.0 ± 0.01^{e}	$0.73\pm0.00^{e,f,g}$	$0.95\pm0.00^{b,c,d,e}$
β-Carotene-ASF	$1.6\pm0.03^{d,e,f}$	1.1 ± 0.00^{f}	1.1 ± 0.00^{f}	$0.84\pm0.03^{d,e,f}$	$0.80\pm0.01^{b,c,d,e}$
Coenzyme Q_{10}-ASF	$1.7\pm0.14^{d,e,f}$	$0.9\pm0.02^{f,g}$	$0.9\pm0.02^{f,g}$	$0.86\pm0.00^{d,e,f}$	$0.67\pm0.03^{e,f,g}$
β-Sitosterol-ASF	$0.7\pm0.10^{d,e,f}$	0.1 ± 0.00^{h}	0.1 ± 0.00^{h}	$0.75\pm0.06^{e,f,g}$	$0.37\pm0.05^{f,g,h}$
0.1 mM NaCl					
Curcumin-ASF	6.8 ± 0.10^{a}	8.8 ± 0.06^{b}	8.8 ± 0.06^{b}	$1.27\pm0.00^{a,b}$	$1.05\pm0.01^{b,c}$
Astaxanthin-ASF	$5.4\pm0.21^{b,c}$	5.5 ± 0.06^{d}	5.5 ± 0.06^{d}	$1.14\pm0.01^{b,c}$	$0.82\pm0.01^{b,c,d,e}$
Cholecalciferol-ASF	5.1 ± 0.07^{c}	3.8 ± 0.02^{e}	3.8 ± 0.02^{e}	$0.70\pm0.01^{f,g}$	$0.94\pm0.00^{b,c,d,e}$
β-Carotene-ASF	$1.9\pm0.19^{d,e}$	1.1 ± 0.01^{f}	1.1 ± 0.01^{f}	$0.94\pm0.01^{c,d,e}$	$0.72\pm0.04^{c,d,e}$
Coenzyme Q_{10}-ASF	2.4 ± 0.29^{d}	$0.4\pm0.00^{g,h}$	$0.4\pm0.00^{g,h}$	$0.69\pm0.02^{f,g}$	$0.37\pm0.02^{g,h}$
β-Sitosterol-ASF	$1.9\pm0.24^{d,e}$	0.1 ± 0.00^{h}	0.1 ± 0.00^{h}	0.57 ± 0.07^{g}	0.14 ± 0.01^{h}
150 mM NaCl					
Curcumin-ASF	$6.3\pm0.51^{a,b}$	9.6 ± 0.37^{a}	9.6 ± 0.37^{a}	1.42 ± 0.03^{a}	$1.13\pm0.02^{a,b}$
Astaxanthin-ASF	$5.3\pm0.16^{b,c}$	6.5 ± 0.06^{c}	6.5 ± 0.06^{c}	$1.03\pm0.04^{b,c,d}$	$1.03\pm0.01^{b,c,d}$
Cholecalciferol-ASF	6.9 ± 0.15^{a}	3.6 ± 0.11^{e}	3.6 ± 0.11^{e}	$0.64\pm0.02^{f,g}$	$0.86\pm0.01^{b,c,d,e}$
β-Carotene-ASF	$0.9\pm0.21^{e,f}$	1.2 ± 0.10^{f}	1.2 ± 0.10^{f}	$1.05\pm0.06^{b,c,d}$	1.40 ± 0.25^{a}
Coenzyme Q_{10}-ASF	$1.3\pm0.11^{d,e,f}$	$0.4\pm0.01^{g,h}$	$0.4\pm0.01^{g,h}$	$0.73\pm0.14^{e,f,g}$	$0.70\pm0.03^{d,e,f}$
β-Sitosterol-ASF	n.d	n.d	n.d	n.d	n.d

The superscripts with different letters (a-e) in a column indicates that the mean values are significantly different ($P < 0.05$).
n.d., not determined due to precipitation. ND., not determined due to software limitation for large molecules.
Abbreviations: ASF, Alkaline soluble pea protein isolate; *K*, effective quenching constant; *n*, substantive binding pockets for the various lipophilic compounds in ASF; K_D, Stern-Volmer quenching constant; K_Q, biomolecular quenching rate constant; *f*, accessible fluorophore fraction; ND, not determined.

Using Eq. 4.1, the Stern-Volmer quenching constant K_D and bimolecular quenching rate constant K_Q were estimated at the linear region of a plot of $\frac{F_0}{F}$ vs. $[Q]$ (Figure 4.6) with data fitting correlation coefficient above 0.95, and the nature of the protein-bioactive compound interactions determined at various ionic strength and the results presented in Table 4.2. At various ionic strength, curcumin and astaxanthin displayed a static quenching behaviour at low concentration and dynamic quenching at concentration above 40 and 60 µM, respectively. This is an indication that the binding mode of these two bioactive compounds is independent of the ionic environment. Cholecalciferol, β-carotene, coenzyme Q_{10} and β-sitosterol displayed mostly static quenching at 0 and 0.1 mM NaCl as evident in the linear plot. At higher ionic strength (150 mM), cholecalciferol, β-carotene, and coenzyme Q_{10} displayed static quenching behaviour at low concentration of the ligand and dynamic quenching above 50, 40 and 25 µM concentrations, respectively. β-Sitosterol demonstrated only dynamic quenching at various ligand concentration at 150 mM ionic strength and the binding parameters could not be determined due to the non-linearity of the plot and precipitation during measurement. Dynamic quenching results from excited state collision between tryptophan residues of protein and the ligand while static quenching refers to ground state complexation.[39,40] This result indicates that there is lower dissociation rate of the protein-bioactive compound complexes formed at lower concentration of the bioactive compound compared to the higher concentration where there is tendency of protein binding site saturation and shifts in chemical equilibrium. At lower ligand concentration, the rate of association exceeded the rate of dissociation but this was reversed as the concentration increased. Lower ionic strength favoured static binding of cholecalciferol, β-carotene, coenzyme Q_{10} and β-sitosterol to ASF while higher ionic strength promoted dynamic quenching mode. The changes in the mode of binding of these lipophilic bioactive compounds at higher ionic strength could be attributed to the effect of

unfavourable polar environment. Therefore, the determination of the optimum ionic environment and stoichiometric ratio of the protein and lipophilic bioactive compound is essential for efficient stabilization and protection, especially during encapsulation and delivery in functional food formulation. The estimated values of K_D and K_Q (Table 4.2) showed that curcumin demonstrated stronger binding to ASF and hence formed the most stable complex followed by astaxanthin and then cholecalciferol whereas β-sitosterol displayed the least binding strength. These binding parameters are correlated with the lipophilicity of the bioactive compounds where those with moderate lipophilicity showed stronger binding than those of higher lipophilicity. This could be because of unfavourable aqueous environment for the interaction. The K_D and K_Q values of the various bioactive compounds are similar at various ionic strength, which could be attributed to the negligible impact of ionic strength on protein hydrophobicity (Figure 4.1). Ionic strength changed the nature of binding of cholecalciferol, β-carotene, coenzyme Q_{10}, and β-sitosterol to ASF from static dominant to static-dynamic binding, but K_D and K_Q were not affected by this factor. Therefore, while the nature of binding of some bioactive compounds could be influenced by ionic environment, K_D and K_Q are heavily dependent on the protein hydrophobicity. The K_Q values for all the lipophilic bioactive compounds-protein complexes are greater than the limiting diffusion rate constant ($K_{dif} = 2.0 \times 10^{10}$ $M^{-1}S^{-1}$) suggesting that static rather than dynamic binding played a major role in the fluorescence quenching.[41] Therefore, the estimated binding parameters (Table 4.2) are not as a result of collision between tryptophan residues and the lipophilic bioactive compounds (dynamic binding) but due to the formation of less fluorescent ground-state complexes (static binding).[39] The K_D and K_Q values (Table 4.2) indicate moderate binding strength and are of the same order of magnitude with values reported in other protein-bioactive compound fluorescence-based interaction studies.[4,5,14,22,24,37] The value estimated for curcumin-ASF

interaction is twice that reported earlier,[14] which can be attributed to the different solvent composition. Earlier report[14] aimed at reducing ethanol composition to ~10% but the present study involves bioactive compounds of higher lipophilicity (Table 4.1), hence requiring higher concentration of ethanol or DMSO for better solubility. Interaction was carried out in 25% ethanol for all ethanol soluble bioactive compounds, including curcumin. The higher the percentage of ethanol, the higher the solubility and hence more molecules of curcumin available for interaction. Studies have shown that 25% ethanol induces negligible structural changes in protein and hence the solvent is adequate for interaction studies.[23,42]

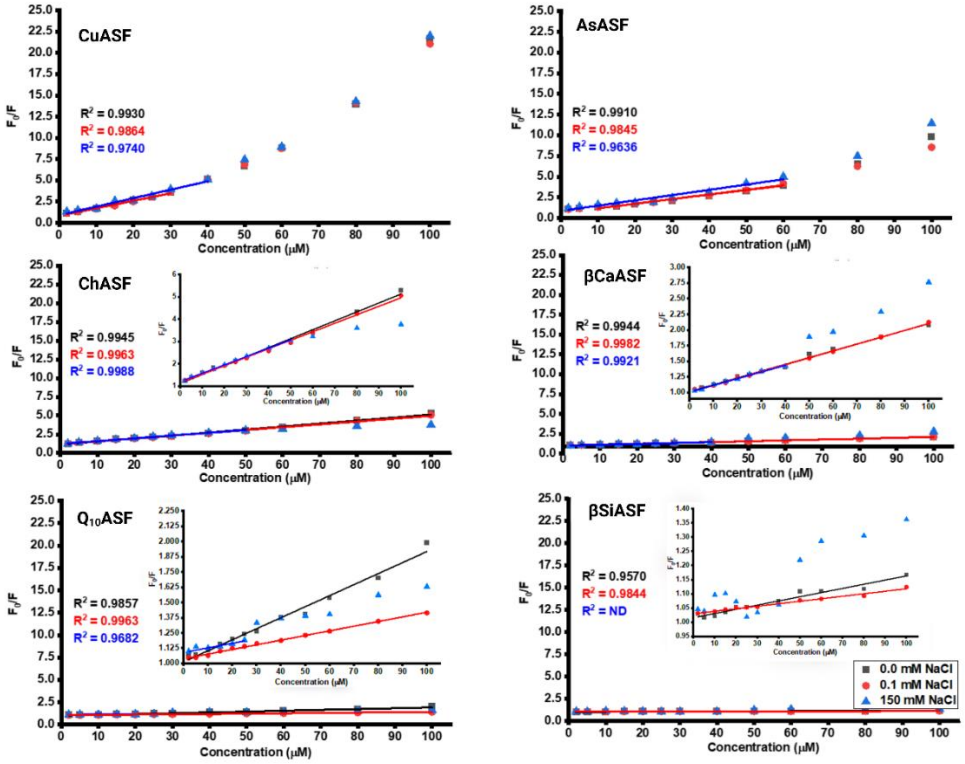

Figure 4.6. Determination of Stern-Volmer constant, K_D and biomolecular quenching constant K_Q in the curcumin-ASF, astaxanthin-ASF, cholecalciferol-ASF, β-carotene-ASF, co-enzyme Q10-ASF and β-sitosterol-ASF complexes through a plot of F_0/F against the concentration of the various lipophilic compounds at 0.0, 0.1 and 150 mM NaCl concentration.

The effective quenching constant, K for the accessible tryptophan residue, also known as the associative binding constant for the protein-bioactive compound complex and the accessible tryptophan fraction, f were determined from the slope ($\frac{1}{fK}$) and intercept ($\frac{1}{f}$), respectively, of the linear regression of a plot of $\frac{F_o}{F_o - F}$ vs. $\frac{1}{[Q]}$ with data fitting correlation greater than 0.97 (Figure 4.7).

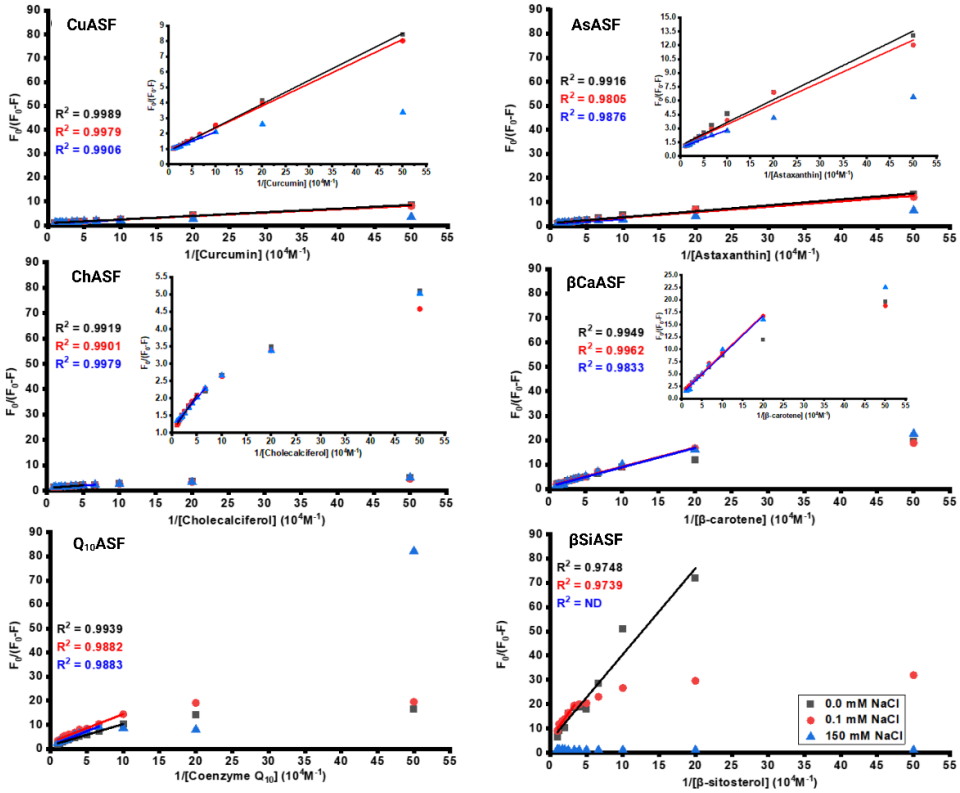

Figure 4.7. Determination of effective quenching constant (K) and the accessible fluorophore fraction (f) in the curcumin-ASF, astaxanthin-ASF, cholecalciferol-ASF, β-carotene-ASF, co-enzyme Q10-ASF and β-sitosterol-ASF complexes at 0.0, 0.1 and150 mM NaCl concentration through a plot of $F_0/(F_0-F)$ vs. 1/[lipophilic compound].

Similar to K_D and K_Q values, K values estimated for curcumin, astaxanthin, and cholecalciferol are significantly larger than those of β-carotene, coenzyme Q_{10} and β-sitosterol (Table 4.2) and hence

demonstrate better interaction. Ionic strength of the interacting medium did not cause any significant effect on the values of K. This further suggests that the main driving force in the ASF-bioactive compound binding is hydrophobic rather than electrostatic interaction because ionic strength mainly influence binding constant when there is distribution of charges on the surface of the protein.[13] This result corroborates our initial assumption from the nature of the fluorescence emission spectra and maximum emission wavelength that the protein-bioactive compound interaction is likely occurring in the hydrophobic protein core hidden from changes in polarity of the environment, and that binding constants, which indicate binding strength of the protein-bioactive compound complex, depend on protein hydrophobicity. Since ionic strength did not have a major effect on the protein hydrophobicity, the values K_D, K_Q and K are not likely to be affected. A previous study showed that the presence of monovalent ion, K^+ had no significant impact on K values for the interaction of biotin with β-lactoglobulin, α-lactalbumin, bovine serum albumin and whey protein isolate. The study equally showed only slight increase in K values at NaCl concentration of 10, 50, and 100 mM, which is attributed to increased surface hydrophobicity as tryptophan residue is exposed on the protein surface at higher ionic strength.[32] Similar observation was not made in the present study probably due to different nature of the protein and ligands.

The estimated accessible fluorophore fraction, f and the substantive binding site, n calculated graphically from Eq. 4.2 and 4.3, respectively are shown in Table 4.2, Figure 4.7 and 4.8. The f values show that curcumin, astaxanthin and cholecalciferol at zero ionic strength are accessible to 100, 81 and 95% tryptophan residues, and this could have contributed to their higher K_D, K_Q and K values compared to β-carotene, coenzyme Q_{10} and β-sitosterol. There was no significant difference in the f values for curcumin, astaxanthin and cholecalciferol with increasing ionic strength, in line with the binding constant values, which were independent of the ionic

concentration. However, there is no clear pattern in *f* values of β-carotene, coenzyme Q_{10} and β-sitosterol. The *n* values (Table 4.2) show that the number of curcumin and astaxanthin that bound per protein is higher than that of other bioactive compounds and independent of ionic environment. Cholecalciferol, β-carotene, coenzyme Q_{10} and β-sitosterol had similar *n* values in the range of 0.57–1.05 at different ionic strength, except for β-carotene whose value surprisingly increased at 150 mM NaCl. The *n* and *f* values reported in this study are similar to previously reported values.[4,5,14,22,24,32,37]

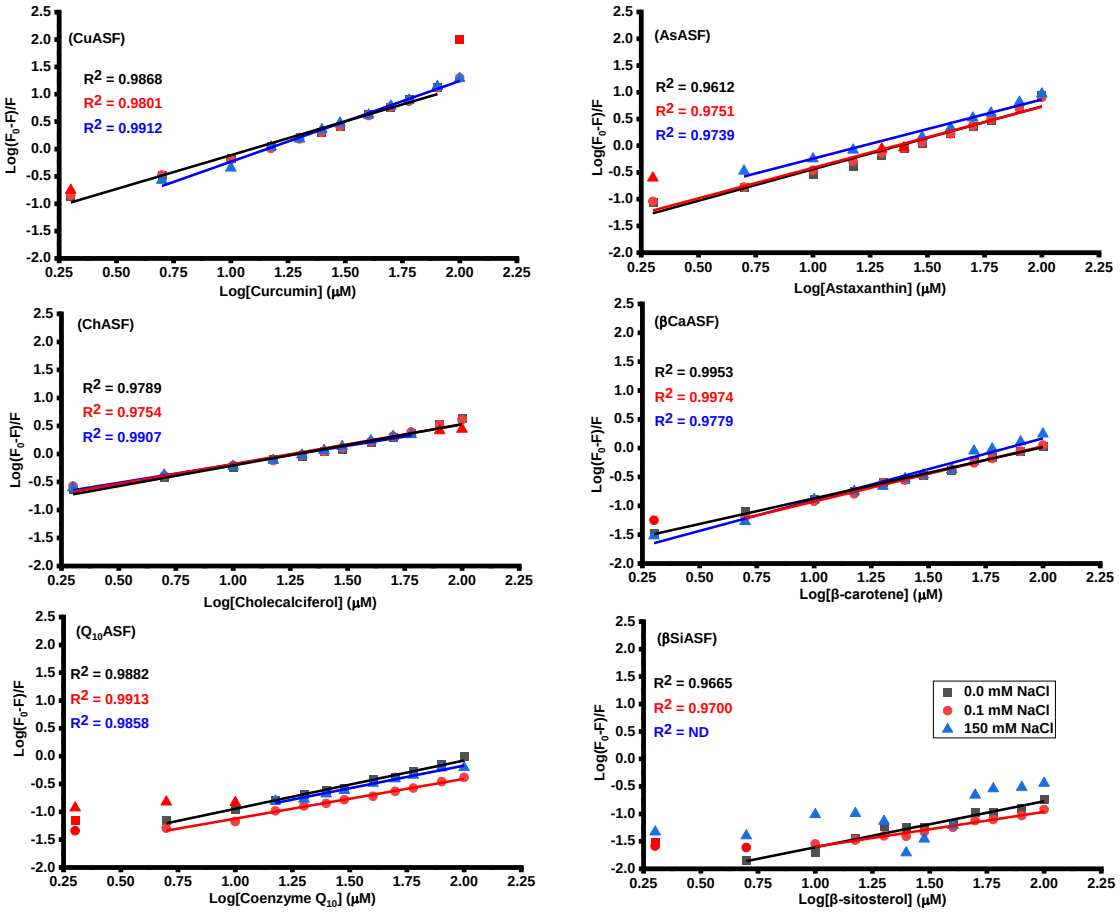

Figure 4.8. Determination of substantive binding site *n* of curcumin, astaxanthin, cholecalciferol, β-carotene, co-enzyme Q10 and β-sitosterol, in ASF at 0.0, 0.1 and 150 mM NaCl concentration.

3.3. Morphological characterization by transmission electron microscopy

The morphology of the protein-bioactive compound complexes was analyzed by transmission electron microscopy and the data presented in Figure 4.9. The images were acquired at different magnification due to the complexity of samples of diverse structural properties (Figure 4.1) and limitation of acquiring images at strictly one magnification without destroying the carbon coated copper grid. The various complexes displayed unique shapes and sizes. Curcumin-ASF interaction formed spherical complexes of ~270 nm, similar to complexes of curcumin with pea globulin, pea albumin,[14] whole pea protein, succinylated pea protein,[4] insect protein,[5] and zein-caseinate-sodium alginate.[43] Astaxanthin and β-sitosterol formed spherical nanoparticles in the size range of 15-50 nm, cholecalciferol and β-carotene formed aggregate complexes in the size range of 0.5-1.5 μm while coenzyme Q_{10} formed mainly fibre-like particles. The differences in the size and morphology of the various nano and micro-complexes could be attributed to their varying degree of lipophilicity. While curcumin, astaxanthin and cholecalciferol have moderate lipophilicity, β-carotene, coenzyme Q_{10} and β-sitosterol have high lipophilicity. This difference would result to varying degree of solubility and precipitation resulting in nano and micro-particles of difference sizes and shapes. The size and shape of astaxanthin and cholecalciferol-protein complexes appear similar to those reported for astaxanthin-loaded β-lactoglobulin nanocomplexes[12] and cholecalciferol encapsulated in pea protein[11]. Therefore, while curcumin, astaxanthin, coenzyme Q10 and β-sitosterol formed mainly nanocomplexes, cholecalciferol and β-carotene formed micro-complexes. The population of the particles formed by curcumin, astaxanthin and cholecalciferol is higher than those formed by β-carotene, coenzyme Q_{10} and β-sitosterol. This is probably due to the lower lipophilicity of the former (Table 4.1) and hence increased solubility and availability of interacting bioactive molecules in the solvent. This result further strengthens the conclusion drawn

from the binding parameters, that the binding strength of curcumin, astaxanthin and cholecalciferol to ASF is greater than those of β-carotene, coenzyme Q_{10} and β-sitosterol because of their lower lipophilicity in aqueous environment.

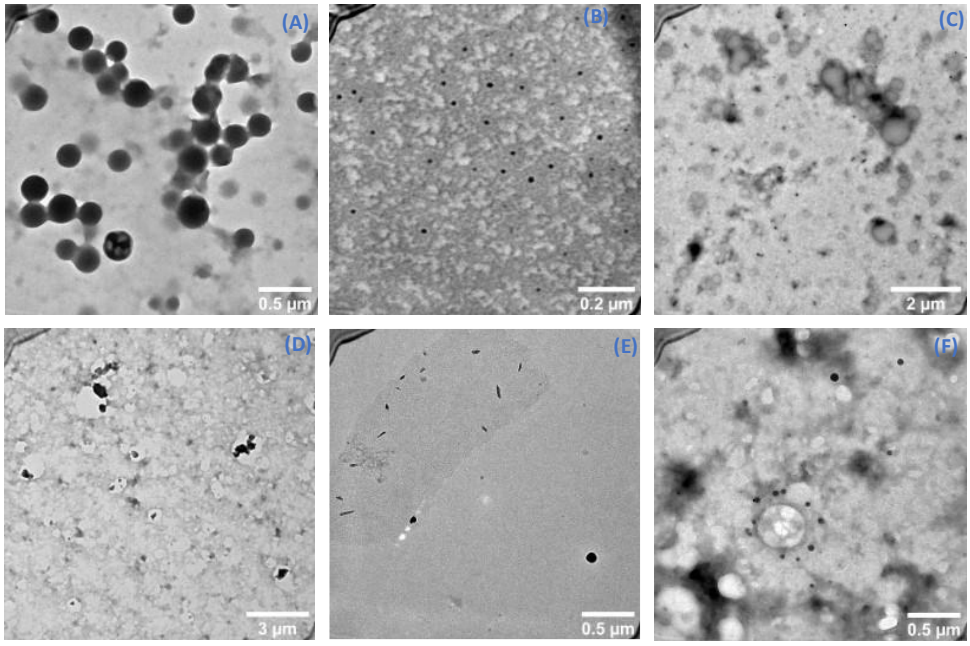

Figure 4.9. Transmission electron microscopy images of colloidal complexes of (A) ASF-curcumin (B) ASF-astaxanthin (C) ASF-cholecalciferol (D) ASF-β-carotene (E) ASF-coenzyme Q10 (F) ASF-β-sitosterol.

3.4. Interaction of protein-lipophilic bioactive compound complexes with calcein-loaded zwitterionic GUV

Understanding the nature of interactions occurring at the bio-nano/micro interface is essential in developing biocompatible and safe encapsulation systems in food formulation. In this study, we used zwitterionic giant unilamellar vesicle as a model biomembrane and ASF-bioactive compound complex as the nano/micro particles. Interaction of nano/micro particles with calcein-loaded GUV could cause membrane disruption leading to calcein leakage and hence increase in calcein

fluorescence intensity. Nano/micro particles can as well bind on GUV surface leading to calcein fluorescence quenching.[29] Calcein undergoes self-quenching at 70 mM and its fluorescence intensity is significantly reduced on encapsulation into a lipid membrane. Disruption of this membrane results in calcein leakage and dilution into the leakage buffer and hence increase in fluorescence intensity. The percentage calcein leakage is estimated from Eq. 4.4. This value can be positive or negative depending on whether interaction of nano/micro particles induced calcein leakage leading to increase in fluorescence intensity or a decrease due to binding of the nano/micro particles on GUV surface.[29] This technique has been explored in investigating the cytotoxicity of organic nanomaterials such as protein aggregates in nanoscale,[44] curcumin-loaded protein and protein-chitosan nano complexes,[29] lysozyme aggregates, amyloid fibril, lysozyme functionalized single-walled carbon nanotube,[28] and semihydrophobic polystyrene nanoparticles.[45] In this study, the impact of protein-bioactive compound complexes of various stability, lipophilicity, sizes, and shapes on GUV loaded with calcein was investigated by monitoring fluorescence intensity changes after interaction. The steady maximum fluorescence emission wavelength at 518 nm (Figure 4.10) after interaction of calcein-loaded GUV with various concentrations of the protein-bioactive compound complexes indicated that the nano and microparticles interacted mainly with GUV and did not form complexes with calcein; hence the structural properties of calcein is unaltered. As shown in Figures 4.10 and 4.11, all the protein-bioactive compound complexes induced calcein fluorescence quenching at various concentrations except for β-sitosterol-protein complex, which induced minimal calcein leakage at low concentrations. This behavior was observed in curcumin-pea protein and curcumin-succinylated pea protein nano complexes, which caused negligible calcein leakage at low concentration and fluorescence quenching at higher doses.[29] Protein complexes of curcumin, astaxanthin, cholecalciferol, and β-carotene that displayed higher binding

strength (Table 4.2) caused major fluorescence quenching in a dose-dependent manner, although this is more pronounced with curcumin-protein and β-carotene-protein complexes. The calcein fluorescence quenching can be attributed to the binding of the complexes on the surface of the GUV without disrupting the vesicle.[29] The magnitude of this quenching effect is estimated by the negative leakage percentage (Figure 4.11); the higher the negative value, the greater the binding and hence more fluorescence quenching. Classic molecular dynamic simulation supports this mechanism of nano/micro particle adsorption to lipid membrane.[47] The micro/nano complex binding to the surface of GUV cannot be electrostatically driven due to the net zero charge of the zwitterionic GUV but hydrophobic interaction may be involved. The role of hydrophobic interaction on particle binding to lipid membrane has been reported.[44,45] Since the alkaline-soluble pea protein fraction has high surface hydrophobicity (Figure 4.2) and the bioactive compounds are highly lipophilic (Table 4.1), hydrophobic interaction could be playing a key role on the adsorption of the nano and micro complexes to the GUV surface. The adsorption of carboxyl end-functionalized polystyrene nanoparticles on neutral supported lipid bilayers is facilitated by hydrophobic interaction and results in membrane disruption.[45] Hydrophobic interaction is also responsible for lipid membrane rupturing due to the binding of neutral liposome to nanoscale amyloid fibril that originated from lysozyme.[44] The nature of the interaction with GUV could not be directly linked to the shapes and sizes of the protein-bioactive compound complexes as the nanoscale spherical complexes (formed by curcumin and astaxanthin) and microscale aggregates (formed by cholecalciferol and β-carotene) (Figure 4.9) showed marked disparities in their quenching effect to the calcein-loaded GUV. The protein complexes of curcumin and β-carotene had the highest adsorption effect on the GUV surface whereas β-sitosterol and coenzyme Q_{10}-protein complexes, which had the lowest binding strength (Table 4.2), displayed the least effect.

The different behaviours could be attributed to the different chemical and structural characteristics as the various complexes contain the same macromolecule (alkaline-soluble pea glutelin fraction) but different lipophilic bioactive compounds. This observation supports our earlier report that encapsulated bioactive compounds play key role in modulating the interaction between the encapsulating macromolecule and GUVs.[29] Therefore, the chemical and structural properties of bioactive compounds and their nature and strength of interaction with macromolecule (protein) play a key role on their impact on lipid vesicles.

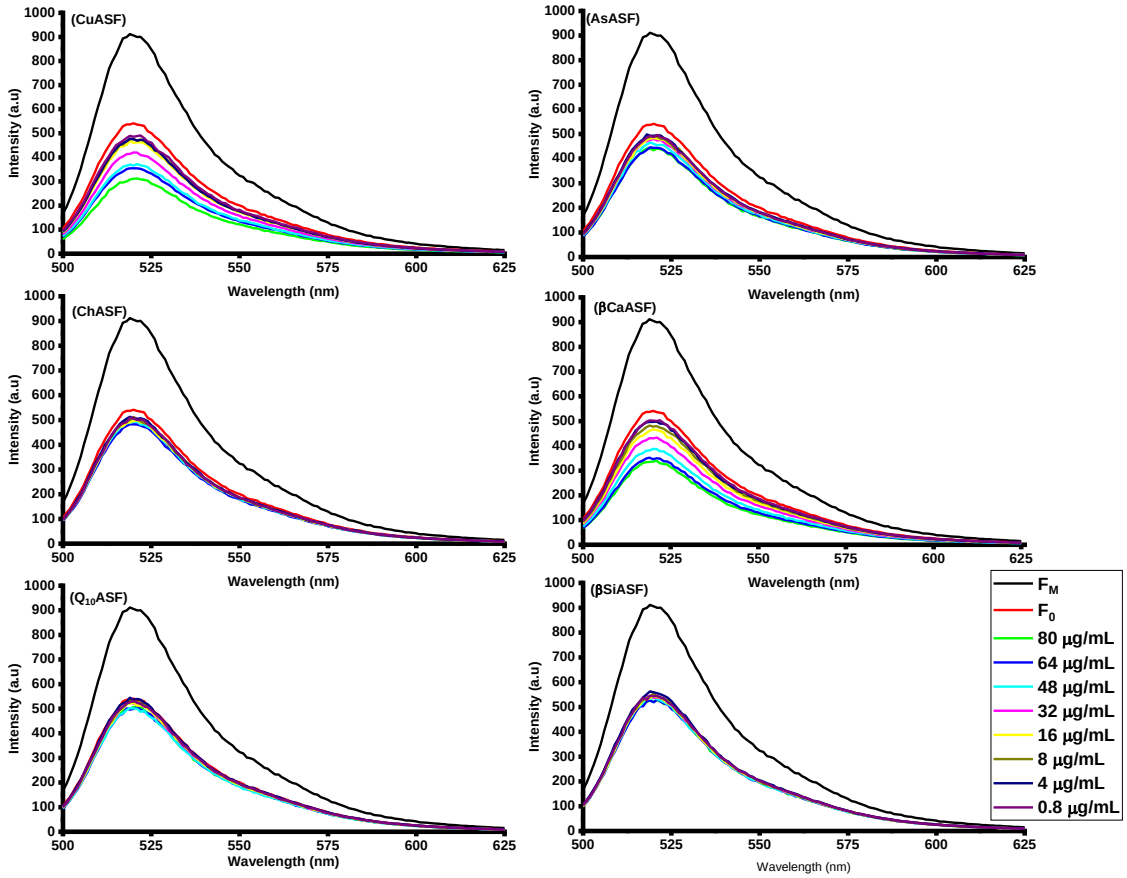

Figure 4.10. Binding-induced fluorescence quenching spectra of calcein-loaded GUV after interaction of different concentrations of ASF-curcumin, ASF-astaxanthin, ASF-cholecalciferol, ASF-β-carotene, ASF-coenzyme Q10 and ASF-β-sitosterol.

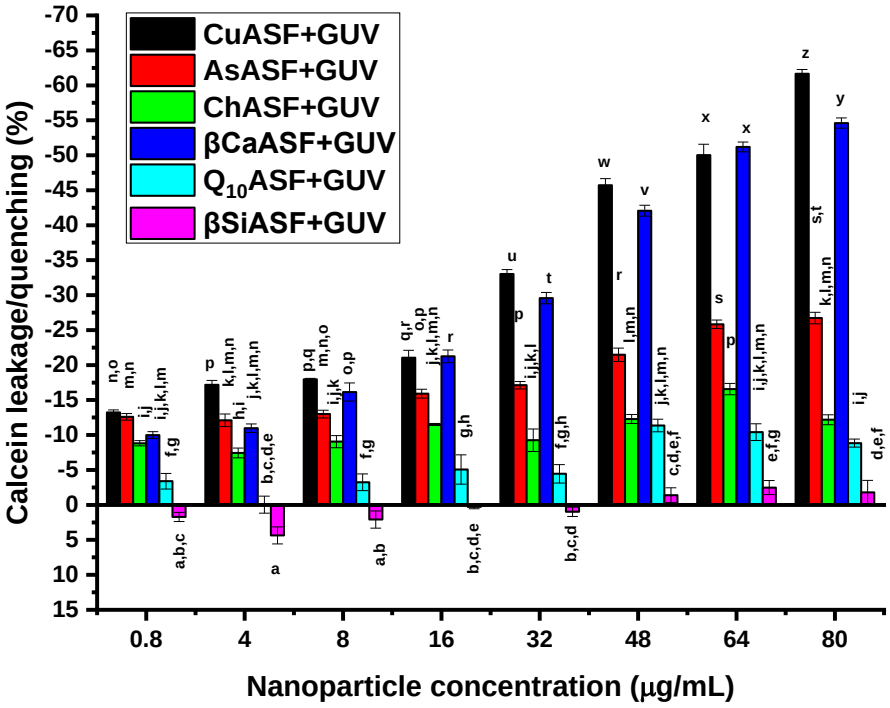

Figure 4.11. Interaction of calcein-loaded GUV with various concentrations of CuASF, AsASF, ChASF, βCaASF, Q10ASF and βSiASF led to calcein quenching/leakage as monitored by fluorescence spectrometry.

Mean values with the same letters in the bar chart are not significantly different at $p < 0.05$.

3.5. Changes in particle characteristics of GUV after interaction with nano/micro complexes

The size, zeta potential and polydispersity index of GUV were monitored before and after interaction with nano/micro complexes of the various protein-bioactive compounds using dynamic light scattering technique and the result presented in Table 4.3. All the various protein-bioactive compound complexes are negatively charged since the protein (ASF) employed in the complexation process is negatively charged (zeta potential -42.9 mV).[14] The charge on the calcein-loaded GUV was not significantly affected after interaction of the various nano/micro complexes.

The size of CuASF, ChASF and βCaASF complexes were slightly higher than sizes obtained from transmission electron microscopy, and this could be attributed to hydrodynamic diameter. In contrast, the size of AsASF, Q_{10}ASF and βSiASF complexes were significantly larger than those of transmission electron microscopy. It is possible that the interaction of astaxanthin and β-sitosterol induced protein aggregation as noted from their PDI and TEM images (Figure 4.9) while fibre formation could have caused disparity in the size of Q_{10}ASF (Figure 4.9). The size of the GUV decreased ~200 folds after interaction with Triton X-100, which was used as the positive control. This result could be attributed to the bursting and clearing of the vesicles, which is responsible for the maximum calcein fluorescence intensity obtained after the addition of TritonX-100 in the leakage assay (Figure 4.10). The addition of the various protein-bioactive compound complexes decreased the size of the GUV significantly. This is contrary to the expectation that nano/micro particle binding on the surface of GUV, as shown by fluorescence quenching in the leakage assay (Figures 4.10 and 4.11), should increase the size. Similar observation was recently reported for curcumin-pea protein complex where the size of GUV decreased from 1933 to 1091 nm after addition of the complex.[29] Two major mechanisms have been postulated for this size reduction. First, protein-bioactive compound complex binding to GUV surface could have induced GUV division into smaller units while retaining the calcein content. The second mechanism involves membrane shrinkage caused by strong hydrophobic interaction between the protein-bioactive compound complexes and the GUV. The latter postulation has been reported to be more feasible as the binding of the protein-bioactive compound complex, which cannot cross the membrane bilayer, could cause osmotic pressure to build up leading to the escape of water trapped in the GUV core while retaining calcein, hence the subsequent size reduction of the vesicle.[29,48] The interaction of serum with PEGylated and non-PEGylated phosphatidylcholine/cholesterol

liposomes caused a reduction in the size of the vesicle following a similar mechanism.[48] Studies have shown that nonspecific binding of charged nanoparticles to large unilamellar vesicles and supported lipid bilayer could reconstruct the elasticity and surface structure of the membrane.[49,50] Loss of hydration has also been reported to be the major cause of size reduction after the binding of anionic polystyrene nanoparticles on large unilamellar vesicles.[50] Overall, the interaction of protein-bioactive compound complexes with calcein-loaded GUV results in nano and microparticle binding on the surface of GUV which shield the fluorescence properties of calcein and caused a size reduction in GUV due to the osmotic pressure induced by the impermeable particle on vesicle surface. The osmotic pressure led to the permeability of water (smaller molecule) while retaining calcein, and hence decrease in the size of GUV.

Table 4.3. Size, polydispersity index and zeta potential of calcein-loaded GUV with and without interaction of protein-bioactive compound complexes.

Samples	Size (nm)	PDI	Zeta potential
lGUV	2009.7 ± 117.6^{a}	0.15 ± 0.07^{b}	$-6.8\pm0.7^{b,c}$
CuASF	382.7 ± 2.6^{f}	0.23 ± 0.03^{b}	$-17.9\pm0.3^{e,f}$
AsASF	1029.6 ± 25.5^{d}	0.25 ± 0.01^{b}	-16.1 ± 0.3^{e}
ChASF	$510.3\pm6.8^{e,f}$	0.39 ± 0.06^{b}	$-19.4\pm0.3^{f,g}$
βCaASF	$1581.3\pm83.7^{b,c}$	0.79 ± 0.04^{a}	-23.6 ± 0.3^{h}
Q_{10}ASF	633.2 ± 5.6^{e}	0.38 ± 0.03^{b}	$-19.5\pm0.6^{f,g}$
βSiASF	360.9 ± 9.6^{f}	0.37 ± 0.04^{b}	$-21.0\pm0.4^{g,h}$
lGUV + CuASF	1112.3 ± 26.8^{d}	0.27 ± 0.07^{b}	-10.1 ± 1.3^{d}
lGUV + AsASF	1362.7 ± 15.3^{c}	0.15 ± 0.07^{b}	$-5.5\pm0.3^{a,b}$
lGUV + ChASF	1605.7 ± 18.0^{b}	0.26 ± 0.08^{b}	$-5.2\pm0.3^{a,b}$
lGUV + βCaASF	1587.0 ± 31.0^{b}	0.31 ± 0.05^{b}	$-9.0\pm0.4^{c,d}$
lGUV + Q_{10}ASF	$1417.7\pm48.3^{b,c}$	0.34 ± 0.13^{b}	$-5.6\pm0.3^{a,b}$
lGUV + βSiASF	$1467.3\pm5.8^{b,c}$	0.37 ± 0.09^{b}	$-5.2\pm0.2^{a,b}$
lGUV + TritonX-100	11.1 ± 0.1^{g}	0.15 ± 0.00^{b}	-3.4 ± 0.4^{a}
Mean values having same letters in a column are not significantly different ($P < 0.05$) Abbreviations: lGUV, calcein-loaded giant unilamelar vesicles; ASF, alkaline-soluble fraction of pea protein isolate; CuASF, curcumin-ASF complex; AsASF, astaxanthin-ASF complex; ChASF, cholecalciferol-ASF complex; βCaASF, β-carotene-ASF complex; Q_{10}ASF, coenzyme Q_{10}-ASF complex; βSiASF, β-sitosterol-ASF complex			

Morphological examination with widefield fluorescence microscopy (Figure 4.12) showed that calcein encapsulation increased the GUV size (Figure 4.12A&B) and enhanced the formation of more orderly spherical vesicles with smooth surface. The addition of the nano/micro complexes significantly decreased the size of the GUVs (Figure 4.12 C-H), which further corroborate the postulated surface binding-osmotic pressure-induced shrinkage mechanism. The addition of the positive control, Triton X-100 resulted in bursting and clearing of all the GUVs (Figure 4.12 I), which also supported the 200-fold decrease in size obtained from dynamic light scattering and the highest fluorescence intensity (Figure 4.10) observed in the leakage assay. The similarities in the size and morphology of the GUV after interaction of the various nano-complexes also support their similar mode of interaction.

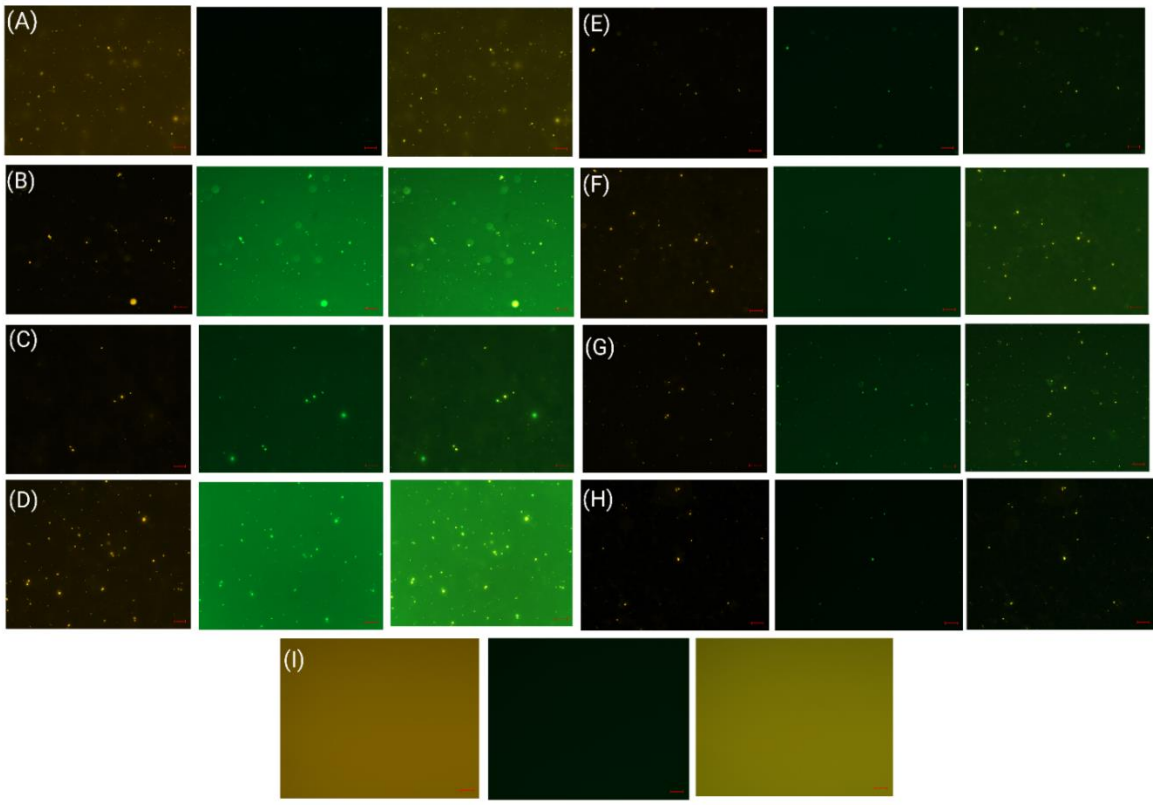

Figure 4.12. Widefield fluorescence microscopy images of (A) empty GUV, (B) calcein-loaded GUV before interaction with colloidal nanocomplexes and after interaction with (C) ASF-

curcumin (D) ASF-astaxanthin (E) ASF-cholecalciferol (F) ASF-β-carotene (G) ASF-coenzyme Q10 (H) ASF-β-sitosterol and (I) Triton X-100. Scale bar is 20 µM.

4. Conclusion

This study demonstrated that physiologically relevant parameter like ionic strength influences the surface hydrophobicity of pea glutelin protein, and the nature and strength of interaction between the protein and bioactive compounds of different lipophilicity. The study also established bio-nano/micro interaction by examining the influence of the various nano/micro protein-bioactive compound complexes formed on zwitterionic giant unilamellar vesicles (GUV). The bioactive compounds with moderate lipophilicity (curcumin, astaxanthin and cholecalciferol) demonstrated higher binding strength than those of high lipophilicity (β-carotene, coenzyme Q_{10} and β-sitosterol). Lower ionic strength promotes mainly static quenching by the lipophilic bioactive compound whereas higher ionic strength promotes mainly dynamic quenching. While K, K_Q and K_D values depend mainly on protein hydrophobicity, ionic strength affected the mode of interaction. Morphological characterization with transmission electron microscopy revealed the formation of nano-range spherical complexes for curcumin-protein, astaxanthin-protein, and β-sitosterol-protein, micro-range aggregate complexes for cholecalciferol-protein and β-carotene-protein, and fibre-like complex for coenzyme Q_{10}-protein. The study shows that the nature of bioactive compounds, lipophilicity, ionic strength, and stoichiometry are essential parameters for rational design of efficient bioactive compound-loaded protein complexes. The non-rupturing of GUVs after interaction with various nano/micro complexes of protein-bioactive compounds suggests their low cytotoxicity. However, further imaging studies are needed to evaluate the binding and distribution of the nano/micro complexes on the GUV surface.

Funding

This research was funded by the Natural Sciences and Engineering Research Council of Canada (NSERC) through the Discovery Grant Program, reference number RGPIN-2018-06839, and the University Research Chairs Program of the University of Ottawa.

Acknowledgement

Authors wish to thank Pulse Canada (Winnipeg, MB, Canada) for donating the dried yellow pea seeds used in this study. We acknowledge the valuable insight of Tyler Avis (Department of Chemistry, Carleton University, Canada) on the leakage assay and for donating calcein and material used for column chromatography.

References

(1) Naoi, M.; Maruyama, W.; Shamoto-Nagai, M. Disease-Modifying Treatment of Parkinson's Disease by Phytochemicals: Targeting Multiple Pathogenic Factors. *Journal of Neural Transmission*. **2022**, 1-17. https://doi.org/10.1007/s00702-021-02427-8.

(2) Chen, J.; Hu, L. Nanoscale Delivery System for Nutraceuticals: Preparation, Application, Characterization, Safety, and Future Trends. *Food Engineering Reviews*. **2020**, 12(1), 14-31. https://doi.org/10.1007/s12393-019-09208-w.

(3) Granado-Lorencio, F.; Hernández-Alvarez, E. Functional Foods and Health Effects: A Nutritional Biochemistry Perspective. *Current Medicinal Chemistry*. **2016**, *23* (26), 2929-2957. https://doi.org/10.2174/0929867323666160615105746.

(4) Okagu, O. D.; Jin, J.; Udenigwe, C. C. Impact of Succinylation on Pea Protein-Curcumin Interaction, Polyelectrolyte Complexation with Chitosan, and Gastrointestinal Release of Curcumin in Loaded-Biopolymer Nano-Complexes. *Journal of Molecular Liquids.* **2020**, 325, 115248. https://doi.org/10.1016/j.molliq.2020.115248.

(5) Okagu, O. D.; Verma, O.; McClements, D. J.; Udenigwe, C. C. Utilization of Insect Proteins to Formulate Nutraceutical Delivery Systems: Encapsulation and Release of Curcumin Using Mealworm Protein-Chitosan Nano-Complexes. *International Journal of Biological Macromolecules.* **2020**, 151, 333-343. https://doi.org/10.1016/j.ijbiomac.2020.02.198.

(6) Feng, S.; Yan, J.; Wang, D.; Jiang, L.; Sun, P.; Xiang, N.; Shao, P. Preparation and Characterization of Soybean Protein Isolate/Pectin-Based Phytosterol Nanodispersions and Their Stability in Simulated Digestion. *Food Research International*. **2021**, 143, 110237. https://doi.org/10.1016/j.foodres.2021.110237.

(7) Feng, S.; Zheng, X.; Luan, D.; Shao, P.; Sun, P. Preparation and Characterization of Zein-Based Phytosterol Nanodispersions Fabricated by Ultrasonic Assistant Anti-Solvent Precipitation. *LWT-Food Science and Technology* **2019**, *107*, 138-144. https://doi.org/10.1016/j.lwt.2019.03.025.

(8) Yi, J.; Lam, T. I.; Yokoyama, W.; Cheng, L. W.; Zhong, F. Beta-Carotene Encapsulated in Food Protein Nanoparticles Reduces Peroxyl Radical Oxidation in Caco-2 Cells. *Food Hydrocolloids.* **2015**, 43, 31-40. https://doi.org/10.1016/j.foodhyd.2014.04.028.

(9) Basar, A. O.; Prieto, C.; Durand, E.; Villeneuve, P.; Sasmazel, H. T.; Lagaron, J. Encapsulation of β-Carotene by Emulsion Electrospraying Using Deep Eutectic Solvents. *Molecules.* **2020**, *25* (4), 981. https://doi.org/10.3390/molecules25040981.

(10) Zanoni, F.; Vakarelova, M.; Zoccatelli, G. Development and Characterization of Astaxanthin-Containing Whey Protein-Based Nanoparticles. *Marine Drugs.* **2019**, *17* (11), 627. https://doi.org/10.3390/md17110627.

(11) Walia, N.; Chen, L. Pea Protein Based Vitamin D Nanoemulsions: Fabrication, Stability and in Vitro Study Using Caco-2 Cells. *Food Chemistry.* **2020**, *305*, 125475. https://doi.org/10.1016/j.foodchem.2019.125475.

(12) Liu, C.; Liu, Z.; Sun, X.; Zhang, S.; Wang, S.; Feng, F.; Wang, D.; Xu, Y. Fabrication and Characterization of β-Lactoglobulin-Based Nanocomplexes Composed of Chitosan Oligosaccharides as Vehicles for Delivery of Astaxanthin. *Journal of Agricultural and Food Chemistry.* **2018**, *66* (26), 6717-6726. https://doi.org/10.1021/acs.jafc.8b00834.

(13) Vinayahan, T.; Williams, P. A.; Phillips, G. O. Electrostatic Interaction and Complex Formation between Gum Arabic and Bovine Serum Albumin. *Biomacromolecules.* **2010**, *11* (12), 3367-3374. https://doi.org/10.1021/bm100486p.

(14) Okagu, O. D.; Udenigwe, C. C. Molecular Interactions of Pea Globulin, Albumin and Glutelin with Curcumin: Formation and Gastric Release Mechanisms of Curcumin-Loaded Bio-Nanocomplexes. *Food Biophysics.* **2021**, *17(1)*, 10-25. https://doi.org/10.1007/s11483-021-09697-5.

(15) Wang, F.; Yang, Y.; Ju, X.; Udenigwe, C. C.; He, R. Polyelectrolyte Complex Nanoparticles from Chitosan and Acylated Rapeseed Cruciferin Protein for Curcumin Delivery. *J Agric Food Chemistry.* **2018**, *66(11)*, 2685-2693. https://doi.org/10.1021/acs.jafc.7b05083.

(16) Mathew, M. S.; Vinod, K.; Jayaram, P. S.; Jayasree, R. S.; Joseph, K. Improved Bioavailability of Curcumin in Gliadin-Protected Gold Quantum Cluster for Targeted Delivery. *ACS Omega.* **2019**, *4(10)*, 14169-14178. https://doi.org/10.1021/acsomega.9b00917.

(17) Alehosseini, A.; Gómez-Mascaraque, L. G.; Martínez-Sanz, M.; López-Rubio, A. Electrospun Curcumin-Loaded Protein Nanofiber Mats as Active/Bioactive Coatings for Food Packaging Applications. *Food Hydrocolloids.* **2019**, *87*, 758-771. https://doi.org/10.1016/j.foodhyd.2018.08.056.

(18) Xue, J.; Zhang, Y.; Huang, G.; Liu, J.; Slavin, M.; Yu, L. (Lucy). Zein-Caseinate Composite Nanoparticles for Bioactive Delivery Using Curcumin as a Probe Compound. *Food Hydrocolloids.* **2018**, *83*, 25-35. https://doi.org/10.1016/j.foodhyd.2018.04.037.

(19) Tapal, A.; Tiku, P. K. Complexation of Curcumin with Soy Protein Isolate and Its Implications on Solubility and Stability of Curcumin. *Food Chemistry.* **2012**, *130(4)*, 960-965. https://doi.org/10.1016/j.foodchem.2011.08.025.

(20) Wang, L.; Gulati, P.; Santra, D.; Rose, D.; Zhang, Y. Nanoparticles Prepared by Proso Millet Protein as Novel Curcumin Delivery System. *Food Chemistry.* **2018**, *240*, 1039-1046. https://doi.org/10.1016/j.foodchem.2017.08.036.

(21) Okagu, O.D.; Wang, B.; Udenigwe, C.C. CHAPTER 4: Food Proteins as Biomaterial for Delivery Functions. In Food Proteins and Peptides: Emerging Biofunctions, Food and Biomaterial Applications. Ed. by Udenigwe, C.C. *Royal Society of Chemistry*, Cambridge, United Kingdom. **2021**, 97-126. https://doi.org/10.1039/9781839163425-00097.

(22) Kanakis, C. D.; Tarantilis, P. A.; Polissiou, M. G.; Tajmir-Riahi, H. A. Probing the Binding Sites of Resveratrol, Genistein, and Curcumin with Milk β -Lactoglobulin. *Journal of Biomolecular Structure and Dynamics.* **2013**, *31(12)*, 1455-1466. https://doi.org/10.1080/07391102.2012.742461.

(23) Belatik, A.; Kanakis, C. D.; Hotchandani, S.; Tarantilis, P. A.; Polissiou, M. G.; Tajmir-Riahia, H. A. Locating the Binding Sites of Retinol and Retinoic Acid with Milk β-Lactoglobulin. *Journal of Biomolecular Structure and Dynamics.* **2012**, *30* (4), 437-447. https://doi.org/10.1080/07391102.2012.682209.

(24) Bourassa, P.; Bariyanga, J.; Tajmir-Riahi, H. A. Binding Sites of Resveratrol, Genistein, and Curcumin with Milk α- And β-Caseins. *Journal of Physical Chemistry B.* **2013**, *117(5)*, 1287-1295. https://doi.org/10.1021/jp3114557.

(25) McClements, D. J.; Xiao, H. Is Nano Safe in Foods? Establishing the Factors Impacting the Gastrointestinal Fate and Toxicity of Organic and Inorganic Food-Grade Nanoparticles. *NPJ Science of Food.* **2017**, *1(1)*, 1-13. https://doi.org/10.1038/s41538-017-0005-1.

(26) Wong, C. Y.; Al-Salami, H.; Dass, C. R. Cellular Assays and Applied Technologies for Characterisation of Orally Administered Protein Nanoparticles: A Systematic Review. *Journal of Drug Targeting*. **2020**, *28(6)*, 585-599. https://doi.org/10.1080/1061186X.2020.1726356.

(27) Yang, L.; Li, M.; Sun, Y.; Zhang, L. A Cell-Penetrating Peptide Conjugated Carboxymethyl-β-Cyclodextrin to Improve Intestinal Absorption of Insulin. *International Journal of Biological Macromolecules.* **2018**, *111*, 685-695. https://doi.org/10.1016/j.ijbiomac.2018.01.077.

(28) Hirano, A.; Uda, K.; Maeda, Y.; Akasaka, T.; Shiraki, K. One-Dimensional Protein-Based Nanoparticles Induce Lipid Bilayer Disruption: Carbon Nanotube Conjugates and Amyloid Fibrils. *Langmuir.* **2010**, *26* (22), 17256-17259. https://doi.org/10.1021/la103615b.

(29) Okagu, O. D.; Abioye, R. O.; Udenigwe, C. C. Curcumin–Induced Stabilization of Protein–Based Nano-Delivery Vehicles Reduces Disruption of Zwitterionic Giant Unilamellar Vesicles. *Molecules.* **2022**, *27* (6), 1941. https://doi.org/10.3390/molecules27061941.

(30) Adebiyi, A. P.; Aluko, R. E. Functional Properties of Protein Fractions Obtained from Commercial Yellow Field Pea (Pisum Sativum L.) Seed Protein Isolate. *Food Chemistry.* **2011,** *128(4),* 902-908. https://doi.org/10.1016/j.foodchem.2011.03.116.

(31) Tetko, I. v.; Tanchuk, V. Y. Application of Associative Neural Networks for Prediction of Lipophilicity in ALOGPS 2.1 Program. *Journal of Chemical Information and Computer Sciences.* **2002**, *42* (5), 1136-1145. https://doi.org/10.1021/ci025515j.

(32) Zhang, Y.; Zhong, Q. Binding between Bixin and Whey Protein at PH 7.4 Studied by Spectroscopy and Isothermal Titration Calorimetry. *Journal of Agricultural and Food Chemistry.* **2012**, *60* (7), 1880-1886. https://doi.org/10.1021/jf2050262.

(33) Zhang, Y.; Zhong, Q. Effects of Thermal Denaturation on Binding between Bixin and Whey Protein. *Journal of Agricultural and Food Chemistry.* **2012**, *60* (30), 7526-7531. https://doi.org/10.1021/jf3021656.

(34) Mantil, E.; Buznytska, I.; Daly, G.; Ianoul, A.; Avis, T. J. Role of Lipid Composition in the Interaction and Activity of the Antimicrobial Compound Fengycin with Complex Membrane Models. *Journal of Membrane Biology.* **2019**, *252* (6), 627-638. https://doi.org/10.1007/s00232-019-00100-6.

(35) Tanger, C.; Müller, M.; Andlinger, D.; Kulozik, U. Influence of PH and Ionic Strength on the Thermal Gelation Behaviour of Pea Protein. *Food Hydrocolloids.* **2022**, *123,* 106903. https://doi.org/10.1016/j.foodhyd.2021.106903.

(36) Lam, A. C. Y.; Can Karaca, A.; Tyler, R. T.; Nickerson, M. T. Pea Protein Isolates: Structure, Extraction, and Functionality. *Food Reviews International*. **2018**, *34(2)*, 126-147. https://doi.org/10.1080/87559129.2016.1242135.

(37) Mantovani, R. A.; Hamon, P.; Rousseau, F.; Tavares, G. M.; Mercadante, A. Z.; Croguennec, T.; Bouhallab, S. Unraveling the Molecular Mechanisms Underlying Interactions between Caseins and Lutein. *Food Research International.* **2020**, *138,* 109781. https://doi.org/10.1016/j.foodres.2020.109781.

(38) Möller, M.; Denicola, A. Protein Tryptophan Accessibility Studied by Fluorescence Quenching. *Biochemistry and Molecular Biology Education*. **2002**, *30(3)*, 175-178. https://doi.org/10.1002/bmb.2002.494030030035.

(39) Lakowicz, J. R. *Principles of Fluorescence Spectroscopy*; Boston, MA: springer US. **2006**. https://doi.org/10.1007/978-0-387-46312-4.

(40) Lehrer, S. S. Erratum: Solute Perturbation of Protein Fluorescence. The Quenching of the Tryptophyl Fluorescence of Model Compounds and Lysozyme by Iodide Ion. *Biochemistry*. **1971**, *10(17)*, 3254-3263. https://doi.org/10.1021/bi00802a602.

(41) Ware, W. R. Oxygen Quenching of Fluorescence in Solution: An Experimental Study of the Diffusion Process. *Journal of Physical Chemistry.* **1962**, *66(3),* 455-458. https://doi.org/10.1021/j100809a020.

(42) Belatik, A.; Hotchandani, S.; Bariyanga, J.; Tajmir-Riahi, H. A. Binding Sites of Retinol and Retinoic Acid with Serum Albumins. *European Journal of Medicinal Chemistry*. **2012**, *48*, 114-123. https://doi.org/10.1016/j.ejmech.2011.12.002.

(43) Liu, Q.; Jing, Y.; Han, C.; Zhang, H.; Tian, Y. Encapsulation of Curcumin in Zein/ Caseinate/Sodium Alginate Nanoparticles with Improved Physicochemical and Controlled Release Properties. *Food Hydrocolloids.* **2019, 93,** 432-442. https://doi.org/10.1016/j.foodhyd.2019.02.003.

(44) Hirano, A.; Yoshikawa, H.; Matsushita, S.; Yamada, Y.; Shiraki, K. Adsorption and Disruption of Lipid Bilayers by Nanoscale Protein Aggregates. *Langmuir*. **2012**, *28* (8), 3887-3895. https://doi.org/10.1021/la204717c.

(45) Jing, B.; Zhu, Y. Disruption of Supported Lipid Bilayers by Semihydrophobic Nanoparticles. *Journal of the American Chemical Society.* **2011**, *133* (28), 10983-10989. https://doi.org/10.1021/ja2040305.

(46) Ambroggio, E. E.; Separovic, F.; Bowie, J. H.; Fidelio, G. D.; Bagatolli, L. A. Direct Visualization of Membrane Leakage Induced by the Antibiotic Peptides: Maculatin, Citropin, and Aurein. *Biophysical Journal.* **2005**, *89* (3), 1874-1881. https://doi.org/10.1529/biophysj.105.066589.

(47) Aydin, F.; Dutt, M. Surface Reconfiguration of Binary Lipid Vesicles via Electrostatically Induced Nanoparticle Adsorption. *Journal of Physical Chemistry B.* **2016**, *120* (27), 6646-6656. https://doi.org/10.1021/acs.jpcb.6b02334.

(48) Wolfram, J.; Suri, K.; Yang, Y.; Shen, J.; Celia, C.; Fresta, M.; Zhao, Y.; Shen, H.; Ferrari, M. Shrinkage of Pegylated and Non-Pegylated Liposomes in Serum. *Colloids and Surfaces B: Biointerfaces.* **2014**, *114*, 294-300. https://doi.org/10.1016/j.colsurfb.2013.10.009.

(49) di Silvio, D.; Maccarini, M.; Parker, R.; Mackie, A.; Fragneto, G.; Baldelli Bombelli, F. The Effect of the Protein Corona on the Interaction between Nanoparticles and Lipid Bilayers. *Journal of Colloid and Interface Science.* **2017**, *504*, 741-750. https://doi.org/10.1016/j.jcis.2017.05.086.

(50) Wang, B.; Zhang, L.; Sung, C. B.; Granick, S. Nanoparticle-Induced Surface Reconstruction of Phospholipid Membranes. *Proceedings of the National Academy of Science, U S A.* **2008**, *105* (47), 18171-18175. https://doi.org/10.1073/pnas.0807296105.

CHAPTER FIVE

POTENTIAL TOXICITY OF PROTEIN–BASED NANO-DELIVERY VEHICLES: INVESTIGATION INTO BIO-NANO INTERACTIONS

Curcumin–Induced Stabilization of Protein–Based Nano-Delivery Vehicles Reduces Disruption of Zwitterionic Giant Unilamellar Vesicles

Ogadimma D. Okagu, Raliat O. Abioye, Chibuike C. Udenigwe

Molecules **2022**, *27*(6), 1941; https://doi.org/10.3390/molecules27061941

DECLARATION FOR THESIS CHAPTER FIVE

Curcumin–Induced Stabilization of Protein–Based Nano-Delivery Vehicles Reduces Disruption of Zwitterionic Giant Unilamellar Vesicles

This is to declare that there is no conflict of interest associated with this work and the contribution of the candidate is as stated below:

Candidate's contribution	Conceptualization of idea, formal analysis, investigation, methodology, validation, visualization, writing, review, and editing	85%

The following co-authors attest to the candidate's participation in a group publication as a component of his thesis and was active in the creation of this publication. The co-authors' permission are as follows:

Name	Signature	Date
Raliat O. Abioye		22/11/2022
Chibuike C. Udenigwe		22/11/2022

Abstract

Curcumin-loaded native and succinylated protein nanoparticles, as well as zwitterionic giant unilamellar vesicles were used in this study as model bioactive compound loaded-nanoparticles and biomembranes, respectively, to assess bio-nano interactions. Curcumin-loaded native protein-chitosan and succinylated protein-chitosan complexes, as well as native protein-chitosan and succinylated protein-chitosan hollow, induced leakage of calcein, encapsulated in the giant unilamellar vesicles. The leakage was more pronounced with hollow protein-chitosan complexes. However, curcumin-loaded native proteins and curcumin-loaded succinylated proteins induced calcein fluorescence quenching. Dynamic light scattering measurements showed that the interaction of curcumin-loaded native pea protein, curcumin-loaded succinylated pea protein, native pea protein-chitosan, and succinylated pea protein-chitosan complexes with the giant unilamellar vesicles caused a major reduction in the size of the lipid vesicles. Confocal and widefield fluorescence microscopy showed rupturing of the unilamellar vesicles after treatment with native pea protein-chitosan and succinylated pea protein-chitosan complexes. The nature of interaction between the curcumin-loaded protein nanoparticles and the biomembranes, at the bio-nano interface, is influenced by the encapsulated curcumin. Findings from this study showed that, as the protein plays a crucial role in stabilizing the bioactive compound from chemical and photodegradation, the encapsulated nutraceutical stabilizes the protein nanoparticle to reduce its interaction with biomembranes.

Keywords: zwitterionic giant unilamellar vesicles; protein; curcumin; protein-chitosan nanocomplexes; biomembrane; succinylation; bio-nano interaction

1. Introduction

Curcumin-loaded native pea protein (CUR/PPI), succinylated pea protein (CUR/SPPI), native pea protein-chitosan (CUR/PPI/CHI) and succinylated pea protein-chitosan (CUR/SPPI/CHI), as well as hollow native pea protein-chitosan (PPI/CHI) and succinylated pea protein-chitosan (SPPI/CHI),[1] and many other bioactive compound-loaded protein nanoparticles[2–8] have demonstrated promising physicochemical properties, such as high encapsulation efficiency, zeta potential, water-dispersibility, small size, increased surface area-to-volume ratio, improved shelf life, low polydispersity index, stability at high ionic strength, pepsin-resistant properties, enhanced gastric stability, and sustained release of bioactive compounds compared to macroparticles. However, there are concerns that changes in the structural and physicochemical properties of proteins, during fabrication or conversion to nanoparticles that promote their food application, could also result in unwanted physiological responses. This is plausible because unfavorable nanoparticle-membrane interaction may impact cell viability, cellular uptake efficacy, exocytosis and endocytosis mechanisms, as well as transepithelial and permeation capacity. The potential outcome of this interaction might affect both the structural integrity of the protein nanoparticles and the gastrointestinal cell membrane, and it could cause inflammation, nanoparticles accumulation, decreased protein digestibility, and considerable side effects in the liver, gut microbiota, and muscles.[9–12]

Although a few studies have investigated the mechanism of cytotoxicity of bioactive compound-loaded protein nanoparticles,[13] possible dose-dependent *in vitro* toxicity data have been reported.[14–16] For instance, curcumin-loaded zein nanoparticles, functionalized with polydopamine in the presence and absence of dodecamer peptide coating, induced cell death (below 20% cell viability) at a nanoparticle concentration above 5 µg/Ml. The nanoparticles induced the generation

of cellular-reactive oxygen species, two-times higher than those of free curcumin, and promoted apoptosis of C6 glioma cells.[14] Curcumin-loaded human serum albumin nanoparticles, coated with HER2 aptamer, induced higher cytotoxicity iN SK-BR3 cell line, compared to free curcumin, and reduced cell viability to 36% after 72 h.[15] While free curcumin reduced the viability of MCF-7 cells to ~60%, self-assembled curcumin-loaded human serum albumin nanoparticles induced significant cell death at a concentration of 50 μM.[16] Although the studies demonstrated the anticancer activities of curcumin-loaded protein nanoparticles, no information was provided on the effect of the nanoparticles on healthy cells. The mechanism of cytotoxicity can be evaluated through the characterization of the interaction of protein-based nano-delivery systems and biomembranes occurring at the nano-bio interface. This information is essential in the rational design and applicability of nutraceutical-loaded, food-grade encapsulating agents in functional food formulation. The underlying mechanism could depend on the physicochemical properties of the loaded nano-encapsulating agents and their nature of interaction with the gastrointestinal membrane. For instance, the shape and mechanical properties of single-walled carbon nanotubes, functionalized with adsorbed lysozyme, its monomer, amorphous aggregate, and amyloid fibril formed by lysozyme, coupled with the nature of their noncovalent interaction, played an important role in the leakage of liposome content.[12] Lysozyme proteins did not disrupt the lipid membrane under physiological saline conditions except when they rearranged or aligned with the single-walled carbon nanotube to form a one-dimensional shape.[12] Poly-L-lysine and polyamidoamine dendrimers, as well as semihydrophobic nanoparticles of polystyrene of various sizes, shapes, functional group, flexibility, surface hydrophobicity, and charge density have been reported to interact with lipid membranes differentially.[17–19] To date, there is no information available for nutraceutical-loaded protein nanoparticles. The physicochemical properties of the engineered

protein nanoparticles, with or without the loaded bioactive compounds, which dictate their delivery function and food matrix compatibility,[1,3,4] could also determine the nature of their interaction with the gastrointestinal cell membrane during oral administration.

Our previous study[1] reported the fabrication of hollow and curcumin-loaded pea protein-based nanoparticles (Scheme 5.1) with the following physicochemical properties: hollow PPI/CHI and SPPI/CHI (size: 151.5 and 176.3 nm, zeta potential: +40.8 and +20.3 mV, respectively, shape: irregular morphology); CUR/PPI and CUR/SPPI (size: 165.6 and 159.9 nm, zeta potential: −46.8 and −53.9 mV, encapsulation efficiency: 34.65% and 24.92%, effective binding constant: 6.9×10^4 M^{-1} and 4.2×10^4 M^{-1}, respectively, shape: well-ordered spherical morphology); CUR/PPI/CHI and CUR/SPPI/CHI (size: 194.5 and 183.3 nm, zeta potential: +20.9 and +12.8 mV, encapsulation efficiency: 85.01% and 62.05%, effective binding constant: 14.5×10^4 M^{-1} and 187.9×10^4 M^{-1}, respectively, shape: well-ordered spherical morphology). The aim of this study was to assess the implication of the interaction occurring at the bio-nano interface for these well-characterized, hollow, and nutraceutical-loaded food-grade nanoparticles of different physicochemical properties, with a giant unilamellar vesicle (GUV) used as a model biomembrane. The specific objectives were to evaluate: (1) food-grade nanoparticle-induced leakage or quenching of calcein-loaded giant unilamellar vesicles; (2) the effect of interactions of food-grade nanoparticles on the physicochemical properties of calcein-loaded biomembrane; (3) the impact of the interaction on the structural integrity of the biomembrane.

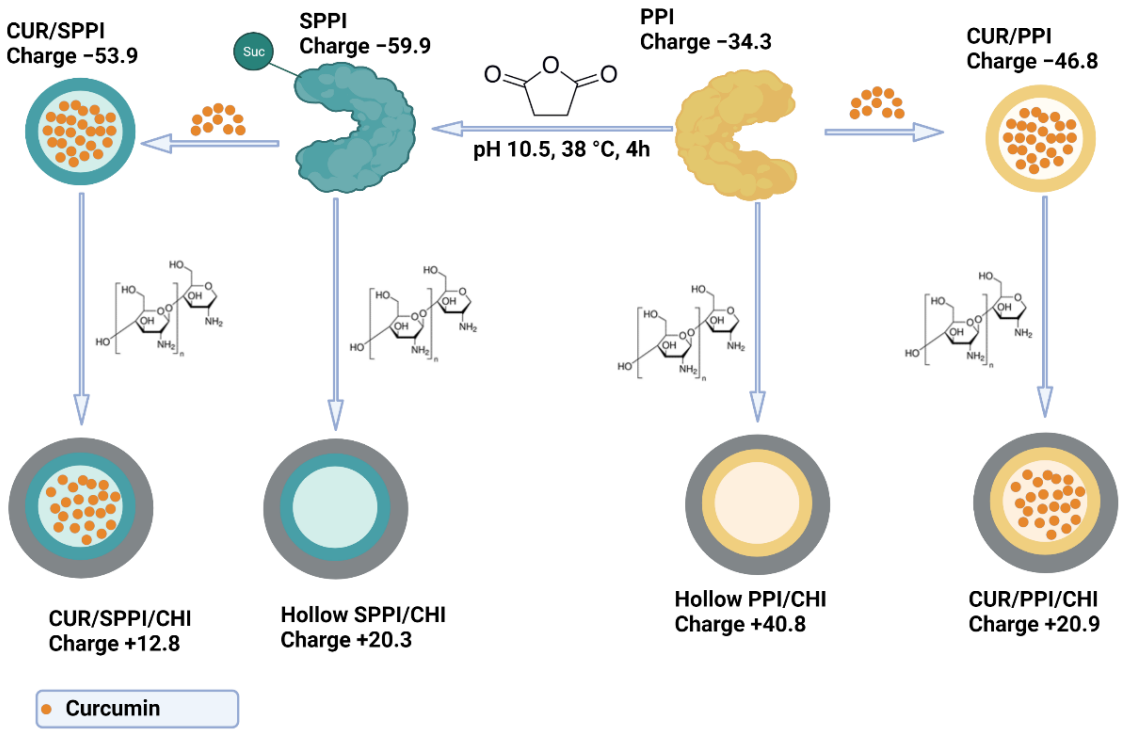

Scheme 5.1. Preparation of hollow and curcumin-loaded protein and protein-chitosan nano-complexes with different physicochemical properties, as previously reported.[1]

2. Materials and methods

2.1. Chemical Materials

The 1,2-Dioleoyl-sn-glycero-3-phosphocholine (≥99%), Chloroform (≥99.5%), 1,2-dioleoyl-sn-glycero-3 phosphoethanolamine-N-(lissamine rhodamine B sulfonyl) (ammonium salt) (≥99%), medium molecular weight chitosan, calcein, succinic anhydride (≥99.5%), curcumin (≥94%), and ethanol were purchased from MilliporeSigma Chemical Co., Ltd. (St. Louis, MO, USA). Tris(hydroxymethyl)aminomethane (Tris-base, ≥ 100.1%), sodium chloride (≥99.0%), Tris-EDTA (99.4–100.6%), and sodium hydroxide (≥98%) were purchased from Thermo Fisher Scientific (Geel, Belgium). Triton X-100 was purchased from VWR (Mississauga, ON, Canada). Yellow pea seed was donated by Pulse Canada (Manitoba, Canada). Milli-Q water was obtained from the water-purification system (Advantage A10 Q-POD Milli-Q Water System), with total

organic carbon level ≤ 5 ppb and resistivity of 18.2 MΩcm at 25 °C. Leakage buffer, which comprises of 1 mM EDTA, 10 mM Tris, and 150 mM NaCl at pH 7.4 was prepared in Milli-Q water. All chemical reagents were of analytical grade and used without further purification.

2.2. Synthesis of Hollow and Curcumin-Loaded Protein Nanoparticles

Pea protein isolate (PPI) with total protein content of 96.1%, as determined from Lowry assay, was extracted from yellow pea seeds (*Pisum sativum*) by the isoelectric precipitation technique and succinylated with succinic anhydride at pH 10.5 and a temperature of 38 °C, as previously reported.[1] Detailed protocol is provided in sections S1.1 and S1.2 of the supplementary information. Hollow and curcumin-loaded protein and protein-chitosan complexes were prepared with the native (PPI) and succinylated pea protein isolates (SPPI), as briefly described in Scheme 5.1; detailed experimental procedures are presented in sections 2.2.1 to 2.2.4.

2.2.1. Preparation of Reaction Solutions

Protein solutions of PPI and SPPI (5 mg/mL) were prepared in Milli-Q water, while solutions of Chitosan (2.5 mg/mL) and curcumin (1 mg/mL) were prepared in acetic acid (1%) and ethanol, respectively. The containers of curcumin solutions were wrapped with aluminum foil to protect curcumin from photodegradation. Protein and chitosan solutions were stirred for 6 h and centrifuged with a Sorvall LYNX 4000 superspeed centrifuge (ThermoFisher Scientific, Waltham, MA, USA) at 40,000× *g* for 30 min. The supernatant was vacuum filtered (Whatman filter paper number 50, pore size 2.7 μm) and degassed with Polylab vacuum desiccator (Singhla Scientific Industries, Punjabi Mohalla, Ambala, Haryana, India) to ensure air bubbles and gaseous impurities are removed.

2.2.2. Preparation of Curcumin-Loaded Native and Succinylated Pea Protein Nano-Complexes

Curcumin-loaded native and succinylated pea protein nano-complexes were synthesized by anti-solvent precipitation, following a previously-reported protocol [1]. Briefly, each curcumin solution in ethanol (1 mg/mL, 0.5 mL) was added, dropwise, to a solution of PPI and SPPI (5 mg/mL, 2.0 mL) in a separate flask, while stirring at 320× *g* for 5 h, until a steady negative zeta-potential was maintained. The colloidal solutions were centrifuged at 7500× *g* for 30 min using an Eppendorf 5430R centrifuge (Eppendorf, Mississauga, ON, Canada). The precipitate obtained was washed twice with Milli-Q water and redissolved in water (5 mL) for dynamic light scattering, microscopic studies, or in leakage buffer for a GUV leakage assay.

2.2.3. Preparation of Curcumin-Loaded Protein-Chitosan Nano-Complexes

The synthesis of curcumin-loaded native/succinylated pea protein-chitosan nano-complexes was carried out by first synthesizing the curcumin-protein nano-complexes (0.5 mL curcumin, 1.5 mL protein) by anti-solvent precipitation, as described in section 2.2.2. After stirring the colloidal solution at 320× *g* for 3 h, chitosan was incorporated through electrostatic deposition method, by dropwise addition of chitosan solution (2.5 mg/mL, 0.5 mL), while maintaining stirring for additional 5 h. The mixture was centrifuged at 7500× *g* for 30 min after obtaining a steady positive zeta-potential. The precipitate obtained was washed twice with water and redispersed, in water or buffer, for further studies.

2.2.4. Preparation of Native/Succinylated Pea Protein-Chitosan Hollow Nano-Complexes

Hollow native and succinylated protein-chitosan nano-complexes were prepared by the electrostatic deposition method, as previously reported [1]. Briefly, each chitosan solution (2.5 mg/mL, 0.5 mL) was gradually added to a separate solution of native and succinylated pea proteins, while stirring at 320× *g* for 5 h. The solution was monitored for steady positive zeta-potential, after

which it was centrifuged at 7500× *g* for 30 min. The precipitate was washed twice with water and redispersed, in water or buffer, for subsequent analysis.

2.3. Interactions of the Protein Nanoparticles with Calcein-Loaded GUV

2.3.1. Preparation of Empty and Calcein-Loaded Giant Unilamellar Vesicles

Zwitterionic giant unilamellar vesicles were prepared, according to a previously reported method,[20] with some modifications. Briefly, a solution of 1,2-dioleoyl-sn-glycero-3-phosphocholine (7.2 mg/mL) was prepared in chloroform in a 50 mL centrifuge tube, covered with aluminum foil, and allowed to dry under a stream of nitrogen for 4 h, followed by vacuum drying for an additional 12 h. Calcein solution (20 mM, 15 mL) was prepared in the leakage buffer (10 mM Tris, 150 mM NaCl, 1 mM EDTA, pH 7.4) and pH adjusted to 7.5 with NaOH (0.2 M). The dried lipid film (36 mg) was rehydrated with this solution to reach a final lipid concentration of 2 mg/mL. The colloidal solution was vortexed for 1 min, sonicated at 30 °C for 1 h, and subjected to five freeze/thaw cycles to enhance the encapsulation of calcein in the vesicle. Each cycle was comprised of 3 min in liquid nitrogen, 5 min in 60 °C water bath, and vortex mixing for 1 min. Size exclusion column (sephadex G-50) was used to separate the calcein-loaded GUV from unencapsulated calcein, using a leakage buffer for equilibration and elution. The eluted calcein-loaded GUV was stored for a maximum of 72 h at 4 °C and used for the leakage study.

Similarly, fluorescence-labeled calcein-loaded and free GUV was prepared for visualizing the impact of nanoparticle interaction. In this case, a mixture of 1,2-dioleoyl-sn-glycero-3-phosphocholine (20 mg) and 1,2-dioleoyl-sn-glycero-3 phosphoethanolamine-N-(lissamine rhodamine B sulfonyl) (ammonium salt) (1 mg) was dissolved in chloroform.

2.3.2. Zwitterionic GUV Leakage Assay

The influence of nanoparticles on the structural integrity of zwitterionic GUV was investigated by fluorescence spectroscopy using Varian Cary Eclipse (Agilent, Santa Clara, CA, USA), as previously reported,[20] with minor modifications. The eluted calcein-loaded GUV was diluted two-fold before mixing, with equal volume of colloidal solutions of hollow, curcumin-loaded protein, and curcumin-loaded protein-chitosan nano-complexes to reach final nanoparticles concentrations of 42 to 140 µg/mL. The spectrofluorometer was first zeroed with pure leakage buffer, and a fluorescence emission scan was performed, from 500 to 625 nm, at the excitation wavelength of 495 nm (calcein) and slit width of 2.5 nm. The fluorescence intensity of the calcein-loaded GUV was monitored for 10 min, to ensure stabilization of the signal, and used as the baseline fluorescence (F_0). Fluorescence intensity (F) was measured after interaction of the calcein-loaded GUV with various concentrations of nanoparticles. The maximum fluorescence intensity, corresponding to the fluorescence intensity of calcein after 100% leakage (F_M), was achieved with equal volume of 10% Triton X-100. The zwitterionic GUV leakage induced by the protein nanoparticles was estimated using to equation 5.1.

$$\%Leakage = \frac{(F - F_0)}{(F_M - F_0)} \times 100 \qquad (5.1)$$

2.4. Morphological Characterization of the Structural Integrity of Zwitterionic GUV after Interaction with Nanoparticles

The effect of interactions of hollow and various curcumin-loaded nano complexes, on the structural integrity of zwitterionic GUV, was visualized with confocal and widefield fluorescence microscopes. Each solution of calcein-loaded GUV (500 µL) was mixed with a solution of the nanoparticles (150 µL, 0.28 mg/mL) or 10% Triton X-100 (150 µL) prepared in a leakage buffer,

vortexed for 1 min, and allowed to stand for 15 min before mounting on glass microscope slides. To image calcein-loaded and empty GUV in the solution after leakage, the morphology was visualized separately in the rhodamine B (λ_{ex} 540, λ_{em} 625) and calcein (λ_{ex} 494, λ_{em} 517) channels, with the Axio Imager 2 fluorescence microscope equipped with an Axiocam 506 monochromatic camera (Carl Zeiss, Oberkochen, Germany) and Zeiss LSM880 AxioObserver Z1 confocal microscope equipped with AiryScan FAST (Carl Zeiss, Oberkochen, Germany). Zen 2.3 pro and 3.4 software (Carl Zeiss, Oberkochen, Germany) were used for image processing and optimization.

2.5. Dynamic Light Scattering Analysis

The impact of GUV-nanoparticle interaction on the particle size, polydispersity index, and zeta potential of calcein-loaded GUV was evaluated with the dynamic light scattering technique, using Nano-ZS Zetasizer (Malvern Instrument Ltd., Malvern, UK). Solutions of the calcein-loaded GUV (500 µL) and nanoparticles (150 µL, 0.28 mg/mL) were mixed and analyzed with the Smoluchowski model at absorption of 0.001, refractive index 1.450, F(ka) 1.50, and backscattered angle of 173° at 25 °C, after triplicate measurements.

2.6. Statistical Analysis

Experiments were conducted in triplicate, and mean values of data from leakage assay and dynamic light scattering were compared by one-way analysis of variance, using the Turkey's test and group mean differences, in Origin 9 software (OriginLab Corporation, Northampton, MA, USA). Significant differences were defined at $p < 0.05$.

3. Results and discussion

3.1. Nanoparticle-Induced Giant Unilamellar Vesicle Disruption at Physiological pH

There is a lack of studies using leakage assays to investigate the interactions occurring at the bio-nano interface, involving protein-based nanodelivery systems and giant unilamellar vesicles.

Existing information on organic compounds, such as antibiotic peptides fengycins,[20] maculatin, citropin, and aurein,[21] showed the disruption of liposomes as a measure of their antimicrobial properties. Liposome leakage data have also been reported for organic nanoparticles, such as lysozyme functionalized single-walled carbon nanotube, amyloid fibril in nanometer-order and lysozyme aggregates,[12] semihydrophobic nanoparticles of polystyrene,[19] and nanoscale protein aggregates,[22] focusing on cytotoxicity of the nanomaterials. In this work, the leakage-induced fluorescence emission spectra of calcein-loaded giant unilamellar vesicles was monitored, after interactions with various hollow and curcumin-loaded protein nanoparticles of different surface chemistry, size, stability, and biocoating, to study the biophysicochemical interactions that occur at the nano-bio interface. This assay is based on measuring the fluorescence intensity of calcein, which is quenched when encapsulated in the lipid vesicle and fluoresce on leakage. Therefore, the fluorescence intensity is directly proportional to the number of moles of calcein released from the model biomembrane.[23] The fluorescence emission scan (Figure 5.1) showed that the interaction of the various nanoparticles with calcein-loaded giant unilamellar vesicles did not cause a major shift in the maximum emission wavelength of encapsulated calcein. This indicates that the nanoparticles do not cause any major modification in the structural properties of calcein. The GUV leakage assay (Figures 5.1 and 5.2) showed that each nanoparticle pair—CUR/PPI and CUR/SPPI, CUR/PPI/CHI and CUR/SPPI/CHI, or PPI/CHI and SPPI/CHI—demonstrated similar modes of interaction with the GUV. This could be attributed to their similar physicochemical properties, such as chemical composition, size, morphology, and zeta potential.[1] CUR/PPI and CUR/SPPI induced minimal calcein leakage at the lowest nanoparticle concentrations (<5.6 μg/mL). At higher concentrations, a dose-dependent quenching of calcein fluorescence was observed, and the effect was more pronounced with CUR/SPPI than CUR/PPI. The extent of the quenching is quantified

by the negative value of percentage leakage (Figure 5.2). The higher the negative percentage leakage, the higher the quenching effect resulting from the nanoparticle-GUV interaction. Curcumin forms a less stable complex with succinylated pea protein isolate (CUR/SPPI), compared to native pea protein isolate (CUR/PPI), based on their Stern–Volmer binding parameters [1]. The higher stability of CUR/PPI, compared to CUR/SPPI, could have resulted to its lower binding to GUV and, hence, lower fluorescence quenching on interaction. The quenching effect is possibly due to binding of the nanoparticles on the GUV surface without rupturing the membrane. The feasibility of this nanoparticle-membrane association mechanism has been well-established through classic molecular dynamic simulation.[24] The net charge of DOPC GUV is zero, thus ruling out the possibility of electrostatically-induced adsorption. Instead, hydrophobic interaction has been reported to play an essential role in the adsorption of liposomes, with zero net charge on nanoscale amyloid fibrils, derived from lysozymes and the subsequent disruption of the membrane.[22] In addition, hydrophobic interaction is responsible for the adsorption of carboxyl end-functionalized polystyrene nanoparticles on neutral-supported lipid bilayers, dragging the lipids from the model cell membrane to the nanoparticles' surface and rupturing the membrane at high nanoparticle concentration.[19]

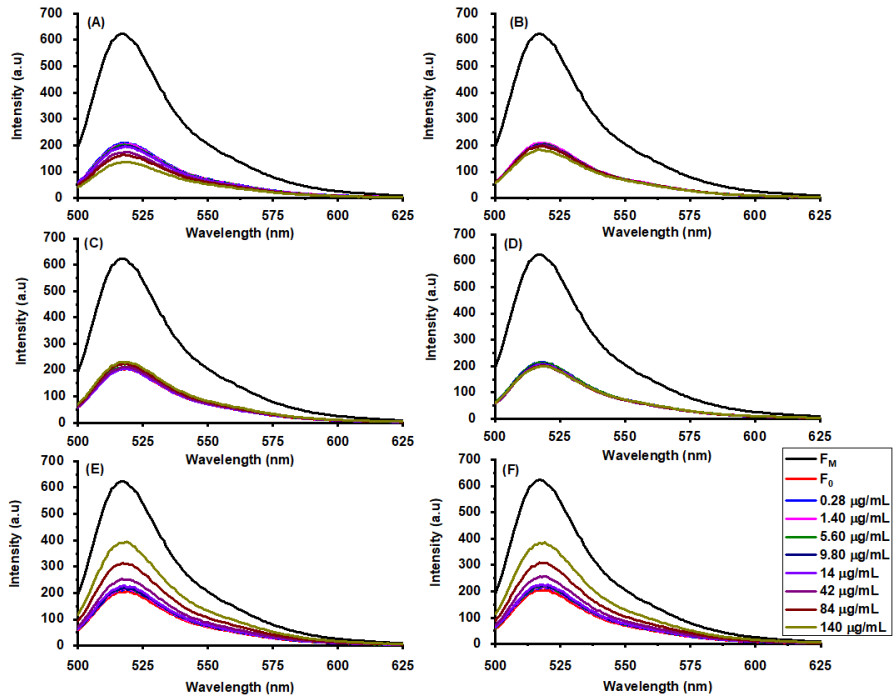

Figure 5.1. Leakage-induced fluorescence emission spectra of calcein, encapsulated in the GUV, after interaction with various concentrations of (A) curcumin-loaded succinylated pea protein, (B) curcumin-loaded native pea protein, (C) curcumin-loaded succinylated pea protein-chitosan, (D) curcumin-loaded native pea protein-chitosan, (E) hollow succinylated pea protein-chitosan, and (F) hollow native pea protein-chitosan complexes.

Interactions of CUR/PPI/CHI and CUR/SPPI/CHI nanoparticles with GUV induced dose-dependent minimal calcein leakage (Figures 5.1 and 5.2) which have a more pronounced effect in the former. Unlike CUR/PPI and CUR/SPPI, the incorporation of chitosan modified the physicochemical properties of the nanoparticles and resulted in calcein leakage rather than quenching. The binding parameters showed that CUR/SPPI/CHI and CUR/PPI/CHI complexes are significantly more stable than CUR/PPI and CUR/SPPI complexes, and the higher stability resulted in minimal interaction with GUV. The leakage could be attributed to the rupturing of the biomembrane by the nanoparticles. The curcumin-protein and curcumin-protein-chitosan

nanoparticles possess opposite surface charges, different sizes, and chemical compositions [1], which could account for their different modes of interaction. The interaction of other nanoparticles of different physicochemical properties, such as amyloid fibril, heat-induced aggregate, and monomer of lysozyme, with liposomes depends on their concentration, shape, and charge. While amyloid fibril induced up to 70% calcein leakage, the lysozyme monomer and aggregates had minimal impact on the liposomes.[12] Carboxylated polystyrene nanoparticles of different sizes, 20 and 100 nm, coated with fetal bovine serum had different effects on the supported lipid bilayer. Unlike the nanoparticle of 20 nm, which had negligible impact on the membrane, quartz crystal microbalance with the dissipation technique showed that 100 nm particles, adsorbed on the supported lipid bilayer, caused a significant decrease in frequency and increase in dissipation to induce rupturing of the membrane.[25] Negatively charged carboxyl-functionalized polystyrene nanoparticles induced local gelation in fluid bilayers, whereas positively charged amidine-functionalized polystyrene nanoparticles caused the fluidization of gelled membrane locally.[26]

Hollow PPI/CHI and SPPI/CHI nanoparticles showed dose-dependent significant leakage within the tested concentrations. As with the curcumin-loaded protein and protein-chitosan pairs, PPI/CHI and SPPI/CHI nanoparticles displayed similar modes of interaction. There was no significant difference in the leakage effect observed at a nanoparticle concentration of 0.28 to 14 µg/mL. However, major leakage of more than 40% was noted at a nanoparticle concentration of 140 µg/mL (Figure 5.2). This effect could be attributed to nanoparticle-induced membrane perturbation. Single-walled carbon nanotubes, functionalized with lysozyme from a chicken egg white, demonstrated similar dose-dependent leakage of calcein from liposomes, attaining ~30% leakage at a particle concentration of 80 ng/mL. The leakage effect of PPI/CHI and SPPI/CHI hollow could be because of the low stability of the nanoparticles, as demonstrated from their low binding

constants (data not shown). The irregular nanostructure of PPI/CHI and SPPI/CHI, coupled with their numerous pores in solution, could also be contributing to the leakage. Pores have been reported to considerably impact membrane integrity.[19,27] Pore-forming toxins employ similar mechanisms to form holes in biomembranes, leading to the death of target cells.[28] Our previous study showed that curcumin encapsulation is essential for the stability of the protein-chitosan complex.[1] The shape of nanoparticles plays an important role in their membrane disruption ability. For instance, one-dimensional shape of single-walled carbon nanotube, coated with lysozyme, was reported to be responsible for liposome disruption.[12]

Based on the findings, we propose that the encapsulated guest compound, which stabilizes the host macromolecule used as the delivery vehicle, influences the nature of interaction of hollow and curcumin-loaded protein, as well as protein-chitosan nanoparticles, with biomembranes. Therefore, as the protein or protein-chitosan complexes play a crucial role in stabilizing the bioactive compound from chemical and photodegradation, the encapsulated compound modulates the interaction of the host macromolecule with biomembranes.

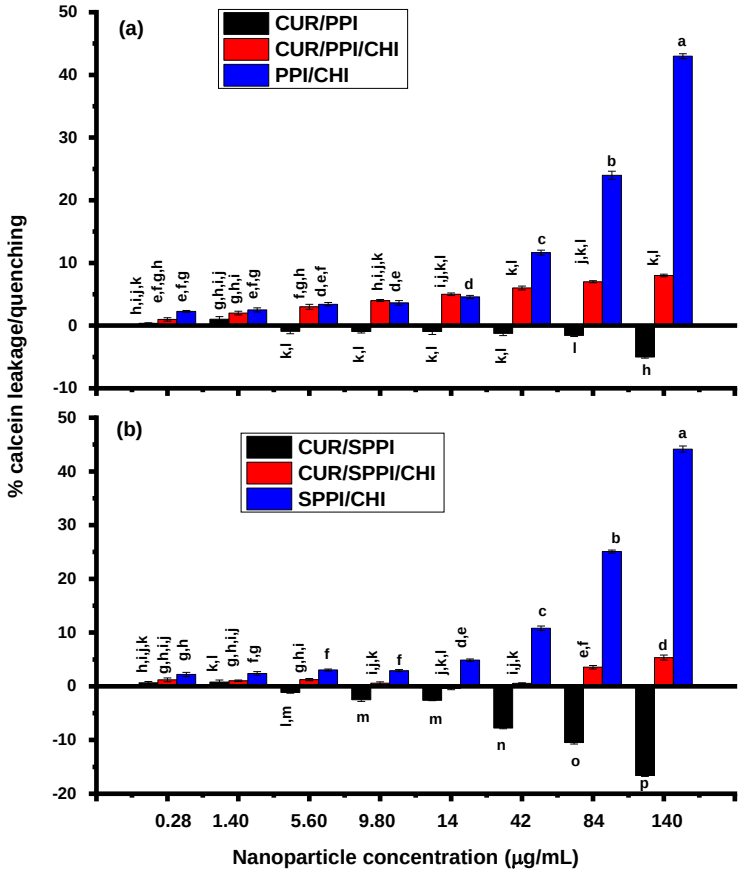

Figure 5.2. Percentage calcein leakage from the GUV, induced by (a) native protein-based nanoparticles and (b) succinylated protein-based nanoparticles, with different surface chemistry and physicochemical properties.

Bars with similar letters represent mean values that are not significantly different at $p < 0.05$.

3.2. Influence of Nanoparticle-GUV Interaction on the Size, Zeta Potential and Polydispersity Index of the Vesicles

Dynamic light scattering measurements showed that the interaction of CUR/PPI and CUR/SPPI with GUV caused a major reduction in the size of the vesicles. This was unexpected because the calcein leakage assay showed a considerable fluorescence quenching effect above 14 µg/mL, attributed to nanoparticle binding on the GUV surface. Hence, one would expect an increase in the size of the GUV-nanoparticle complex. The reduction in size after binding of the nanoparticles

could be because of strong hydrophobic interaction between the nanoparticles and GUV, resulting in a shrinking of the membrane. Another reason could be due to nanoparticle-induced GUV division, into smaller particles, while retaining the content of the membrane. The former mechanism seems more likely, as the exposure of PEGylated and non-PEGylated phosphatidylcholine/cholesterol liposomes to serum resulted in the shrinking of the biomembrane.[29] The binding of proteins that are impermeable to the membrane triggered a high osmotic pressure that caused the escape of water from the core of the liposome and, hence, the reduction in liposome size.[29] This mechanism can explain the observed shrinking of GUV, after interaction with CUR/PPI and CUR/SPPI, with the membrane selectively allowing the escape of water while retaining calcein at high osmotic pressure, resulting in reduced calcein fluorescence. Other studies have shown that the surface structure and elasticity of supported lipid bilayers, or large unilamellar vesicles, can be reconstructed by nonspecific adsorption of charged nanoparticles.[25,26] For instance, the binding of anionic polystyrene nanoparticles, of different charge density and similar size, on large unilamellar vesicles resulted in the shrinking of the vesicles, due to local fluid-to-gel transition of the lipid, which equally caused the reduction in area per molecule and loss of hydration.[26]

The size of the calcein-loaded GUV, before and after interaction with CUR/PPI/CHI and CUR/SPPI/CHI (Table 5.1), was comparable, suggesting minimal impact of the nanoparticles on the vesicles. This result supports the minimal GUV leakage (Figure 5.2) related to the higher stability of the curcumin-protein-chitosan nano-complexes. Although weaker than the effect of 10% Triton X-100, PPI/CHI and SPPI/CHI hollow caused a significant decrease in the size of the GUV (Table 5.1). This effect could be attributed to direct bursting of the GUV on interaction with the nanoparticles, which corroborates the significant calcein leakage (Figure 5.2). There was no

definite pattern of zeta potential of the calcein-loaded GUV, before and after interaction with the various nanoparticles, as the charges were contributed by the nanoparticles, leakage buffer, or calcein since the zwitterionic GUV has a net zero charge. The polydispersity index of the GUV, after interaction with PPI/CHI and SPPI/CHI hollow (Table 5.1), indicates the formation of a more heterogeneous mixture (Figure 5.3). The rupturing of ~40% of the vesicles by the hollow nanoparticles means that the remaining 60% intact GUV resulted in a heterogeneous mixture (Figure 5.3). The positive control, Triton X-100, decreased the size of the GUV by ~200-fold due to direct bursting and clearing of the vesicles. This is supported by results from confocal (Figure 5.4h) and widefield fluorescence microscopy (Figure S5.1i). Triton X-100 is a well-known surfactant that causes almost 100% leakage or disruption of liposome vesicles; thus, it is commonly used to estimate the percentage leakage of fluorophore from loaded vesicles (Section 2.3.1.).[20]

Table 5.1. Changes in size, polydispersity index, and zeta potential of calcein-loaded GUV after interaction with the hollow or curcumin-loaded protein nanoparticles or Triton X-100.

Samples	Size (nm)	PDI	Zeta Potential (mV)
lGUV	1933.3 ± 29.0 ^{b}	0.30 ± 0.03 ^{a,b,c}	-5.7 ± 0.2 ^{b}
lGUV + CUR/PPI	1091.3 ± 5.0 ^{e}	0.33 ± 0.04 ^{a,b,c}	-10.0 ± 0.1 ^{e,f}
lGUV + CUR/SPPI	1028.7 ± 26.2 ^{e}	0.25 ± 0.02 ^{a,b,c}	-11.5 ± 0.3 ^{f,g}
lGUV + CUR/PPI/CHI	1689.7 ± 55.2 ^{c}	0.42 ± 0.10 ^{a,b}	-9.6 ± 0.3 ^{d,e}
lGUV + CUR/SPPI/CHI	2222.7 ± 36.4 ^{a}	0.18 ± 0.05 ^{b,c}	-7.9 ± 0.4 ^{c,d}
lGUV + PPI/CHI	1464.7 ± 64.8 ^{d}	0.41 ± 0.06 ^{a,b}	-11.8 ± 0.2 ^{g}
lGUV + SPPI/CHI	1551.7 ± 20.0 ^{c,d}	0.43 ± 0.05 ^{a}	-7.4 ± 0.2 ^{b,c}
lGUV + Triton X-100	10.7 ± 0.0 ^{f}	0.10 ± 0.00 ^{c}	-1.0 ± 0.8 ^{a}

Mean values with different letters in a column are significantly different ($p < 0.05$) Abbreviations: CUR/SPPI, curcumin-succinylated pea protein complex; CUR/PPI, curcumin-pea protein complex; CUR/SPPI/CHI, curcumin-succinylated pea protein-chitosan complex; CUR/PPI/CHI, curcumin-pea protein-chitosan complex; SPPI/CHI hollow, succinylated pea protein-chitosan shell; PPI/CHI hollow, native pea protein-chitosan shell; lGUV, giant unilamelar vesicles loaded with calcein.

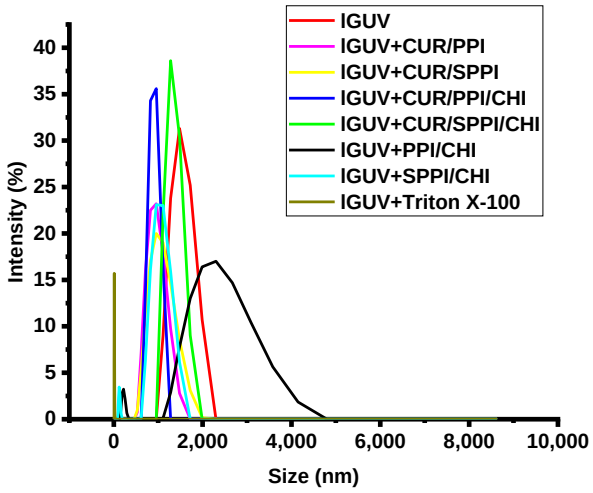

Figure 5.3. Dynamic light scattering size distribution curve of calcein-loaded giant unilamellar vesicles (lGUV), before and after interaction with hollow (PPI/CHI and SPPI/CHI) and curcumin-loaded protein nanoparticles (CUR/PPI, CUR/SPPI, CUR/PPI/CHI and CUR/SPPI/CHI) and Triton X-100.

3.3. Morphological Properties of the GUV after Interaction with Nanoparticles

The images from confocal and widefield microscopy further corroborate the findings. The morphology of the GUV, after interaction with CUR/SPPI, CUR/PPI, CUR/SPPI/CHI, and CUR/PPI/CHI nano-complexes (Figure 5.4a–d and Figure S5.1c–f), looks similar to that of the calcein-loaded GUV in the absence of the nanoparticles (Figure 5.4g and Figure S5.1b). This

suggests minimal impact of the nanoparticles to the biomembrane. The size range of the nanoparticles <200 nm [1] falls outside the range of the light microscope, making it difficult to capture the nanoparticles on the surface of the GUV, as postulated for CUR/SPPI and CUR/PPI, or in the vicinity of the GUV for CUR/SPPI/CHI and CUR/PPI/CHI nano-complexes. Figure 5.4e–f and Supplementary Figure S5.1g–h confirmed membrane disruption and calcein leakage induced by the hollow SPPI/CHI and PPI/CHI nanocomplexes, with impact more visible in SPPI/CHI. The morphology of the empty GUVs (Figure 5.4i and S5.1a) indicates that calcein encapsulation stabilizes the vesicles, thus giving it a definite structure. Taken together, the calcein leakage and microscopy results show two distinct nanoparticle-GUV interaction mechanisms, as illustrated in Figure 5.5.

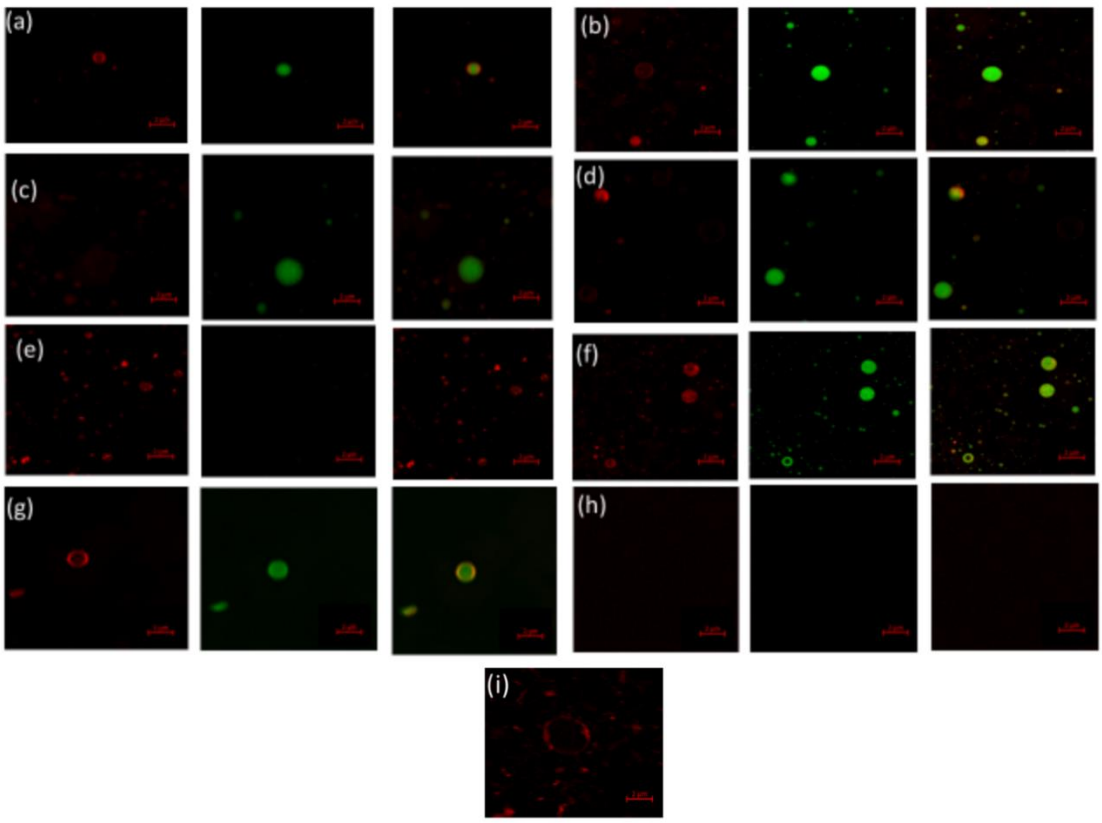

Figure 5.4. Confocal microscopy images of calcein-loaded GUV, after interaction with (a) CUR/SPPI, (b) CUR/PPI, (c) CUR/SPPI/CHI, (d) CUR/PPI/CHI, (e) SPPI/CHI, (f) PPI/CHI

nanoparticles, and (g) calcein-loaded GUV, in the absence of nanoparticles, (h) calcein-loaded GUV after treatment with Triton X-100 (10%) positive control, and (i) GUV without calcein.

Images in the first column were acquired at rhodamine B channel (GUV labeled with rhodamine), the second column is at calcein channel, and the third column is the merger of both. Scale bar is 2 µm.

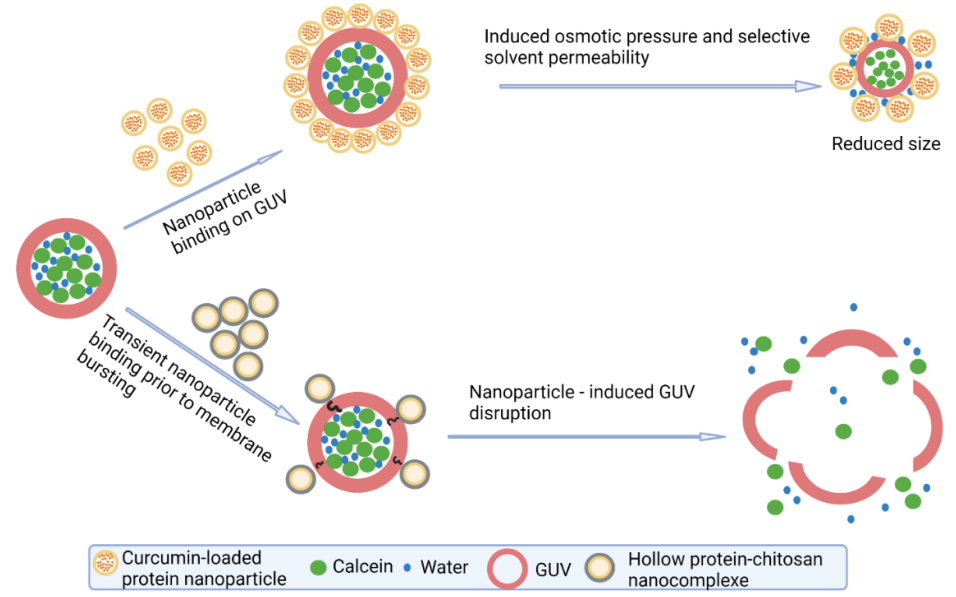

Figure 5.5. Proposed nanoparticle-giant unilamellar vesicle interaction mechanisms.

4. Conclusion

The bio-nano interaction of nutraceutical-loaded protein nanoparticles was investigated using hollow and curcumin-loaded protein nanoparticles of different surface chemistry (with or without chitosan or curcumin) and physicochemical properties (size, zeta potential, morphology, binding strength) as model delivery vehicles, with GUV as model biomembranes. Protein nanoparticle-lipid membrane interaction is mainly influenced by the composition, physicochemical property, and surface chemistry of nanoparticles. Interaction of CUR/PPI and CUR/SPPI nanoparticles,

which have a smaller size range, higher negative zeta potential, spherical morphology, and lower binding strength, compared to CUR/SPPI/CHI and CUR/PPI/CHI, where calcein-loaded GUV led to the quenching of calcein fluorescence. Unlike CUR/PPI/CHI (effective binding constant 14.5×10^4 M^{-1}) that induced minimal calcein leakage, interaction of CUR/SPPI/CHI nanoparticles (effective binding constant 187.9×10^4 M^{-1}) with calcein-loaded GUV did not cause significant change in the morphology and structure of GUV or calcein fluorescence. Conversely, PPI/CHI and SPPI/CHI hollow with irregular morphology caused major rupturing of calcein-loaded GUV, leading to increased calcein leakage. Therefore, we propose two mechanisms for the nanoparticle-membrane interactions: 1) nanoparticle binding on membrane surface induces osmotic pressure, resulting in water escape from the membrane and consequent shrinkage; 2) nanoparticle binding on the membrane induces GUV bursting. The former was demonstrated by CUR/PPI and CUR/SPPI nanoparticles, while CUR/SPPI/CHI, CUR/PPI/CHI, PPI/CHI, and SPPI/CHI displayed the latter mechanism. CUR/SPPI/CHI nanoparticles with the highest stability and, hence, minimal impact to the biomembrane could be potentially less deleterious during delivery of bioactive compounds. Therefore, as protein and protein-chitosan complexes protect the bioactive compounds from photo and chemical degradation, the encapsulated nutraceutical could modulate the interaction of the protein-based nanoparticle with the gastrointestinal cell membrane. This study provides the first evidence of the implication of interactions, occurring at the bio-nano interface, for food protein-based nanodelivery systems. This information will guide the design of delivery systems that safely interact with biological membranes, while ensuring the protection of the guest compound from degradation and its sustained release at the target location in the body.

Acknowledgments: The authors are grateful to Tyler Avis (Department of Chemistry, Carleton University, Canada) for valuable insight on the leakage assay and for donating calcein and material for column chromatography.

Funding: This research was supported by the University Research Chair Program of the University of Ottawa, and the Discovery Grant Program (RGPIN-2018-06839) of the Natural Sciences and Engineering Research Council of Canada (NSERC).

References

(1) Okagu, O.D.; Jin, J.; Udenigwe, C.C. Impact of succinylation on pea protein-curcumin interaction, polyelectrolyte complexation with chitosan, and gastrointestinal release of curcumin in loaded-biopolymer nano-complexes. *Journal of Molecular Liquids.* **2020**, *325*, 115248. https://doi.org/10.1016/j.molliq.2020.115248.

(2) Guo, Q.; Bayram, I.; Zhang, W.; Su, J.; Shu, X.; Yuan, F.; Mao, L.; Gao, Y. Fabrication and characterization of curcumin-loaded pea protein isolate-surfactant complexes at neutral pH. *Food Hydrocolloids.* **2021**, *111*, 106214. https://doi.org/10.1016/j.foodhyd.2020.106214.

(3) Okagu, O.D.; Udenigwe, C.C. Molecular Interactions of Pea Globulin, Albumin and Glutelin with Curcumin: Formation and Gastric Release Mechanisms of Curcumin-loaded Bio-nanocomplexes. *Food Biophysics.* **2021**, *17*, 1–16. https://doi.org/10.1007/s11483-021-09697-5.

(4) Okagu, O.D.; Verma, O.; McClements, D.J.; Udenigwe, C.C. Utilization of insect proteins to formulate nutraceutical delivery systems: Encapsulation and release of curcumin using mealworm protein-chitosan nano-complexes. *International Journal of Biological Macromolecules.* **2020**, *151*, 333–343. https://doi.org/10.1016/j.ijbiomac.2020.02.198.

(5) Wang, F.; Yang, Y.; Ju, X.; Udenigwe, C.C.; He, R. Polyelectrolyte Complex Nanoparticles from Chitosan and Acylated Rapeseed Cruciferin Protein for Curcumin Delivery. *Journal of Agricultural and Food Chemistry.* **2018**, *66*, 2685–2693. https://doi.org/10.1021/acs.jafc.7b05083.

(6) Sneharani, A.H. Curcumin–sunflower protein nanoparticles—A potential antiinflammatory agent. *Journal of Food Biochemistry.* **2019**, *43*, e12909. https://doi.org/10.1111/jfbc.12909.

(7) Wei, Y.; Wang, C.; Liu, X.; Liao, W.; Zhang, L.; Chen, S.; Liu, J.; Mao, L.; Yuan, F.; Gao, Y. Effects of microfluidization and thermal treatment on the characterization and digestion of curcumin loaded protein-polysaccharide-tea saponin complex nanoparticles. *Food & Function.* **2021**, *12*, 1192–1206. https://doi.org/10.1039/d0fo02283g.

(8) Mirpoor, S.F.; Hosseini, S.M.H.; Yousefi, G.H. Mixed biopolymer nanocomplexes conferred physicochemical stability and sustained release behavior to introduced curcumin. *Food Hydrocolloids.* **2017**, *71*, 216–224. https://doi.org/10.1016/j.foodhyd.2017.05.021.

(9) McClements, D.J.; Xiao, H. Is nano safe in foods? Establishing the factors impacting the gastrointestinal fate and toxicity of organic and inorganic food-grade nanoparticles. *Npj Science of Food* **2017**, *1*, 1–13. https://doi.org/10.1038/s41538-017-0005-1.

(10) Wong, C.Y.; Al-Salami, H.; Dass, C.R. Cellular assays and applied technologies for characterisation of orally administered protein nanoparticles: A systematic review. *Journal of Drug Targeting.* **2020**, *28*, 585–599.

(11) Yang, L.; Li, M.; Sun, Y.; Zhang, L. A cell-penetrating peptide conjugated carboxymethyl-β-cyclodextrin to improve intestinal absorption of insulin. *International Journal of Biological Macromolecules.* **2018**, *111*, 685–695. https://doi.org/10.1016/j.ijbiomac.2018.01.077.

(12) Hirano, A.; Uda, K.; Maeda, Y.; Akasaka, T.; Shiraki, K. One-dimensional protein-based nanoparticles induce lipid bilayer disruption: Carbon nanotube conjugates and amyloid fibrils. *Langmuir.* **2010**, *26*, 17256–17259. https://doi.org/10.1021/la103615b.

(13) Araújo, F.; Shrestha, N.; Granja, P.L.; Hirvonen, J.; Santos, H.A.; Sarmento, B. Safety and toxicity concerns of orally delivered nanoparticles as drug carriers. *Expert Opinion on Drug Metabolism & Toxicology.* **2015**, *11*, 381–393.

(14) Zhang, H.; Van Os, W.L.; Tian, X.; Zu, G.; Ribovski, L.; Bron, R.; Bussmann, J.; Kros, A.; Liu, Y.; Zuhorn, I.S. Development of curcumin-loaded zein nanoparticles for transport across the blood-brain barrier and inhibition of glioblastoma cell growth. *Biomaterials Science.* **2021**, *9*, 7092–7103. https://doi.org/10.1039/d0bm01536a.

(15) Saleh, T.; Soudi, T.; Shojaosadati, S.A. Aptamer functionalized curcumin-loaded human serum albumin (HSA) nanoparticles for targeted delivery to HER-2 positive breast cancer cells. *International Journal of Biological Macromolecules.* **2019**, *130*, 109–116. https://doi.org/10.1016/j.ijbiomac.2019.02.129.

(16) Saleh, T.; Soudi, T.; Shojaosadati, S.A. Redox responsive curcumin-loaded human serum albumin nanoparticles: Preparation, characterization and in vitro evaluation. *International Journal of Biological Macromolecules.* **2018**, *114*, 759–766. https://doi.org/10.1016/j.ijbiomac.2018.03.085.

(17) Lee, H.; Larson, R.G. Lipid bilayer curvature and pore formation induced by charged linear polymers and dendrimers: The effects of charge density, concentration, molecular size and shape. *In Proceedings of the AIChE Annual Meeting, Conference Proceedings*, Philadelphia, PA, USA, 16–21 November 2008.

(18) Mecke, A.; Majoros, I.J.; Patri, A.K.; Baker, J.R.; Banaszak Holl, M.M.; Orr, B.G. Lipid bilayer disruption by polycationic polymers: The roles of size and chemical functional group. *Langmuir.* **2005**, *21*, 10348–10354. https://doi.org/10.1021/la050629l.

(19) Jing, B.; Zhu, Y. Disruption of supported lipid bilayers by semihydrophobic nanoparticles. *Journal of the American Chemical Society.* **2011**, *133*, 10983–10989. https://doi.org/10.1021/ja2040305.

(20) Mantil, E.; Buznytska, I.; Daly, G.; Ianoul, A.; Avis, T.J. Role of Lipid Composition in the Interaction and Activity of the Antimicrobial Compound Fengycin with Complex Membrane Models. *Journal of Membrane Biology.* **2019**, *252*, 627–638. https://doi.org/10.1007/s00232-019-00100-6.

(21) Ambroggio, E.E.; Separovic, F.; Bowie, J.H.; Fidelio, G.D.; Bagatolli, L.A. Direct visualization of membrane leakage induced by the antibiotic peptides: Maculatin, citropin, and aurein. *Biophysical Journal.* **2005**, *89*, 1874–1881. https://doi.org/10.1529/biophysj.105.066589.

(22) Hirano, A.; Yoshikawa, H.; Matsushita, S.; Yamada, Y.; Shiraki, K. Adsorption and disruption of lipid bilayers by nanoscale protein aggregates. *Langmuir*. **2012**, *28*, 3887–3895. https://doi.org/10.1021/la204717c.

(23) Alkhammash, H.I.; Li, N.; Berthier, R.; De Planque, M.R.R. Native silica nanoparticles are powerful membrane disruptors. *Physical Chemistry Chemical Physics.* **2015**, *17*, 15547–15560. https://doi.org/10.1039/c4cp05882h.

(24) Aydin, F.; Dutt, M. Surface Reconfiguration of Binary Lipid Vesicles via Electrostatically Induced Nanoparticle Adsorption. *Journal of Physical Chemistry B.* **2016**, *120*, 6646–6656. https://doi.org/10.1021/acs.jpcb.6b02334.

(25) Di Silvio, D.; Maccarini, M.; Parker, R.; Mackie, A.; Fragneto, G.; Baldelli Bombelli, F. The effect of the protein corona on the interaction between nanoparticles and lipid bilayers. *Journal of Colloid and Interface Science.* **2017**, *504*, 741–750. https://doi.org/10.1016/j.jcis.2017.05.086.

(26) Wang, B.; Zhang, L.; Sung, C.B.; Granick, S. Nanoparticle-induced surface reconstruction of phospholipid membranes. *Proceedings of the National Academy of Sciences, USA.* **2008**, *105*, 18171–18175. https://doi.org/10.1073/pnas.0807296105.

(27) Chan, H.; Král, P. Nanoparticles Self-Assembly within Lipid Bilayers. *ACS Omega.* **2018**, *3*, 10631–10637. https://doi.org/10.1021/acsomega.8b01445.

(28) Cabezas, S.; Ho, S.; Ros, U.; Lanio, M.E.; Alvarez, C.; van der Goot, F.G. Damage of eukaryotic cells by the pore-forming toxin sticholysin II: Consequences of the potassium efflux. *Biochimica et Biophysica Acta - Biomembranes.* **2017**, *1859*, 982–992. https://doi.org/10.1016/j.bbamem.2017.02.001.

(29) Wolfram, J.; Suri, K.; Yang, Y.; Shen, J.; Celia, C.; Fresta, M.; Zhao, Y.; Shen, H.; Ferrari, M. Shrinkage of pegylated and non-pegylated liposomes in serum. *Colloids and Surfaces B: Biointerfaces* **2014**, *114*, 294–300. https://doi.org/10.1016/j.colsurfb.2013.10.009.

SUPPLEMENTARY INFORMATION

Curcumin–induced stabilization of protein–based nano-delivery vehicles reduces disruption of zwitterionic giant unilamellar vesicles

Ogadimma D. Okagu, Raliat O. Abioye, Chibuike C. Udenigwe

Molecules **2022**, *27*(6), 1941; https://doi.org/10.3390/molecules27061941

S1. Methodology

S1.1. Pea protein extraction

Isoelectric precipitation technique was employed in extracting pea protein isolate (PPI) from yellow pea seeds (*Pisum sativum*) as previously reported.[1] Briefly, dehulled yellow pea seeds were ground and sieved, the flour (200 g) extracted with NaOH solution (0.05 M, 2L) at pH 12.7 after 4 h of stirring in a magnetic stirrer (Thermo Scientific, Waltham, MA, USA). The resulting slurry was centrifuged at 25 °C and 5600 ×*g* for 30 min. The supernatant was separated from the residue and pH adjusted to 4.5 with HCl (1 M) to precipitate PPI. The mixture was again centrifuged for 30 min and PPI collected, washed twice with Milli-Q water and pH adjusted to 7. The PPI paste was frozen at -80 °C for 24h, and lyophilized (Labconco, Kansas, MO, USA) at -52 °C and 0.2 mbar. The total protein content as determined by Lowry assay was 96.1 %.

S1.2. Succinylation of the pea protein isolate

Pea protein isolate was succinylated according to a previously reported method [1]. It involves drop-wise addition of a solution of succinic anhydride (0.5 M, 4 mL) to a pre-heated solution of PPI (100 mL, 2% w/v, 38 °C, pH 11) and the pH maintained at 10.5 with NaOH (1 M) while stirring for 4 h. The mixture was dialyzed against deionized water with a membrane of molecular weight cut-off of 3.5 kDa for 48 h at 4 °C. The retentate was lyophilized and the powder store at -20 °C.

Figures

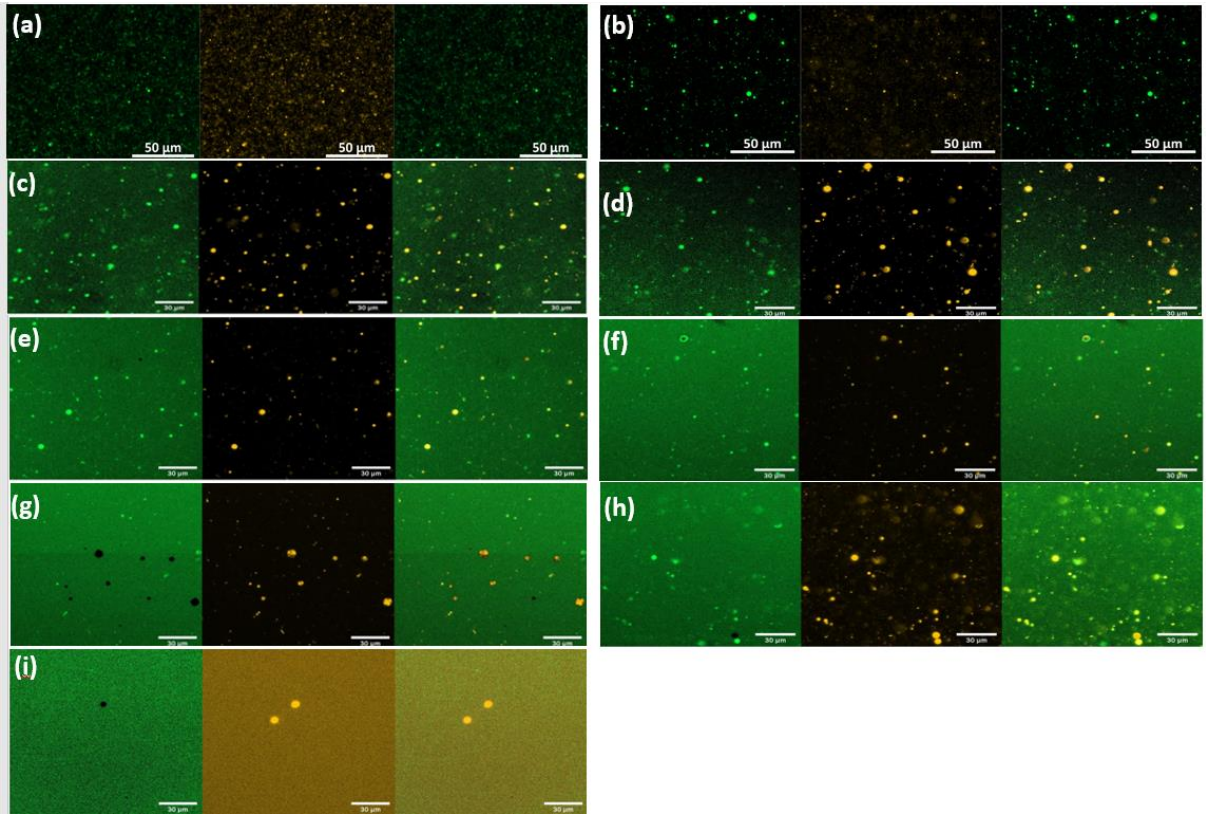

Figure S5.1. Widefield fluorescence microscopy images of (a) empty GUV (b) GUV-loaded calcein in the absence of nanoparticles, and after interaction with (c)CUR/SPPI (d) CUR/PPI (e) CUR/SPPI/CHI (f) CUR/PPI/CHI (g) SPPI/CHI (h) PPI/CHI nanoparticles and (i) Triton-X-100 (10%) positive control. Images in the first column were acquired at calcein channel, second column at rhodamine B channel (GUV labeled with rhodamine), and third column is the merger of both.

Reference

(1) Okagu, O.D.; Jin, J.; Udenigwe, C.C. Impact of succinylation on pea protein-curcumin interaction, polyelectrolyte complexation with chitosan, and gastrointestinal release of curcumin in loaded-biopolymer nano-complexes. *J. Mol. Liq.* **2020**, *325*, 115248. https://doi.org/10.1016/j.molliq.2020.115248.

CHAPTER SIX

CONCLUSION

The main objective of this thesis was to investigate the structural basis of guest-host interaction in the gastrointestinal delivery of lipophilic bioactive compounds. This knowledge is expected to guide the rational design of delivery vehicles for the encapsulation, protection, and release of unstable, biodegradable, and insoluble bioactive compounds with low bioaccessibility and bioavailability. The four research objectives that motivated this research is based on the seven key research questions listed in chapter one.

The first, second and third research questions, which are the first core objective of this thesis, were addressed in chapter two. Using native pea protein and succinylated pea protein isolate as model natural and modified proteins, respectively, a comparative study conducted showed that native and succinylated pea proteins and their chitosan complexes could be used to create curcumin-loaded biopolymer nano-complexes. The process of succinylation raised the protein negative charge, facilitating electrostatic interaction with chitosan, but it also reduced the protein surface hydrophobicity, reducing hydrophobic interaction with curcumin. The solubility and stability of curcumin were improved via hydrophobic interaction with the protein in the protein-chitosan polyelectrolyte complex. For curcumin encapsulation with the polyelectrolyte complex, it is crucial to achieve a balance during succinylation to ensure an increase in negative charge with little to no effect on the protein hydrophobicity. Curcumin demonstrated some degree of dynamic binding to both the natural and succinylated proteins, whereas the addition of chitosan favoured static binding. The succinylated protein hydrophobicity was restored by the electrostatic interaction with chitosan, which also increased curcumin binding. The native protein-chitosan combination had the highest encapsulation efficiency of curcumin due to the stronger binding. There was a lower amount of curcumin released from succinylated protein-curcumin compared to native protein-curcumin due to weaker binding and stabilisation occurring in the former. While

complexes stabilised with chitosan provided superior protection in the stomach phase, native protein-curcumin complexes were more effective at reducing the release of curcumin in the salivary phase. These actions culminated in the same quantity of curcumin reaching the intestinal phase and correspondingly identical bioaccessibility for both complexes. Therefore, without protein modification by succinylation or polyelectrolyte complexation with chitosan, our investigation showed that pea protein isolate successfully encapsulated and controlled-released significant amounts of curcumin in a simulated gastrointestinal tract.

The second objective, which is based on the fourth research question, was explored in chapter three and like in the first objective, the study further strengthened the finding that curcumin binding to protein depends on the surface hydrophobicity of the protein. The key finding in this study is that the structural and physicochemical properties of protein influence not only curcumin binding but the release of the bioactive compound at different gastric conditions. The research demonstrated that structural compatibility plays a key role in bioactive compound binding and stabilization in gastric phase of digestion. The structural modification in the protein as a result of its interaction with curcumin increased its thermal stability. Curcumin was successfully encapsulated into well-ordered, spherical nanocomplexes as revealed by transmission electron microscopy. In summary, using the antisolvent precipitation approach, spherical, pepsin-resistant, and thermostable curcumin-protein fraction nanocomplexes were synthesized. The various pea protein fraction complexes of curcumin released curcumin during gastric digestion by two separate mechanisms: a pepsin-dependent process as observed for water- and alkaline-soluble pea protein fractions and salt-dependent mechanism for salt-soluble pea protein fraction. The potential use of these complexes in the gastrointestinal administration of curcumin is suggested by their high encapsulation efficiency, stability in gastric fluid, and resistance to pepsin degradation.

The fifth and sixth research questions, which fall under the third objective of this research, were aimed at understanding the influence of lipophilicity of bioactive compounds and ionic strength of the gastrointestinal fluid on the stability of protein-bioactive compound complexes. The study showed that the nature of protein interaction with bioactive compounds of varying lipophilicity is influenced by ionic strength. Curcumin, astaxanthin, and cholecalciferol, which have moderate lipophilicity, showed greater binding strength than β-carotene, coenzyme Q_{10}, and β-sitosterol with high lipophilicity. While higher ionic strength promoted primarily dynamic quenching, lower ionic strength mostly favoured static quenching by the lipophilic bioactive molecules. Ionic strength impacted the mechanism of association while protein hydrophobicity mostly determined the K, K_Q, and K_D values. Transmission electron microscopy (TEM) morphological analysis demonstrated the formation of nano-range spherical particles for the protein complexes of curcumin, astaxanthin, and β-sitosterol, micro-range aggregate complexes for the protein-loaded with cholecalciferol and β-carotene, and fiber-like complexes for the protein complex of coenzyme Q_{10}. The research demonstrates that stoichiometry, ionic strength, lipophilicity, and the type of the bioactive compounds are critical factors in the rational design of effective protein complexes for the purpose of bioactive compound delivery.

The final research objective, which represents the last research question, focuses on bio-nano interaction and understanding of the nature of interaction occurring at the bio-nano interface between protein-based nano delivery agents of various structural, physicochemical, and surface functionality and the biomembrane. This research threw more light into the concern of potential nanoparticle toxicity as many researchers believe that the same features that make nanoparticles promising in food and pharmaceutical applications could trigger unwanted physiological responses depending on the nature of nanoparticle interaction with mucus barrier, gastrointestinal lining, or

nature of protein corona formation. This research investigated the underlying mechanism of nanoparticle interaction with giant unilamellar vesicles, a model biomembrane, and revealed two major mechanisms. First is osmotic pressure build-up induced by the nanoparticle binding to the membrane surface, as demonstrated by curcumin-protein nanoparticles, which causes water to escape from the membrane and leads to shrinking in vesicle size. Second is membrane bursting because of nanoparticle binding as shown by curcumin-protein-chitosan and protein-chitosan nanoparticles. The study further showed that hollow nanoparticles without curcumin caused major disruption to the membrane and hence suggests that as the protein or protein-chitosan complexes plays the role of stabilizing curcumin, the bioactive compound modulates the interaction of the macromolecule with the biomembrane. This study is the first to demonstrate the implications of interactions at the bio-nano interface for food protein-based nano delivery systems. This knowledge will help in the development of delivery systems that interact with biological membranes in a safe manner, protect the guest bioactive compound from deterioration, and enable sustained release of the compound at the intended site in the body.

Overall, all four of the thesis objectives, which were derived from the research questions in chapter one, have been accomplished. The findings showed correlation between the structural properties of proteins, structural modification, solubility, hydrophobicity, lipophilicity of bioactive compounds, and ionic strength of the environment, and their important roles on the nature and strength of binding. The study further showed how the strength and mode of binding influence the encapsulation and release efficiencies. The mechanism of release of bioactive compounds depends on the structural and physicochemical properties of protein and the nature of the environment. Macromolecular encapsulating agents play the role of encapsulation, protection, and release of bioactive compounds while the loaded bioactive compound equally stabilizes the encapsulating

agent to the reduce the impact on biomembrane. Taken together, the four objectives of this study have provided the structural basis of interaction of bioactive compounds with proteins to enable the rational design of nano delivery vehicles.

Future direction

Although the goals set out in this research have been fulfilled, for full utilization of protein-based nanoparticles in functional food formulation, further research is required to understand the influence of various ions in the saliva, gastric and intestinal juice. The present study investigated the impact of Na^+ and Cl^- ions which are quite abundant in physiological fluids. Therefore, there is need to study the influence of other ions such as K^+, $H_2PO_4^-$, HCO_3^-, CO_3^{2-}, Mg^{2+}, NH_4^+ and Ca^{2+}. It is only when the contributions of the various ions in physiological fluids have been fully analyzed for their stabilizing or destabilizing effect to bioactive compound-loaded protein complex, that a more accurate conclusion can be made to guide the preparation of protein-based encapsulation systems.

Furthermore, there is need to investigate an encapsulation technique that will accommodate the different structural and physicochemical properties of protein and various bioactive compounds. The encapsulation technique employed in this study is peculiar to curcumin and hence gave rise to heterogeneous nano and micro-complexes of coenzyme Q_{10}, β-carotene, cholecalciferol, and β-sitosterol.

Finally, it will be important to understand the influence of complex macromolecules in the gastrointestinal tract that can cause nanoparticle modification leading to protein-bioactive compound stabilization, degradation, or toxicity. For instance, there is need to investigate the nature of protein corona formed around the surface of the nanoparticles in the saliva, gastric fluid,

intestinal fluid, and mucus barrier that could mask the engineered properties of protein-based nano delivery systems. This study will ensure that bioactive compounds are delivered to their target site and hence reduce the complications associated with the release of drug molecules in off-target cell populations.

APPENDICES

Appendix A: Copyright and Consent Notes

Appendix A1

Consent by co-authors

Names	Signature	Date
Chibuike C. Udenigwe		December 19, 2022
Jian Jin		Nov. 22, 2022
Raliat O. Abioye		11/21/2022
Caleb Acquah		22/11/2022
Bo Wang		22.11.2022

Appendix A2

Copyright from RSC

CCC Marketplace

Special Requests > Special Request Details

Review Cart

Food Proteins and Peptides : Emerging Biofunctions, Food and Biomaterial Applications

Article: CHAPTER 4. Food Proteins as Biomaterial for Delivery Functions

GENERAL INFORMATION

Request ID	Request Date
600102784	18 Nov 2022
Request Status	**Price**
Accepted	0.00 CAD

ALL DETAILS

COMMENTS

Add Comment / Attachment

21 Nov 2022 5:58:39 PM, by Publisher Representative

Permission is granted as long as the chapter is fully acknowledged and a link is given back to the article on our Platform. Please go to rsc.li/permissions for details. Please note that if the material specified above or any part of it appears with credit or acknowledgement to a third party then you must also secure permission from that third party before reproducing that material.

Please ensure all co-authors are aware your chapter will be published in your thesis. View Less

18 Nov 2022 3:46:15 PM, by Ogadimma Okagu

I wish to include part of this chapter which I co-authored in my PhD thesis.

Review Cart

Appendix A3

Copyright from Elsevier

ELSEVIER LICENSE
TERMS AND CONDITIONS

Nov 21, 2022

This Agreement between Mr. Ogadimma Okagu ("You") and Elsevier ("Elsevier") consists of your license details and the terms and conditions provided by Elsevier and Copyright Clearance Center.

The publisher has provided special terms related to this request that can be found at the end of the Publisher's Terms and Conditions.

License Number	5433791029755
License date	Nov 21, 2022
Licensed Content Publisher	Elsevier
Licensed Content Publication	Elsevier Books
Licensed Content Title	Encyclopedia of Food Chemistry
Licensed Content Author	Ogadimma D. Okagu,Bo Wang,Caleb Acquah,Chibuike C. Udenigwe
Licensed Content Date	Jan 1, 2019
Licensed Content Pages	8
Start Page	719
End Page	726
Type of Use	reuse in a thesis/dissertation
I am an academic or government institution with a full-text subscription to this journal and the audience of the material consists of students and/or employees of this institute?	No
Portion	full chapter
Circulation	1
Format	electronic
Are you the author of this Elsevier chapter?	Yes
How many pages did you author in this Elsevier book?	8
Will you be translating?	No
Title	Structural Basis of Guest-Host Interaction in the Gastrointestinal Delivery of Lipophilic Bioactive Compounds using Protein-based Vehicles
Institution name	University of Ottawa
Expected presentation date	Jan 2023
Order reference number	08066955250
Requestor Location	Mr. Ogadimma Okagu 2460 Southvale Crescent, Unit 1114 Ottawa, ON K1B 4L8 Canada Attn: Mr. Ogadimma Okagu
Publisher Tax ID	GB 494 6272 12
Billing Type	Invoice

Appendix A4

Copyright from Journal of Molecular Liquids

CCC Marketplace

This is a License Agreement between Ogadimma Desmond Okagu/University of Ottawa ("User") and Copyright Clearance Center, Inc. ("CCC") on behalf of the Rightsholder identified in the order details below. The license consists of the order details, the Marketplace Order General Terms and Conditions below, and any Rightsholder Terms and Conditions which are included below.

All payments must be made in full to CCC in accordance with the Marketplace Order General Terms and Conditions below.

Order Date	18-Nov-2022	Type of Use	Republish in a thesis/dissertation
Order License ID	1291762-1		
ISSN	0167-7322	Publisher	ELSEVIER BV
		Portion	Chapter/article

LICENSED CONTENT

Publication Title	Journal of molecular liquids	Rightsholder	Elsevier Science & Technology Journals
Article Title	Impact of succinylation on pea protein-curcumin interaction, polyelectrolyte complexation with chitosan, and gastrointestinal release of curcumin in loaded-biopolymer nano-complexes	Publication Type	Journal
		Start Page	115248
		Volume	325
Date	01/01/1969		
Language	English, French, German		
Country	Netherlands		

REQUEST DETAILS

Portion Type	Chapter/article	Rights Requested	Main product
Page Range(s)	1-13	Distribution	Worldwide
Total Number of Pages	13	Translation	Original language of publication
Format (select all that apply)	Electronic	Copies for the Disabled?	No
Who Will Republish the Content?	Academic institution	Minor Editing Privileges?	Yes
		Incidental Promotional Use?	No
Duration of Use	Life of current edition		
Lifetime Unit Quantity	Up to 499	Currency	CAD

NEW WORK DETAILS

Title	Structural Basis of Guest-Host Interaction in the GastrointestinalDelivery of Lipophilic Bioactive Compounds using Protein-based Vehicles	Institution Name	University of Ottawa
		Expected Presentation Date	2023-01-16

Appendix A5

Copyright from Food Biophysics

SPRINGER NATURE LICENSE
TERMS AND CONDITIONS

Nov 18, 2022

This Agreement between Mr. Ogadimma Okagu ("You") and Springer Nature ("Springer Nature") consists of your license details and the terms and conditions provided by Springer Nature and Copyright Clearance Center.

License Number	5432070418689
License date	Nov 18, 2022
Licensed Content Publisher	Springer Nature
Licensed Content Publication	Food Biophysics
Licensed Content Title	Molecular Interactions of Pea Globulin, Albumin and Glutelin With Curcumin: Formation and Gastric Release Mechanisms of Curcumin-loaded Bio-nanocomplexes
Licensed Content Author	Ogadimma D. Okagu et al
Licensed Content Date	Oct 21, 2021
Type of Use	Thesis/Dissertation
Requestor type	academic/university or research institute
Format	electronic
Portion	full article/chapter

Appendix A6

MDPI open access permission for Molecules

All articles published by MDPI are made immediately available worldwide under an open access license. This means:

- everyone has free and unlimited access to the full-text of *all* articles published in MDPI journals;
- everyone is free to re-use the published material if proper accreditation/citation of the original publication is given;
- open access publication is supported by the authors' institutes or research funding agencies by payment of a comparatively low **Article Processing Charge (/about/apc)** for accepted articles.

Permissions

No special permission is required to reuse all or part of article published by MDPI, including figures and tables. For articles published under an open access Cre BY license, any part of the article may be reused without permission provided that the original article is clearly cited. Reuse of an article does not imply endorse authors or MDPI.

External Open Access Resources

Those who are new to the concept of open access might find the following websites or the *Open Access Explained!* video informative:

- **Wikipedia article on Open Access (https://en.wikipedia.org/wiki/Open_access)**
- **Open Access Network (https://open-access.network/en/information/open-access-primers/what-does-open-access-mean)**

Meaning of Open Access

Open Access I

Open Access E

In accordance with major definitions of open access in scientific literature (namely the Budapest, Berlin, and Bethesda declarations), MDPI defines *open access* by the following conditions:

- peer-reviewed literature is freely available without subscription or price barriers,
- literature is immediately released in open access format (no embargo period), and
- published material can be re-used without obtaining permission as long as a correct citation to the original publication is given.

Until 2008, most articles published by MDPI contained the note: "© *year* by MDPI (http://www.mdpi.org). Reproduction is permitted for noncommercial purposes". During 2008, MDPI journals started to publish articles under the **Creative Commons Attribution License (https://creativecommons.org/licenses/by/4.0/)** and are now using the latest version of the CC BY license, which grants authors the most extensive rights. All articles published by MDPI before and during 2008 should now be considered as having been releas 2008 Creative Commons Attribution License.

This means that all articles published in MDPI journals, including data, graphics, and supplements, can be linked from external sources, scanned by search eng text mining applications or websites, blogs, *etc.* free of charge under the sole condition of proper accreditation of the source and original publisher. MDPI believe access publishing fosters the exchange of research results amongst scientists from different disciplines, thus facilitating interdisciplinary research. Open access provides access to research results to researchers worldwide, including those from developing countries, and to an interested general public. Although MDPI pu journals under the open access model, we believe that open access is an enriching part of the scholarly communication process that can and should co-exist wi communication and publication, such as society-based publishing and conferencing activities.

Important Note: some articles (especially *Reviews*) may contain figures, tables or text taken from other publications, for which MDPI does not hold the copyrigh license the published material. Please note that you should inquire with the original copyright holder (usually the original publisher or authors), whether or not thi re-used.

Advantages of Open Access for Authors

The High Availability and Visibility of our open access articles is guaranteed through the free and unlimited accessibility of the publication over the Internet. E access and download the full text of all articles published with MDPI: readers of open access journals, *i.e.*, mostly other researchers, do not need to pay any sut per-view charges to read articles published by MDPI. Open access publications are also more likely to be included in search engines and indexing databases.

The Higher Citation Impact of open access articles results from their high publicity and availability. Open access publications are demonstrably more frequentl

Lower Publishing Costs: Open access publishers cover their costs for editorial handling and editing of a paper by charging authors' institutes or research fund cost of handling and producing an article is covered through the one-time payment of an **article processing charge (APC) (/about/apc)** for each accepted artic open access publishers are only a fraction of the average income per paper earned by traditional, subscription-based publishers. MDPI's **article processing ch (/about/apc)** is the same, irrespective of article length, because we wish to encourage publication of long papers with complete results and full experimental or details [3].

Appendix A7

Copyright from Journal of Agricultural and Food Chemistry

Every conceivable effort has been taken to provide credit to the rightful proprietors of any copied materials. Any copyright holder who has been left out or erroneously acknowledged should get in touch with me.

Thank you